

**POST MORTEM MICROSTRUCTURAL CHANGE TO THE SKELETON**

**Lynne Sevon Bell**

**A Thesis Submitted for the Degree of  
Doctor of Philosophy**

**Faculty of Science  
Department of Anatomy and Developmental Biology  
University College London  
University of London**

**October 1995**

**- 1 -**



## ABSTRACT

The microstructural impact of diagenetic or post mortem alteration has been assessed in predominately human skeletal tissues. The method of assessment selected was microscopical analysis, mainly using backscattered electron imaging in a scanning electron microscope and, to a lesser extent, confocal reflection microscopy. The microstructural morphologies of post mortem alteration were investigated in archaeological material, both normal and pathological, from terrestrial and marine contexts. Further studies were undertaken on a case-by-case basis on skeletal material which offered some unique pathology, environmental context, spatial relationship, time variable, or mortuary practice. Additionally, the effect of diagenetic change on mitochondrial DNA (mtDNA) recovery and the potential location of DNA within the skeletal tissues were investigated. Two quantitative studies were undertaken to validate and measure the observed mineral density changes.

The investigations showed that post mortem alteration or diagenetic change to skeletal material can be extensive, and can occur shortly after death. Diagenesis did not represent a post burial phenomenon as the term diagenesis suggests, but was found to have begun above ground in a range of exposure contexts. The implication of gut bacteria in the promotion of early bacterially-related microstructural change was strong, and it is proposed that body status at the point of, or soon after, death is important. Post mortem alteration to skeletal microstructure can provide environmental information, since terrestrial and marine contexts exhibited distinct morphologies. It may also provide localized environmental



information within a stratigraphic matrix. Characterizing the post mortem microstructural and density changes to bone has helped to elucidate the preservational status of mtDNA in terms of its relative retrieval in archaeological specimens, and the potential location of mtDNA in bone. It is proposed that the shift in mineral density that was found in bacterially-remodelled specimens from terrestrial contexts, relative to the excellent preservation of marine specimens, may help to explain why marine vertebrates far outnumber terrestrial ones in the fossil record, since bacterially driven microstructural change is here considered to be a destructive form of fossilisation.

## ACKNOWLEDGEMENTS

This thesis could not have been completed without the unstinting support of my doctoral supervisor Sheila J. Jones. Throughout the long duration of this study she has always been ready to offer encouragement, tactful criticism, endless patience, grammatic enlightenment and kindness. For all of this I am most grateful.

I also gratefully acknowledge the help and guidance Alan Boyde has given throughout this study. Certainly many aspects of this work could not have been undertaken without him. In addition, I would like to offer warmest thanks to Mo Arora and Roy Radcliffe for their expert technical assistance and friendship.

Many other people have generously provided their time, interest and skeletal material. Of these people I particularly wish to thank Ann Stirland who not only introduced me to the Mary Rose material, but who has remained the best of colleagues and the best of friends. Peter Andrews and Theya Molleson have always given freely of their ideas and material, and provided me with many inspirational moments. Mark Skinner provided essential forensic material at a critical time. Andy Elkerton has provided valuable stratigraphic information on the Mary Rose wreck. Erika Hagelberg, Franti Wong and Jim Elliott collaborated on the DNA and microtomographic work. Sue Stallibrass kindly provided animal bone material and has always been very patient of my enquiries. Gill Stroud has been a valuable and knowledgeable friend. The many other people to whom I am greatly indebted and owe thanks to, are, Paul Bahn, Don

Brothwell, Rosalie David, Chris Dean, Paul Dieppe, Helen Donohue, Ebba During, Roger Flinn, Mark Garrison, Robert Hedges, Marianne Hester, Mike McCarthy, Douglas Owsley, John Paddock, Juliet Rogers, Margaret Rule, Alan Saville, Derek Stirland and Noreen Tuross.

To my friends who have collectively endured this project I am particularly grateful. I owe special thanks to Jane Gill for her expert help with the Figures and to Lynx Training for allowing me multifarious access to their resources. I gratefully acknowledge the financial assistance of the Medical Research Council.

Finally, none of this work could have been concluded without the loving support of Bee and her daughter Edith.

## TABLE OF CONTENTS

Top page	1
Abstract	2
Acknowledgements	4
List of Figures	9
List of Tables	14
 <b>CHAPTER 1: MICROSTRUCTURAL CHANGES TO SKELETAL TISSUES AND RELATED ISSUES</b>	 15
1.1 Defining definitions	15
1.2 The micromorphology of diagenesis in the skeletal tissues	20
1.3 The micromorphology of diagenesis in teeth	20
1.4 The micromorphology of diagenesis in bone	26
1.5 Terrestrial and marine decomposition	40
1.6 Ante mortem microbial changes to the skeleton	44
1.7 Aims of this study	46
 <b>CHAPTER 2: THE MORPHOLOGY OF DIAGENETIC CHANGE IN HUMAN BONE AND TEETH</b>	 48
2.1 PART I: Soil-buried contexts	48
2.2 Introduction	48
2.3 Diagenetic morphology in archaeological normal and pathological human bone	48
2.4 Materials and methodology	49
2.5 Results and discussion	51
2.6 Conclusion	75
2.7 PART II: Terrestrial versus marine	76
2.8 Introduction	76
2.9 Materials and methodology	76
2.10 Results and discussion	77
2.11 Conclusion	82
 <b>CHAPTER 3: PAGET'S DISEASE: POST MORTEM ALTERATION AND BONE PATHOLOGY</b>	 99
3.1 Introduction	99
3.2 Aims of this study	100
3.3 Materials and methodology	100
3.4 Results	101
3.5 Discussion	102
3.6 Conclusion	109
 <b>CHAPTER 4: THE MARY ROSE WRECK: A UNIQUE SEA BURIAL</b>	 110
4.1 Introduction	110
4.2 Historical background	110
4.3 Depositional history	112
4.4 Microstructural changes to marine substrates	113
4.5 The aims of this study	114
4.6 Materials and methodology	114
4.7 Results	115
4.8 Discussion	131
4.9 Conclusion	134

<b>CHAPTER 5: A NEOLITHIC LONG CAIRN: LONG TERM SKELETAL EXPOSURE</b>	<b>135</b>
5.1 Introduction	135
5.2 Historical background	135
5.3 Microstructural evidence of exposure	137
5.4 Aims of this study	139
5.5 Materials and methodology	139
5.6 Results	142
5.7 Discussion	143
5.8 Conclusion	160
 <b>CHAPTER 6: THE SPEED OF POST MORTEM CHANGE TO THE HUMAN SKELETON AND ITS TAPHONOMIC SIGNIFICANCE</b>	 <b>161</b>
6.1 Introduction	161
6.2 Aims of this study	163
6.3 Materials and methodology	163
6.4 Results	165
6.5 Discussion	167
6.6 Conclusion	180
 <b>CHAPTER 7: BUTCHERY AND DELIBERATE MUMMIFICATION</b>	 <b>181</b>
7.1 Introduction	181
7.2 Butchery in an archaeological context	181
7.3 Mummification in an archaeological context	182
7.4 Aim of this study	184
7.5 Materials and methodology	185
7.6 Results	187
7.7 Discussion	188
7.8 Conclusion	193
 <b>CHAPTER 8: SKELETAL DNA</b>	 <b>194</b>
8.1 PART I: Microstructural preservation and DNA recovery	194
8.2 Introduction	194
8.3 Aim of this study	196
8.4 Materials and methodology	196
8.5 Results	197
8.6 Brief summary of DNA results	199
8.7 Discussion and conclusion	206
8.8 PART II: Mineralised osteocytes: a possible location of bone DNA	207
8.9 Introduction	207
8.10 Materials and methodology	213
8.11 Results	213
8.12 Discussion and conclusion	221
 <b>CHAPTER 9: QUANTITATION</b>	 <b>223</b>
9.1 Introduction	223
9.2 Bone	223
9.3 Bone mineral density	224
9.4 SEM/BSE imaging and bone density	225
9.5 Aims of this study	228
9.6 Materials and methodology	228
9.7 Results	231
9.8 Discussion	237
9.9 Conclusion	238

<b>CHAPTER 10: SUMMARY AND CONCLUSIONS</b>	<b>240</b>
<b>REFERENCES</b>	<b>246</b>
<b>APPENDICES</b>	<b>265</b>
Appendix 4.1 Data set of tubule diameters	266
Appendix 4.2 Data set of maximum ingress	267
Appendix 7.1 Context description: Old Grapes Lane, Carlisle	268
Appendix 10 Publications arising from this study	270

## LIST OF FIGURES

Figure 2.1		62
2.1a	Image of modern cranial bone	
2.1b	Topographical image of above	
2.1c	Image of modern bone periosteal aspect	
2.1d	Topographical image of above	
2.1e	Image of modern mid-cortical bone	
2.1f	Topographical image of above	
Figure 2.2		65
2.2a	Image of archaeological bone which has been diagenetically altered	
2.2b	Topographical image of above	
2.2c	Single osteon diagenetically altered	
2.2d	Topographical image of above	
2.2e	Bone at periosteal aspect affected by diagenesis	
2.2f	Topographical image of above	
Figure 2.3		68
2.3a	Diagenetically altered trabeculum	
2.3b	Cortical field of bone altered by diagenesis	
2.3c	Extensive diagenetic remodelling of cortex	
2.3d	Extensive diagenetic remodelling of single osteon	
2.3e	Circumferential lamellae intact above field of diagenetically altered bone	
2.3f	Primary osteonal bone affected by diagenesis, located on periosteal aspect	
Figure 2.4		71
2.4a	High power view of altered primary osteonal bone	
2.4b	Topographical image of above	
2.4c	De and remineralisation centred within single osteon	
2.4d	Diagenetic foci centred on osteocyte lacunae	
2.4e	Non-survival of circumferential lamellae	
2.4f	Distribution of diagenetic foci around single osteon	
Figure 2.5		74
2.5a	High power view of 2.4f	
2.5b	Single osteon which has increased in overall density due to diagenesis	
2.5c	Diagenetic foci orientated around vascular spaces in pathological specimen	
2.5d	High power view of above	
2.5e	Normal alveolar crest, dentine and cementum	
2.5f	Diagenetic alteration to cementum and alveolar bone	
Figure 2.6		86
2.6a	Montage of soil-buried tooth	
2.6b	Montage of marine-buried tooth	

Figure 2.7		89
2.7a	Diagenetically remodelled maxillary lamellar bone	
2.7b	Alveolar crest with unique marine-type change	
2.7c	Unaffected dentine, enamel and calculus	
2.7d	Enamel white-spot lesion	
2.7e	Microcavitation of carious lesion	
2.7f	Unaffected field of dentine and enamel	
Figure 2.8		92
2.8a	Secondary dentine diagenetically altered	
2.8b	Extensive diagenetic alteration to dentine and cementum	
2.8c	Normal dentine	
2.8d	Preserved interglobular dentine	
2.8e	Diagenetic demineralisation foci streaming along dentine's incremental planes	
2.8f	Peritubular dentine evident within diagenetic foci	
Figure 2.9		95
2.9a	Loss of peritubular dentine and splitting	
2.9b	Possible combined activity of caries and post mortem alteration	
2.9c	Marine-type change undermining enamel	
2.9d	Cementum with soil-related change	
2.9e	Distribution of diagenetic foci within Sharpey fibre bone	
Figure 2.10	Cementum tunnelled by marine-type micro-organism	98
Figure 3.1		104
3.1a	Possible Pagetic cranial bone	
3.1b	Irregularly defined soft tissue spaces and hypermineralised reversal lines	
3.1c	Irregular osteocyte lacunae	
3.1d	Two osteonal systems	
3.1e	High power centre field of above	
3.1f	Rapidly remodelling bone	
Figure 3.2		107
3.2a	Small diagenetic foci present in cranial bone	
3.2b	Radius with classic "mosaic" morphology	
3.2c	Enlarged soft tissue spaces	
3.2d	Periosteal circumferential lamellae intact	
3.2e	Osteoclastic resorption lacunae	
3.2f	Diagenetic foci strongly orientated with collagen direction	
Figure 4.1	Medieval picture of the Mary Rose warship	111
Figure 4.2	Distribution of sample group over ship	116
Figure 4.3	Diagram of sample sites per specimen	117



Figure 4.4		122
4.4a	Enamel undermined by post mortem tunnelling	
4.4b	Dentine totally remodelled	
4.4c	Internal reflection artefact of tunnel direction	
Figure 4.5		125
4.5a	Alveolar bone invaded by tunnelling	
4.5b	Maximum ingress measurement	
4.5c	Maximum post mortem tubule diameter	
Figure 4.6	Distribution of tubule diameters	126
Figure 4.7	Cumulative silt phase schematic of ship	129
Figure 4.8	Graphical representation of maximum ingress	130
Figure 5.1	Contour map of long cairn	136
Figure 5.2	Spatial representation of total bone scatter	138
Figure 5.3	Spatial representation of specimen location	140
Figure 5.4		146
5.4a	Dentine invaded by bacterial-type attack	
5.4b	Cementum unaffected	
5.4c	Post mortem change as reflective globular features	
Figure 5.5		149
5.5a	Post mortem enlargement of alveolar bone	
5.5b	Dentine tunnelled to enamel dentine junction (EDJ)	
5.5c	Dentine extensively remodelled post mortem	
Figure 5.6		152
5.6a	Enlargement of osteocytic spaces in alveolar bone	
5.6b	Centre field of above	
5.6c	Apical cementum altered post mortem	
Figure 5.7		155
5.7a	Tooth extensively remodelled post mortem	
5.7b	Dentine extensively remodelled to the EDJ post mortem	
5.7c	Radicular dentine extensively altered post mortem	
5.7d	Peritubular dentine preserved within a post mortem demineralisation focus	
Figure 5.8		157
5.8a	Post mortem bacterial foci changing direction at the CDJ	
5.8b	Unaffected tooth	
5.8c	Region of interglobular dentine	
5.8d	Unaffected cementocytes	
Figure 6.1		170
6.1a	3 months (m) post mortem. Subperiosteal demineralisation foci	

6.1b	3 m post mortem.	Intracortical demineralisation	
6.1c	15 m post mortem.	Bacterial-type remodelling	
6.1d	15 m post mortem.	Bacterial-type foci located on osteocyte lacunae	
Figure 6.2			173
6.2a	15 m post mortem.	Bacterial-type change in two osteons	
6.2b		Small diagenetic focus	
6.2c	2 years (yrs) post mortem.	Marine-type tunnelling to tooth	
6.2d	2 yrs post mortem.	Tunnels penetrating dentine	
Figure 6.3			173
6.3a	7 yrs post mortem.	Radicular cementum with two localised post mortem foci	
6.3b	70 yrs post mortem.	Diffuse peripheral band of demineralisation to periosteal aspect of a rib	
6.3c		High power view of above	
Figure 7.1		Schematic of modern carcass division in Britain	182
Figure 7.2			191
7.2a		Extensive post mortem alteration to bone	
7.2b		Small localised post mortem voids	
7.2c		Extensive diagenetic change to trabecular bone	
7.2d		Peripheral demineralisation at periosteal aspect	
7.2e		Small intracortical diffuse demineralisation focus	
Figure 8.1			202
8.1a		Diagenetic change to bone at periosteal aspect	
8.1b		Mid-cortical osteonal systems exhibiting localised diagenetic foci	
8.1c		Single trabeculum with containing small diagenetic foci	
8.1d		Only the circumferential lamellae are unaffected	
8.1e		Mid-cortical bone with moderate diagenetic change	
8.1f		Cortical bone close to medullary aspect diagenetically altered	
8.1g		Bone below periosteal aspect extensively diagenetically remodelled	
8.1h		Mid-cortical region altered post mortem	
8.1i		Medullary aspect bone extensively altered post mortem	
Figure 8.2			205
8.2a		Extensive diagenetic remodelling next to periosteal aspect	
8.2b		Small area of mid-cortical bone extensively altered post mortem	
8.2c		Medullary aspect and adjoining trabeculae altered post mortem	
8.2d		Mid-cortical region of intact bone bordering a diagenetically altered region of bone	

8.2e	Specimen with normal micromorphology	
8.2f	Small focus of demineralisation at periosteal aspect	
Figure 8.3		217
8.3a	Two 'mineral infilled osteocyte lacunae' (MIOL)	
8.3b	Field of MIOL	
8.3c	Layed and partially infilled MIOL	
8.3d	A single MIOL abutting a diagenetic focus	
8.3e	Higher power view of MIOL from above	
Figure 8.4		220
8.4a	Field of MIOL close to band of peripheral demineralisation	
8.4b	MIOL with internal structure similar to cell nucleus	
8.4c	As above	
8.4d	Field of MIOL	
8.4e	As above	
8.4f	MIOL in bone close to calcified cartilage	
Figure 9.1	Diagram of specimen set-up and radial motion for microtomography	229
Figure 9.2	Tomogram of Barton femur with high density diagenetic component	233
Figure 9.3	Tomogram of Barton femur recalibrated	234
Figure 9.4	Diagenetic shift in sample group	235
Figure 9.5	Maximum diagenetic shift	236

## LIST OF TABLES

Table 1.1	Stages of Decomposition for Land and Water	41
Table 4.1	Translated Data Grades	128
Table 6.1	Forensic Sample Group	164
Table 7.1	Animal Sample Group	186

## CHAPTER 1: MICROSTRUCTURAL CHANGES TO SKELETAL TISSUES AND RELATED ISSUES

### 1.1 Defining definitions

The aim of this dissertation is to assess the microstructural impact of post mortem change to primarily human bone and teeth. The study is therefore a taphonomic one, of a phenomenon called diagenesis which can occur in forensic, archaeological and fossil skeletal material. The terms or nomenclature used in this study originate historically from overlapping disciplines and as such vary in their use and comprehension. A short discussion of this nomenclature follows by way of clarification.

Taphonomy means literally 'the laws of burial'. Arguably, the German geologist Weigelt, whose classic treatise published in 1927 described how organisms die, decay and become encased in sediment, was the first to outline taphonomic study, calling it "biostratinomy". However, historically, the term "taphonomy" was first coined by the Russian vertebrate palaeontologist Efremov (1940) who outlined a more systematic approach to the study of the transitional phases between death, entombment and final lithification. Efremov wanted to establish predictive laws in order to understand just why and how fossil groupings display bias in terms of species representation. He suggested that if one could account for the factors which control successful fossilisation, then the resultant bias could be understood and corrected for, allowing for the theoretical reconstruction of fossil communities (Efremov, 1940).

Both Weigelt and Efremov (although Efremov was more explicit) were working within, and arguing for, a theoretical framework for taphonomic study based

on uniformitarianism. Uniformitarianism, outlined by Lyell in "Principles of Geology" in 1830, stated that a) processes are uniform throughout time and b) natural laws are constant in space and time. (This theory opposed the Catastrophist ruling paradigm which asserted that geological strata were created out of environmental catastrophies, the most recent being the Noachian Flood, which all occurred after Creation 4004 BC [Daniel, 1975].) Taphonomy is theoretically based upon the latter aspect of uniformitarianism and has been called methodological uniformitarianism (Gould, 1965). It has also been referred to as actualistic and neotaphonomic, which essentially means that methodological inferences can be made about past events by direct analogy to the present, since the processes which governed events in the past will proceed identically to those in the present (Lyman, 1994). Hence, 'actualistic' experiments which model or observe a taphonomic event in either a cross-sectional or longitudinal time-frame will have legitimate relevance to interpreting comparable historical skeletal assemblages.

Diagenesis is a geological term and refers to the physical, physicochemical and biochemical events which can occur during the formation of a sedimentary deposit. The events referred to are here understood to mean: -

"...compaction, dessication, deformation, corrosion, bleaching, oxidation reduction, crystal inversion, recrystallization, intercrystalline bonding, cementation, decementation, mineral growth and mineral replacement, particle accretion, flocculation, sediment mixing, boring, decomposition and synthesis of organic compounds...incorporation of biota...and excludes the effects of high temperature and pressure." (Lapedes, 1978: 153)

Biota or faunal remains can constitute a greater or lesser percentage of a sedimentary deposit and as such are necessarily included within the term "diagenesis". It is this inclusion, however, that has led to the now

common use of the term diagenesis within archaeological literature and refers to any microstructural post mortem alteration to skeletal material. Unfortunately, this has introduced an implicit and potentially erroneous assumption that post mortem alteration begins after burial and is controlled by soil cofactors stretched into geological time (Piepenbrink & Schutowski, 1987). Indeed, part of this problem hangs upon the question of when exactly diagenesis begins. Recently, workers have taken to stating that diagenesis begins at the point of burial (Lyman, 1994; Retallack, 1990) and that any changes which occur prior to that are 'biostratinomic'. Essentially this is the correct view and considered earlier by Lawrence (1971) as a necessary distinction. However, the theoretical practicality of such an approach is questionable. Purdy (1968) readily admitted in his study of carbonate diagenesis that diagenesis is a "vague" concept which is difficult to define, particularly at the beginning and end of its effects on sediments: "the impossibility of clearly distinguishing between diagenesis and metamorphism because diagenesis is, in fact, the beginning of metamorphism.... (and) the distinction between depositional and post-depositional processes is equally arbitrary" (Purdy, 1968: 184). Rolfe and Brett (1969) attempted to solve this problem by subdividing diagenesis into three stages, where the earliest stage is referred to as "syndiagenesis", which involves only the activity of bacteria in shallow sediments metabolizing organic matter in skeletal tissue. This subdivision, although refining terminology, goes no further towards solving the problem other than stating that diagenetic processes begin postburial. Indeed, the entomological and microbial aspects of decay, whether above or below ground, may be considered identical processes and therefore descriptively diagenetic.

This problem is further added to by the prefixure of "forensic", "archaeological" and "fossil" to date skeletal material. A forensic specimen can generally be defined as an individual who has been dead, buried or unburied, for up to 50-100 years and is also of no interest to the County Coroner (Burial Act 1857, section 25). In other parts of the world this generality may vary usually for legal reasons, but also for political reasons, as in the reburial issues surrounding the Israeli, Amerindian, Aboriginal and Maori skeletal collections (Watzman, 1995; Ubelaker & Grant, 1989).

An archaeological specimen is more difficult to define due to the historical origins of archaeology. A discussion of the origins of archaeology would be lengthy and inappropriate here, but generally, modern archaeology is concerned with all aspects of human social organisation where there is evidence of people and their material culture (Hodder, 1991; Daniel, 1975). It no longer necessarily involves the study of human evolution as it did during the 1800's, nor is it treasure hunting as it was at the turn of the century. Instead, it has become a global discipline which examines evidence of social organisation dating from Mesolithic hunter gatherer societies onwards. In Britain this can be clearly defined as beginning 10,000 years BP (at the end of the last glaciation), but other parts of the world may pre or post date this.

A fossil can mean all things to all people. The nineteenth century biblical scholars believed that Creation began 4004 years BC, and consequently found fossils to be the irksome protagonists of new evolutionary schemes in geology and biology (Desmond, 1982). Even today,



Jehovah's Witnesses will argue that fossils have been placed in geological deposits, by God, in order to test our faith - an argument difficult to dispute! Indeed, one notable and extant professor has called enamel a "living fossil", it being effectively dead and almost totally mineralized within the living mouth (Boyde, pers. comm.). However, from a geological standpoint a fossil constitutes any evidence of past life which is, or was, situated in a geological deposit (Lapedes, 1978). Fossils fall within four main groups: -

1. **Unaltered remains** such as frozen woolly mammoths or animals and insects preserved in oil seeps and oil shales.

2. **Petrified fossils** produced by perimineralization, where mineral is added to natural microscopic voids within specimens; by replacement of minerals by substitution at a molecular level; and by distillation where organic tissues are carbonised via the liberation of carbon dioxide and water, leaving only a carbon copy.

3. **Molds, casts and imprints** of animals etc are created when a creature is surrounded by a deposit and latterly lost leaving only an impression of itself.

4. **Tracks, trails and burrows** are the final subgroup where life has passed over or through a deposit and subsequently that feature is preserved as an interface or morphological discontinuity within the deposit.

(After Lapedes, 1978: 247-8)

Hence, fossils can be thought of as specimens of some great antiquity which have been preserved as distinct features or inclusions within geological deposits and relatively predate the beginning of the Mesolithic period. However, two major inconsistencies remain: one is the problem of when diagenesis begins and therefore the various processes of fossilisation; and

secondly, archaeological specimens are usually inhumations from cemetery sites, and as such, are intrusively buried deep within a sediment, and therefore considered to be both archaeological and fossil.

This thesis will use all the terms referred to in this section. It will as a result try to unravel some of the processes and contradictions manifest in an eclectic area of study.

### 1.2 The micromorphology of diagenesis

In the previous century and well into this one, the internal micromorphology of diagenesis, or post mortem alteration to bone and teeth, was observed only as a curiosity. Latterly, diagenesis has come to represent an irksome source of contamination for various archaeological and forensic techniques which rely heavily on the anorganic integrity of skeletal tissues. As a source of information in itself, diagenesis has had few admirers, and much of the microscopic work has concentrated on the taphonomic relevance of surface changes to the periosteal circumferential lamellae of bone (Andrews, 1990; Teaford, 1988).

### 1.3 The micromorphology of diagenesis in teeth

The original description and first important histological study of post mortem change to human bone and teeth was undertaken by Wedl (1864). Wedl's study began by accident when a batch of teeth stored in water had become fouled by a possible fungus. He observed microscopic tunnelling extending into the dentine from the neck and peripheral aspect of the root. He then went on to conduct a unique experimental study where teeth were immersed in growth media containing the original micro-organism. His

results revealed that the micro-organism, considered to be a fungus, was capable of penetrating the dentine via the neck and peripheral aspect of the root but had no effect on enamel. Penetration of the dentine occurred within 13-17 days of immersion, resulted in canals with transverse diameters of 7 microns and invaded dentine without any regard to its structure. Wedl repeated his experiment with a section of horse rib and found the same invasive tunnelling by the micro-organism. He then examined several fossil species of teeth in order to determine the antiquity of this alteration, and also to evaluate the relationship between tooth morphology and distribution of the micro-organisms' attack. He found that some of the fossil specimens exhibited the previously observed post mortem alteration and that the enamel remained unaffected by such changes no matter what the structural arrangement of the dental tissues. He concluded that the change itself must have occurred after death since the morphology of the attack was different from that of any known caries; that it was caused by a fungus; that the fungus fed on the collagenous fraction of the skeletal tissues and therefore could not compromise enamel, it being almost entirely mineral; and that this particular post mortem change was itself of great antiquity.

Other histological investigations followed Wedl's initial study. Tomes (1892) examined a human tooth "picked up in a graveyard" and found similar tunnelling to that of Wedl. He noted that invasive tunnels had three directional tendencies: to invade along the dentine tubules, to invade at right angles to dentine tubule direction and, thirdly, to invade in any direction without regard to dentine structure at all. Previous to Tomes' study, Roux (1887) and Schaffer (1895, 1889, 1890) examined fossil bone and

teeth of over 90 million years and found similar microscopic tunnelling. Later Duckworth (1901) passed brief comment on post mortem microscopic tunnelling in a human tooth fragment, and in 1903 Hopewell Smith re-examined Tomes' cited specimen and, unsurprisingly, observed exactly the same changes to microstructure as those reported by Tomes.

The next extensive piece of research undertaken in the the area of post mortem alteration to human teeth was not reported until Sognnaes' work during the 1950's (1949, 1955, 1956, 1959). He collected a large group of human teeth from several different historical contexts and periods from Palestine, Egypt, Greece, Iceland, Norway and Guatemala. All the teeth were embedded and sectioned and were examined for evidence of post mortem alteration (Sognnaes 1949, 1955). Tunnelling was observed extending from the neck of teeth (as reported by Wedl), or extending from the neck and from the pulpal dentine. The tunnels had diameters varying between 2-10, 15-25 and 50-100 microns. Respectively, these tunnels could traverse the entire width of the dentine in a corkscrew like manner; the commonest type formed branched arrays; whilst the largest tunnels were characterized by ampulla-shaped widenings. Again the enamel remained unaffected by this type of invasion. Sognnaes felt that no time relationship existed between his specimens in terms of the severity of post mortem attack, but that was not to deny that the proportion of teeth affected was different between population groups. Sognnaes remained puzzled as to the identity of the responsible micro-organism, but suggested that the tunnelling may occur soon after death in the aerobic shallow layer of soil prior to bacterial and gaseous putrefaction. In a later paper Sognnaes (1959) suggested a

saprophytic agent for the branching type of tunnelling and extensively dismissed the notion of in vivo caries as a possible cause.

Syssoeva (1958) undertook the first systematic study to ascertain the speed with which post mortem alteration to teeth could occur. He examined a total of 196 teeth from soil-buried individuals who had been dead from between 6 months to 70 years and buried for 10 years or more. He observed macroscopic changes to teeth, although no obvious change to microstructure were evident in these teeth, or in any others of the sampled group. However, an x-ray study did show a slight decrease in density in specimens which had been in the ground for 65-70 years. Hence, Syssoeva's study appeared to show that post mortem alteration, if it were to occur at all, would begin no earlier than 70 years after burial and possibly some considerable time thereafter. It is curious however, that the unspecified macroscopic changes to teeth observed, were not detectable microscopically.

Work by Clement (1958, 1963) and Falin (1961) addressed post mortem alteration to teeth only as a subjunct to assessing evolutionary aspects of tooth development from the early anthropoids through to the Bronze Age period. Both workers found evidence of Sognnaes' commonest type of tunnelling (some of which were infilled with mineral presumed to originate from the soil), and agreed that mechanisms governing the presence and severity of such changes could not be time-dependent. As a result of these findings Falin suggested that the work of Syssoeva (1958) needed reassessment, presumably because no post mortem alteration had been found in his specimens other than pulp degradation in the first 10 years.

Werelds examined 300 human teeth excavated from a sandy soil (1961), 72 human teeth from a clay soil (1962) and a set of human teeth deliberately exposed to soil and marine burial (1967). The age of his specimens spanned approximately 1000 years. The sandy specimens yielded the same tunnelling as described by previous workers (a type of mycetes was suggested as the causative agent), but Werelds also felt he had identified a new type of post mortem change, described as an apparent "disaggregation of the dentine" (1961: 60) and later described it as a "multitude of galleries" (1962: 589). In his examination of the clay based specimens he found the same array of post mortem change to dentine and cementum - buried for approximately 300 years - and concluded that time was not a pertinent factor in this process of change. Werelds then buried and immersed freshly extracted teeth in an attempt, similar to Wedl's (1864) work, to induce post mortem alteration experimentally. The soil buried specimens exhibited post mortem alteration in the third year of burial and the water immersed specimens suffered tunnelling within a few months (Werelds, 1967). Hence, Werelds demonstrated, as did Wedl, that post mortem alteration could occur soon after death and as a corollary that the presence and severity of such changes were unlikely to have a linear relationship with time.

Electron microscopic work undertaken to investigate the survival of fossil dentine collagen (Isaacs & Little, 1963; Doberenz, 1967; Doberenz & Wyckoff, 1967) also provided inadvertent evidence of the identity of and route taken by an invasive micro-organism post mortem. Fossilised rod-shaped bacteria/inclusions were found packed inside dentine tubules of a *Brontotherium* tooth (Doberenz & Wyckoff, 1967). An attempt was made to cultivate these inclusions to check that they were not a recent laboratory

contaminant: the cultures proved negative. Cold incineration with ionized oxygen, which would have converted any carbon to carbon dioxide, also proved negative. The authors felt it unlikely that the bacteria were carious in origin since no regional breakdown in the structure of the surrounding dentine, indicative of present day disease, was apparent. It was felt that the most likely period for the introduction of the bacteria was soil related, either during decomposition or at a much later stage.

A new post mortem alteration to enamel was detected and described as "pseudocaries" by Poole and Tratman (1978). Twelve Mesolithic human teeth excavated in a limestone cave were examined using ordinary light and polarized microscopy. Macroscopically, teeth appeared free of any carious lesions; however, on microscopic inspection, zones of demineralisation (morphologically characteristic of caries) affected the surface area of whole crowns, and extended pulpally approximately one third to one half of the total enamel thickness. This alteration was considered to have been caused by slow demineralisation and created internal lesions that were identical to those created by oral micro-organisms, but the distribution of this change was totally unlike that of dental caries. The dentine situated beneath such lesions showed no disaggregation or reparative response. In addition, post mortem tunnelling extended both peripulpally and perpendicular to dentine tubule direction, with tunnel diameters of 2-5 microns, and was only detected in specimens free of enamel pseudocaries. The authors considered post mortem alteration to the affected dental tissues probably began soon after death when a range of microbial colonies would have been present as part of decomposition. However, they remained puzzled as to why the overwhelming presence of limestone had not inhibited

the observed acidification of the enamel. The authors mention, almost as an aside, that they buried a set of human and dog teeth in a Bristol cemetery for 6 months, but that on reinspection no post mortem alteration was evident.

At this point work which considered the internal micromorphology of post mortem alteration to dental tissues either stopped or went unreported. Instead, work shifted toward ascertaining the elemental and organic composition of dental tissues. This change of emphasis in archaeologically related research was largely technique driven and itself originated from the emerging science-based 'New Archaeology'. However, the shift was largely a taphonomic and geochemical one, and as such, post mortem alteration to skeletal tissues became known as diagenetic change, with all the incumbent problems associated with that term.

#### 1.4 The micromorphology of diagenesis in bone

Historically, the first histological observation of post mortem change within bone, as in teeth, was made by Wedl (1864). In addition to his experimental work on teeth with a fungal type isolate, he inoculated a section of horse rib and observed that similar tunnelling occurred within four days. The tunnels had the same morphology as those previously observed in dentine, but their distribution was not detailed by Wedl. He also observed extensive tunnelling in the fossil rib bone of a warbler (from the Leitha Mountains); and reported that the distribution of this change was peripheral, with tunnels invading the cortex most intensively from the periosteal aspect with decreasing penetration deeper to the surface. The tunnels themselves had diameters of 4 microns, invaded no



deeper than 250 microns and appeared unaffected by the collagenous arrangement of the bone. Other fossil material studied by Roux (1887), Schaffer (1895, 1889, 1890) and Thomasett (1931) extended and confirmed Wedl's initial observations that post mortem tunnelling, alongside other post mortem changes, could be found in a range of species, including dinosaurs, mammals and fish.

Graf (1949) undertook a histological study to assess the preservation of soft and bony tissue in human Egyptian mummy and Swedish skeletalized soil-buried material and made some interesting observations. He found a range of preservation states: all bone belonging to the mummy material was intact; whereas, the skeletonized material from different soil contexts showed a "derangement of the Haversian systems" (ibid: 245). This alteration was different in morphology from that described by Wedl, and was figured by Graf as a picture of enlarged osteocyte lacunae, with enlargement and funnelling of the osteocyte canaliculae, which collectively fused to create greater, irregular and continuous defects. Often, however, the lamellae nearest the Haversian canal were unaffected. Graf was puzzled by the mechanism which caused this post mortem alteration, but noted that specimens exhumed from dry earth and gravel contexts exhibited less high grade destruction than those from moist earth. Interestingly, or in Graf's terms "astonishing", a Viking skeleton revealed remnants of blood vessel walls within a Haversian canal, red blood corpuscles and erythrocytes, alongside non-identifiable ovoid bodies which Graf suggests were worm eggs. He reasoned that the Haversian canals deep to the central area of compact bone offered protection, over some considerable time, from the destructive processes which removed the soft tissues of the skeleton. Finally, in

order to study early post mortem changes, Graf attempted a small "flower pot" experiment where a cadaver rib was acquired, allowed to sit unfixed for a fortnight, and then potted on for a year. When examined no discernible change to bone was evident, although "the endoplasma of the osteocytes and their nuclei were still to be seen....but necrotic in appearance....erythrocytes in blood vessels had fused to form an amorphous mass....white corpuscles were clearly outlined but shrunken....remnants of bone marrow were observed and contained primitive blood cells" (ibid: 246-7). Graf concludes that post mortem alteration to bone is not a time dependent phenomenon and that the cellular components of bone can potentially survive partially intact for some centuries.

Other histological observations by Morganthaler and Baud (1956), Enlow and Brown (1956), Cook et al. (1962), Little et al. (1962), Berg (1963) and Sergi et al. (1972) extended and confirmed Graf's work. They all found evidence for a range of post mortem alteration dating from the Triassic and Eocene through to approximately 1800 AD. Morganthaler and Baud observed minute canaliculae which disrupted osteon lamellar structure, some of which were filled with what appeared to be brownish septate filaments. They were unable to cultivate any of these filaments. Cooke et al. (1962) commented that under polarized light specimens which were unaffected by tunnelling (ie had good morphology) exhibited "the pattern of concentric striations imposed on the living osteon by the fibrillar organisation of collagen.....this implied a substitution of mineral matter for the original organic matter at the submicroscopic or macromolecular level" (ibid:494). Hence, Cook et al. (1962) suggest that even when good bone morphology is evident at the microscopic level, post mortem degradation of the collagen

protein will still have occurred. Similar collagen degradation was observed in human bones dating approximately to 1800 AD by both Little et al. (1962) and Berg (1963). Berg (1963) asserted that such changes to bone microstructure occur gradually over 1000-2000 years post mortem. Sergi et al. (1972) made ultrathin sections of bone and found that unaltered bone had very thin needle-like crystals (width 8.5 nm) typically aligned with the major axis of the lamellae, but in some areas the crystals changed direction and formed obtuse angles with previous and following groups, giving an overall impression of collapsed tissue. In areas of bone which had undergone considerable and diffuse or "mottled" post mortem alteration, large irregular and interconnecting voids opened up with bordering walls which were very thin (only a few crystals thick) and "labyrinth-like" in structure (crystallite size and orientation is not reported). Again there is general agreement amongst the authors that the post mortem process of change is not a time related one.

Marchiafava et al. (1974) undertook a morphological investigation into the "osteoclastic activity" of a *Mucor* fungus on buried bone. Initially fragments of human vertebrae, dissected from cadavers, were buried in flower pots with garden earth. The earth was kept wet at 20°C. After a few days a white mould masked the surface of the bone fragments. Three fungal isolates were obtained from this mould and subsequently reseeded individually onto autoclaved bone. Only *Mucor* grew under these controlled conditions and bone changes were observed within 15-20 days. The penetrating hyphae were 2-6 microns in diameter and tubular in structure. Marchiafava et al. noted that two different patterns of invasion were present. In one, hyphae with normal appearance produced penetrating

tubules within bone which showed no evidence of decalcification resorption and was smooth up to the free edge. In the second pattern of invasion, bone matrix was undergoing fungal decalcification: closely packed collagen fibrils with clearly recognisable 64 nm periodicity were alongside small aggregates of crystals. The affected tissue appeared as thin strips surrounding the tubules created by the fungal hyphae which showed evidence of aging, containing intrahyphal lipid droplets. Exactly how *Mucor* managed to tunnel into bone without using decalcifying agents remained a puzzle. However, the authors postulate that aging hyphae may have utilised a possible combination of acid, pectinase and cellulase, as is the case with pathogenic fungi.

In 1978 two papers by Stout (1978) and Stout and Teitelbaum (1978) advanced an argument for standard microscopic screening of bone as an error-check for other investigative techniques involving archaeological bone. After examining both cadaver and archaeological human bone using basic staining technology, polarizing light (Stout & Teitelbaum, 1978) and microradiography (Stout, 1978), the authors realised that post mortem alteration to bone could be not only extensive intracortically but also cause a general reduction in overall mineral density. Stout casts doubt over the efficacy of various histological aging techniques which rely on osteon integrity and also on photon-absorptiometry due to marked changes to mineral density.

An in-depth study, probably seminal, of post mortem alteration to human bone was undertaken by Hackett in 1981. His initial interest was to ascertain information on the survivability of pathological conditions

sufficient for histological analysis, and he conceived a four-tiered classification of post mortem change. Hackett believed that the micro-organisms responsible originated from the soil, initially scavenging on the decomposing soft tissues of the body, and later progressing to bone intracortically via the endosteal and periosteal aspects. Invasion of osteonal systems themselves was via Haversian canals, but Hackett saw no evidence that the "destructive foci" were influenced by osteocyte lacunae and associated canaliculae. Hackett considered that the micro-organisms, once within bone, fed on collagen via a process of systematic demineralisation. Mineral redeposition was noted as "cuffing" around smaller foci, the composition of which is considered to be reconstituted bone mineral. This process of demineralisation and remineralisation was considered by Hackett to be a seasonally episodic event, which was aided by the corresponding rise and fall of moisture levels within soil: "burials 100 years old might be expected to have experienced many major annual tides" (Hackett, 1981: 248). Hackett ruled out secondary feeding by one set of micro-organisms on another and proposed that foci, demineralised and remineralised by the same micro-organisms, enlarge in area with a consequent overall decrease in mineral density. Hence, the seasonal creep of water allows for various changes in mineral density as a driving co-factor to episodic attacks by the same micro-organisms. Once a bone is exhumed and allowed to dry out, the bone's micromorphology is considered by Hackett to be "fixed".

Hackett's classificatory system is considered in detail below:-

1. Wedl: named after Wedl's (1864) original description. In Hackett's study only 2 specimens exhibited this change, and so it was an infrequent

morphological type. Although Wedl's specimen was water-immersed and similar to tunnelling described by Marchiafava et al. (1974), the environmental history of Hackett's specimens was not well documented. The tunnelling had a uniform diameter of 5-10 microns and exhibited no remineralisation at the free edge. The distribution of the tunnelling was peripheral, spreading inwards from the periosteal and endosteal aspects of the cortices, and was unaffected by the cellular and collagenous network of bone. A fungus was considered responsible.

2. Linear longitudinal: this type of tunnelling had similar dimensions to Wedl ie. 5-10 microns, but occasionally formed "cuffed" rims. Hackett stated that microradiography showed the tunnels to be dark, and that these tunnels "stream" together in many longitudinal arrays, being limited only by cement lines. Occasionally, tunnels passed transversely across lamellae. In addition, when tunnels left the mid-zone of the cortex and approached the outer region, the morphology of post mortem change altered to large round dark foci, 30-50 microns in diameter, which were fibrillar with refractile rims. These foci were often concentrated within a single osteon. Hackett considered that bacteria were responsible.

3. Budded: "frond-like" tunnels followed osteonal canals and often filled them and were approximately 30 microns in diameter. Budded side shoots formed at irregular intervals and measured 80-90 microns across. This type of change was considered to be produced by episodic demineralisation and remineralisation events, which led to further episodes of demineralisation. Consequently, large amounts of mineral were removed, resulting in the formation of voids or empty tunnels. Again, this morphology was considered by Hackett to result from bacterial activity.

4. Lamellate: described as a "mosaic pattern or round jigsaw shapes". The

foci were usually rounded in shape and curved in transverse section, following the curvature of osteonal systems. They were often found near the surfaces of the cortices, localising around osteonal systems, occasionally crossing cement lines, and ranged in size from small foci of 10-20 microns and larger ones ranging between 60-250 microns. Within a single focus, lamellation was visible, suggesting that collagen may have survived in some form. Bony bars, usually of 3-5 microns, surrounded the circumference of each lamellate focus. This lamellate pattern was considered by Hackett to have the potential to survive for centuries, assuming that the focal destruction began soon after burial. Again, bacteria were considered the causal agent.

Hackett also undertook a small experimental investigation. He did obtain changes to bone within a year, but the experiment itself was uncontrolled and so was uninformative.

Sea water burial effects have been investigated by Arnaud et al. (1978) and by Ascenzi and Silverstrini (1984) and their studies are considered together here for simplicity. Both confirmed that human bone, both archaeological and recent, deposited in sea water may exhibit tunnelling features. Arnaud et al. examined archaeological material (900 AD) and found many peripherally invasive tunnels with diameters similar to Marchiafava et al. (1974). Ascenzi and Silverstrini undertook an experimental study immersing fresh bovine metatarsal cortical bone, without soft tissue, in sea water to an equivalent depth as the retrieved bone examined in the Arnaud et al. study. They found a variety of micro-organisms present in a complicated network of boring channels which had

diameters of 6-10 microns, and again similar to those induced by Marchiafava et al. (1974), although bacteria and algae were not considered directly involved. Instead, protozoans of the amoebic type were found to contain aggregations of bone crystals intracellularly when observed by transmission electron microscopy. The authors suggested that cells may initially cause solubilization of the hydroxyapatite, but could not explain the resultant take-up of hydroxyapatite crystals.

Work by Piepenbrink (1986) assessed post mortem change in archaeological human bone from two distinct environmental contexts. The 1986 study encompassed microbiology, x-ray diffraction and histology. In brief, Piepenbrink isolated four fungi from freshly excavated archaeological bone and subsequently re-innocolated them onto samples of histologically normal bone from the same specimens. The results were inconclusive as none of the innocolants produced any tunnelling, although *Stachybotrys cylindrospora* did produce a combination of non-identified antibiotics which fluoresced yellow green concentrically around Haversian canals. Histologically, Piepenbrink found varying degrees of Hackett's "lamellate" form of post mortem change and identified these areas as apatitic. Piepenbrink considered that soil micro-organisms, probably bacteria, were responsible for the lamellate change and that the mechanism of change began at the point of skeletonization within the soil. He cast doubt on the validity of techniques which detect organic components of the bone matrix and which do not employ checks for post mortem alteration. In his 1989 work he reported similar findings to those in the previous paper, but also observed a peripheral change of demineralisation concentrated as a discrete band around the periosteal aspect of two medieval bones (respectively sand and



gravel contexts). He also discovered a similar distribution of staining in bone inoculated with a fungus, *Cryosporium*.

In 1987 Piepenbrink and Schutkowski assessed the microscopical integrity of archaeological human bone from a dry desert context. The results from microradiography illustrated the many "micro-fissures" present as cracks which partially bisected osteonal systems and tracked along cement lines. Large crystals of calcite were identified within these cracks, alongside a significant decrease in phosphorus relative to calcium. The authors commented that light microscopy proved ineffective for histological analysis, microradiography being a more powerful method for highlighting structural changes and relative mineralisation states. A curious alteration in mineralisation was observed within lamellar groups where one lamella may be hyper or hypomineralised relative to another. The authors were unsure as to whether this change was an *in vivo* pathological condition or a post mortem alteration.

The presence of fluorescence as pathology was further postulated by several workers (Rothschild & Turnbull, 1987; Rothschild, 1988; Keith & Armelagos, 1988; Cook et al., 1989) all of whom observed concentrically fluorescing lamellar groups within osteonal and trabecular systems. As previously mentioned, Piepenbrink considered this type of fluorescence a diagenetic co-product of fungal activity, but this view has been disputed. Keith & Armelagos (1988) cited an example of *in vivo* tetracycline labelling within Sudanese Nubian skeletons (350-550AD), where a yellow green fluorescence was detected within cortical osteonal systems. This fluorescence was interpreted as a result of the therapeutic ingestion of tetracycline. The

authors point out that if this were a product of diagenesis, then the distribution of the fluorescence would only occur at sites of natural porosity ie Haversian canals and osteocyte lacunae, and this was not the case. Similar results were obtained by Cook et al. (1989) where the same distribution of yellow green fluorescence in Egyptian material (400-500 AD) was attributed to the ingestion of grain contaminated by a *Streptomyces*. Perhaps most controversial, and entertaining, was an argument which took place in Nature, over the apparent identification of syphilis in a Pleistocene bear using a fluorescing polyclonal antibody method (Rothschild & Bruce, 1987). Clearly incensed, Neiburger (1988) attacked the results stating that polyclonals are notoriously non-specific and the observed fluorescence was more likely to be some other pathological condition, or, nothing more than a post mortem artefact. Rothschild's (1988) retort accused Neiburger of having a poor understanding of pathology, little faith in the power of modern scientific techniques and less than no understanding of the durability of antigens over millions of years.

In further studies, Hanson and Buikstra (1987) and Garland (1987, 1988, 1989) made observations on the microscopical distribution of diagenetic change to bone microstructure. Interestingly, Hanson & Buikstra (1987) found that approximately 25% of 119 skeletons exhibited diagenetic change to microstructure. Of the femora and ribs examined, the ribs tended to be more profoundly affected and this was attributed to the greater porosity of ribs allowing more access to soil micro-organisms. The authors contended that the composition of the soil matrix, its microflora and its pH are important contributory factors to diagenetic change, even though their investigation was inconclusive in those regards. Garland's (ibid) work

employed standard stain technology in light microscopy to assess its usefulness in determining the internal microstructure of human bone. In terms of diagenetic change many of his observations confirm the work of previous authors such as Hackett (1981), and have added further information on the presence of iron compounds and fungal inclusions within the vascular and cellular spaces of bone.

An important study was undertaken in Japan by Yoshino et al. (1991) which investigated the speed of diagenetic change in human bone microstructure in three different environmental contexts. Fifty-one human bone samples of known date, ranging from 0-15 years post mortem, were used. Of this group, 33 were exposed, 14 buried in soil (depth not given) and 4 immersed in sea water (depth not given). Information on the preparation of bone samples is not provided. On retrieval, the samples were either embedded without fixation or dehydration for microradiography and SEM; or fixed, decalcified and embedded for TEM and UV fluorescence microscopy. Of the three environmental contexts, air, soil and marine, the bone from the air context was least affected by post mortem alteration to microstructure. Only one specimen, exposed for 15 years, exhibited a post mortem change which extended inwards from the subperiosteal aspect as a discrete band of demineralisation to an approximate depth of 200 microns. Inside this band was located a mass of micro-organisms. Of the soil-buried material, the first changes to microstructure were noted in one sample at 2.5 years, although changes generally began 5 years post mortem. This change consisted of foci of 5-10 microns in diameter which contained a "labyrinth-like" structure of smaller tubules of 0.5-1 micron in diameter. The thin boundaries between foci were composed of collagen fibrils, but within the

0.5-1 micron tubules the walls contained a combination of degenerative collagen fibrils and bacterial waste. Haversian canals were also observed to be packed with bacteria, although no lytic erosion was noted. In the marine specimens post mortem tubules were detected in samples left for 4-5 years. The distribution of this change was peripheral extending approximately 100 microns inwards from the subperiosteal aspect, penetrated by tubules ranging in diameter from 5-10 microns. These tubules were separated by thin walls of collagen fibrils, but contained none of the inner labyrinth-like smaller tubules of the soil specimens. Also, it was generally noted for all 3 environments that UV-fluorescence decreased linearly over the 15 year period. The authors conclude that soil and marine post mortem changes differ in type and morphology; and bacterial changes to bone cannot occur until the body has reached the point of skeletonization - considered here as 5 years - whereupon soil bacteria can gain access.

In 1993 Grupe et al. reported that they had experimentally demonstrated bacterial degradation of the protein/mineral bond of bone. Compact bone from pig and pine marten was "macerated" (the meaning of this is unclear), immersed in water and sterilised by irradiation. The bacterial inoculants were cultured at 4°C for 12 months, or at warmer optimum temperatures for 6 weeks. A strong brown stain was associated with one bacterial inoculant only, *Actinomadura madurae*, which had been cultured optimally for 6 weeks. Under transmitted light a dark staining was observed peripherally (similar to that previously reported by Yoshino et al. [1991]), extending from the periosteal aspect intracortically for a short distance. Under polarized light the same field exhibited a considerable loss of birefringence which

the authors equated with degradation of the protein/mineral bond. However, no tunnelling was observed in any of the experimental group.

Maat (1993) reported the extraordinary survival of fossilized red blood cells, sickle cells, fungal spores and bacterial cocci in human skeletal material (2200 BP) from Kuwait. The author ascribes the unusual survival of the blood cells to an extremely high evaporation rate of groundwater, which caused a substantial and constant ascending flow of groundwater in the desert conditions (the opposite of temperate and tropical conditions); and also to anoxic burial conditions. The latter reason is puzzling, since one would assume that ascending water from a freshwater lens would serve to oxygenate rather than deoxygenate the burial environment. However, the survival of blood cells alongside microbial spores, when all other tissues have been decomposed, serves to illustrate the complex nature of preservation and decomposition.

Hence, the findings of workers studying post mortem alteration to bone microstructure concur with those of the dental studies previously outlined. Post mortem alteration to bone is considered only to occur after skeletonization, when either aerobic, soil, lacustrine or marine micro-organisms can gain access. Given the variation in skeletonization rates (Galloway et al., 1989), time is subsequently thought to be the least important co-factor involved in post mortem change. Post mortem alteration to bone has also been shown to be extensive and exhibit the same morphological types of change as those observed in teeth. Again, diagenesis is a term which has become synonymous with this type of microstructural change.

### 1.5 Terrestrial and marine decomposition

This section is not intended to be an exhaustive appraisal of the literature concerning the decomposition process, but is instead a concise synthesis of work relevant to bacterial degradation. To this end the differences between terrestrial and marine decomposition are generalised, with particular regard to putrefaction and blood lividity.

After death the decomposition of a body will progress through several stages prior to skeletonization. These stages are represented in Table 1.1 for terrestrial and water contexts (Simpson & Knight, 1985). Putrefaction has been defined as the:-

"...gradual dissolution of the tissues into gases, liquids and salts. This transformation is caused mainly by proteolytic and other enzymes produced by bacteria." (Gordon et al., 1988: 43).

Putrefaction is initially mediated by the body's own indigenous microflora and this can be seen to manifest itself as "marbling" of the skin within 2-3 days after death. This marbling appears as a green discolouration of the flanks and abdomen and progresses to the superficial branching veins of the chest, neck and groin appearing red in colour (Simpson & Knight, 1985).

This effect is caused by the translocation of anaerobic gas-forming bacteria from the small intestine into the entire vascular system via the portal vein, where the blood is initially haemolysed (causing red colouration) with the subsequent evolution of S-methaemoglobin (which is green). The speed of this translocation may vary, but an experimental in-vitro system demonstrated intestinal translocation within 15 hours post mortem (Kellerman et al., 1976). Eventually the vasculature ruptures as a result of this bacterial activity, and can as a consequence involve

Table 1.1

**STAGES OF DECOMPOSITION FOR LAND AND WATER**

Period	Land	Water
Hours	<i>Cooling</i>	
0-12	1°C (approx) per hour	1.5°C (average) per hour
12-24	0.5°C (approx) per hour	0.75°C (average) per hour
10-12	Body <i>feels</i> cold	At 5-6 hours, body <i>feels</i> cold
20-24	Body <i>is</i> cold	At 8-10 hours body <i>is</i> cold
Hours	<i>Lividity</i>	
3-5	<i>Post mortem</i> lividity developing	Cutis anserina and whitening of skin No lividity until at rest
Hours	<i>Chemical changes</i>	
12-72	Vitreous humour <i>Kries</i> steadily	Slight retardation only
Hours	<i>Rigor mortis</i>	
5-7	Rigor appearing in face, jaw and neck muscles	Onset delayed by cold and often lasting longer
7-9	Spread to arms and trunk, and reaching legs	
12-18	Rigor fully established	
24-36	Rigor passing away in same order	Rigor may still be present Skin markedly wrinkled in hands and feet sodden Rigor passing off 2-4 days
Days	<i>Putrefaction</i>	
2	Green staining in flanks	
2-3	Green and purple staining over abdomen and some distension.	
3-4	Marbling of veins. Further spread of stains into neck and limbs	Discoloration at root of neck
5-6	Gaseous swelling and distruption internally. Skin blebs	Neck and face discoloured and swollen. Body floats 5-8 days (period halved in hot weather)
Weeks		
2	Abdomen distended to tight tension. Swelling of body marked, and blebbing with purple transudate widespread. All organs disrupted by gas	Decomposition well established in trunk but little distension Cutis peeling and hair loosening easily pulled out Nails pulled out with difficulty
3	Vesicles bursting and tissues softening and disrupting. Eyes bulging. Organs and cavities bursting. Disfiguration to extreme	Face bloated. Eyes and tongue protruding
4	General slimy liquefaction and disruption of all soft tissues	Body greatly swollen with gases and organs crepitant Hair easily wiped away Nails (fingers easily, toes less easily) pulled away Casts of hands and feet separating
Months	<i>Adipocere</i> (if conditions suitable)	
4-5	Adipocere of face, head and breasts	Slightly slower adipocere development in proportion to lower temperature
	Adipocere of arms, legs and internally	

Table adapted from Simpson and Knight (1985)

exogenous bacteria in internal body decomposition (Gordon et al, 1988; Simpson & Knight, 1985).

It is a common misconception that blood immediately clots after death. The reverse is true and in most cases it remains permanently incoagulable (Gordon et al., 1988). This phenomenon is known as post mortem lividity and causes blood to leak from capillaries into the body creating bluish areas, which appear similar to bruising. The blood remains liquid due to the release of fibrinolysin (inhibits the clotting action of fibrin) from small calibre vessels within 30-60 minutes after death (Gordon et al., 1988), and this must facilitate the transmigration of motile bacteria throughout the vasculature. Indeed, bacteria can also produce fibrinolysin as a kinase, known as plasmin, and this additionally will contribute to post mortem blood liquidity. During the 1930's a Russian worker called Yudin (1936) made use of the post mortem liquidity of blood and transfused cadaver blood to living patients. He reported that he lost only 7 patients out of a total 1000 through bacterially contaminated blood! This practice continued for 30 years and was only picked up latterly by American workers in the 1960's when a report from Kevorkian and Bylsma (1961) described undertaking 4 successful transfusions of cadaver blood. This practice ceased on the creation of the live donor scheme for blood collection.

The given order of decomposition of the internal organs including the circulatory system varies according to author. Simpson and Knight (1985) stated that the intestines, stomach, liver blood, heart blood and circulation, and heart muscle are first to decompose, followed by lungs, liver, brain and spinal cord, kidneys, bladder and testis, voluntary



muscles, uterus and prostate. However, Gordon et al. (1988) reported that the eyeballs liquify first, that the heart muscle is not immediately decomposed and that the capsules of the liver, spleen and kidneys resist putrefaction the longest.

The speed at which the decay process proceeds largely depends upon the temperature of the body after death. In a temperate climate, a fully clothed body will cool to match the external environment within 18-24 hours and will match the process of decomposition out-lined in Table 1.1 (Simpson & Knight, 1985). For an unclothed body, or a body which is buried, or a body which has been submersed in cold water, cooling is much faster so that bacterial growth is slowed. If a body is stored below 4°C, bacterial growth is fully inhibited. Dehydration prior to death can also inhibit decomposition, since water is an important prerequisite for bacterial growth. Conversely, extreme humidity will cause rapid decomposition, whilst extreme aridity will cause rapid drying and hence mummification (Gordon et al., 1988; Micozzi, 1991). If the body has suffered traumatic damage to vasculature and/or the soft tissues, either ante or post mortem, then the progress of decomposition may be faster, due to predation by external microfauna and megafauna (Lyman, 1994; Gordon et al., 1988; Smith, 1986; Simpson & Knight, 1985).

The putrefaction of a body which is immersed in water is slower than terrestrial putrefaction, partly because the body will cool much faster, unless the water is warm or sewage infested. The body will float face downwards and oxygenated blood gravitates towards the head and neck region. After 6 days bacterial decomposition will be concentrated in the

head and neck and by 10 days the skin will have become sodden and begun to peel away. After 4 weeks have elapsed the body starts to disarticulate (Simpson & Knight, 1985). Gordon et al. (1988) state that stagnant water, or water with slow movement, will increase the speed of decomposition.

Clearly, the rate of decomposition is highly variable depending on body status and the depositing environment, and as a consequence, skeletonization is enhanced or delayed accordingly (Galloway et al., 1989). Previous work has consistently implicated bacteria and fungi as causal agents of microstructural change to the skeletal tissues. The micro-organisms responsible have been assumed to be exogenous in origin, gaining access at a point near or after skeletonization. However, this section has served to illustrate that indigenous bacteria are known to migrate to all parts of the body, including the skeleton (Haines & Scott, 1940; Ingram, 1952), very early on in the decay process, and as a result, need to be taken into account.

#### **1.6 Ante mortem microbial changes to the skeleton.**

It has been reported that a single human body acts as host to more micro-organisms than there are people on the planet (Andrews, 1978). In healthy individuals the bulk of this constituent microflora inhabits the skin, the mouth and gastro-intestinal tract, the respiratory tract and genito-urinary tract. However, under certain conditions, micro-organisms - particularly bacteria - can invade any body system, including the bones and joints, causing a range of pathological conditions (Duerden et al., 1993). This invasion is usually acute, although chronic conditions such as gastric ulcers can be caused by a single bacterium taking-up permanent residence

e.g. *Helicobacter pylori* on the gastric mucosa. Only bacterial activity in the mouth, which localises on teeth and surrounding soft tissues, can cause microstructural change to the skeleton, in the form of tooth caries. In all other pathological situations involving a bacterial insult to the bony skeletal tissues, the inflammatory response will always involve either bone formation and/or bone resorption.

Tooth caries is a pathology caused by bacteria which can effect the microstructure of enamel, dentine and cementum. The mechanism of change to microstructure is caused by the combined actions of bacterially produced organic acids, proteolytic enzymes and chelative agents. The attack is thought to be mediated by a consortia of bacteria which attach themselves to an organic film covering the enamel called the acquired pellicle (Newman & Poole, 1974). Coccal bacterial forms appear to colonize the tooth surface first, followed by filamentous forms. This build-up of bacteria and other interbacterial matrix is called plaque and begins to mineralise to become calculus. Phasic layering has been identified in calculus indicating time-related incremental growth (Jones, 1987). The internal micromorphology of calculus replicates bacterial forms and has been identified in archaeological material (Dobney & Brothwell, 1988). Carious microstructural changes to enamel are caused by demineralisation of mineral (of which enamel is almost entirely composed), which causes a net loss of mineral and so density (Jones & Boyde, 1987; Williams & Elliott, 1979). The lesions appear to funnel pulpally and the central body of the lesion may become micro-cavitated. Remineralisation of the surface aspect of the lesion can occur due to the supersaturation of saliva with calcium and deposition of caries crystals. Root caries involves the cementum and

dentine and comprises a combination of demineralisation and collagenous degradation. The microstructural appearance is one of localised diffuse demineralisation of the cementum and with similar changes to dentine. Jones & Boyde (1987) reported observing a striking reduction in density of dentine, due to carious insult, which tracked at right angles to dentine tubule direction i.e. following and emphasizing the incremental plane and dentine tubule branching. Once this type of root damage has occurred, no natural restoration of the dentine is possible, although secondary dentine may form on the pulpal aspect. Hence, any carious damage caused to enamel, or dentine or cementum will remain permanently and will therefore be the only ante mortem site of bacterially driven microstructural degradation of the skeletal tissues which can be observed post mortem.

#### **1.7 Aims of this study**

The central aim of this dissertation is to assess the microstructural impact of diagenetic or post mortem change to predominately human skeletal tissues. The method of assessment will be microscopical, utilizing scanning electron microscopy in backscattered electron mode and, to a lesser extent, confocal reflection microscopy. The intention is to characterize the microstructural morphologies of post mortem alteration in archaeological material, both normal and pathological, from terrestrial and marine contexts. Further studies will then be undertaken on a case-by-case basis on archaeological and forensic specimens which offer some unique pathology, environmental context, spatial relationship, time variable, body status, or mortuary practice, in order to understand what processes have led to any observed change to skeletal microstructure. Additionally, the effect of diagenetic change to skeletal microstructure on DNA recovery will

also be assessed, and favoured locations for the retention of DNA within the skeletal tissues identified. Quantitation of mineralisation density will be undertaken to assess the effects of diagenetic change to bone mineral.

## CHAPTER 2: THE MORPHOLOGY OF DIAGENETIC CHANGE IN HUMAN BONE AND TEETH

### 2.1 PART I: Soil-buried contexts

#### 2.2 Introduction

This chapter is divided into two parts and sets out to establish the usefulness of backscattered electron (BSE) imaging in a scanning electron microscope (SEM) for the characterisation of diagenetic change to archaeological human bone and teeth from terrestrial and marine contexts.

#### 2.3 Diagenetic morphology in archaeological normal and pathological human bone

This study was undertaken to consider the morphological effects of diagenesis on normal and pathological archaeological bone with particular regard to any relative density variations found intracortically. SEM/BSE imaging has been little applied to bones and teeth in the study of archaeological materials. To date most work in the archaeological field has been concerned with the atomic number (Z) composition of metals, ceramics and glassware (Meeks, 1988), even though scanning electron microscopy has been utilised extensively to study surfaces on many different types of archaeological material (see Olsen, 1988). Dobney & Brothwell (1988) applied the same technique to the structure of dental calculus in archaeological samples. Other workers have employed the technique in wider studies and, in particular, to tooth enamel structure during primate evolution (Martin et al., 1988). BSE imaging is a method already utilized in basic medical research to illustrate density changes within bone and it has allowed the study of mineralisation during growth and bone turnover and of impaired mineralisation in certain pathological conditions such as Paget's

disease, fluorosis, osteomalacia and osteogenesis imperfecta (Boyde et al., 1986). BSE imaging was considered to be an entirely appropriate method to adopt for this archaeological bone study.

#### 2.4 Material and methodology

The skeletal material used in this study was adult human femora and tibiae taken from archaeological and modern sources. The archaeological material was taken from soil-buried medieval contexts and was adult but of unknown age and sex. One sample consisted of presumed normal bone in that it had no obvious gross pathology and was taken from a macroscopically well preserved skeleton. The remaining archaeological bone examined was considered pathological, it being affected by the non-specific condition of 'periostitis', and was drawn from a miscellaneous group of bone. Two specimens were examined from this latter group: the first (specimen 1), an adult femur, macroscopically and on X-ray presented with slight striations of new bone distributed anteriorly and posteriorly along the femoral shaft; the second specimen (specimen 2), an adult tibia, showed extensive subperiosteal changes to the entire shaft and in complete longitudinal section showed that the entire medullary cavity had become infilled with bone so that no trabeculae were evident. The absence of the medullary cavity had not been clear from the x-ray, instead the medullary area appeared undefined and irregularly radiodense. The modern material was adult but of unknown age and sex. It had been prepared after Tompsett (1970), and had been used as a laboratory specimen for several years. This specimen was considered normal in that it had no obvious gross pathology and had been provided as normal/non-pathological bone.



Mid-shaft transverse and longitudinal sections, 10mm<sup>2</sup>, were taken from the femora and similarly from the mid-shaft medial and lateral aspects of the tibiae. The sections were cut using a wet diamond-edged circular saw and then allowed to air-dry. They were then placed into reflux columns containing 50:50 chloroform and methanol to remove any residual water present through natural humidity within the bone. Ordinarily, reflux is used to remove any fatty material and water present in fresh specimens (see Boyde et al, 1986). Whilst this procedure is not necessarily required for deproteinized or anorganic specimens - vacuum embedding being a perfectly adequate alternative - it was done so that the results could, if necessary, be compared with fresh material. Reflux continued for two weeks. The sections were then removed and put through three changes of liquid polymethylmethacrylate (PMMA) every 24 hours and subsequently placed in an oven set at 32°C until the PMMA solidified. The methylmethacrylate had been prepared by the 'flash distil' method outlined by Boyde et al. (1986) which prevents bubbling in the methacrylate. Latterly specimens were embedded in methacrylate which had been distilled after Howell & Boyde (1994). The embedded specimens were polished using graded abrasives and finished with a water-dispersed 1 micron diamond abrasive on a rotary lap. Each block was mounted individually on an aluminium stub and the block face received a sputter coating of silver or carbon to render it electrically conductive and therefore suitable for SEM study in the backscattered electron imaging mode.

The specimens were examined using a Cambridge Stereoscan S4-10 SEM, operated in BSE mode, working at 20 kV beam voltage and about 10 amps probe current. The BSE flat section images were created using a solid state BSE detector in a four-



segmented ring configuration and the topographical images were obtained by subtracting the east and south quadrants simultaneously from the north and west. Topographical images were necessary for the identification of bubbles, holes, edges or scratches which may have contributed to the overall signal artefactually by altering the escape volume and hence trajectories of backscattered electrons (Howell & Boyde, 1994). The images of flat sections gave qualitative relative assessments of density changes within the specimen alongside any morphological changes. Such changes in density appear as a density map composed of dark areas which are less dense and light areas which are relatively more dense. This density dependence is the result of backscattered high energy electrons, which have an approximate escape depth of 1 micron, being released from the specimen so that backscattering increases steeply with increasing Z values. Hence, any local variations in Z composition within the specimen will give variations in intensity and so image, due to modulations in the BSE signal (Boyde et al., 1983, 1986; Watt, 1985).

## **2.5 Results and discussion**

All the prepared archaeological specimens, both normal and pathological, showed dramatic diagenetic change. In all specimens, the extensive changes had removed, changed or obscured the characteristic morphology and density associated with adult human bone. Such changes therefore placed limitations on the interpretation of any pathological conditions present within the specimens but at the same time offered the chance to investigate the morphological and density variations present during the little understood process of diagenesis.

## **Normal modern and archaeological bone**

### **Circumferential lamellae: subperiosteal bone**

The results from the specimens, both modern and archaeological, support the view expressed by Garland (1987) that macroscopic studies of the subperiosteal surface of bone to determine preservation and any pathological change is, on its own, a very uncertain practice. Macroscopic study relies upon the basic premise that the circumferential lamellae of the subperiosteal bone [Fig. 2.1a & b] survive the burial environment. However, even in the modern bone, the circumferential lamellae of the subperiosteal region was found to have been extensively removed [Fig. 2.1c & d], whereas the general osteonal architecture remained intact, although some cracks were present [Fig. 2.1e & f]. This irregular removal of the superficial bone, which had cleaved along natural fracture planes, could be differentiated from a surface produced by osteoclastic resorptive activity (as seen preserved in the reversal line in [Fig. 2.1a & b]), since this type of surface would be characterised by a scalloped profile passing through and across secondary osteonal bone, quite irrespective of any natural cleavage planes. This post mortem removal of the superficial bone was not detectable to the naked eye and must have occurred simply by students handling the specimen over the years. Not surprisingly, some of the archaeological specimens examined exhibited similar destructive removal of the circumferential lamellae [Fig. 2.2a & b]. When the lamellae could be seen, the bone had usually undergone extensive diagenetic change in the form of localised areas or foci of decreased or increased density [Fig. 2.2a & b].

### **Cortical bone: osteonal region**

The qualitative morphology of the normal archaeological transverse sections exhibited a similar pattern throughout the bone examined. The diagenetic changes were extensive [Figs. 2.2 - 2.3b]; only in the most central area of the cortex was there evidence of much bone being retained [Fig. 2.3b]. Areas of changed density compared with the density of bone in the same field, were present as discrete, irregularly shaped regions having dimensions of between 20 and 150 microns. These presumably represented recrystallization where bone mineral would have been removed and then mineral redeposited in the same bone matrix. Alternatively (or additionally) crystals may have formed in altered organic material and/or even extended into areas where no matrix remained at all. Areas of markedly decreased density, with similar dimensions, also occurred in all samples. Thus, two extremes of diagenetic change were noted in the BSE images: areas of bone which appeared uniformly very dense and areas from which the mineral seemed to have completely dissolved to create an appearance of holes in the matrix. However, the specimens also exhibited areas of intermediate density between these two extremes. The borders of the altered regions were always clearly defined and of greater density than the surrounding, apparently unaffected, bone. The borders were continuous and enclosed regions which were often of lower density, giving the appearance of encapsulation. Within the altered region, the general density varied from that of the intervening bone, and was not uniform within any one region. Two main textural patterns were evident: holes of approximately 2-3 microns in diameter, and a finer texture which represented the fibrous component of the bone. It was notable on the topographic images [Fig. 2.2b & d] that the most continuously dense altered

regions were proud of the apparently unaffected bone, and this was proud of the zones of diagenesis which were not uniform in density, having been abraded more in polishing. Regions which were of negligible or very low density in the BSE images were most heavily abraded but mostly showed some texture. This whole arena of varying density was interpreted as diagenesis in progress, proceeding at rates defined by the numerous factors which contribute to promote diagenesis.

The artefact of cracking was noted in both modern [Fig. 2.1e & f] and archaeological specimens [Fig. 2.2c & d]. This cracking could have occurred during diagenesis. Additionally, the cracking might have resulted in part from the preparation procedure of the specimens, presumably at the stage of reflux or solidification of the PMMA when shrinkage and expansion could have occurred. The cracks have presumably followed points of natural cleavage within the specimen. It was often noted that the cracks partly encircled single osteons, suggesting that notwithstanding extensive diagenetic change locally within and around the osteons, original fracture planes could be retained [Fig. 2.2c & d]. The archaeological specimens also exhibited cracking which appeared to track from and through the foci of changed density [Fig. 2.3a & b]. These cracks crossed morphologically identifiable areas of secondary osteonal systems, as well as cracking for some distance through islands or foci of recrystallization. Also much smaller cracks were noted within actual foci of recrystallization, often bisecting such features either totally or in part, remaining entirely within the feature or extending beyond it for just a short distance. It would therefore appear that the artefact of cracking shows two important features: firstly, that natural fracture planes can be retained and may play a role in the orientation of

the diagenetic process, giving rise to Hackett's "lamellate" structure (Hackett, 1981); and secondly, the foci of changed density have not only orientated planes of weakness within themselves, but also aided cleavage across areas of morphologically identifiable bone, appearing to ignore natural or ante mortem fracture or cleavage planes. Osteocyte lacunae were also noted to be connected to one another by post mortem cracking, or to be completely bisected by such a crack.

Structurally recognisable but not necessarily unchanged bone could be seen amongst a complicated array of obvious diagenetic change in the archaeological bone. Osteonal systems within the cortex could be clearly observed, as could osteonal and interstitial lamellae, osteocyte lacunae and canaliculae. However, even where bone tissue was identifiable, areas of localised changes in morphology and density were invariably present, even within one osteonal system [Fig. 2.3b]. The central regions of mid-cortical bone were best preserved, whilst the subperiosteal and endosteal aspects were found to be poorly preserved with extensive fields almost entirely affected by diagenesis. The importance of the osteonal canals in the initial spread of diagenetic change was clearly evident in those regions where most of the original bone structure remained [Fig. 2.3b]. The bone trabeculae of the medullary region often retained good morphological detail, displaying lamellar structure, areas of remodelling, osteocyte lacunae and canaliculae [Fig. 2.3a]. This potential for preservation may be due to the protected location within the medulla; if so, it is perplexing that the endosteal aspect of the cortex undergoes such dramatic diagenetic change by comparison.

This study does not address directly the problem of the diagenetic changes that occur in the organic matrix of the bone. Where structurally recognisable bone was retained, it was the fibrous component that was evident, although mineralised cement lines round osteonal systems were also sometimes present [Fig. 2.3b]. It is probable that, during demineralisation, the mineral-protected collagenous component is more resistant to disruption than the non-collagenous protein phase. Where this is less well preserved its loss might provide a track for the primary stages of diagenesis to extend along the collagen planes.

Longitudinal sections, taken from the transverse mid-shaft specimens, showed similar features of extensive diagenetic change with small areas of bone preserved. Regions of changed density which were curvilinear in transverse sections now appeared elongated as though following the lamellae of the osteonal systems [Fig. 2.2e & f]. These elongations extended approximately 200 microns in the plane of the polished longitudinal facet and are highly suggestive of demineralization and recrystallization tracking in three dimensions along the fibrous structural organization of both the osteons and the circumferential lamellae at the subperiosteal surface. This extension and eventual conjoining is presumably aided by the highly porous network of spaces within bone produced by osteonal canals, osteocyte lacunae and interconnecting canaliculae, and the natural boundary planes.

#### **Pathological archaeological bone**

The pathological sections [Figs. 2.3c - 2.5d] support in general the previous observations made in the non-pathological material. The subperiosteal

circumferential lamellar bone was almost invariably absent [Fig. 2.4e], but where present, its lamellae were often preserved [Fig. 2.3e]. Diagenesis was frequently extensive [Fig. 2.3c], particularly in peripheral regions of the cortex, the altered regions having similar size and distribution to those observed in the non-pathological material. The artefact of cracking intracortically was also seen to track along natural and non-natural fracture planes.

The specimen which macroscopically presented with slight striations of periostitis (pathological specimen 1) was investigated to advantage by the BSE imaging technique [Figs. 2.3d - 2.4b]. Primary osteonal bone was clearly seen extending as a branching band partly enclosing vascular spaces which ran longitudinally. The new bone had undergone extensive diagenesis with recrystallization [Fig. 2.4a & b]. However, and perhaps suprisingly, the pathological periostitic, or primary osteonal bone, which is friable on archaeological specimens, had been preserved to its subperiosteal limit, together with a small field of osteoclastic activity [Fig. 2.3d & f]. This is in contrast with the non-pathological specimens which, although apparently robust, had lost most of their subperiosteal circumferential lamellae.

Information on the relationship of diagenesis to bone structure was obtained from intracortical locations in both pathological specimens (specimen 1: Figs. 2.3c - 2.4d; specimen 2: Figs. 2.4e - 2.5d). It was noted in transverse sections of the more pronounced periostitic/osteitic specimen (specimen 2) that obvious diagenetic change seemed to be located preferentially in the lamellar bone close to the vascular canals [Fig. 2.5c & d]. As with the non-pathological bone, it is

difficult not to envisage the canals and osteocyte lacunae offering the primary route for diagenesis to begin and thereby extend deeper into the surrounding bone. Figures 2.4f - 2.5d show this process clearly: firstly the creation of demineralised zones; and secondly, infilling with an unidentified crystalline material. Figures 2.4d and 2.5a show an osteocyte lacuna situated within these foci of recrystallization in which the lamellar or fibrous organisation is still evident. The foci of increased density do not always appear to be centred on osteocyte lacunae. However, this does not necessarily mean that osteocyte lacunae are only accidentally included in areas of recrystallization and thereby play no part in initiating diagenetic change. Many of the smaller lesions do have osteocyte lacunae present and their frequency plus the distribution of early lesions with increased density is very similar to that of the osteocyte lacunae.

It was also noted in the more pronounced periostitic specimen (specimen 2), which had its medullary cavity infilled with bone, that an interesting comparison could be made with the observed diagenetic changes noted on those archaeological specimens with a medullary cavity. In the archaeological specimens which had an endosteal aspect, extensive diagenesis was noted both at this aspect and subperiosteally. These changes extended intracortically leaving more morphologically identifiable bone present in the most central area of the cortex. In contrast, the pathological specimen (specimen 2) which had no endosteal aspect due to the infilling of the medulla with bone, exhibited no such changes at its most inner aspect - that is the mid-point of the once present medulla. This was the region least affected by diagenesis. However, extensive diagenetic changes were well represented in its subperiosteal region, corresponding with previous



observations on the archaeological specimens (both non-pathological and pathological). Therefore, where the endosteal aspect did not exist (specimen 2), the extensive effects of diagenesis had not occurred. This suggested that the highly porous nature of the medullary cavity in non-pathological and pathological archaeological bone contributed positively towards the extensive diagenetic changes noted.

A point counting technique was used to quantify this phenomenon. A systemic scheme was preferred as diagenesis has been considered from previous observations in this study to be a non-random process of events. A small x60 SEM/BSE montage was created from an unembedded transverse section of the pronounced periostitic specimen (specimen 2) with a field width of 1880 microns, extending from its subperiosteal aspect to the bone-infilled approximate mid-point of the once present medulla. A grid containing 11 x 11 intersections, each with an approximate interval of 115 microns, was used to systemically sample the central area of the entire montage counting bone to non-bone (counts falling within vascular spaces were recorded but excluded from the non-bone totals). This provided a total of 8 counting grids. From the results of a correlation carried out on the number of intersections falling on bone to non-bone, it was found that a significant negative association existed between the two variables ( $\rho = -0.976$ ,  $N = 8$ ). Therefore, at the subperiosteal aspect one finds more non-bone, decreasing in sampled frequency with a strong negative gradient, as one approaches the bone infilled mid-point of the medulla. No gradient was present in the distribution of vascular spaces which represented 9.7 % of the total number of grid intersections.

## **CAPTIONS**

**Figure 2.1**

2.1a Bone from cranial vault 10 yr girl. Relatively younger bone can be seen centre field relative to older interstitial areas of bone which appear darker. SEM/BSE, PMMA-embedded bone. Field width 855 microns.

2.1b Topographic image of same field as Fig. 2.1a, using BSE detector with E and W quadrants subtracted. Polishing artefacts due to hardness and collagen orientation variation are evident and would contribute to the density image. Field width 855 microns.

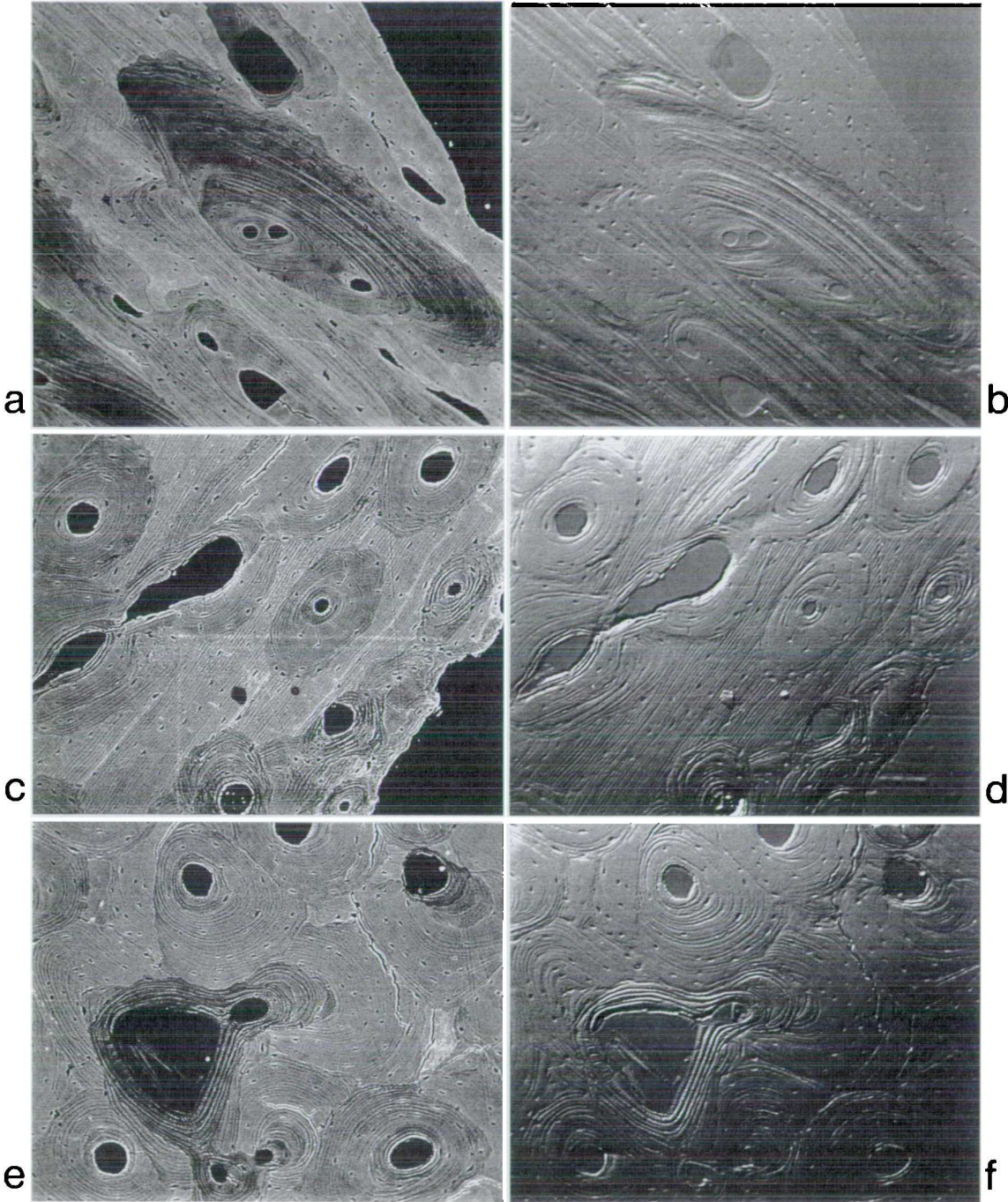
2.1c Transverse section (TS) lateral modern midshaft tibia showing clearly the loss of the subperiosteal circumferential lamellae. This removal is distinct from osteoclastic action as it follows the natural cleavage planes. The dark spots (centre left field) are dust particles in specimen surface. SEM/BSE, PMMA-embedded bone. Field width 690 microns.

2.1d Topographical image of same field as Fig. 2.1c showing the removal of the subperiosteal lamellae follows clearly the natural cleavage planes provided by the bone. Field width 690 microns.

2.1e TS lateral midshaft modern tibia. Mineral density variation associated with secondary osteonal remodelling is comparable to that resulting from normal bone turnover. Note the cracking which follows the natural cleavage planes within the specimen. SEM/BSE, PMMA-embedded bone. Field width 930 microns.

2.1f Topographical image of same field as Fig. 2.1e showing varying topography created by polishing PMMA-embedded section of bone with the secondary remodelling of normal bone turnover. Note the increased topography in the less well mineralized bone: this reflects the different collagen fibre orientations and contributes to the BSE image. Field widthFW 930 microns.

Figure 2.1



**CAPTIONS**

## Figure 2.2

2.2a TS of lateral midshaft archaeological tibia. A small region of the subperiosteal lamellae was preserved intact with osteocyte lacunae morphologically identifiable. Extensive diagenetic change is present in the form of increased and decreased density. SEM/BSE, PMMA-embedded bone. Field width 145 microns.

2.2b Topographical image of same field as Fig. 2.2a. The relative topography associated with extensive diagenetic change results from lesions of increased density standing proud of the apparently unaffected bone and areas of reduced or mixed density which appear as depressions in the overall matrix. The full interpretation of Fig. 2.2a cannot be made without the topographic information. Field width 145 microns.

2.2c TS of lateral midshaft archaeological tibia. A single osteon is enclosed and surrounded by extensive diagenetic change. An original cleavage plane has been preserved and can be seen partially encircling the osteon. The diagenetic foci are curved following the lamellae of the osteon. SEM/BSE, PMMA-embedded bone. Field width 185 microns.

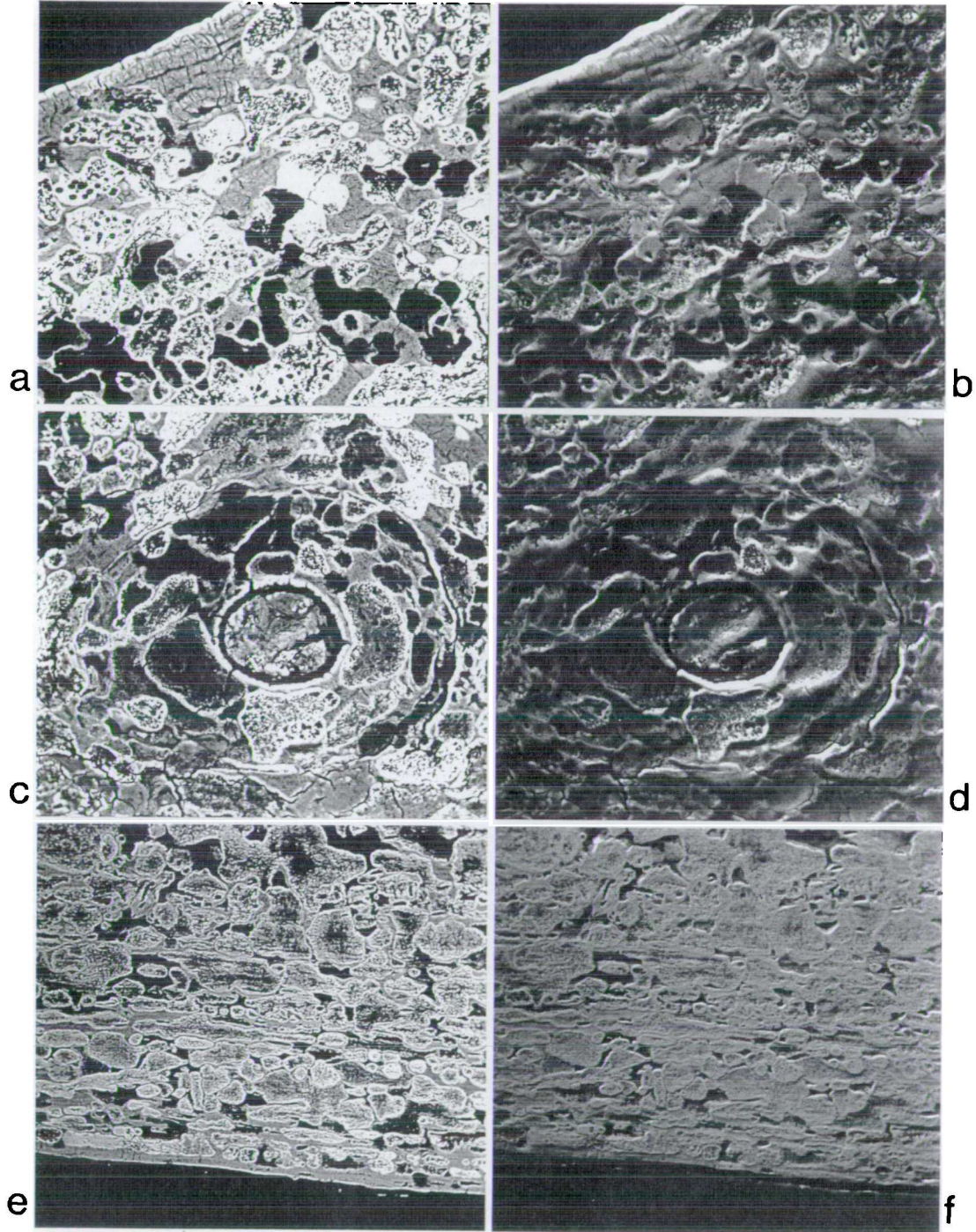
2.2d Topographical image of the same field as Fig. 2.2c. Cracks partially encircle and cross a single osteon. The osteon had undergone extensive diagenetic change which is curvilinear or "lamellate" in shape. Note the raised rim surrounding diagenetic foci, indicating peripheral increased density. Field width 185 microns.

2.2e Longitudinal section (LS) of anterior midshaft archaeological femur. There is extensive diagenetic change with elongation of some areas of changed density, which had been curvilinear in transverse section. Such elongations are considered to follow the lamellae of osteonal systems. SEM/BSE, PMMA-embedded bone. Field width 325 microns.

2.2f Topographical image of the same field as Fig. 2.2e. The outermost circumferential lamellae appear intact but generally the field is one of extensive diagenesis. Elongations of some of the focal lesions can be seen and most appear to follow the lamellae of the osteonal systems. Field width 325 microns.



Figure 2.2



## **CAPTIONS**

.



### Figure 2.3

2.3a LS of anterior midshaft archaeological femur. The trabecular bone is relatively well preserved with only small foci of changed density. Some cracking is evident within the central area of changed density which has been partially bisected. SEM/BSE, PMMA-embedded bone. Field width 315 microns.

2.3b TS of medial midshaft archaeological tibia, showing a field from the most central area of the cortex with improved bone survival. The focal changes of diagenesis are located preferentially around osteonal canals. Cracks are present crossing natural cleavage planes to bisect foci of changed density for some distance. SEM/BSE, PMMA-embedded bone. Field width 620 microns.

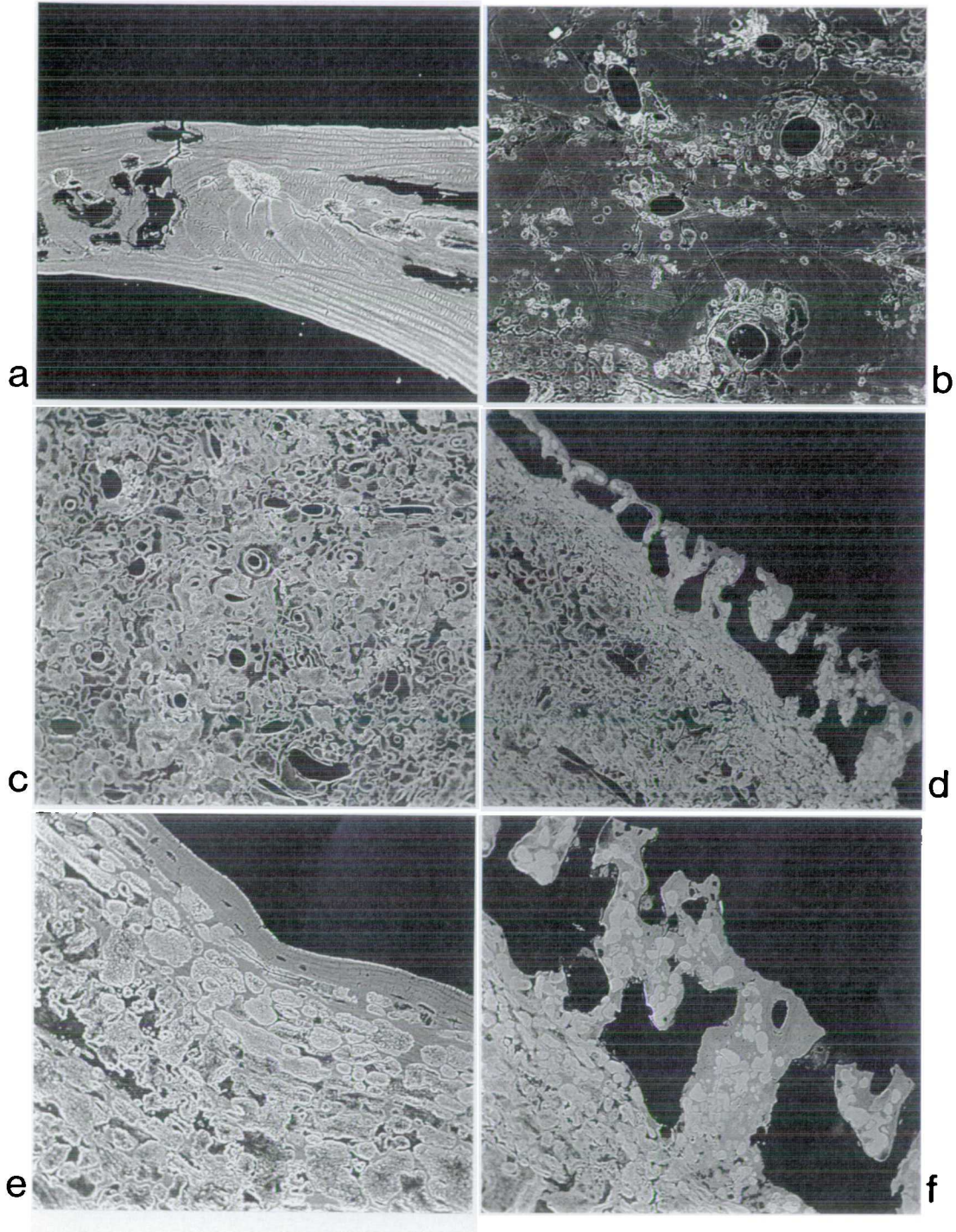
2.3c Pathological (specimen 1) archaeological bone. TS midshaft femur, shows extensive diagenesis toward the endosteal aspect of the cortex. Hardly any identifiable bone is evident. SEM/BSE, PMMA-embedded bone. Field width 1200 microns.

2.3d Pathological (specimen 1) archaeological bone. TS anterior midshaft femur. Primary osteonal bone extending as a branching band, partly enclosing vascular spaces which ran longitudinally, has survived at the subperiosteal limit although diagenetic changes are extensive. SEM/BSE, PMMA-embedded bone. Field width 1200 microns.

2.3e Pathological (specimen 1) archaeological bone. LS anterior midshaft femur; subperiosteal surface taken from the same specimen as Fig. 2.3d, in the region of macroscopic pathology. This does not have primary osteons at the surface, which is still intact. SEM/BSE, PMMA-embedded bone. Field width 300 microns.

2.3f Pathological (specimen 1) archaeological bone. TS anterior midshaft femur. Osteoclastic activity is evident (centre field) as a scalloped resorptive border to the primary osteonal bone. Diagenetic foci have extended well into this new bone. SEM/BSE, PMMA-embedded bone. Field width 300 microns.

Figure 2.3



## **CAPTIONS**

.

#### Figure 2.4

2.4a Pathological (specimen 1) archaeological bone. TS anterior midshaft femur, showing survival of bone with at its subperiosteal limit. Note the irregularly shaped and larger osteocyte lacunae of rapidly formed bone. Diagenesis in this area is generally of increased density. SEM/BSE, PMMA-embedded bone. Field width 300 microns.

2.4b Topographical image of the same field as Fig. 2.4a, showing raised areas in the polished surface associated with the extensive increase in overall relative density to bone. (Two bubbles can be seen in the PMMA.) Field width 300 microns.

2.4c Pathological (specimen 2) archaeological bone. TS apical/anterior midshaft tibia. There is considerable survival of bone endosteally with visible cement lines, osteocyte lacunae and osteonal lamellae. Focal lesions are situated within and bridging osteonal systems and some are partially bisected by cracks. SEM/BSE, PMMA-embedded bone. Field width 300 microns.

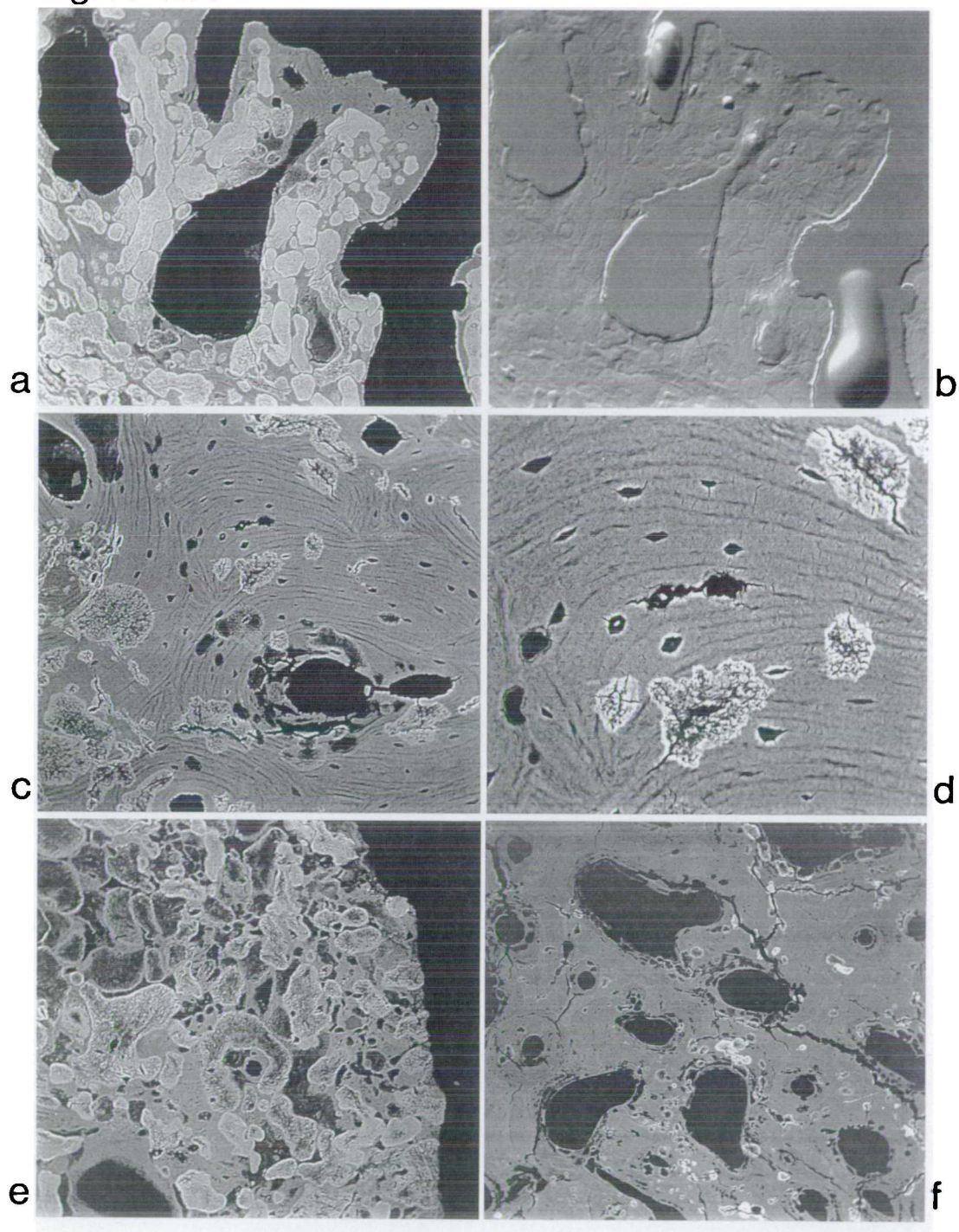
2.4d Pathological (specimen 2) archaeological bone. TS apical/anterior midshaft tibia. Higher magnification of field in Fig. 2.4c: the focal lesions appear to be centred on osteocyte lacunae. SEM/BSE, PMMA-embedded bone. Field width 120 microns.

2.4e Pathological (specimen 2) archaeological bone. TS apical/anterior midshaft tibia. There is extensive diagenetic change and the total absence of the subperiosteal circumferential lamellae. Loss of altered bone has also occurred. SEM/BSE, PMMA-embedded bone. Field width 315 microns.

2.4f Pathological (specimen 2) archaeological bone. TS apical/anterior midshaft tibia. Cracks track for some distance across natural cleavage planes, partially bisecting focal areas of changed density. SEM/BSE, PMMA-embedded bone. Field width 1275 microns.



Figure 2.4



## **CAPTIONS**

## Figure 2.5

2.5a Higher power of central region of Fig. 2.4f, showing details of the focal lesions situated around osteonal canals. Cracks bisect focal lesions, cross and exploit natural cleavage planes. SEM/BSE, PMMA-embedded bone. Field width 315 microns.

2.5b Pathological (specimen 2) archaeological bone. TS apical/anterior midshaft tibia. Two secondary osteons with extensive curvilinear diagenetic foci/lesions are shown. Note the centrifugal spread of diagenesis from the osteonal canals. SEM/BSE, PMMA-embedded bone. Field width 300 microns.

2.5c Pathological (specimen 2) archaeological bone. TS apical/anterior midshaft tibia. Diagenetic change occurred preferentially around vascular spaces. SEM/BSE, PMMA-embedded bone. Field width 1275 microns.

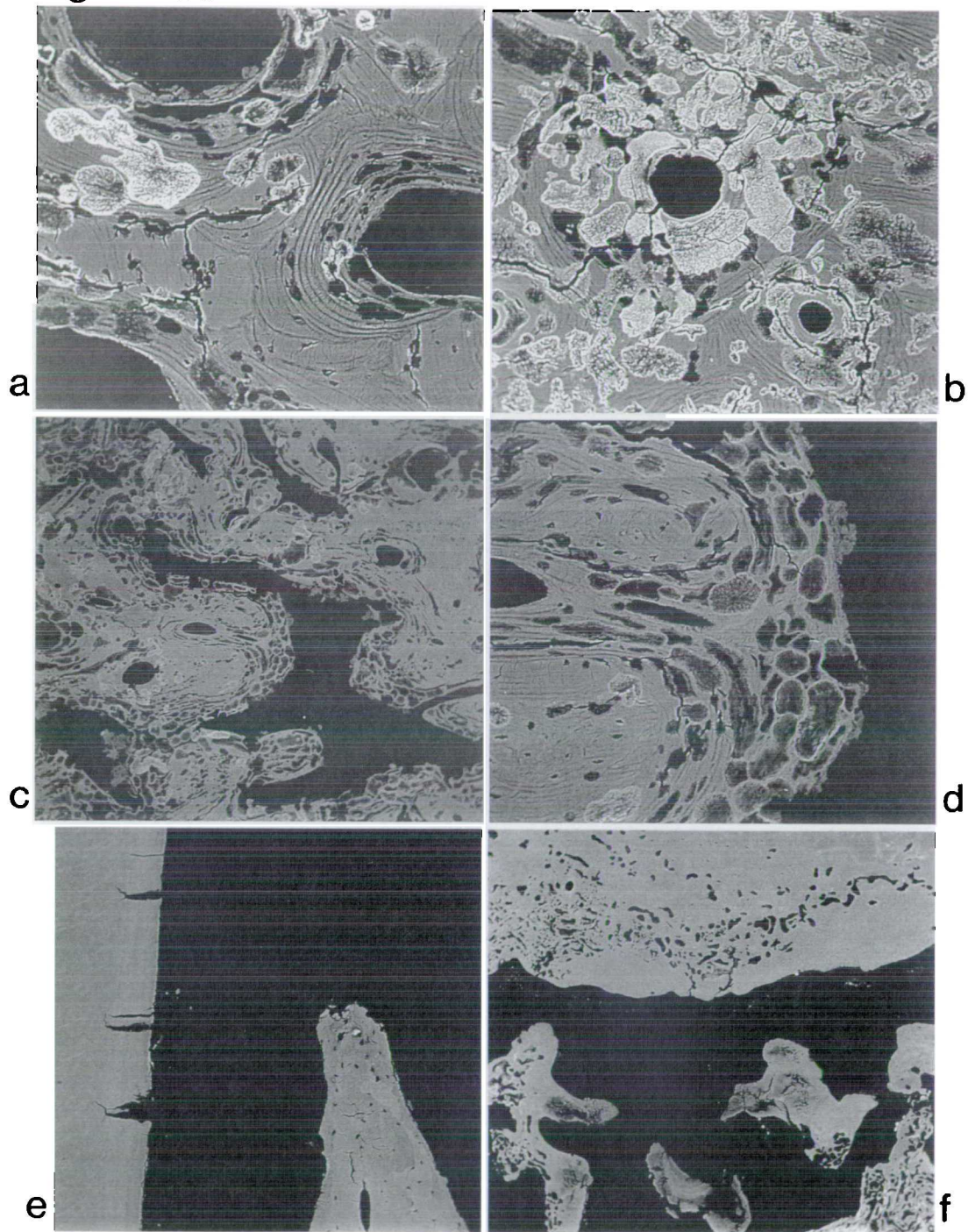
2.5d Higher power of central field of Fig. 2.5c. The focal changes followed the orientation of osteonal lamellae as well as vascular spaces. The border of the focal regions is generally more highly mineralized. SEM/BSE, PMMA-embedded bone. Field width 315 microns.

2.5e Soil-buried mandibular second premolar in-situ showing dentine and cementum (left) and alveolar crest (right) unaffected by diagenesis. BSE image. Field width 885 microns.

2.5f Soil-buried maxillary canine in-situ: both apical cementum and alveolar bone are extensively altered by diagenesis. BSE image. Field width 1660 microns.



Figure 2.5





## 2.6 Conclusion

Clearly, to understand the structural dynamics of diagenesis in human bone, be it pathological or otherwise, one needs to consider the role played by the extensive porous network provided by osteonal canals, osteocyte lacunae and canaliculae and also the influence of the subperiosteal and endosteal zones. The orientation and structure of those areas of changed morphology and density are also highly suggestive of the inherent ante mortem fibrous structure of bone influencing the pattern and progression of diagenesis to produce Hackett's (1981) "lamellate" structure, which he and others consider to be initiated by the complex actions of fungi and bacteria (Hackett, 1981; Wedl, 1867; Marchiafava et al., 1973; Ascenzi et al., 1984). The results from this study confirm the view of these authors that changes in bone are not randomly distributed but reflect the lamellar nature of bone and the distribution of external and internal surfaces. Furthermore, the variation of density within diagenetically altered bone, dramatically illustrated by BSE imaging, may result both from the wide ranging elemental composition of the remineralised archaeological bone and from its stage of diagenesis.

An analysis of diagenetic changes in archaeological bone is therefore limited by the need to deduce the sequence of diagenesis. Further experimental investigation of the progression of diagenetic alterations in accelerated systems, particularly with regard to mineral density, should provide a valuable insight into this process in normal and pathological bone. It should be recognised that not only can unrecognised or discounted diagenesis invalidate ones interpretation of pathology in archaeological specimens but also pathology can play an important role in the progression of diagenesis itself.

## **2.7 PART II: Terrestrial versus marine**

### **2.8 Introduction**

What is lacking in all previous studies is a method which allows morphology, density and total distribution of diagenesis to be assessed in one section, with skeletal and dental tissues present and retained in their anatomical locations. This section presents a method whereby the investigation of diagenesis in archaeological material was extended to advantage using SEM/BSE imaging.

The study presented here examines the use of SEM/BSE imaging to assess the effects and distribution of diagenesis in teeth retained in-situ in their supporting bone. The two important benefits of taking this approach are that all the hard tissues can be cross-compared in a single section; and that the contribution of a natural joint space can be assessed.

### **2.9 Material and methodology**

Macroscopically intact archaeological human mandibles and maxillae from five different soil-buried contexts (all cemeteries, Bronze Age to Medieval) and one marine context (the sudden sea burial of the crew of the Mary Rose, Portsmouth, 1545 A.D.) were used for this study. A single tooth and accompanying socket was removed from the mandible or maxilla by cutting the entire tooth and socket free using a wet, diamond-edged circular saw. Each section was then rinsed in tepid tap water and allowed to air dry. These sections were placed in methylmethacrylate and 5% (by volume) styrene, placed in a 32°C oven and removed after the monomer had polymerised to polymethylmethacrylate (PMMA). The methacrylate monomer had been prepared by the flash distil method described by

Boyde et al. (1986). The embedded specimens were then cut longitudinally buccolingually using an Isomet-11-1180 circular saw, polished using graded abrasives and finished with 1 um diamond abrasive on a rotary lap. Each block face received a coating of carbon in vacuum and was then mounted on an aluminium stub. The specimens were examined using a Cambridge Stereoscan S4-10 SEM, operated in BSE mode working at 20 kV beam voltage.

## 2.10 Results and discussion

All the hard tissues observed in this study, excepting enamel, had undergone quite radical diagenetic change. Further, the marine burial tissues proved to have a different and highly distinctive morphology when compared to soil-buried material.

### Bone

The diagenetic effects in the soil-buried alveolar bone were similar to those found in long bones previously detailed. The alveolar bone in all but one of the specimens [Fig. 2.5e] was extensively affected by diagenetic alteration and appeared to have furnished no lasting protection to the enclosed root [Figs. 2.5f & 2.6a]. The primary or initial route of entry and spread of the micro-organisms in the soil-buried contexts [Fig. 2.7a], as in previous observations, appeared to follow the vascular and cellular network of bone and also had a strong orientation parallel to gross collagen direction. In the Mary Rose marine specimen such a spread/distribution was not present. Instead, the route of entry of the micro-organisms almost completely ignored the vascular, cellular and collagenous network of the bone, dentine and cementum [Fig. 2.6b]. The

periodontal ligament "space", which once would have comprised the natural joint for the tooth, could not be implicated as a route for the spread of the main post mortem attack. The major tissue destruction was located peripherally from the necks of the teeth crossing to the periosteal aspect of the alveolar crest and continuing peripherally around the entire distance of the subperiosteal bone of the mandible [Fig. 2.7b]. Very limited diagenesis was present in some regions bordering the ligament space.

### Enamel.

The enamel in the study, whether covered by calculus or not, appeared unaffected by diagenesis [Figs. 2.6b & 2.7c]. No general demineralization of the enamel surface was observed, although some apparently 'classic' carious lesions in the enamel were found [Fig. 2.7d & e]. In the limited regions where such an attack had taken place, the cross striations of the enamel prisms could be seen more clearly than elsewhere, the approximately weekly incremental striae of Retzius were more prominent and a denser surface zone was evident. Micro-cavitation within the body of the lesion which resulted from partial localised removal of enamel, presumably by acid dissolution, was also present. The characteristic survival of this "white spot" type of carious lesion, and other more extensive enamel caries observed in this study, underlines the enamel's ability to be free of attack from body and soil flora, even when it's own microstructure had apparently been compromised by ante mortem attack. It is recognised, however, that enamel can suffer post mortem degradation to its surface as observed by Poole & Tratman (1978). The pattern of distribution of dental caries is characteristically localized, but the physicochemical changes

that occur in acid dissolution of this tissue would be similar whatever the origin of the protons. In this study no such generalized changes were seen and so it is concluded that the total depositional environment of both the soil and marine contexts studied were not conducive to such changes occurring. The acidity of the soils/sediments during the time of burial is unfortunately unknown.

### **Dentine.**

In striking contrast to the enamel, the soil-buried dentine was observed to have undergone extensive diagenetic change to its microstructure. These changes tended not to affect the mantle and adjacent circumpulpal dentine of the crown [Fig. 2.7f], but were instead concentrated quite extensively both peri-pulpally in the root and crown [Fig. 2.8a] and peripherally in the root [Fig. 2.8b]. The enamel appeared to have protected the underlying dentine from external attack [Fig. 2.8c]. Interglobular spaces in the dentine below the enamel were also maintained without change [Fig. 2.8d] but in the root the granular layer of Tomes was often not discernible because of extensive diagenesis [Fig. 2.8b]. Where diagenetic changes to the dentine had occurred, streaming foci tended initially to orientate along the long axis of the collagen, following incremental planes, approximately at a 90° angle to the dentine tubules [Fig. 2.8e]. Peritubular dentine was often preserved in the diagenetic destruction foci [Fig. 2.8f], in contradistinction to *in vivo* carious attack, which frequently initially follows and locates itself within the dentine tubules, demineralization then spreading to intertubular regions. With the formation of liquifaction foci, carious micro-organisms move outwards into the intertubular dentine (Jones & Boyde, 1987;

Jones, 1987). By contrast, diagenetic destruction foci were primarily placed in the intertubular dentine region, and the foci were discrete with clear boundaries between affected and unaffected tissue. Changes in the dentine became extremely difficult to interpret or pick out when diagenetic alteration had been superimposed over an ante mortem carious assault on the dentine [Fig. 2.9a & b]. The full distribution of diagenesis was obvious only where it deviated from ante mortem microbial carious distribution. Consequently, if one were able to decide that the overall pattern and location of altered dental tissues could not have been produced by carious attack alone, and the supporting alveolar bone shows evidence of diagenesis, then it would be reasonable to assume a degree of diagenetic intervention in the tooth.

The marine-buried dentine had an altogether different diagenetic morphology and distribution from that of the affected soil-buried material. The attack, as mentioned above, was peripheral and therefore possibly short-lived [Fig. 2.6b]. The dentine was primarily attacked at the cervical margin where the enamel was partially undermined for a short distance [Fig. 2.9c]. The full spread of this post mortem attack appeared to have been self-limiting and only affected the root dentine to a level above the alveolar crest [Figs. 2.6b & 2.9c]. The invading micro-organisms appeared somewhat less affected by the collagenous network of the dentine but some tunnels followed incremental planes and may have utilised the coronal system of tubule side branches. Many tunnels either tracked along dentine tubules at the advancing edge of the attack, but some also crossed dentine tubule boundaries in almost any direction. There was no evidence of demineralization around any of these boring tunnel-like features, the smallest of

which had diameters of approximately 5 microns. Boring channels or tunnels from a marine context have been reported previously by Ascenzi & Silvestrini (1984), who found a variety of micro-organisms present inside the tunnels themselves. These authors implicated protozoans of the amoebic type as principal candidates for the tunnelling (ruling out bacteria and algae due to their absence). The actual in-situ distribution of the boring tunnels was not demonstrated.

#### **Cementum.**

Soil-buried cementum, like bone and dentine, also underwent diagenetic change. Figure 2.8b shows considerable tissue alteration, and cracking which may have been due in total, or in-part, to the methacrylate shrinking during polymerisation and possibly also expanding due to the exothermic heat of polymerisation. The diagenetic foci were clearly observable as partially demineralised and remineralised regions of varying densities [Fig. 2.9d] similar to those observed in the alveolar bone [Fig. 2.9e] and those detailed previously in long bones. The orientation of these foci appeared less clearly defined than those in dentine although they sometimes predominated at one incremental level, as seen in the longitudinal sections. Collagen order in cementum is similar to that of Sharpey fibre bone, the extrinsic fibres being approximately normal to, and the intrinsic fibres, where present, parallel to, the developing surface of the bone. On the whole, cementum was less affected by diagenesis than the related alveolar bone, presumably because it lacks the access routes provided by vascular canals.

The marine-buried cementum seemed hardly affected by diagenesis due to it's location mostly within the preserved joint space [Fig. 2.9f]. However, the small

amount that was affected, in a band horizontal above the alveolar crest, showed similar tunnelling to that previously described in the marine bone and dentine [Fig. 2.10]. Where cervical cementum was entirely absent, it was not possible to say whether this was due to ante mortem or post mortem loss, or whether root caries had complicated the picture.

## 2.11 Conclusion

BSE imaging of the dental and supporting bony tissues proved a simple and effective method for investigating the changes in mineral density and morphology that accompany diagenesis. All the hard tissues other than the enamel underwent diagenetic change to microstructure, and the microstructure of each calcified connective tissue influenced the pattern of diagenesis. A striking comparison was made possible between soil versus marine contexts examined in this study, illustrating the necessity of not only taking total account of the distribution and morphology of diagenesis throughout the hard tissues, but the contribution of the joint space to this whole process. It became clear from this study that had the teeth not been retained in-situ of their alveolar and basal bone, the unique distribution of the soil to marine contexts would have been lost. Previous studies have not used this method of presentation but it provides an important step toward understanding the microbial environment which promoted the consequent diagenetic morphologies.

It is clear from this study that the effects of diagenesis can be extensive even in apparently well preserved dental and supporting skeletal tissues. Sampling protocols for biochemical and mtDNA extraction studies could gain considerable



benefit from identifying and locating microscopically the distribution of diagenesis before removal of bone or dentine. Moreover, rather than considering diagenesis as an irksome contaminative factor alone, it instead represents a little exploited taphonomic resource which could be of great use and interest to archaeological and forensic science.

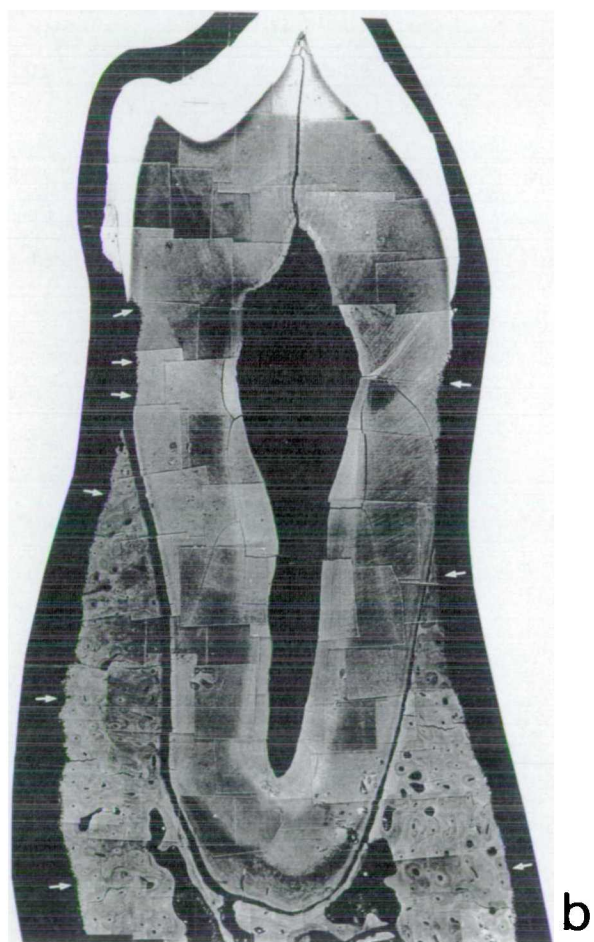
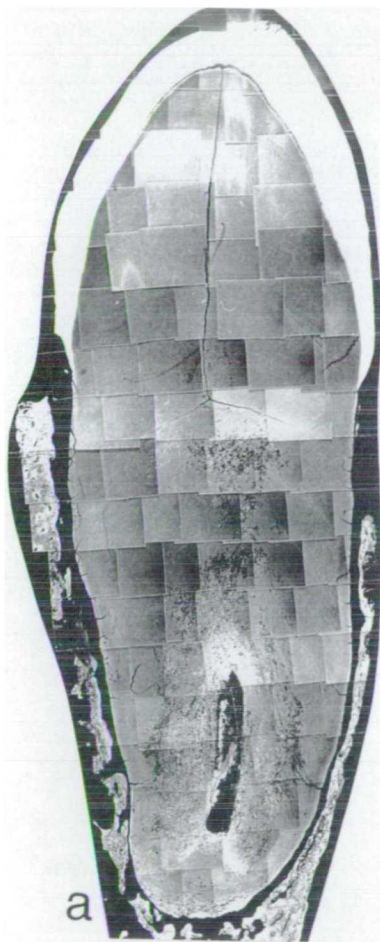
## **CAPTIONS**

**Figure 2.6**

2.6a Montage of soil-buried maxillary canine and supporting bone. Diagenesis had affected all tissues except enamel. The tooth bears calculus and had ante mortem caries confined to enamel. BSE image. Max. field width 7 mm.

2.6b Montage of marine-buried second premolar retained in mandibular bone. Diagenesis was confined to the surfaces arrowed. BSE image. Max. field width 9 mm.

Figure 2.6



## **CAPTIONS**

.

## Figure 2.7

2.7a Discrete diagenetic foci of varying mineral density in soil-buried maxillary lamellar bone. Spread of diagenesis was via the vascular and cellular network and incremental layers. BSE image.

Field width

410 microns.

2.7b Alveolar crest of marine-buried mandibular canine. Tunnels extend for a limited distance from the external surface (right). The Sharpey fibre bone of the socket wall is unaffected except at the margin of the socket. BSE image. Field width 855 microns.

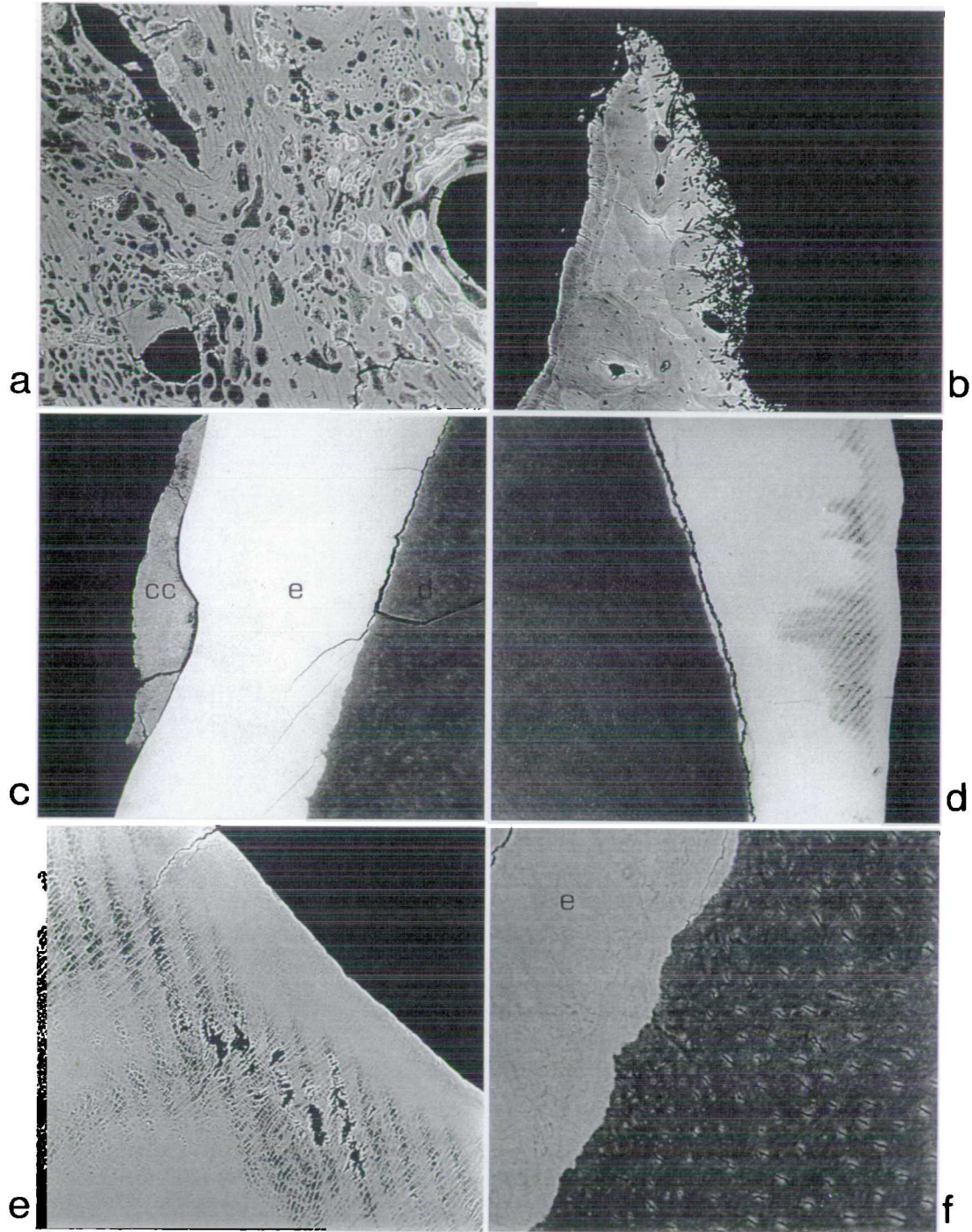
2.7c Soil-buried mandibular canine: the dentine (d), enamel (e) and calculus (cc) were unaffected by diagenesis. BSE image. Field width 855 microns.

2.7d White spot carious lesion in enamel showing characteristic peaks in spread of demineralization and intact surface layer: soil-buried maxillary canine; high power of Fig. 2.6a. BSE image. Field width 1660 microns.

2.7e Higher power of Fig. 2.7d. Cross striations in the enamel prisms and incremental Brown Striae of Retzius are more prominent in the carious lesion, which has cavitated. BSE image. Field width 430 microns.

2.7f Unaffected enamel (e) and adjacent, protected, dentine (d) in soil-buried mandibular canine. BSE image. Field width 180 microns.

Figure 2.7



## **CAPTIONS**



**Figure 2.8**

2.8a Secondary dentine bordering pulp chamber riddled by diagenetic foci of varying density in a soil-buried maxillary canine. BSE image. Field width 855 microns.

2.8b Extensive post mortem alteration to dentine (d) and cementum (c) structure in soil-buried second premolar. BSE image. Field width 895 microns.

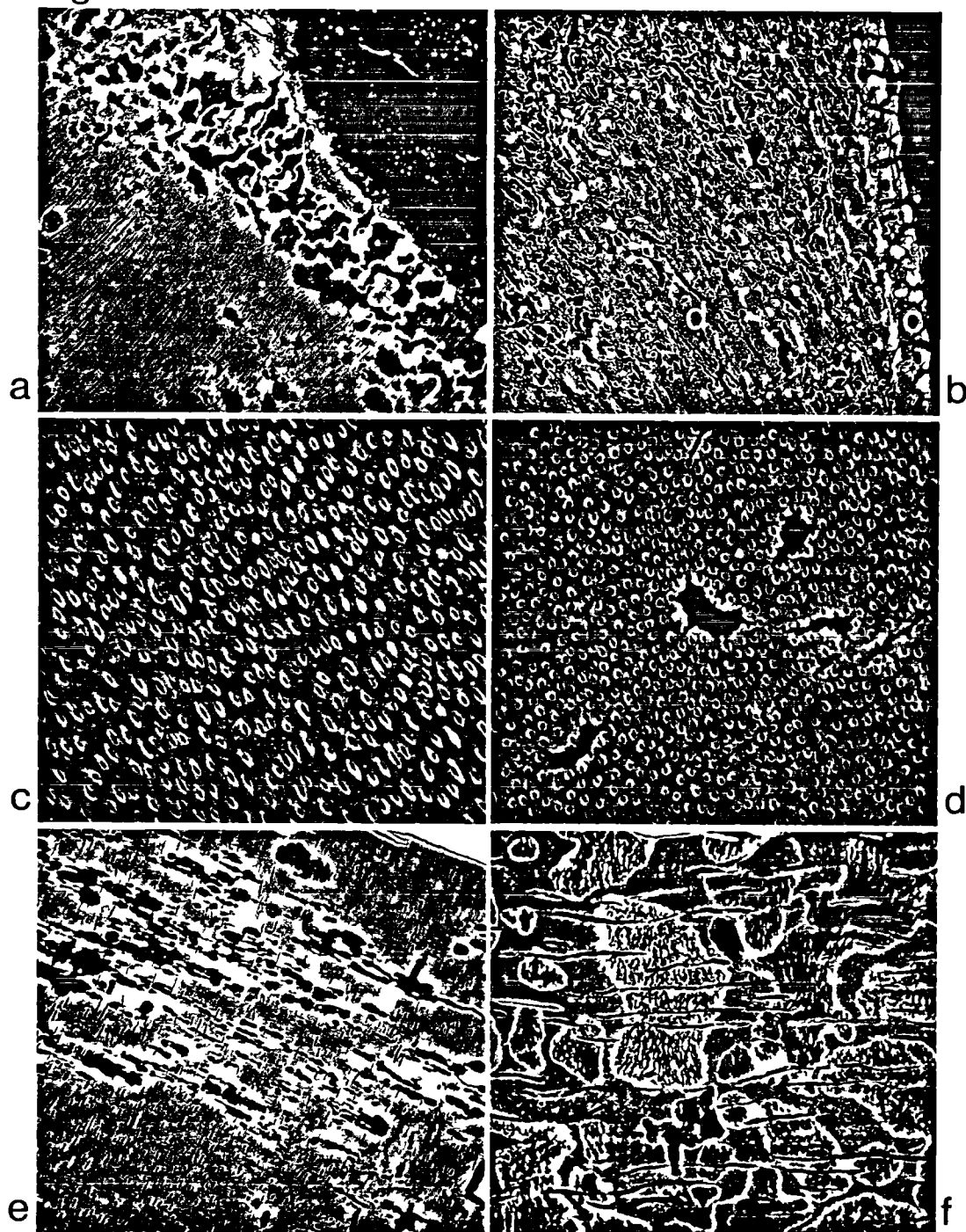
2.8c Peritubular and intertubular dentine in the body of coronal dentine, unaffected by diagenesis: the varied diameter of the tubules is a feature of normal dentine. Soil-buried mandibular second premolar. BSE image. Field width 170 microns.

2.8d Well preserved interglobular dentine in a soil-buried maxillary canine crown. BSE image. Field width 170 microns.

2.8e Diagenetic foci extending along incremental planes in radicular dentine of a soil-buried upper canine. BSE image. Field width 430 microns.

2.8f Same tooth as Fig. 2.8e. Note the variation in mineralization, the preservation of peritubular dentine and the peripheral hypermineralization of the diagenetic foci. BSE image. Field width 170 microns.

Figure 2.8



## **CAPTIONS**

## Figure 2.9

2.9a Second maxillary premolar showing possible loss (l) of peritubular dentine and splitting (s) of decayed intertubular dentine. Soil-buried specimen. BSE image. Field width 170 microns.

2.9b Same tooth as Fig. 2.9a showing a demineralized and cavitated area within the ante mortem carious dentine which could have been secondarily affected by diagenesis. BSE image. Field width 170 microns.

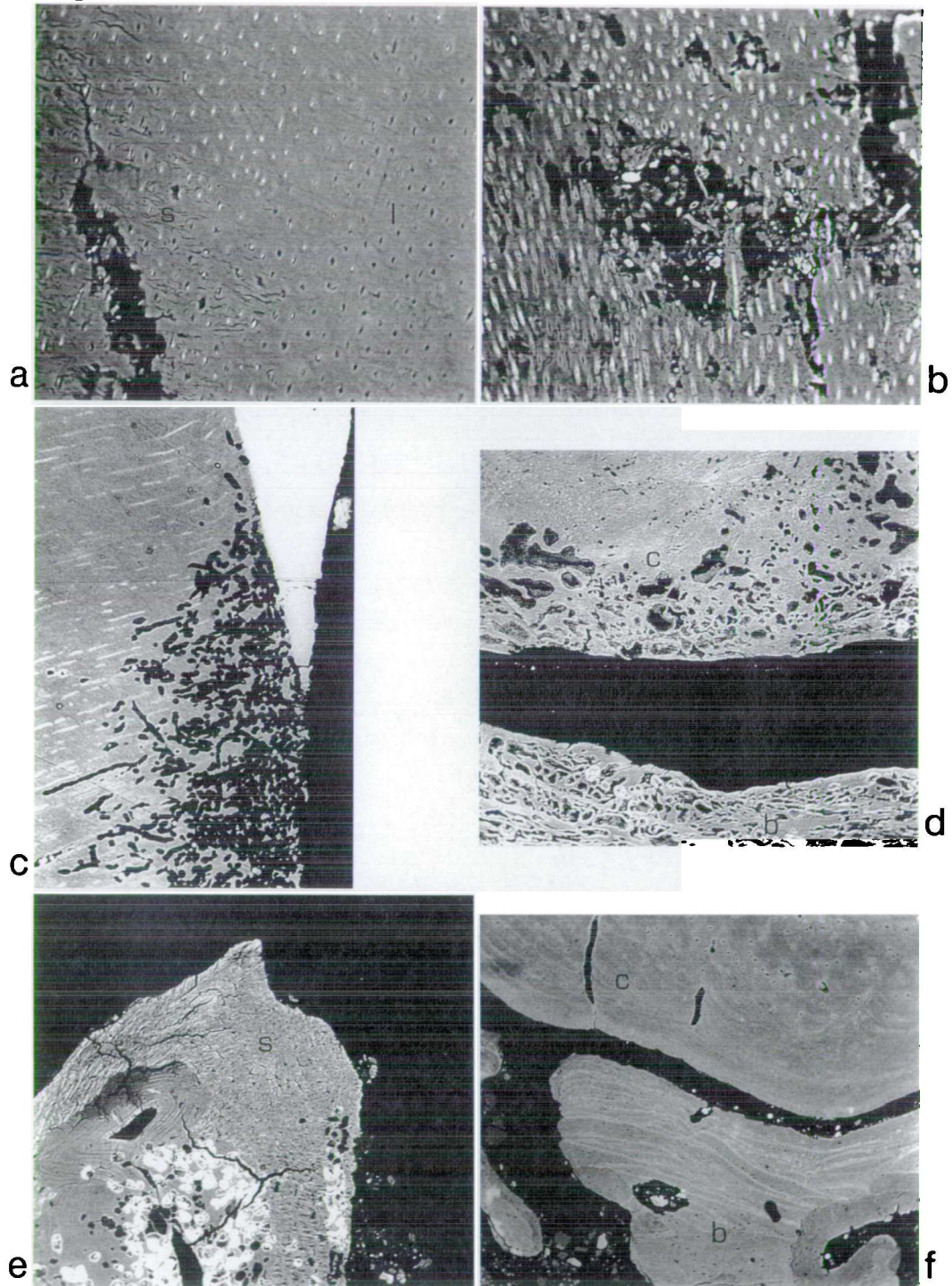
2.9c Marine-buried mandibular canine exhibiting diagenetic attack to dentine with tunnels undermining enamel for a short distance. The invading tunnels follow dentine tubule direction, the incremental planes and also directions apparently unrelated to dentine microstructure. BSE image. Field width 430 microns.

2.9d Soil-buried maxillary canine showing diagenetic demineralized and remineralized foci within the apical cementum (c) and alveolar bone (b). BSE image. Field width 855 microns.

2.9e Soil-buried alveolar crest exhibiting several discrete diagenetic foci of differing densities. The Sharpey fibre bone (s) contains post mortem lesions which followed intrinsic fibre incremental planes. In the osteon and adjacent bundle bone note the large area of demineralization (arrowed). BSE image. Field width 855 microns.

2.9f Marine-buried mandibular second premolar and supporting alveolar bone (b) in region unaffected by diagenesis. The clefts in the cellular cementum (c) are not of diagenetic origin but anatomical features of the root apex. Sediment inclusions are present in ligament and vascular spaces. BSE image. Field width 1805 microns.

Figure 2.9



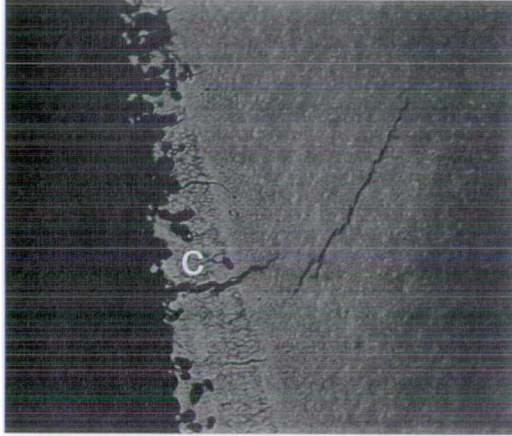
## **CAPTIONS**

.

**Figure 2.10**

2.10 Marine-buried mandibular canine: cellular cementum (c) at neck of tooth affected by boring tunnels only above the alveolar crest level. Same specimen as Fig. 2.6a. BSE image. Field width 430 microns.

Figure 2.10





## CHAPTER 3: PAGET'S DISEASE: POST MORTEM ALTERATION AND BONE PATHOLOGY

### 3.1 Introduction

Two potential cases of Paget's disease in archaeological human bone have been investigated to ascertain the effects of diagenesis on this particular bone pathology, and also the influence of bone pathology on the post mortem microstructure itself.

Paget's disease of bone derives its name from Sir James Paget's original description of 'osteitis deformans' in 1877. It is a disease of considerable antiquity and affects most bones of the skeleton (Ortner & Putschar, 1985). Histologically it is characterised by excessive or rapid resorption and formation of bone. Consequently it has a higher frequency of immature forms of bone, a greater number of reversal lines and larger osteocyte lacunae with less well mineralized walls, giving an overall "mosaic" like appearance (Boyde et al., 1986; Chappard et al., 1984) although, in the early stages of the disease this mosaic appearance will be less obvious (Tillman, 1962). In archaeological material, Paget's disease is usually assessed from the gross and radiological appearance of the bones (Ortner & Putschar, 1985; Wells, 1959; Denniger, 1933).

Microscopical reports on such archaeological bone are rare and the potentially complicating effects of diagenesis on bone structure have not been addressed in palaeopathological material. Diagenesis is known to alter and reorganise bones and teeth extensively after death (Garland, 1989; Hackett, 1981; Poole & Tratman, 1978; Clement, 1963). This reorganisation is believed to be mediated by the separate or combined actions of bacteria

and fungi (Hackett, 1981; Piepenbrink, 1986; Marchiafava et al., 1974; Wedl, 1864); although in marine contexts other micro-organisms have been implicated (Ascenzi & Silverstrini, 1984). In this study two cases thought to be Paget's disease from macroscopic and radiological findings have been examined for microstructural evidence supporting these tentative diagnoses.

### 3.2 Aims of this study

The aims were to investigate the effects of post mortem alteration to a specific bone pathology, in this instance Paget's disease; and to ascertain the applicability of SEM/BSE imaging as a useful diagnostic adjunct.

### 3.3 Material and methodology.

The skeletal material used in this microscopic study came from two adult inhumations from separate medieval cemeteries: St. Margaret Incumbusto, Norwich (SMI) and Sandwell Priory, Sandwell (SP). The gross and radiological distribution of SMI Paget's was postcranial (Stirland, 1991), whilst the SP skeleton was only affected cranially and was not x-rayed (Flinn, pers. comm.). The macroscopic condition of the SMI was excellent, whereas that of the SP material was poor, being fragmentary and chalky.

A tranverse midshaft section was removed from the left humerus and left radius (SMI), and a thick sagittal section was removed from the occipital bone (SP). The sections were then put in methylmethacrylate (with added styrene for stability), placed in a 32°C oven, and removed after the methylmethacrylate had polymerised to polymethylmethacrylate (PMMA). The embedded specimens were then cut transversely using an Isomet-11-1180 circular diamond saw, polished using graded abrasives, and finished with a

1 micron diamond abrasive on a rotary lap. Each block face received a coating of carbon in vacuo.

The specimens were examined using a Cambridge Stereoscan S4-10 SEM, operated in backscattered electron (BSE) mode working at 20 keV beam voltage. A four-segment solid-state BSE detector was used for compositional imaging, collecting BSE electrons at all four segments and summing the signal from all four segments. The images were dominated by differences in the mean atomic number of the volume probed by the scanning beam and so provided a sensitive indicator of mean density and micromorphology (Boyde & Jones, 1983).

### 3.4 Results.

Examination by SEM/BSE imaging showed that the cranial SP bone, although considered poorly preserved macroscopically, had extensive regions unaffected by diagenesis. By contrast, the SMI material which was considered in excellent macroscopic condition, was profoundly altered by diagenesis.

The Sandwell Priory bone.

The specimen had the appearance of a high bone turnover condition not dissimilar to the early stages of Paget's disease referred to by Tillman (1962). There was evidence of increased vascularity [Fig. 3.1a], with irregularly defined vascular canals [Fig. 3.1b], large osteocyte lacunae within poorly organized collagen lamellae [Figs. 3.1c - e], and an increased number of reversal lines [Figs. 3.1e & f] which were easily seen in the BSE image because they were hypermineralised compared with the

surrounding tissue. Small focal diagenetic lesions were evident on the endocranial aspect, located at sites where osteocyte lacunae would once have been [Fig. 3.2a]. These focal alterations were distinguishable from osteoclastic activity.

The St. Margaret Incumbusto bone.

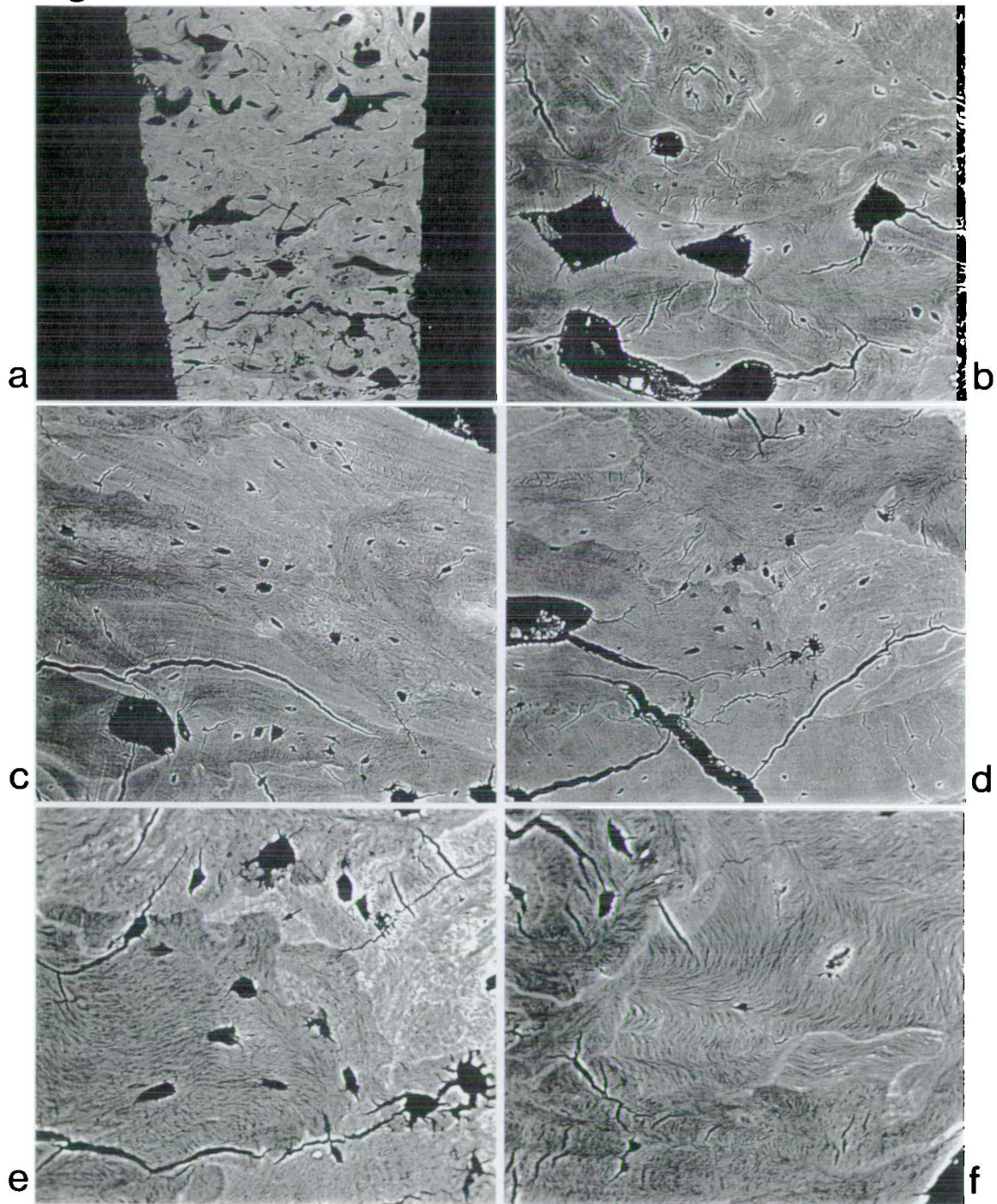
The SMI bone had been extensively altered by diagenesis and little of the original bone tissue was recognisable. The left radial SMI specimen had the classic mosaic pattern of Pagetic bone which had been retained, or rather replicated, by the diagenetic process [Fig. 3.2b]. Similarly, the left humerus exhibited large irregular vascular canals within a field of diagenetically altered bone [Fig. 3.2c]. At the subperiosteal aspect of both specimens there was survival of circumferential lamellae, external to regions of the bone with greatly diagenetically changed micromorphology and altered density [Fig. 3.2d]. Internally, many regions of resorption lacunae profiles could be identified edging the much enlarged vascular spaces [Fig. 3.2e]. The diagenetic foci (as described in detail in Chapter 2) have a strong orientation along the long axis of gross collagen direction [Figs. 3.2d & f]. Thus, although at a microscopic level very little bone with its correct structure and density was intact, the overall structure was coarsely replicated by the diagenetic process itself. It was therefore possible to read evidence for increased remodelling in the original bone even in regions where none had apparently survived.

### 3.5 Discussion.

The chalky fragmented appearance of the SP specimen presented a gloomy prospect in terms of ascertaining any useful information to add to the

## **CAPTIONS**

Figure 3.1



**CAPTIONS**

### Figures 3.2

3.2a SP specimen. Small focal diagenetic lesions were evident on the endocranial aspect of the section. The diagenetic foci all had this type of morphology and were mostly located within osteonal systems. Field width 875 microns.

3.2b St. Margaret Incumbusto (SMI) left radius midshaft transverse section (TS). The classic "mosaic" pattern of Paget's disease replicated by the diagenetic process. Very little of the original bone with its characteristic morphology and density is evident. Field width 1910 microns.

3.2c SMI left humerus midshaft TS. Enlarged soft tissue spaces characteristic of increased bone turnover found in a small area of the humeral cortex. Again diagenetic ingress is virtually total. Field width 1665 microns.

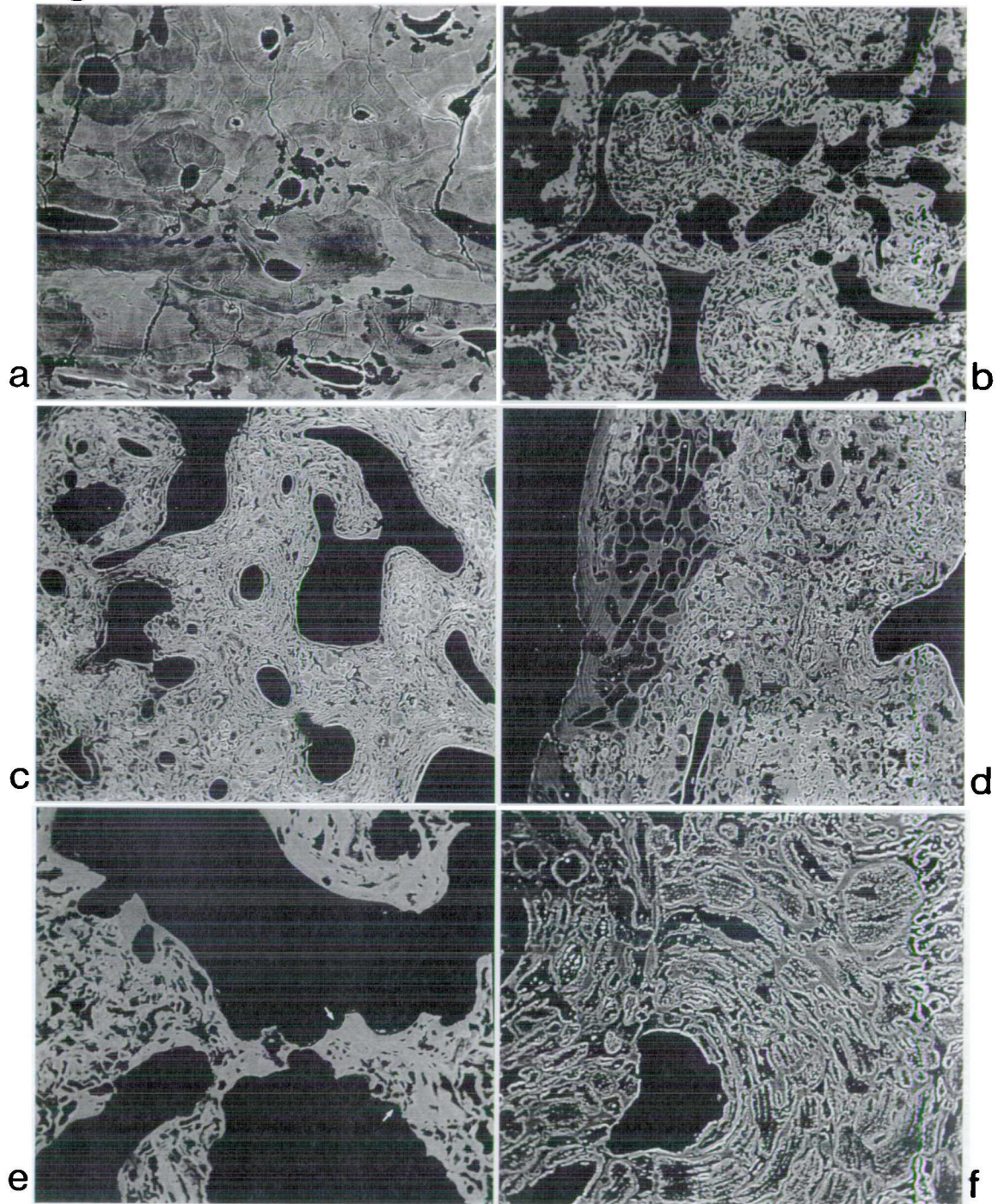
3.2d SMI left humerus midshaft TS. The subperiosteal circumferential lamellae in both specimens often survived intact. However, regions just below the lamellae were entirely diagenetically reorganised in terms of morphology and density. Field width 810 microns.

3.2e SMI left radius midshaft TS. Osteoclastic resorption lacunae are clearly evident as scalloped edging at the periphery of enlarged soft tissue spaces (arrowed). Although the diagenetic ingress is extensive, bone with its characteristic density is present at the periphery of the vascular spaces. Field width 955 microns.

3.2f SMI left humerus midshaft TS. The orientation of diagenetic ingress is seen to orientate itself strongly with general collagen direction. Also a reversal line (top left centre) is highlighted by two different orientations of diagenetic ingress. Field width 410 microns.



Figure 3.2



assessment of a potential pathology. It was therefore a pleasant surprise to find the microstructure of the bone in such good condition. Although the micromorphology indicated a high bone turnover pathology, this did not in itself prove that Paget's disease was the cause of the condition. However, the microscopic study did add valuable information, and poor macroscopic survival of the bone should not pose a deterrent to microscopic investigation.

By contrast the SMI specimens, although in excellent macroscopic condition and exhibiting both the gross and radiological appearance of Paget's disease, had been almost entirely remodelled by diagenesis. Although it might be supposed that the diagenetic alteration made it difficult to observe any signs of high rates of resorption and apposition, the retention of the original vascular arrangement characteristic of Paget's disease, and the mosaic pattern with many interrupted arcs mimicking the organisation of the original lamellar groups, could be read as evidence for high bone turnover. This pattern was observed clearly in the grossly deformed SMI left radius, whilst the less altered SMI left humerus had a small area of enlarged soft tissue spaces within the cortex. Such characterisation allowed validation of X-rays: the invasive lesions coarsely replicated the collagenous arrangement of the pathology with sufficient resolution for gross x-ray analysis. This observation however, should not be considered the rule, since it has been shown in Chapter 2 and by others that diagenesis can have other micromorphologies (Hackett, 1981; Ascenzi & Silverstrini, 1984). It would therefore be prudent to ascertain the nature and type of diagenetic ingress microscopically before presenting important pathological case studies.

The investigation of the microstructure of the bone was greatly simplified by the use of PMMA embedding: no further crumbling or fracturing of the archaeological bone occurred, whatever its original state of preservation. The bone was embedded intact without decalcification. All the histopathological information was revealed in a single polished facet of the block, but sequential planes could have been prepared either by further polishing or micromilling the blocks. Backscattered electron imaging was particularly useful because subtle changes in the degree of mineralisation present were easily detected; these were of great value in the microscopical analysis of the bony tissues and in the appreciation of diagenetic changes. The sensitivity of the method (Reid & Boyde, 1987) exceeds that of microradiography (Kelly, 1961), and it is particularly apposite for palaeopathological specimens.

### 3.6 Conclusions.

Recent developments in the microscopy of bone, and in particular the SEM/BSE imaging method, have provided highly useful investigative tools for palaeopathological study. The information yielded by this microscopical analysis has emphasised the need to be critical of macroscopic assessments of preservation, the requirement to validate the use of x-rays, and the opportunity to obtain further diagnostic information from the surviving microstructure in archaeological material.

## CHAPTER 4: THE MARY ROSE WRECK: A UNIQUE SEA BURIAL

### 4.1 Introduction

The unique nature of the Mary Rose wreck, both as a sea burial and as a maritime excavation, cannot be overstressed and represents a highly valuable and well documented taphonomic context. The only wreck comparable to the Mary Rose in these terms is the Swedish warship Vasa which sank under similar circumstances (Daring, 1990).

### 4.2 Historical background

The Mary Rose was a Tudor warship built in Portsmouth between 1509 and 1511. Her design was very different from previous medieval warships, which were essentially floating castles, and enabled accurate broadsides to be fired for the first time. She underwent a major rebuild in 1536 when guns were placed in the hull and protruded through lidded gunports [Fig. 4.1]. On the evening of the 19th July 1545 this fiercesome Vice Flagship of Henry VIII sailed into the Solent from Portsmouth Harbour in calm waters and was to engage the French Fleet in battle, but sank with all hands lost. Historical documents numbered the crew complement at 415. The French claimed that the Mary Rose sank due to canon fire, but English records claim that overloading and poor handling caused the ship to rapidly keel over and sink long before reaching the French Fleet. Whatever happened, the fact remains that she sank suddenly in 12-14 metres of water, under the gaze of Henry VIII, with a tragic loss of life (Rule, 1983).

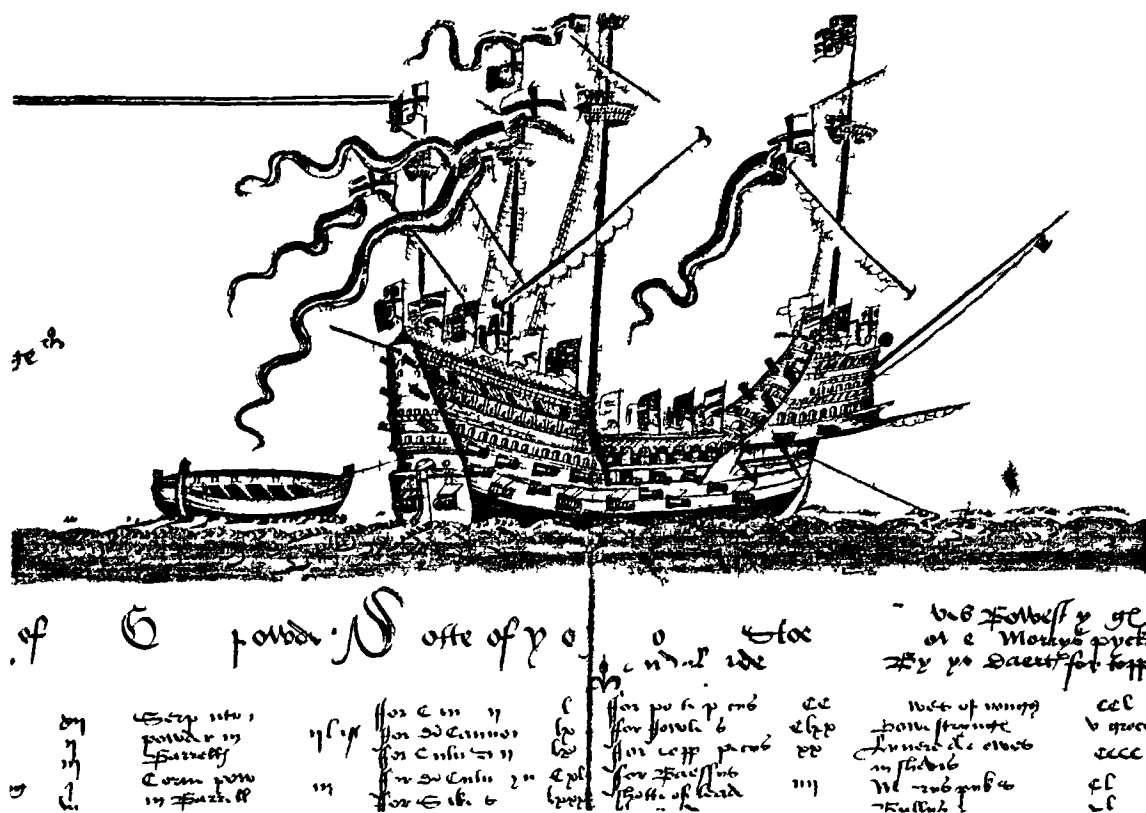


Figure 4.1 The Mary Rose warship as depicted in a 16th century list of the King's ships (Mary Rose Trading Ltd., 1980).

#### 4.3 Depositional history

The depositional history of the wreck itself was not understood until after its excavation and lifting. However, it was known that prior to lifting the wreck had suffered intrusive damage from salvage attempts during the 1800's and more recently by deliberate bomb blasting by the Royal Engineers! At the beginning of the excavation the ship was entirely buried in marine sediment (Rule, 1983).

After sinking, the ship came to rest on the seabed stern down on her starboard side which caused a shifting of the ballast within the hold. The hull rapidly became in-filled with current-borne estuarinal grey clay silts which settled within the calm waters of the ship. This distinct layer was deposited quite rapidly over a period of a few months and constituted the first Tudor layer. During the slower formation of the second Tudor layer, which consisted of light grey clay and seaweed lenses, the upper structure of the hull collapsed. This resulted in the hull decks becoming exposed to an open seabed environment. During the formation of the Tudor layers scouring action, produced by current direction and turbulence, caused redeposition of silt outside the ship, along the hull, and at certain localised sites within the hull. The ship was not encased by sediment until the third layer was deposited during the late 16th and 17th centuries, which consisted of a hard grey clay and broken shelly material. The fourth and final layer constituted the modern mobile seabed, which was wholly or partially removed at different intervals by current action. Water temperature (during excavation) had a seasonal winter summer variation of 12-13°C and 18-20°C respectively (Elkerton pers. comm., Mary Rose Trust).

As the ship sank there was inevitable movement of men and objects. On excavation it was apparent that guns had torn from their holdings and gunports either remained open or were forced open. The skeletal remains were found generally in a disarticulated and commingled state (one sailor was found pinned beneath a large canon), but with good representative survival and retrieval of all bones of the skeleton. Of the 415 men present (Rule, 1983) only 179 were identifiable from minimum number analysis conducted on the skulls and mandibles contained within the ship (Stirland, 1985). Bones retrieved from the area extending 1 m<sup>2</sup> (full extent of excavation) from the hull of the ship were not included. This was due to provenance problems, although given the depositional history of decks collapsing, this is regrettable.

#### **4.4 Microstructural changes to marine substrates**

Post mortem alteration to skeletal, calcareous and wooden materials by tunnelling or microboring is known to occur in the marine environment and is connected to microbial fouling. Arnaud et al. (1978) reported tunnelling in human skeletal material in association with a mediterranean wreck; whilst Ascenzi et al. (1984) experimentally submersed defleshed bovine bone in a similar marine context for 1 year and found equivalent tunnelling. Microboring in living coral reefs, caused by the cyclical attack of algae between the months of May to September, has also been reported (Highsmith, 1981). Other microorganisms such as polychaetes (Sato-Okoshi, 1990) and thraustochyrids (Chamberlain & Moss, 1988; Porter & Lingle, 1984), which are silt sensitive and have a cyclical nature of attack, produce similar small tunnels and tend to colonize substrates peripherally. Cynobacteria (Raghu-Kumar, 1989) have also been implicated



with shell boring, as have some marine fungi (Zeff & Perkins, 1979). Golubic et al. (1975) gave a fascinating review of tunnelling in relation to fossilisation processes, calling this type of penetration "endolithic" and the microorganisms which cause it "endoliths". He suggested that differing endoliths will create type-specific tunnelling and their activity will be affected by depth, temperature and light penetration. He referred to experimental work which demonstrated that endolithic penetration can occur very quickly, within 12 days to 2 months (Golubic et al., 1975: 247). Similarly, wooden timbers from the Mary Rose wreck underwent penetrative tunnelling which decreased in intensity towards the inner core of affected wood (Jones & Rule, 1993). Other larger organisms such as octopii (Nixon & Maconnachie, 1988), sea snails (Symth, 1988), sea urchins (McClanahan & Kurtis, 1991) and sea sponges (Young & Nelson, 1985) are also capable of creating much larger holes/borings within calcareous substrates.

#### **4.5 The aims of this study were twofold:-**

1. To assess the extent of the post mortem marine-type change in a three dimensional sample taken from the Mary Rose wreck.
2. To determine whether a relationship existed between the extent of post mortem attack and silt phase progression within the ship.

#### **4.6 Materials and methods**

A sample of 17 mandibles and maxillae were taken from all decks and silt phases, excluding the modern seabed. At excavation the ship itself was arbitrarily divided into 3 m<sup>2</sup> quadrants and the location of each specimen from the sample group is represented per quadrant in Figure 4.2.



The preparation of the specimens followed the same procedure as that outlined in chapter 2, where a single tooth and accompanying socket was removed from either mandible or maxilla by cutting the entire tooth and socket free using a diamond-edged circular saw. The specimens were then embedded in PMMA, cut in longitudinal transverse section buccolingually and polished on a rotary lap using graded abrasives and finished with a 1 micron diamond paste.

The uncoated blocks were then dry mounted and individually examined under a Lasertec 1LM11 confocal reflection microscope (CRM) using a helium neon light source. This microscope has increased resolution over a standard optical reflection microscope and allowed for identification of tissue morphology and characterisation of post mortem alteration, due to slight topographical relief created by polishing. The Lasertec's integrated software is capable of accurate measurement of x, y and z dimensions within 0.25 microns (Jones et al., 1992). For the measurement of tubule diameters and maximum ingress, only x and y measurements were taken.

All measurement data was collected blind without prior knowledge of specimen location within the ship's stratigraphy. The distribution of post mortem tubule invasion was recorded in terms of total morphology and distribution, maximum ingress, and maximum tubule diameter at 8 different sites per specimen [Fig. 4.3]. Given the disarticulated and non-anatomical deposition and orientation of mandibles and maxillae within the ship, the buccal and medial aspects of specimens were considered to have been rendered anatomically meaningless, and so the 8 sample sites per specimen were based on block face orientation alone. The results from the

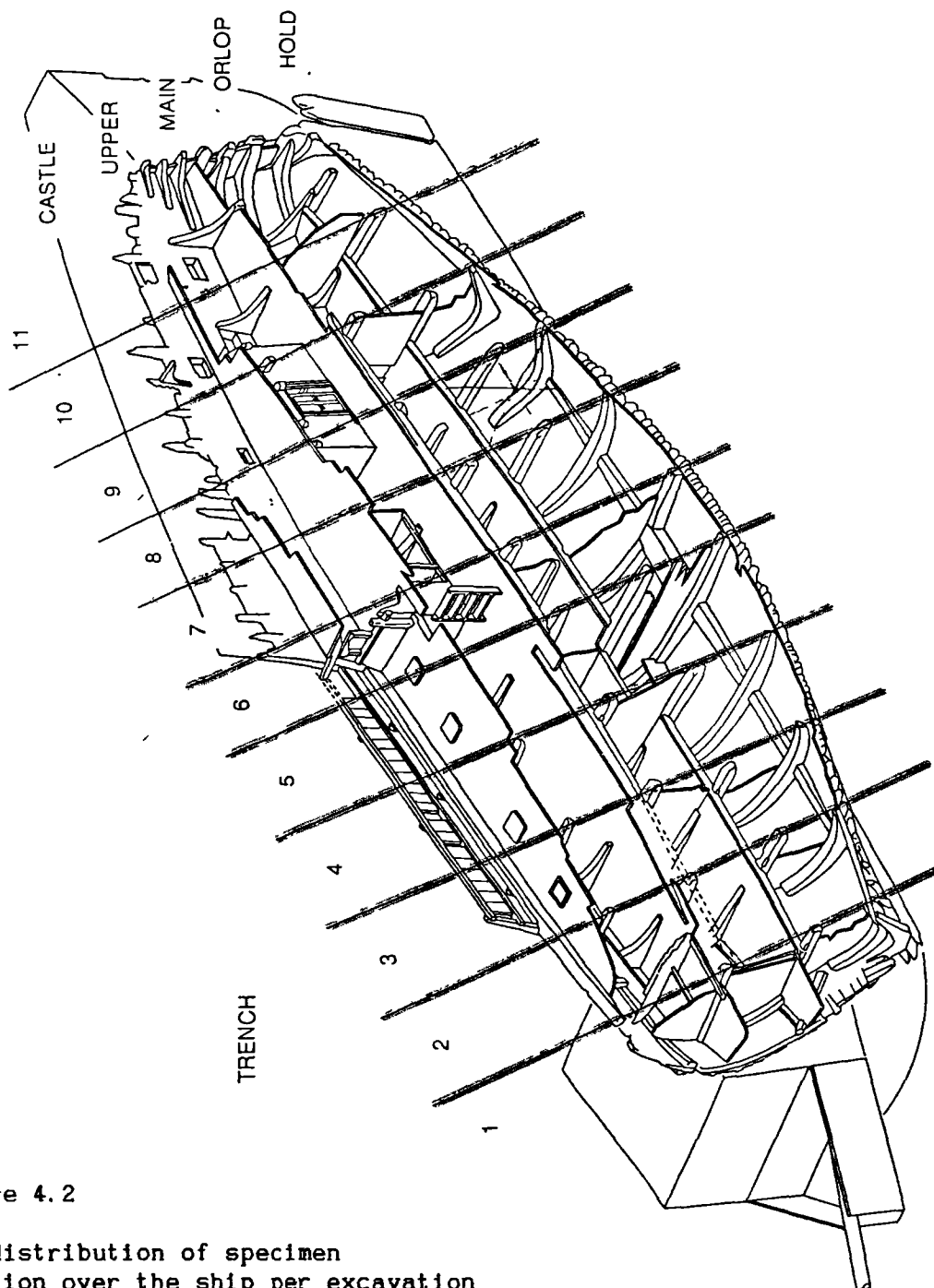


Figure 4.2

The distribution of specimen location over the ship per excavation quadrant (turn image to view). Diagram adapted from an original provided by the Mary Rose Trust.

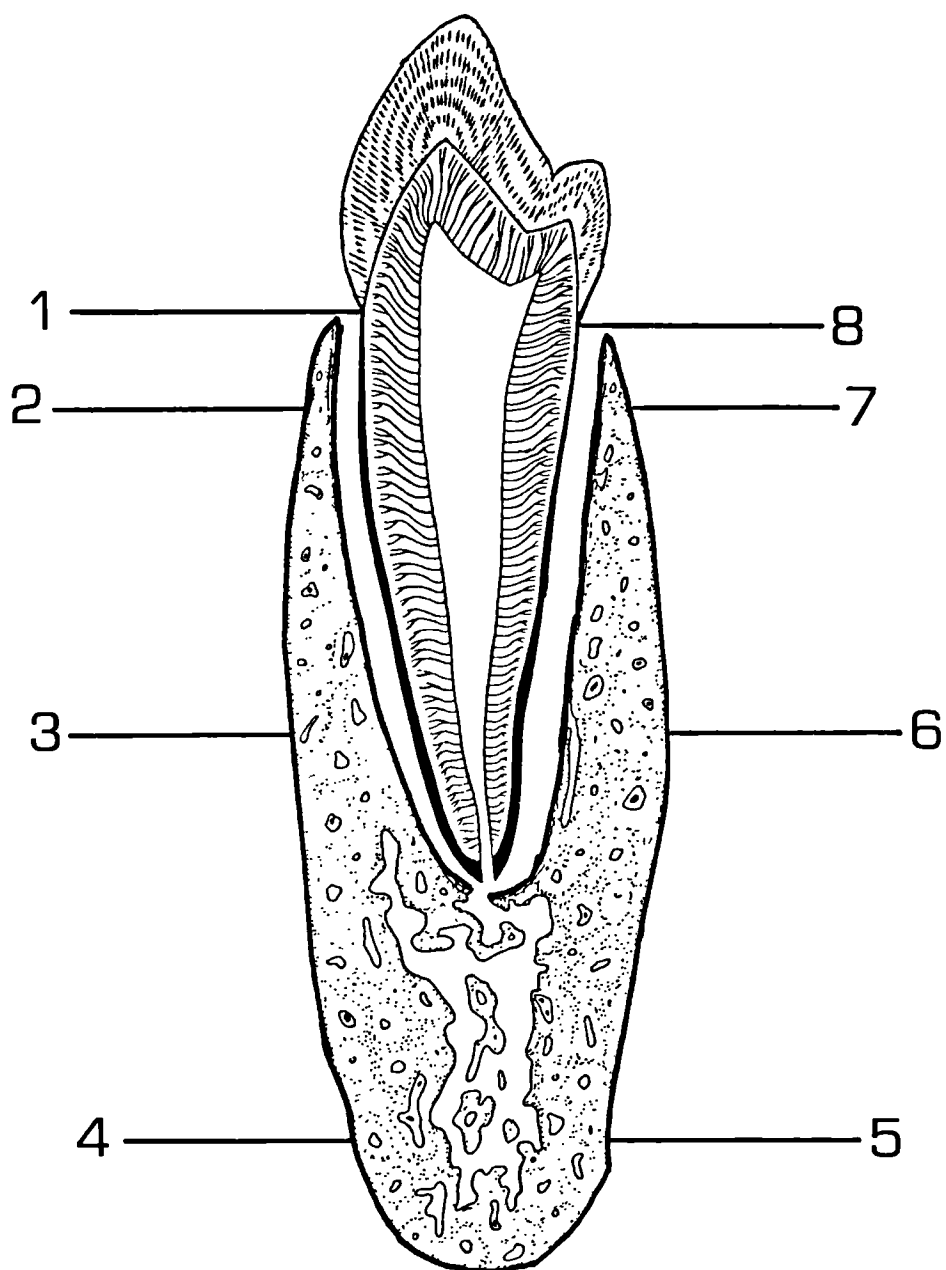


Figure 4.3 Diagram of sample sites per mandibular specimen. Invert image for maxillary specimens.

assessment of maximum ingress were regraded into 3 arbitrarily predetermined ranges where: -

Grade 1 = slight = < 100 mm

Grade 2 = moderate =  $\geq$  100 mm - < 200 mm

Grade 3 = deep =  $\geq$  200 mm - pulp cavity

Total distribution of invasive tunnelling was recorded as unaffected (0) or bilateral (B). The results from this regrading were then related to the ship's stratigraphy and plotted onto the culmulative silt phase schematic. The invasion, or not, of the periodontal joint (PDJ) space was also assessed.

#### 4.7 Results

The Lasertec 1LM11 CRM proved to be an excellent tool for the rapid screening of specimens and enabled the identity, location and distribution of post mortem change to be accurately assessed and measured. The marine-type change observed in chapter 2 was found replicated in all specimens affected by microstructural post mortem alteration. This was the only post mortem alteration observed in the sample group.

The distribution of the change itself varied from one specimen to another in terms of invasive depth and distribution, but was always peripheral leaving the PDJ unaffected, excepting in one case (specimen 14), where the PDJ space had been totally invaded. The enamel too (including calculus) was unaffected, although it was characteristically undermined by the microborings [Fig. 4.4a]. In intensely remodelled areas of dentine (tooth neck), no obvious directionality could be observed amongst the post mortem tunnels [Fig. 4.4b]; although at the invasive front of the tunnels or

microborings, an internal reflection artefact usefully demonstrated the course and direction of single tunnels once they dipped beneath the block face [Fig. 4.4c]. This suggested that dentine tubule direction and branching probably facilitated or influenced the initial direction of tunnelling. However, it is postulated that once a post mortem tunnel has been established, this intrusive feature will itself act as an avenue for further tunnelling. Alveolar bone similarly underwent peripheral tunnelling which typically (and descriptively) began at the alveolar crest and tracked round the external aspect to connect with the opposing alveolar crest. The invasive tunnels also lacked directionality in terms of the bony and vascular microstructure [Fig. 4.5a]. The depth of invasion in all the hard tissues was measured using the Lasertec system's integrated software [Fig. 4.5b], and was found to vary between specimens. Maximum tubule diameter was also measured at each measuring site [Fig. 4.5c].

The minimum and maximum diameter of the tunnels ranged between approximately 5-19 microns (nearest 0.5 micron) in all those tissues affected [Appendix 4.1]. Within this range of diameters two separate subgroups were distinguishable between 5-8 and 11-19 microns respectively [Fig. 4.6]. The commonest tunnel diameter fell within the first subgrouping, which represented 84% of total diameters measured. Circular sections of tunnels were identified and chosen for this measurement, and it is acknowledged that slight sectional obliquity may have contributed to an overall increase in tunnel diameters. However, this alone cannot account for the larger diameters recorded in the second subgrouping.

## **CAPTIONS**

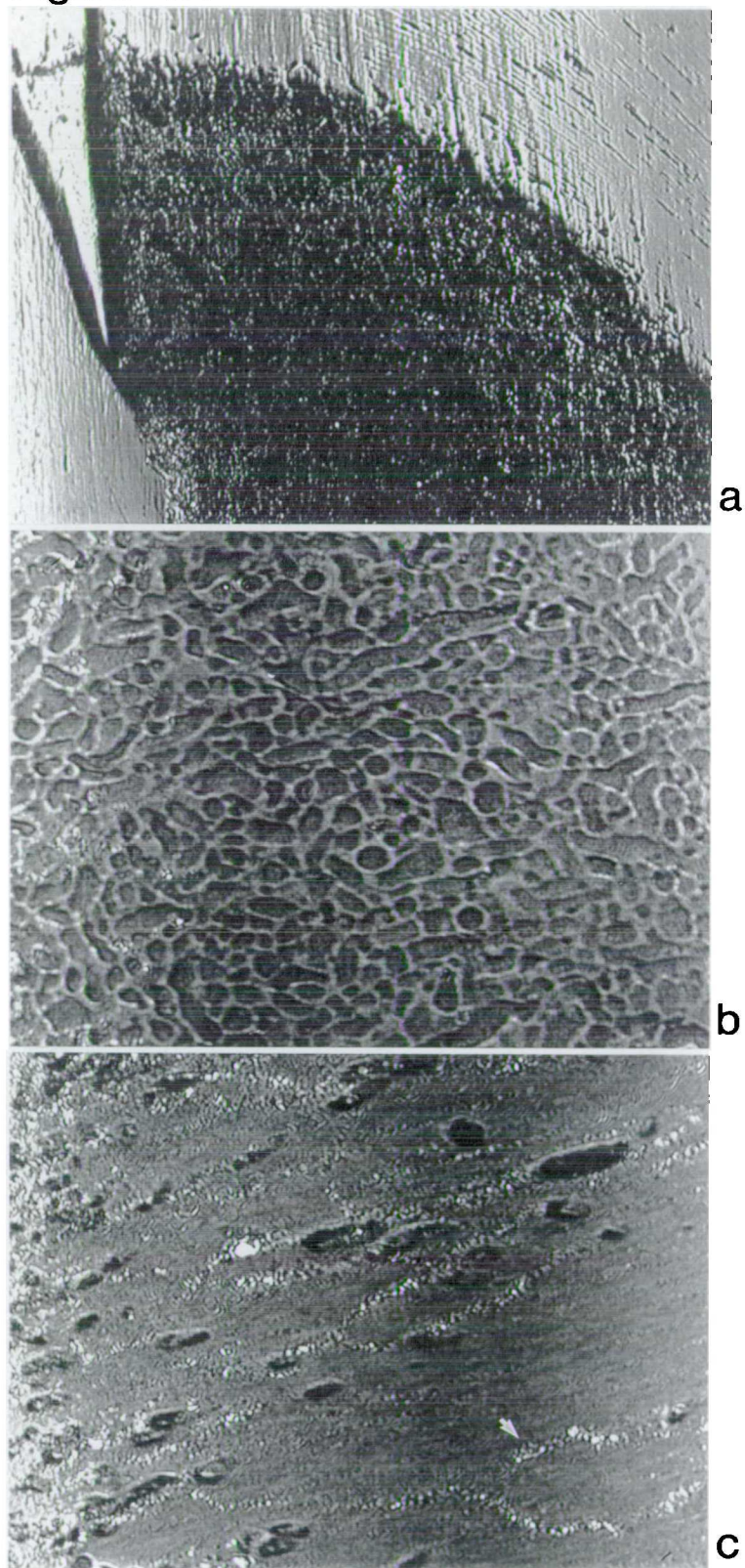
**Figure 4.4**

4.4a Enamel undermined by post mortem tunnelling. Field width 1100microns.

4.4b Dentine totally remodelled by post mortem invasion. Field width 130 microns.

4.4c Internal reflection artefact showing subsurface direction of post mortem tunnelling (arrowed). Field width 150 microns.

Figure 4.4





## **CAPTIONS**

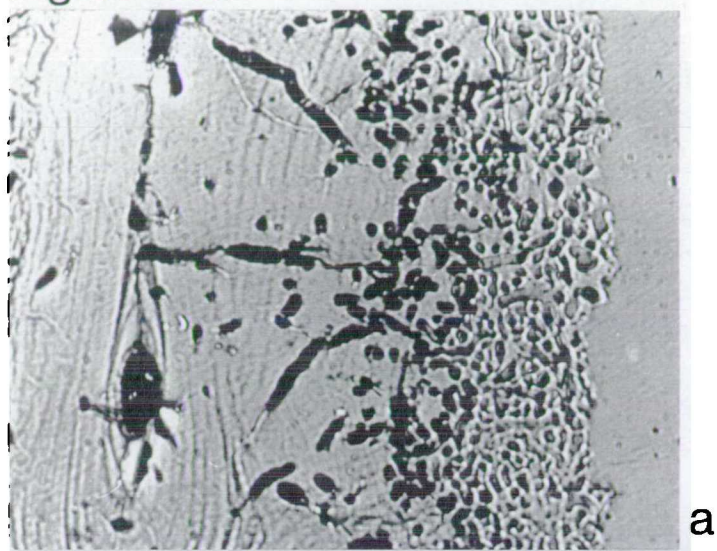
**Figure 4.5**

4.5a Alveolar bone affected by peripheral post mortem tunnelling. The darker tunnels are those which have not been penetrated by the embedding medium. Field width 400 microns.

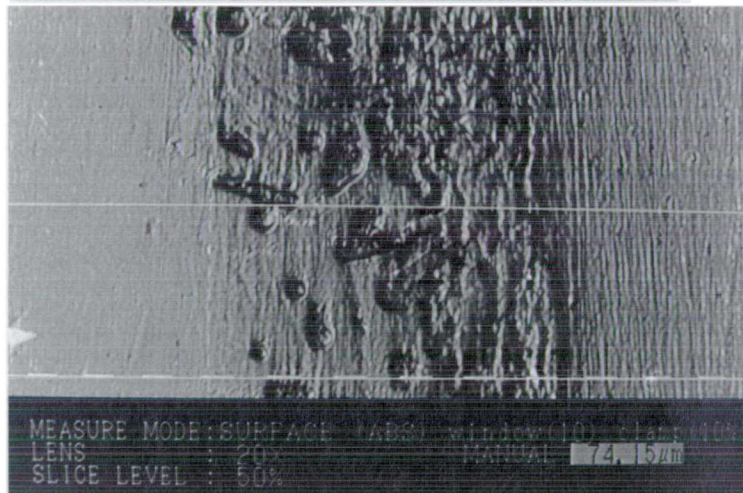
4.5b Alveolar bone measurement of maximum ingress at specimen sample site.

4.5c Alveolar bone measurement of post mortem tubule diameter at a specimen sample site.

Figure 4.5



a



MEASURE MODE: SURFACE (ABS) window( 0) clamp(10%)  
LENS : 20X MANUAL 74.15um  
SLICE LEVEL : 50%

b

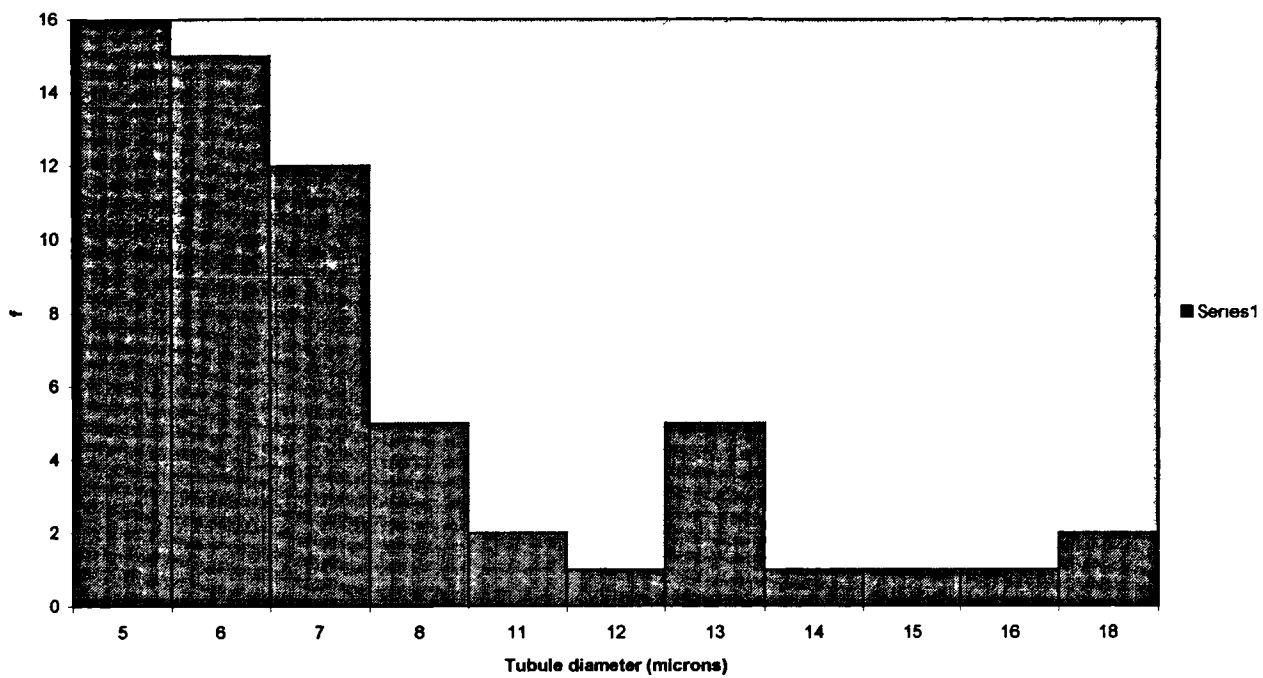


MEASURE MODE: SURFACE (REL) window( 0) clamp(10%)  
LENS : 80X MANUAL  
SLICE LEVEL : 50%

c

Figure 4 6

DISTRIBUTION OF TUBULE DIAMETERS (microns)



The blind study results from measuring maximum ingress per specimen [Appendix 4.2] were translated into slight (1), moderate (2) and deep (3) levels or gradations of invasion. In addition, total distribution was recorded as either unaffected (0) or bilateral (B) [Table 4.1]. The results from each specimen were then plotted onto the cumulative silt phase schematic [Fig. 4.7]. It was found that most of the sample group deposited in the initial Tudor layer exhibited no post mortem alteration. Only two specimens were affected by post mortem tunnelling: specimen 15 (mid silt phase, Orlop deck quadrant 9) exhibited slight bilateral tunnelling mostly to the mandibular alveolar bone; whilst specimen 14 (mid/lower silt phase, Hold quadrant 10) proved to have doubtful provenance and is considered to have originated from the second Tudor layer within the hold (Elkerton pers. comm., Mary Rose Trust). Those specimens deposited in the second Tudor layer were all affected by post mortem tunnelling, which tended to be bilateral in distribution with a graded depth of 2-3 [Fig. 4.8]. Two specimens from the main and upper decks exhibited slight attack with bilateral distribution, whilst two specimens from the hold and the Orlop deck were invaded fairly equally. One specimen, situated in the third layer, was found to be heavily invaded by post mortem tunnelling, with no evidence of bilateralism. This specimen was found within an area of localised scouring and may, at some juncture, been pushed intrusively upwards from the second layer and thus redeposited into the third (Elkerton pers. comm., Mary Rose Trust). No specimens were examined or present in the modern seabed layer.

The PDJ space was unaffected by post mortem tunnelling in all specimens excepting one, and this confirms earlier observations made on the Mary Rose

Table 4.1

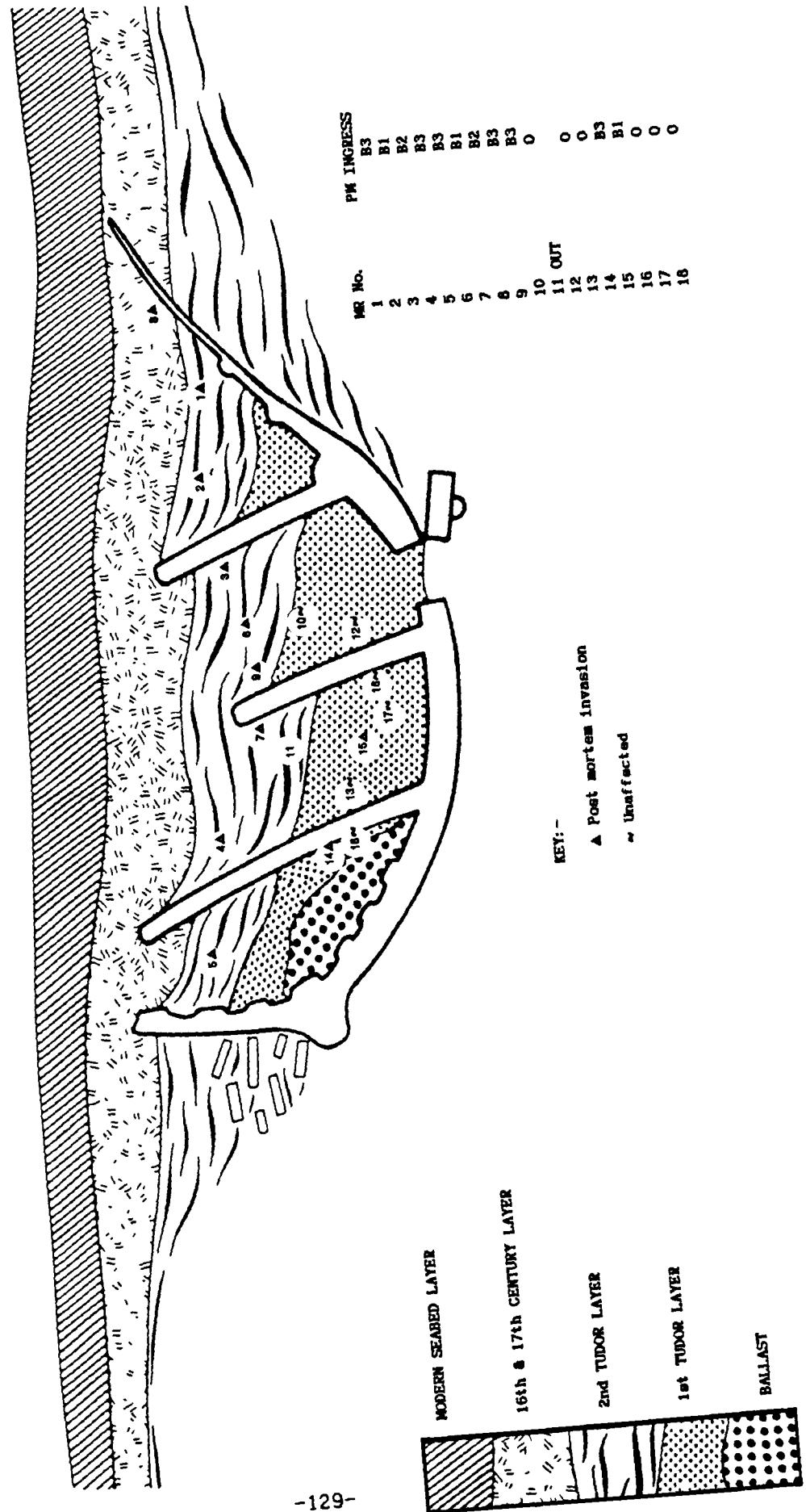
**TRANSLATED DATA GRADES**

MR No.	LSB No	SITES								Orientation	Final grad.
		1	2	3	4	5	6	7	8		
1	53	2	2	3	2	2	1	1	1	B	B3
2	52	0	0	0	0	1	1	1	1	B	B1
3	57	0	0	0	0	2	0	0	0	B	B2
4	64	3	3	3	3	3	3	2	3	B	B3
5	68	3	3	3	3	3	3	3	3	B	B3
6	58	0	0	0	0	0	1	1	1	B	B1
7	62	1	1	1	2	1	1	1	0	B	B2
8	54	3	3	3	3	0	0	0	3	B	B3
9	55	3	3	3	3	0	0	1	1	B	B3
10	59	0	0	0	0	0	0	0	0	O	O
11	61	OUT	-	-	-	-	-	-	-	-	-
12	60	0	0	0	0	0	0	0	0	O	O
13	63	0	0	0	0	0	0	0	0	O	O
14	70	3	3	3	3	3	2	3	3	B	B3
15	67	1	1	1	0	0	1	1	0	B	B1
16	65	0	0	0	0	0	0	0	0	O	O
17	66	0	0	0	0	0	0	0	0	O	O
18	69	0	0	0	0	0	0	0	0	O	O

Key:-

*B* bilateral*O* unaffected

Figure 4.7 Cumulative Silt Phase Schematic



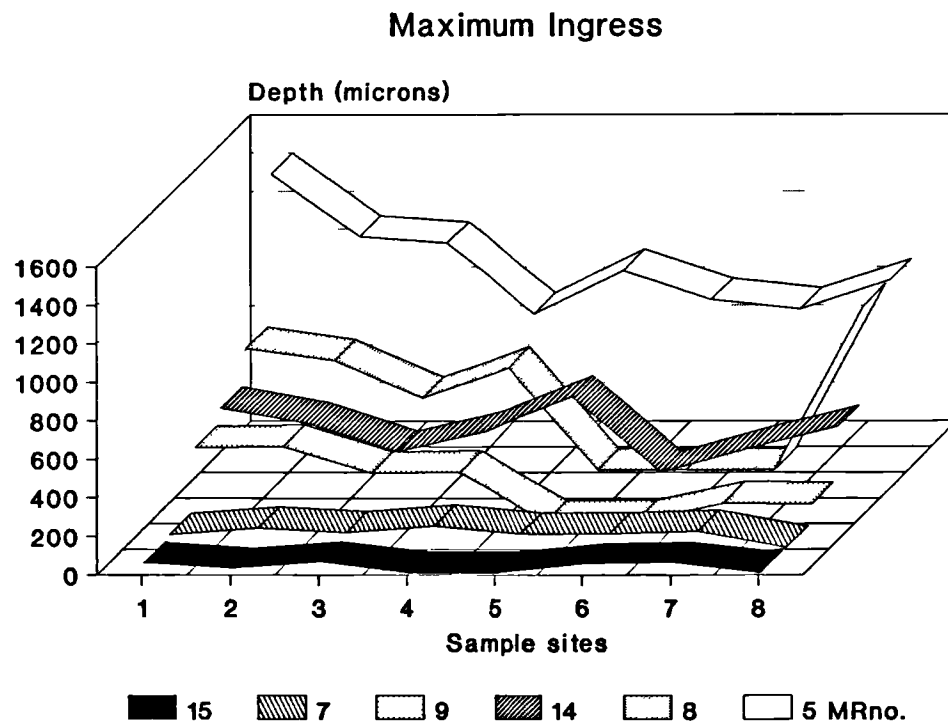
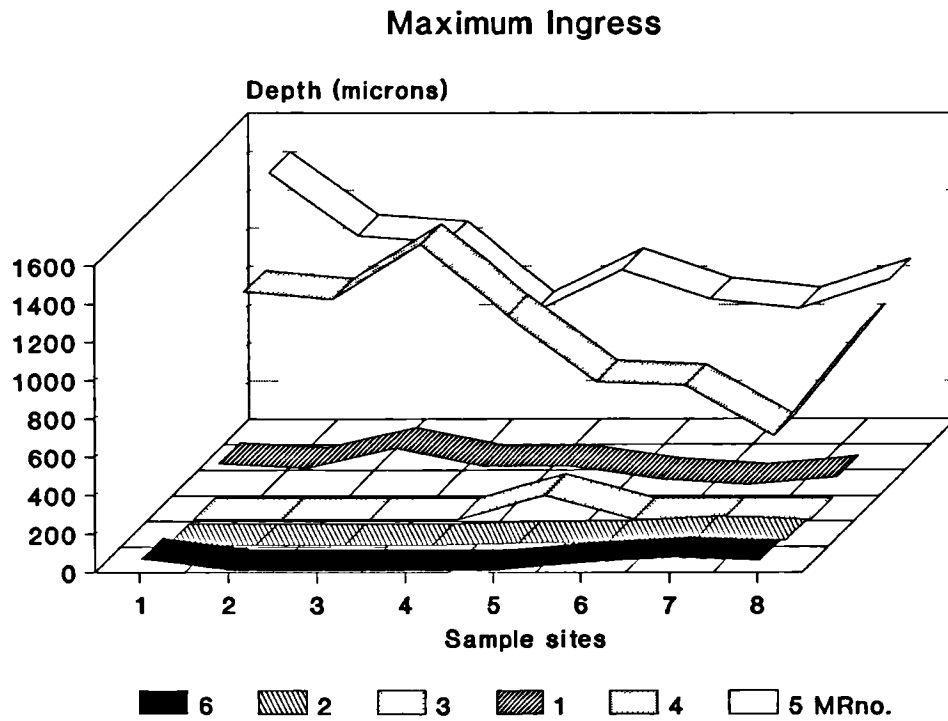


Figure 4.8 Bilateral ingress of post mortem tunnelling per specimen affected in the sample group. Specimen 5 is represented in both 3-axis graphs for scale.



material. The post mortem tunnelling, when present, consistently crossed from the neck of the tooth and progressed across an invisible line to continue peripherally from the alveolar crest. Occasionally, the tunnelling dipped slightly lower than the alveolar crest into the region of the PDJ, where tunnelling of the cementum and dentine could be observed on one aspect of the joint, with equivalent attack on the opposing medial aspect of the alveolar crest. The anomalous specimen 14 which exhibited pronounced post mortem tunnelling throughout the PDJ space, also had the identical peripheral distribution as the other specimens, and the diameters of the tubules for this specimen fell within the first sub-grouping.

#### 4.8 Discussion

The results from this study demonstrate for the first time, that a relationship can exist between microstructural post mortem change and site stratigraphy. This study also confirms and validates the notion that post mortem alterations to skeletal microstructure represent important, and to date unrecognised, taphonomic and environmental indicators.

A discussion of the results now follows layer by layer. The first Tudor layer represents a period of rapid silting which occurred immediately after the ship sank and lasted for a few months only. The specimens examined from this layer generally (excepting one specimen which was very slightly tunnelled) exhibited no post mortem changes whatsoever. Why is this? It is important to remember that after the ship sank all those individuals who were below topdeck had little chance of escape: they were trapped and must have either drowned or died immediately from traumatic injury. Their bodies will have cooled rapidly at a depth of 12-14 metres, and after

approximately 2-4 weeks the sodden bodies will have started to disarticulate, where bones and skin separate (Simpson & Knight, 1985; Smith, 1986). During this period the bodies would have floated around the decks or compartments freely unless pinned down by debris, and this accounts for the observed scattering of bone in all layers and on all decks. This also allows enough time for decomposition to be close to skeletonization prior to the rapid formation of the first Tudor layer. If this was not the case, one would have expected to see partially or totally articulated bodies encased within the first layer, and this was not the case. Another important factor is that the ship rested on her starboard side, which essentially meant that this aspect became the ship's bottom, and therefore was the coolest and darkest part of the ship. The ship sank in mid July and so the first layer would have been completed by mid winter. The fact that no post mortem tunnelling was observed in this layer suggests that conditions were not conducive to the endolithic micro-organism responsible for the observed profuse tunnelling in the second layer, or perhaps, simply there was not enough time.

The second Tudor layer formed much more slowly than the first, taking years rather than months to form. Specimens examined from this layer were all tunnelled and the overall distribution of this tunnelling showed considerable bilateralism. The depositional history of this layer is very interesting. The layer itself consists of a fine grey clay, full of seaweed lenses. This suggests that sufficient light and water currents were permeating this part of the ship to sustain seaweed growth, and that the seaweed itself would have contributed some stability to the silt bed. During this period, the upper superstructure of the ship collapsed leaving

all decks, including the hold, exposed to an open seabed environment (Elkerton pers. comm., Mary Rose Trust). This would have had the net effect of opening up a semi-enclosed system to more light, heat, increased current borne fauna and detritus. Hence, human skeletal material situated in this part of the ship would have provided an ideal substrate for an endolith which potentially required light, a slight increase in temperature, a silt free environment for feeding on detritus or other microscopic fauna, and which had the capacity to recolonise cyclically. This, deductively, is exactly what was absent during the formation of the first Tudor layer and is highly suggestive of either a silt sensitive polychaete, thraustochyrid or algae as the responsible micro-organism for most of the tunnelling. This type of substrate fouling would also help explain the observed differences in invasive depth and bilateral distribution, since deeper tunnel ingress could be achieved with the upside being preferable for recolonisation than the silt-side-down aspect. It is interesting to note that the two poorly provenenced specimens, the anomalous specimen 14, situated in the hold (1st Tudor layer) and specimen 8 on the upper deck (3rd layer), were both deeply tunnelled and this could reflect a change of orientation during scouring and at redeposition as well as long term marine exposure.

The results from this investigation are also highly relevant to the question of why marine organisms survive as fossils in far greater numbers than terrestrial ones:

"...sessile benthos or infauna (animals living in sediments forming the sea floor)...are more likely to survive (as fossils) than other aquatic creatures, and aquatic creatures more likely

to survive than terrestrial" (Rolfe & Brett, 1969: 218).

The skeletal remains of the sailors of the Mary Rose wreck represent terrestrial animals buried in an aquatic environment and, as such, are no different from the post mortem deposition of any aquatic mammal. The swift accumulation of the 1st Tudor layer elegantly illustrates the preservational properties of rapid silting. It is therefore likely that rapid silting plays a significant role in the survival of any skeletal tissue into the fossil record since it will inhibit the kind of substrate fouling observed here.

#### 4.9 Conclusion

The Mary Rose as a unique marine context, with well documented stratigraphy, has helped to demonstrate for the first time that microstructural changes to skeletal material (human or animal) can give or confirm information on stratigraphy as environmental indicators, and also provide taphonomic information on the post mortem history of a specimen: in this case, rapid burial and long term marine exposure. This aspect is particularly relevant to interpretative archaeology, forensic science and palaeontology.

## CHAPTER 5: A NEOLITHIC LONG CAIRN: LONG TERM SKELETAL EXPOSURE

### 5.1 Introduction

The total excavation of the Cotswold-Severn Neolithic chambered long cairn at Hazleton was unusually meticulous and represents an excellent example of long term skeletal exposure (Saville, 1990).

### 5.2 Historical background

The total excavation of the Neolithic long cairn at Hazleton took place between 1979 and 1982. The tomb was laterally-chambered, with a north and south chamber located approximately 25 metres from the widest end of the enclosing long cairn [Fig. 5.1]. The cairn was built using Cotswold limestone and at excavation was covered by turf. During the Neolithic period the south chamber remained intact and only minor structural disturbance was evident at its entrance. The north chamber had suffered a partial roof collapse during the Neolithic period, although burial did continue in the passage area. In both chambers the skeletal material was in an extremely disarticulated state, and the north chamber partial roof collapse probably contributed to some of the observed post depositional disturbance. At some point after the Neolithic period both chambers became infilled with cairn material, including loose soil, due to monument subsidence (Saville, 1990).

The skeletal material was meticulously recorded during excavation. As each bone, or bone fragment was uncovered, it was drawn and photographed in the normal way, and additionally given an individual number (routinely, individual numbers are attributed to whole or partial skeletons only). A

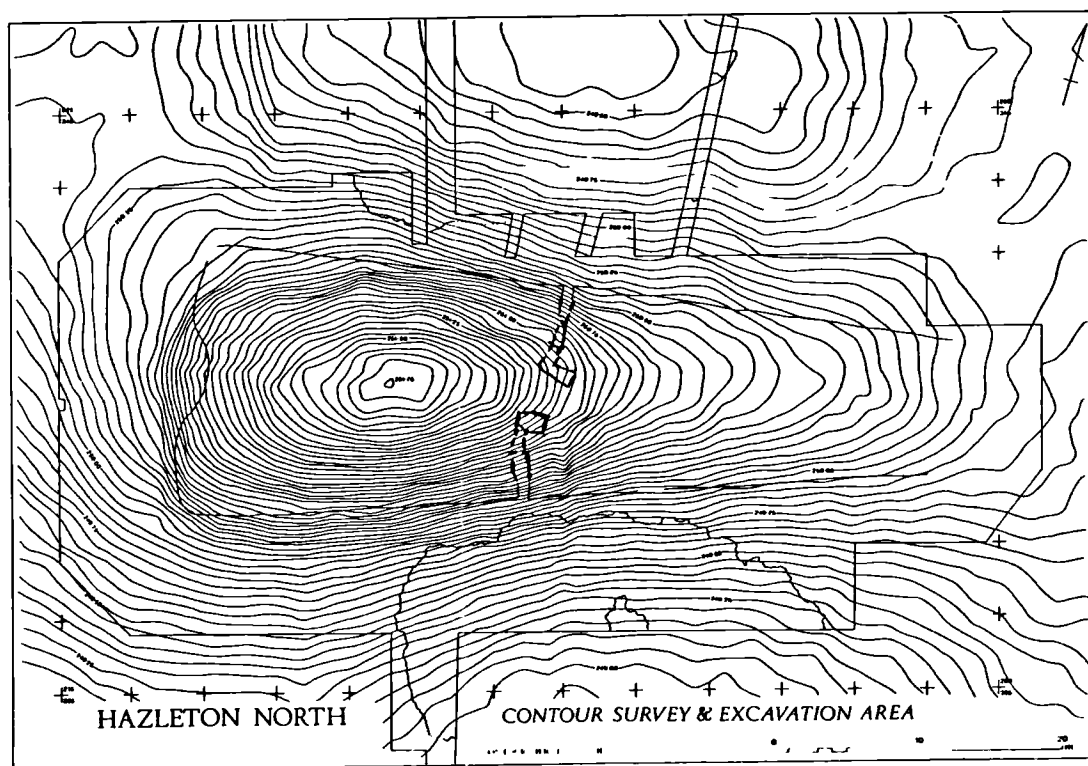


Figure 5.1

Contour map of long cairn illustrating the location of the two chambers (after Saville, 1990).

total of 9000 numbered human bones and fragments were assessed in this way (Saville, 1990). Owing to the extremely disarticulated state of the skeletal material [Fig. 5.2], individual numbering was essential if disarticulation and dispersion were to be mapped within each chamber. After excavation, specialist analysis provided information on conjoined fragments, bone pairing, bone articulation, dental occlusion between skull and mandible and individually matched pathology. From this information dispersal patterns could be mapped between related bones and bones belonging to distinct individuals. Two individuals were identified in the south chamber and four in the north. Dispersal was significant for all those individuals identified (Rogers, 1990). In addition, using minimum number analysis, a total of 14 adults and 11 children were identified as present in the south chamber and 7 adults and 8 children within the north chamber (Rogers, 1990).

The long cairn itself dates from about 3800 BC and burial activity is considered to have extended over a period of 300 years (Saville, 1990). Saville (1990) considered burial took place by direct inhumation into the chambered areas, and that subsequent burials necessitated the disturbance of previous burials causing the observed disarticulation and scatter of bones. No evidence of cut marks were found but rodent gnaw marks of an unknown date were evident (Rogers, 1990).

### **5.3 Microstructural evidence of exposure**

Information on terrestrial exposure of skeletal material has tended only to examine changes to external surfaces and much of this research has concentrated on skeletal dispersion and macroscopic post mortem damage such

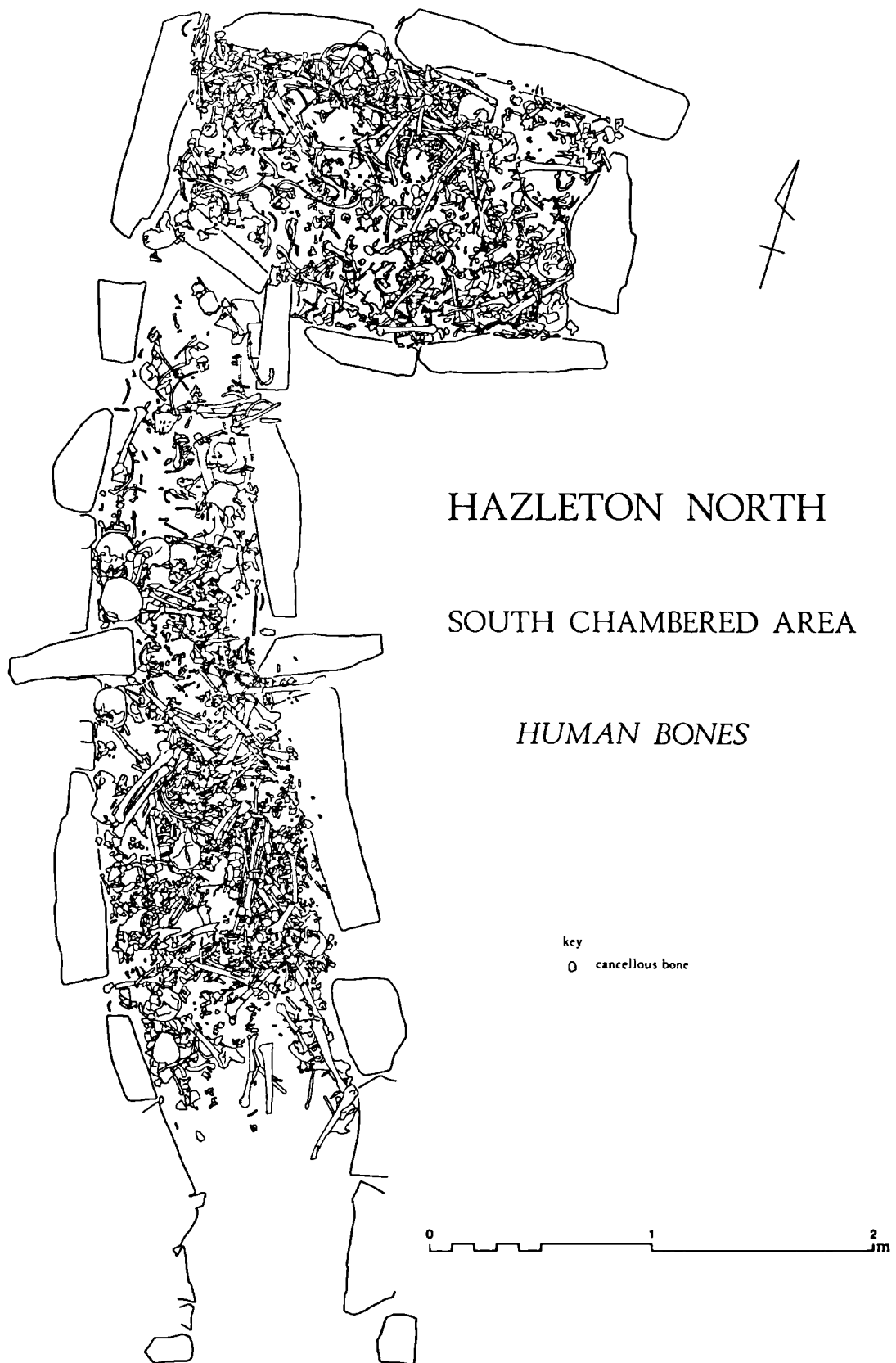


Figure 5.2

Spatial representation of total scatter of bones in the South Chamber  
(adapted from Saville, 1990).



as trampling fractures and gnaw marks (Lyman, 1994; Shipman, 1988; Weigelt, 1927). Little is known about internal microstructural changes to skeletal material related to exposure. Only one histological study by Yoshino et al. (1991) has addressed and documented an exposural change to one human bone out of 15 that had been experimentally exposed for 15 years. The micromorphology of that change consisted of a thin band of demineralisation, which extended from the periosteal aspect intracortically.

#### **5.4 Aims of this study**

Given the paucity of information regarding exposure-related microstructural change to skeletal material, it was decided to examine a well documented and unequivocal case of long term exposure. The meticulous excavation of the Neolithic long cairn at Hazleton presented an unique opportunity to do just that. The aims of this study were twofold:-

1. To identify post mortem microstructural change, if any, to skeletal material within each chamber.
2. To ascertain whether microstructural alteration differed between related specimens which had been spatially separated by post mortem disarticulation and dispersal.

#### **5.5 Material and methodology**

An occlusally matching skull and mandible were removed from each chamber and are spatially represented in Figure 5.3. The south chamber specimens belonged to Individual E (FDI: 26, 36), a juvenile aged approximately 12-15 years. The north chamber specimens belonged to Individual G (FDI: 65, 75), a child of approximately 3-4 years (Rogers, 1990).

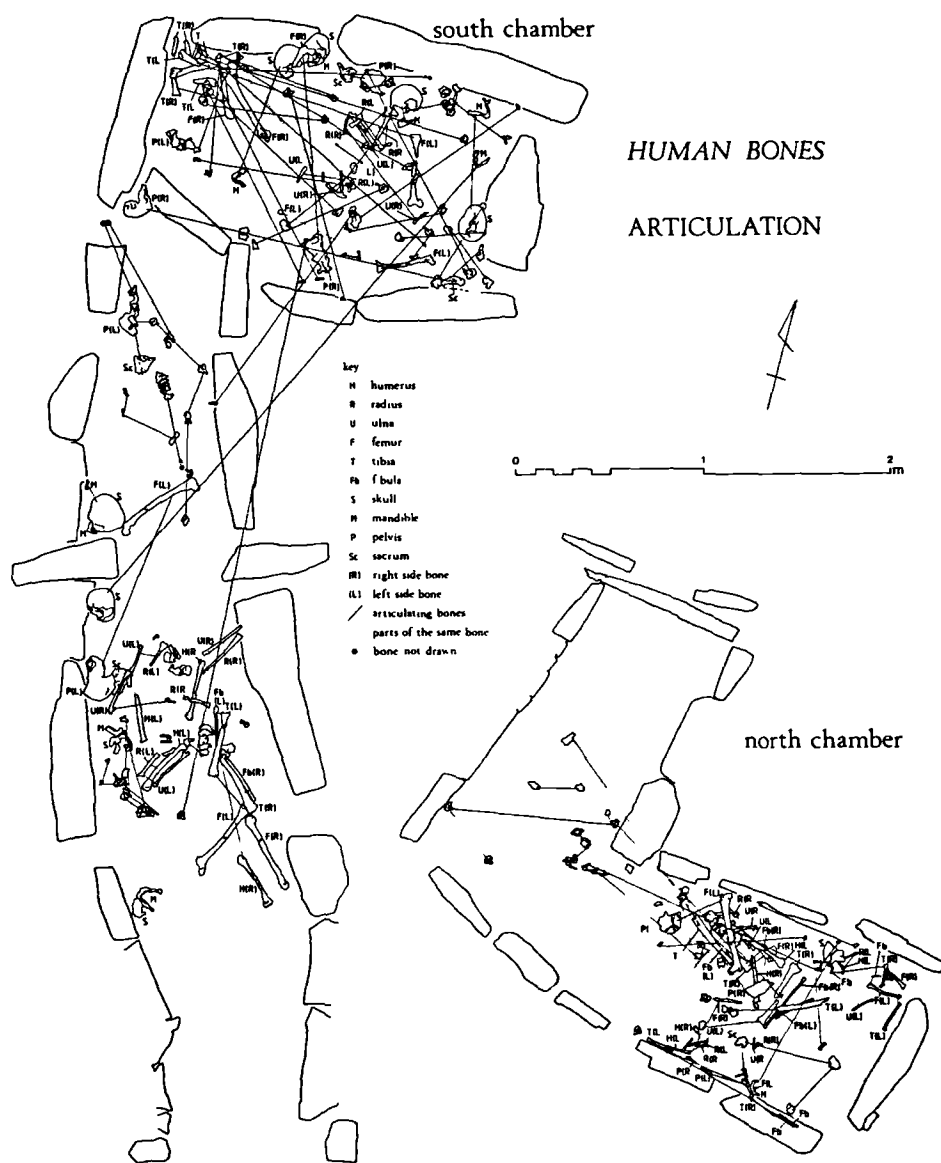


Figure 5.3

Spatial representation of 94, 95, 96 & 97 within each chamber (adapted from Saville, 1990).

The preparation of the specimens followed the same procedure as that outlined in chapter 2, where a single tooth and accompanying socket was removed from the mandible and the maxilla by cutting the entire tooth and socket free using a diamond-edged circular saw. The specimens were then embedded in PMMA and cut in longitudinal transverse section buccolingually. One face of the block was then polished on a rotary lap using graded abrasives and finished with a 1 micron diamond paste.

The uncoated blocks were then individually examined in turn under a Lasertec 1LM11 confocal reflection microscope (CRM) using a helium neon light source. This microscope has increased resolution over a standard optical reflection microscope and enabled identification of tissue morphology and characterisation of any potential post mortem alterations, due to the slight topographical relief created by polishing (Jones et al., 1992).

The specimens were then carbon coated and examined in a Zeiss DSM 962 SEM, operated in BSE mode at 10 kV. A four-segment solid-state BSE detector was used: for compositional imaging the signal used was the sum deriving from all four detector quadrants; whilst topographical images were produced by subtracting the South and East quadrants from the North and West. Hence, compositional images gave information on relative skeletal density and microstructure, since backscattering of high energy electrons increases proportionally with increasing atomic number (Boyde & Jones, 1983 a & b; Watt, 1985), whilst topographical images identified any surface topography which could have contributed artefactually to the backscattered electron signal (Howell & Boyde, 1994).

## 5.6 Results

The results from this study confirm that post mortem change to skeletal microstructure can occur in contexts involving long term exposure. The type of change found was typical of post mortem bacterial ingress, but only affected those specimens taken from the south chamber. No changes were observed in specimens belonging to the north chamber.

### South chamber

Individual E was dispersed widely within the south chamber, and specimens 96 and 97 were separated by a relatively large distance [Fig. 5.3]. The Lasertec CRM analysis revealed that alteration to specimen 96 was characteristic of post mortem bacterial ingress (demonstrated in chapter 2) where the enamel remained unaffected and dentine exhibited large scale coronal and radicular post mortem microstructural change [Figs. 5.4a - c]. Cementum in this specimen appeared unaffected [Fig. 5.4b]. The alveolar bone had also undergone extensive post mortem bacterial remodelling [Fig. 5.5a]. Specimen 97 exhibited the same distribution and type of post mortem alteration [Figs. 5.5b - 5.6b], except that the apical cementum was also affected [Fig. 5.6c] and the alteration to the alveolar bone was not as extensive as in specimen 96.

The SEM/BSE analysis of specimen 96 confirmed that the post mortem alteration detected using the Lasertec CRM was typical of that associated with bacterial ingress previously documented in chapter 2. The skeletal tissues other than enamel had all been extensively altered [Fig. 5.7a]. The dentine itself exhibited a range of demineralised and remineralised post mortem foci located extensively throughout the coronal and radicular

areas [Figs. 5.7b & c]. Characteristically, the peritubular dentine often remained intact, even when encased by post mortem demineralisation foci [Fig. 5.7d]. The cementum was also unaffected by bacterial remodelling and this is thought to be due to the poorly porous acellular layer acting as a natural barrier [Fig. 5.7c]. This barrier may also partly explain why post mortem foci often change their orientation at the CDJ, being forced to track along the numerous terminal branches of the radicular dentine tubules as well as the effect of the hypomineralized spaces provided by the granular layer of Tomes just below the acellular cementum [Fig. 5.8a].

#### **North chamber**

The dispersal of Individual G was not as great as Individual E, but the occlusally paired specimens were still spatially distinct [Fig. 5.3]. Specimens 94 and 95 exhibited no post mortem alteration to hard tissue morphology [Figs. 5.8b - d].

#### **5.7 Discussion**

The results from this study confirm that post mortem alteration of the hard tissues can occur in archaeological contexts involving long term exposure. However, the observed bacterial change to specimens taken from the south chamber is not one previously associated with exposure (see Chapter 2), and is unlike the type of exposural change reported by Yoshino et al. (1991). Further, this type of change was not seen in those specimens examined in the north chamber and this is curious, since both north and south chambers presented similar, if not identical, semi-enclosed aerobic burial environs. The only two known structural differences which differed between the two chambers was a compacted soil floor in the south chamber, and a roof

**CAPTIONS**

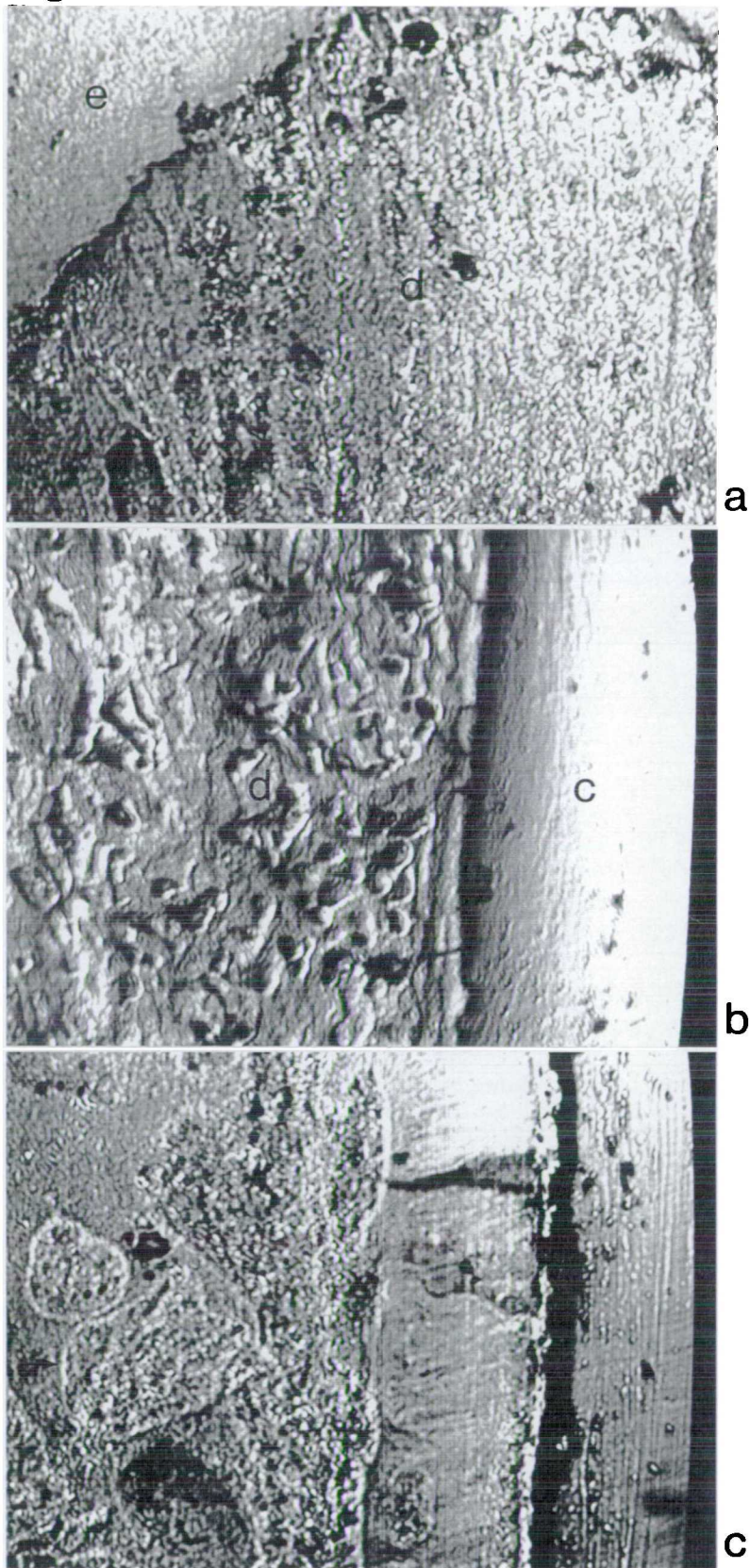
**Figure 5.4**

5.4a Specimen 96. Coronal dentine (d) showing extent of post mortem change. The enamel (e) is unaffected. Field width 120 microns.

5.4b Specimen 96. Radicular dentine (d) affected by post mortem ingress, but cementum (c) unaffected. Incremental lines of Salter are evident in the acellular cementum. Field width 970 microns.

5.4c Specimen 96. Close-up field of bacterial-type post mortem change in dentine, seen as large globular-like reflective features. 160 microns.

Figure 5.4





**CAPTIONS**

**Figure 5.5**

5.5a Specimen 96. Post mortem change to alveolar bone. Parallel ridging is due to differential wear of successive lamellae. Field width 970 microns.

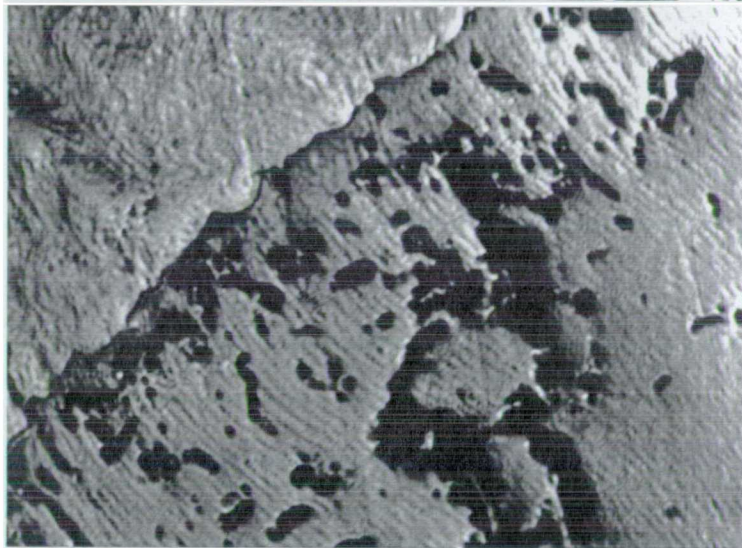
5.5b Specimen 97. Post mortem change evident in dentine at the enamel dentine junction. Field width 100 microns.

5.5c Specimen 97. Field of dentine extensively remodelled by post mortem alteration. The diagenetic foci appear randomly orientated. Field width 150 microns.

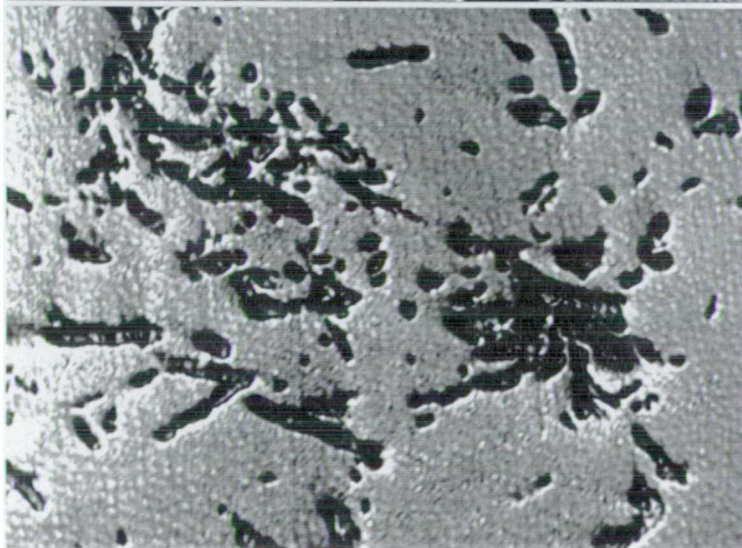
Figure 5.5



a



b



c

## **CAPTIONS**

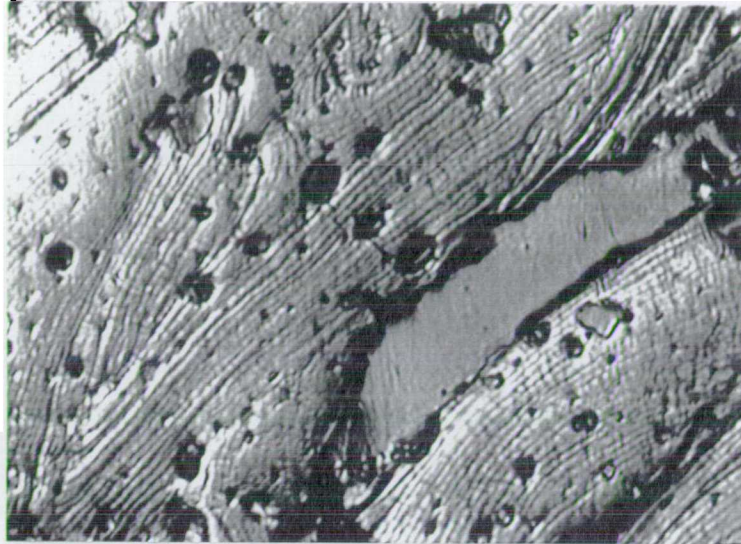
**Figure 5.6**

5.6a Specimen 97. Post mortem enlargement of alveolar bone osteocytic lacunae. The lamellae ridging is caused by polishing. Field width 970 microns.

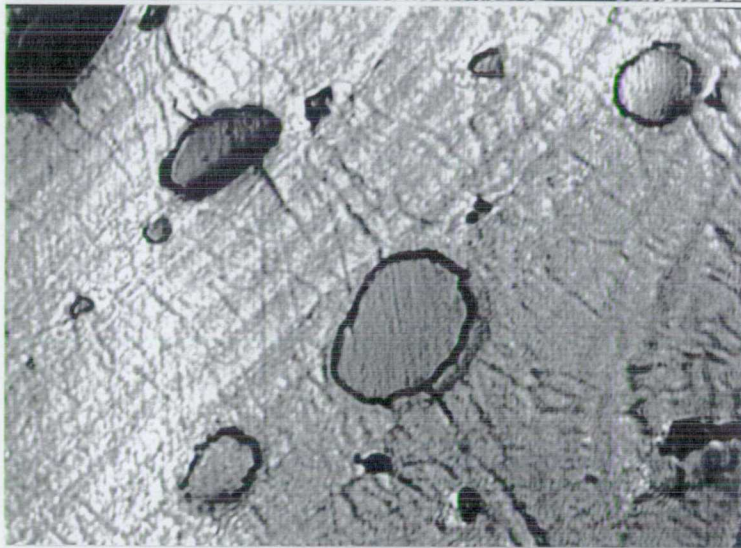
5.6b Specimen 97. Centre field of Fig. 5.6a showing enlargement of osteocyte lacunae alongside unaffected osteocyte lacunae. Field width 160 microns.

5.6c Specimen 97. Cementum in root apex affected by post mortem change. Post mortem change may be due to vascularization in this area, or to the lower mineralisation and cellularity. Field width 970 microns.

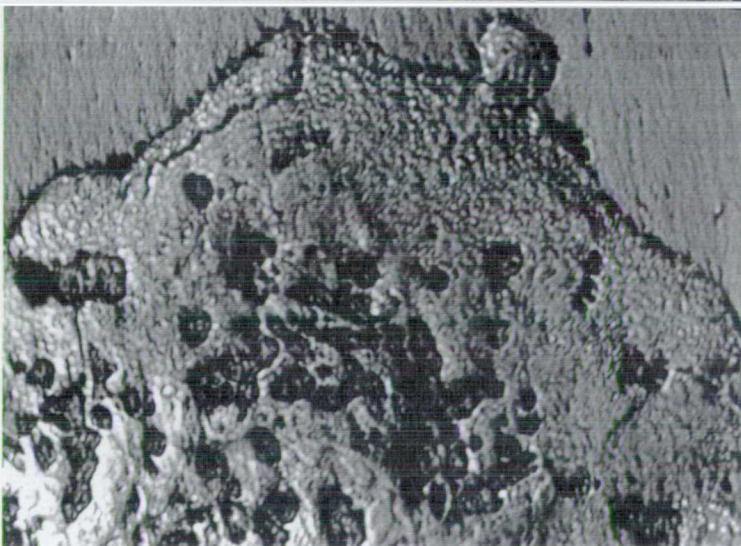
Figure 5.6



a



b



c

## **CAPTIONS**



## Figure 5.7

5.7a Specimen 96. The extensive distribution of post mortem change within this tooth and associated alveolar bone is evident. The alteration of dentine and bone mineral density is apparent. Magnification = scale bar.

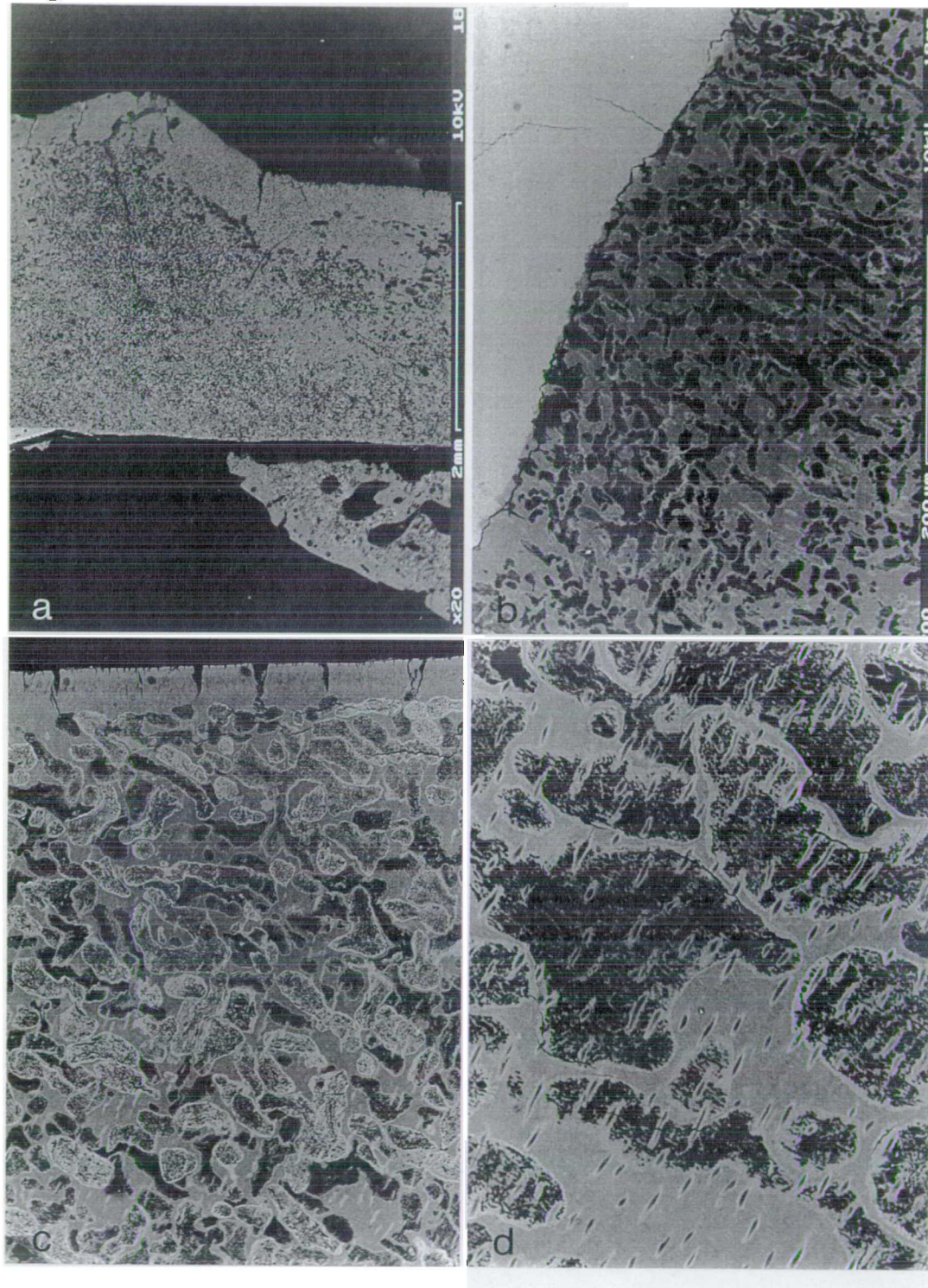
5.7b Specimen 96. Dentine extensively altered right up against the enamel dentine junction. Generalised demineralisation is apparent in this field. The enamel is unaffected. Magnification = scale bar.

5.7c Specimen 96. Radicular dentine extensively altered post mortem, whilst the cementum has remained unaffected. The post mortem foci are of increased and decreased density and appear to change direction at the cement dentine junction. Field width 350 microns.

5.7d Specimen 96. Diffuse demineralisation of dentine (single focus) with peritubular dentine passing through it apparently unaffected. The incremental plane is evident within the post mortem foci. Field width 140 microns.



Figure 5.7



**CAPTIONS**

### Figure 5.8

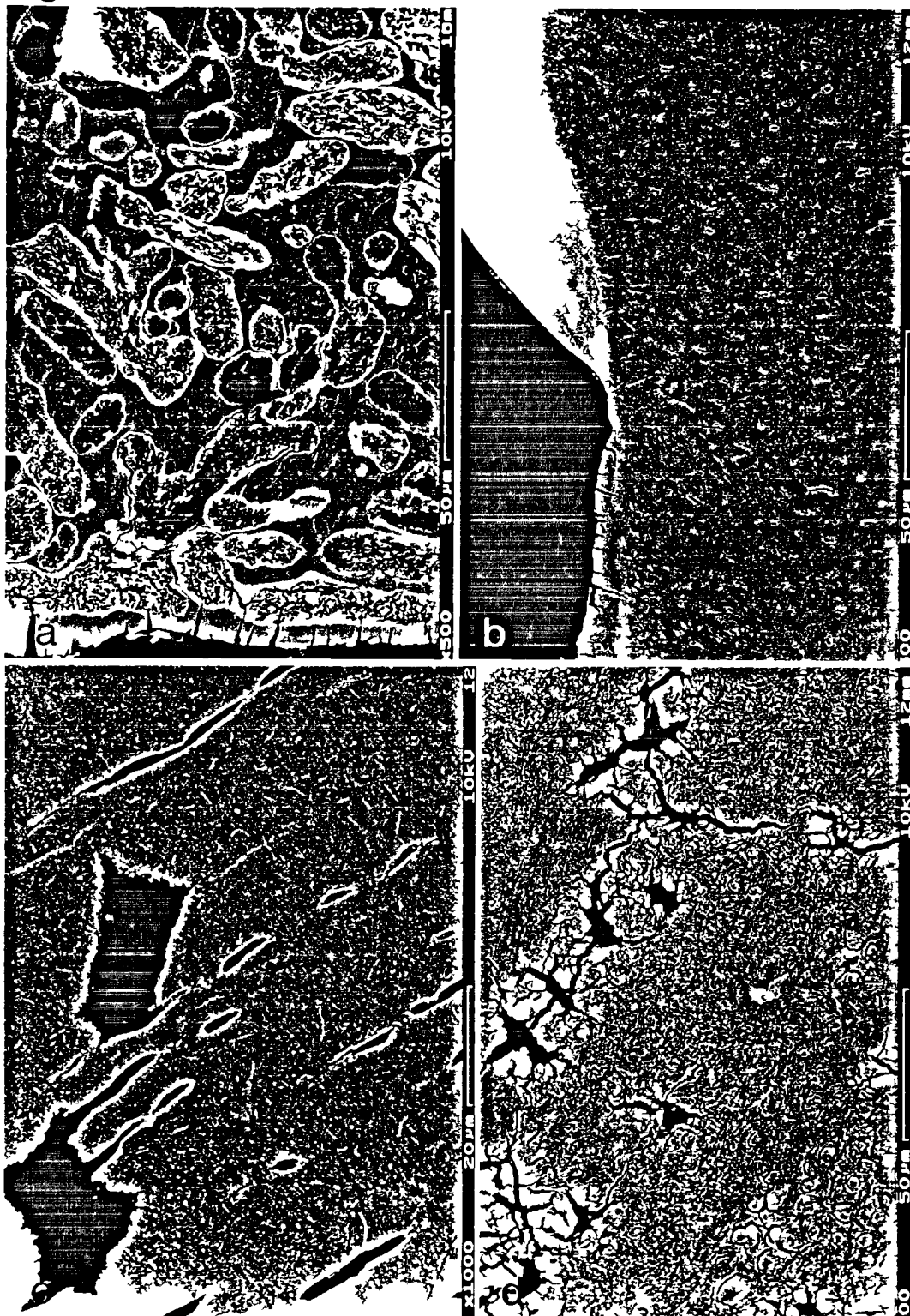
5.8a Specimen 96. Higher power view of cementum (left) with changed orientation of post mortem foci. These post mortem foci probably track along the terminal branches of the dentine tubules as well as being affected by the unmineralised spaces of the granular layer of Tomes. Again the post mortem foci are both increased and decreased in density relative to unaffected areas of dentine and cementum. Magnification = scale bar.

5.8b Specimen 94. Low power view of cement enamel dentine junction. All tissues appear normal. The cracks in the cementum are artefactual and are caused by forces exerted on the specimen during the exothermic polymerisation of the PMMA. The cracks themselves appear to have tracked along the orientation of the extrinsic fibres. Magnification = scale bar.

5.8c Specimen 94. Two regions of interglobular dentine within dentine which appears normal. Magnification = scale bar.

5.8d Specimen 94. Cementocyte lacunae and canaliculae appear normal, as do the Sharpey fibres which are mineralised peripherally with unmineralised cores i.e. extrinsic fibres. Magnification = scale bar.

Figure 5.8



collapse which affected the stone paved north chamber (Saville, 1990). On the basis of these differences it could, therefore, be argued that soil bacteria from the floor of the south chamber gained access to skeletonized individual E more readily than if the floor had been stone paved, as was the case with individual G in the north chamber. Or conversely, that soil bacteria played no role at all, given that monument subsidence introduced soil into both chambers at some time post Neolithic.

There appeared to be no differences that could be ascribed to spatial separation between those specimens examined from either chamber. The altered specimens from Individual E in the south chamber exhibited the same type, extent and distribution of post mortem change, even though both specimens were separated by a considerable distance. This is interesting because previous researchers have always asserted that post mortem alteration to skeletal tissues are environmentally driven, beginning at the point of skeletonization (or after) and that time as a variable is irrelevant to this whole process (see Chapter 1). If this model is correct, then one could expect to identify microstructural differences between anatomically related but disarticulated specimens, since their localised environments would have been slightly different, with post mortem attack potentially occurring or reoccurring at different times for each specimen over the past 4500 years. Whilst this should not effect the actual type of attack, the duration and intensity of bacterial ingress would have been likely to differ, due to intra-chamber microclimates. Since the Hazleton results do not fit this model, does this mean they are merely anomalous, or that the dominant model is wrong? If one accepts the idea of microclimates existing within the chambers, then it is likely that the

observed post mortem changes affecting Individual E occurred when the skull and mandible were still anatomically connected i.e. prior to or perhaps soon after skeletonization. The fact that Individual G remained unaffected by post mortem alteration suggests that other unknown co-factors were operating in this context of long term exposure.

## 5.8 Conclusion

The results from this study have confirmed that post mortem alteration of the hard tissues can occur in archaeological contexts involving long term exposure. The type of change observed was typically bacterial in its morphology, and has not been previously associated with long term exposure. That differences existed between the two individuals examined from each chamber is difficult to explain, unless the bacterial remodelling to the skeletal tissues began prior to, or at the point of, skeletonization; or, that each chamber had differing microclimatic or unknown factors operating to produce such distinct differences between the two individuals. It is therefore concluded that the dominant model for post mortem change to microstructure should be extended to include events prior to skeletonization, and that the co-factor of time may be highly pertinent to this whole process of change.

## CHAPTER 6: THE SPEED OF POST MORTEM CHANGE AND ITS TAPHONOMIC SIGNIFICANCE

### 6.1 Introduction

The speed of post mortem change to human skeletal remains has become an increasingly important question with regard to the efficacy of forensic techniques which rely on anorganic microstructural integrity (Gordon et al., 1988; Iscan & Kennedy, 1989; Zimmerman & Angel, 1986), including the retrieval of mitochondrial DNA from bone, where post mortem change is known to be detrimental (Chapter 8). The taphonomic significance of post mortem change has been little investigated.

That skeletal microstructure can change post mortem has been known from as early as 1864 (Wedl, 1864). The changes are caused by either the separate or combined actions of bacteria, fungi and other microflora (Wedl, 1864; Hackett, 1981; Marchiafava, 1974; Ascenzi & Silverstrini, 1984). The morphology and distribution of post mortem change has been documented by several authors (Hackett, 1981; Clement, 1963; Falin, 1961; Garland, 1989; Piepenbrink, 1986; Piepenbrink & Schutkowski, 1987; Poole & Tratman, 1978; Sognnaes, 1955; Stout & Teitelbaum, 1978) and has been reported to vary with the type of invading micro-organism, the terrestrial or marine depositing environment (Chapter 2; Ascenzi & Silverstrini, 1984), and the presence of ante mortem skeletal pathology (Chapters 2 & 3). Most authors who have examined archaeological human material consider time the least important contributory factor in the process of post mortem change, generally agreeing that post mortem alteration begins at the point of skeletonization (Piepenbrink, 1986; Piepenbrink & Schutkowski, 1987), whenever that occurs (Galloway et al., 1989), and once begun progresses at



an unknown rate over an unknown period of time. The earliest moment such a change can occur is unknown.

An important recent experimental study by Yoshino et al. (1991) investigated the potential speed of change to post mortem human bone in three different environmental contexts. Human bone samples were either exposed, buried in soil or immersed in sea water for 0-15 years. Specimens were periodically retrieved and microscopically assessed. The earliest post mortem alteration was observed in a soil specimen at 2.5 years post mortem, although this was considered unusual, the bulk of change to soil-buried specimens beginning after a 5 year period. Post mortem change to marine and exposure specimens were respectively 4-5 and 15 years (only one exposure specimen out of 15 was affected).

Previous experimental studies have produced results conflicting with those of Yoshino et. al. (1991). Syssoeva (1958) examined teeth buried between 6 months to 70 years and found no change to microstructure. Marchiafava et al. (1974) buried defleshed bone and observed fungal tunnelling in bone within 15-20 days. Hackett (1981) buried bone for 1 year and found bacterial-type post mortem alteration. Ascenzi and Silverstrini (1984) conducted a marine experiment immersing defleshed bovine bone in sea water and found post mortem change after 1 year. Wedl (1864) also undertook a water immersion experiment and obtained changes to dentine within 13-17 days. Clearly, the stage and rate of decomposition, the origin and type of invasive microbial flora and the environment, whether terrestrial or marine, all contributed as co-factors to the puzzling variation in experimental results. What conditions predetermine change from one bone to



another are also little understood, and all previous experimental work has been based on the premise that changes begin at the point of, or after skeletonization.

## **6.2 Aim of this study**

The aim of this study was to assess the potential speed of post mortem alteration to skeletal microstructure by examining a small group of forensic specimens retrieved from differing environs and time periods. The advantage of this approach over an experimental one was that true or actual speed of change could be assessed against differing natural environmental contexts, without setting experimental parameters on the sample group.

## **6.3 Materials and Methodology**

A sample of 11 human skeletal specimens from different Canadian environmental contexts was examined (all material was provided by Dr M. Skinner, Simon Fraser University [see Table 6.1]). The post mortem interval was calculated from the date of disappearance to the date of recovery. The sample extended over a range of 3 months to 83 years post mortem. The age and sex of each individual was known.

Thick sections were removed from bones and teeth using a wet diamond-edged circular saw. Bone sections were cut transversely, whilst teeth were sectioned longitudinally bucco-lingually. The sections were rinsed in water, allowed to air dry, and then placed in three 24 hour changes of 95% (by volume) distilled methylmethacrylate with 5% styrene (by volume) and 0.2% (by weight) 2,2'-azo-bis (2-methylpropionitrile). The specimens were transferred to an oven at 32°C and removed after the monomer had

TABLE 6. 1

## SAMPLE GROUP

Time since death	Anatomical location	Description
3 m	Tibial shaft	Female 86 yrs old. Environ: wet coastal. Possible exposure death. Fragment recovered from carnivore scat.
1 yr +	Rib 4th	Male 24 yrs old. Environ: dry, cold. Surface exposure.
15 m	Rib 4th	Male 91 yrs old. Environ: dry interior. Surface exposure in waterlogged muskeg bog.
2 yr	Rib 5th	Male 55 yrs old. Environ: mild wet coastal. Surface decomposition in leaf litter and shrubs.
2 yr	Tooth 4-5	Male 22yrs old. Environ: intertidal zone of salt water.
7 yr	Tooth 4-2	Male 69 yrs old. Environ: dry interior, lacustrine. Decomposition in water and partial burial of skull at high water mark in tree roots.
8 yr	Tooth 2-2 C2	Male 5.6 yrs old. Environ: dry interior, Surface decomposition, bones highly weathered and whitened.
70 yr	Rib 12th	Male 24 yrs old. Environ: Dry interior. Wood coffin burial 6 ft deep with unslaked lime on top. Executed.
78 yr	Rib 12th	Male 32 yrs old. Environ: as previous entry. Executed.
83 yr	Rib 12th	Male 28 or 34 yrs old. Environ: as previous entry. Executed.

polymerised to polymethylmethacrylate (PMMA). The embedded specimens were then re-cut transversely or bucco-lingually using an Isomet-11-1180 circular saw, polished using graded abrasives, and finished with a 1 micron

diamond paste on a rotary lap. Each block face received a coating of carbon in vacuo and was mounted on an aluminium stub.

The specimens were then examined using a Cambridge Stereoscan S4-10 or Zeiss DSM 962 scanning electron microscope (SEM), operated in backscattered electron (BSE) mode at 10 and 20 kV. A four-segment solid-state BSE detector was used: for compositional imaging the signal used was the sum deriving from all four detector quadrants; whilst topographical images were produced by subtracting the South and East quadrants from the North and West. Hence, compositional images gave information on relative skeletal density and microstructure (since backscattering of high energy electrons increases proportionally with increasing atomic number (Boyde & Jones *ab*, 1983; Watt, 1985)), whilst topographical images identified any surface topography which could have contributed artefactually to the backscattered electron signal (Howell & Boyde, 1994).

#### 6.4 Results

The earliest post mortem change was found 3 months after death [Fig. 6.1a & b]. The affected tibial fragment was recovered from a carnivore scat, which was considered scavenged from an exposure death, situated in a wet coastal environment. The microstructure and relative density of the specimen was characteristic of normal cortical bone. However, two sites of focal demineralisation were detected; one at the abraded periosteal aspect [Fig. 6.1a] and one intracortically [Fig. 6.1b]. The periosteal alteration was concentrated within a single osteon and exhibited three demineralisation foci located around enlarged osteocyte lacunae. The intracortical change had the same morphology as the periosteal change, but

extended inwards from the Haversian canal of a single osteon. No remineralisation in association with increased density was observed at either site.

The next post mortem change occurred in a 4th rib recovered 15 months post mortem. The recovered body was a surface exposure in a waterlogged muskeg bog, located in the dry interior of British Columbia. The rib was extensively affected throughout with what Hackett (1981) characterised as bacterial alteration to bone. The altered tissue itself was concentrically orientated along gross collagen lamellar planes in transverse section [Figs. 6.1c & d]. The post mortem foci did not cross cement lines and were localised around post mortem voids and enlarged osteocyte lacunae [Figs. 6.1d & 6.2a]. Both remineralised and demineralised foci exhibited intra-organisation of cavitation or of internal arrays of 1 micron diametered vacuoles [Fig. 6.2b].

The next observed change to microstructure occurred 2 years post mortem. The tooth came from a drowned individual recovered from an intertidal zone of salt water. The post mortem alteration was characterised by peripheral tunnelling around the neck of the tooth invading both the cementum and dentine and was identical to the marine change documented amongst the sailors of the Mary Rose wreck (Chapter 2). Although undermined for a short distance the enamel was unaffected [Fig. 6.2c]. The invading tunnels were approximately 5-7 microns in diameter and extended peripherally to a depth of approximately 300 microns [Fig. 6.2d]. No demineralisation was associated with the leading aspect of the tunnelling, nor was there any sign of remineralisation at the tunnel boundaries. The organisation of the

tunnels themselves appeared to have little regard for dentine tubule direction, but it is possible that dentine tubule branching may have contributed to or facilitated the invasion.

Two further post mortem changes were observed. At 7 years post mortem a slight change was observed in the cementum of a tooth [Fig. 6.3a], retrieved from a lacustrine/burial context. The change was two small post mortem foci, sited approximately half way down the root, of approximately 70 and 30 microns maximum width. The foci comprised slight demineralisation of the cementum, with a clear remineralised leading band of increased density. The second change was found in a 12th rib, 70 years post mortem. This individual had been executed and buried 6 feet down in a wooden coffin with unslaked lime on top. The change was located as a diffuse band of demineralisation around the whole periphery of the rib [Fig. 6.3b]. The band itself extended intracortically for approximately 50-100 microns from the periosteal aspect [Fig. 6.3c]. Most of the intracortical area of the rib and the entire endosteal aspect were unaffected.

## 6.5 Discussion

The results from this study confirm that post mortem alteration to skeletal tissues can occur very soon after death, change being identified in the earliest specimen examined at 3 months post mortem. Of the other changes detected, the bacterial type occurred within 15 months and the intertidal salt water zone specimen, with typically marine type alteration, within 2 years. The results set a new in-situ time frame for both these morphological types. The other findings, occurring within 7 and 70 years

**CAPTIONS**

**Figure 6.1**

6.1a SEM/BSE image of demineralisation foci (arrowed) situated at the periosteal aspect. 3 months since death. Recovered from carnivore scat.

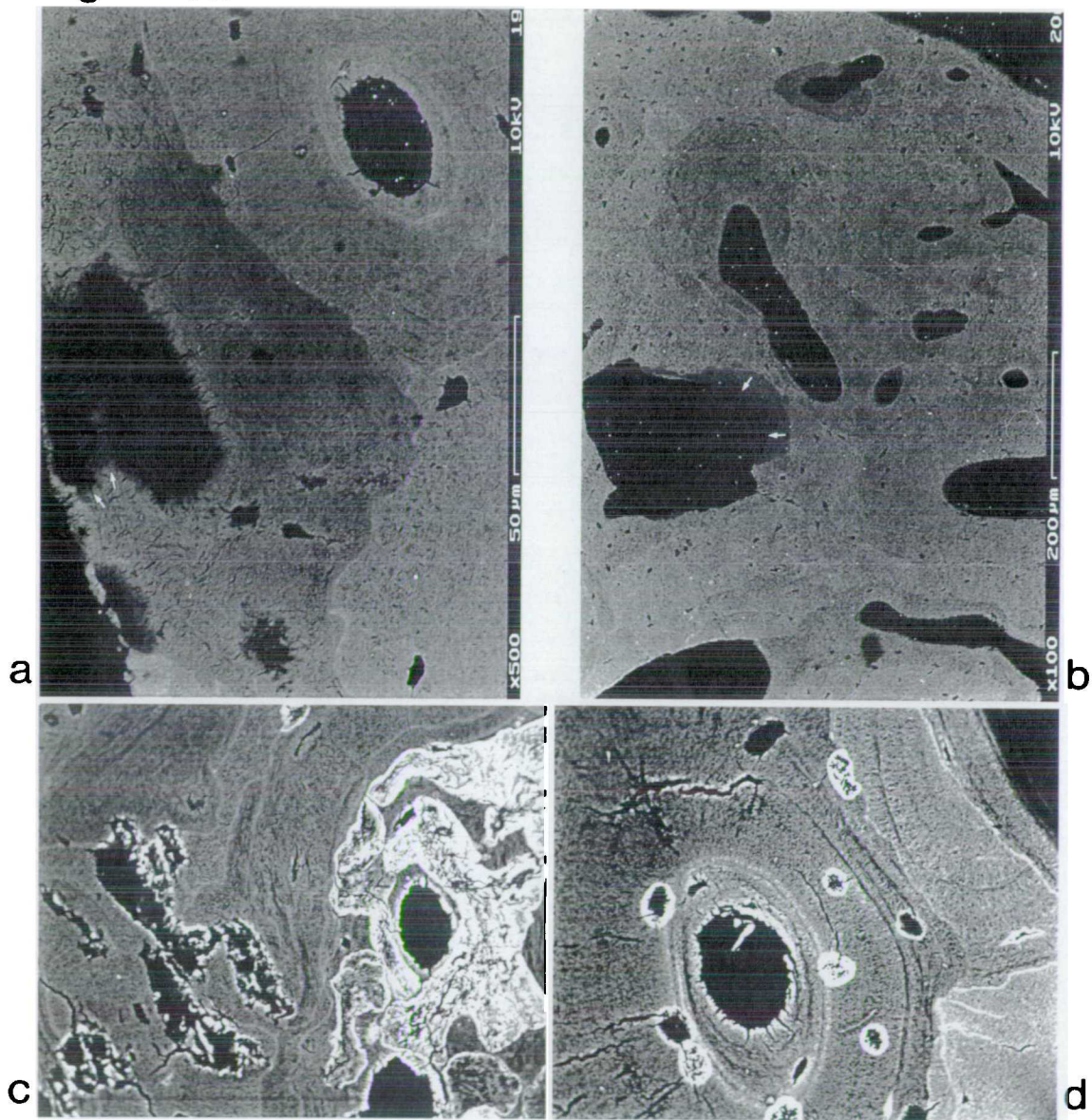
Field width = magnification bar.

6.1b SEM/BSE image of demineralisation zone located intracortically. 3 months since death. Recovered from a carnivore scat. Field width = magnification bar.

6.1c SEM/BSE image of bacterial-type alteration concentrically orientated along gross lamellar planes within an osteonal system. 15 months after death. Recovered as a surface exposure. Field width 110 microns.

6.1d SEM/BSE image of bacterial-type alteration located within a single osteonal system, which do not cross cement lines and are located at sites of osteocyte lacunae with a corresponding increase in mineral density. 15 months after death. Recovered as a surface exposure. Field width 110 microns.

Figure 6.1





## **CAPTIONS**

## Figure 6.2

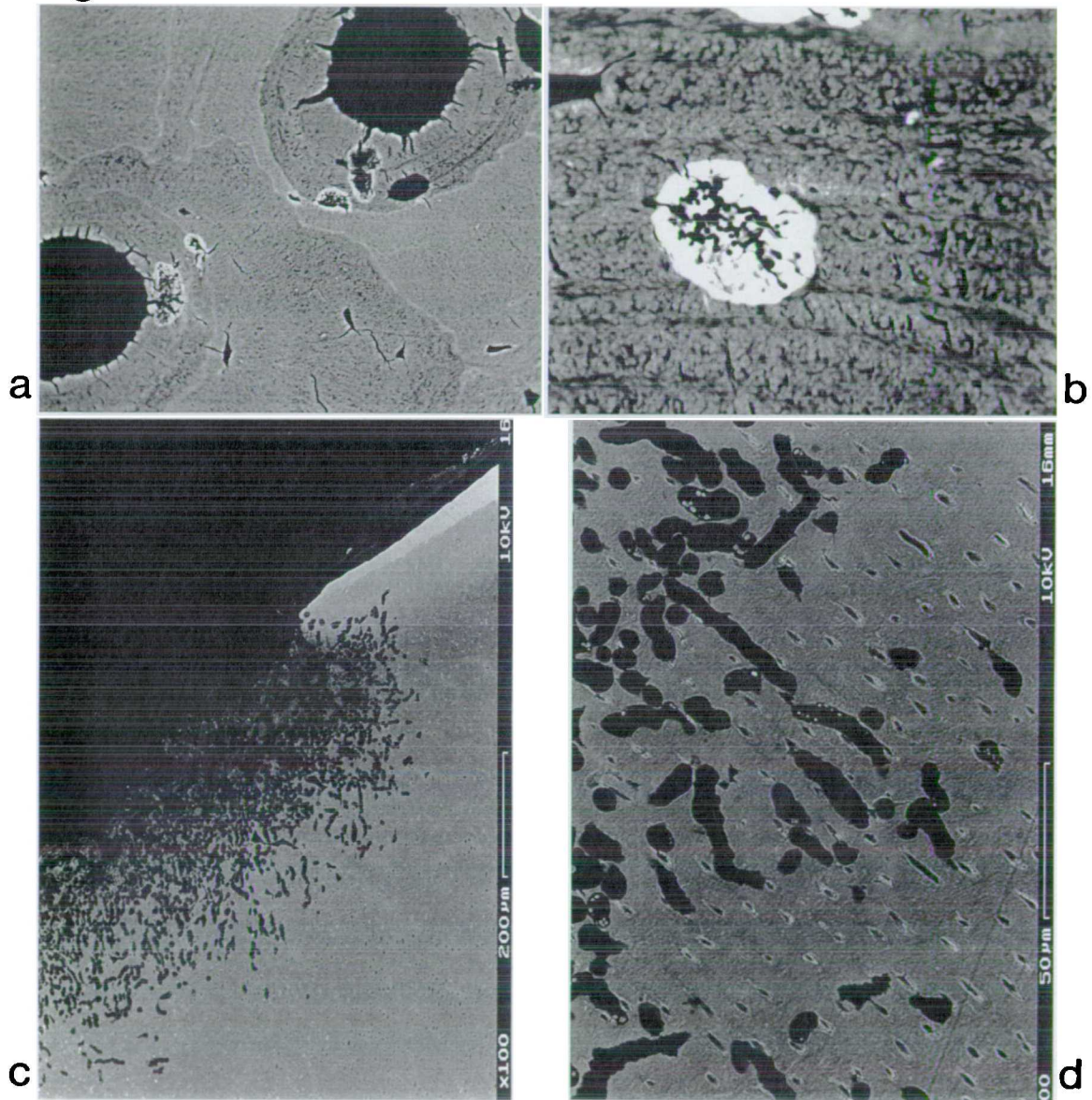
6.2a SEM/BSE image of bacterial-type alteration located within a single osteonal system, which do not cross cement lines and are located at sites of osteocyte lacunae with a corresponding increase in mineral density. 15 months after death. Recovered as a surface exposure. Field width 270 microns.

6.2b SEM/BSE image of single bacterial-type alteration displaying an overall increase of mineral density and containing an internal array of 1 micron vacuoles. 15 months after death. Recovered as a surface exposure. Field width 30 microns.

6.2c SEM/BSE image of tooth neck where cementum and dentine has been peripherally invaded by tunneling to an approx. depth of 300 microns. Although undermined by the invasive tunnelling the enamel remained unaffected. 2 years since death. Drowned, intertidal zone of salt water. Field width = magnification bar.

6.2d SEM/BSE image of invasive tunnels (diameter 5-7 microns), penetrating dentine without any evidence of remineralisation at tunnel boundaries. 2 years since death. Drowned, intertidal zone of salt water. Field width = magnification bar.

Figure 6.2



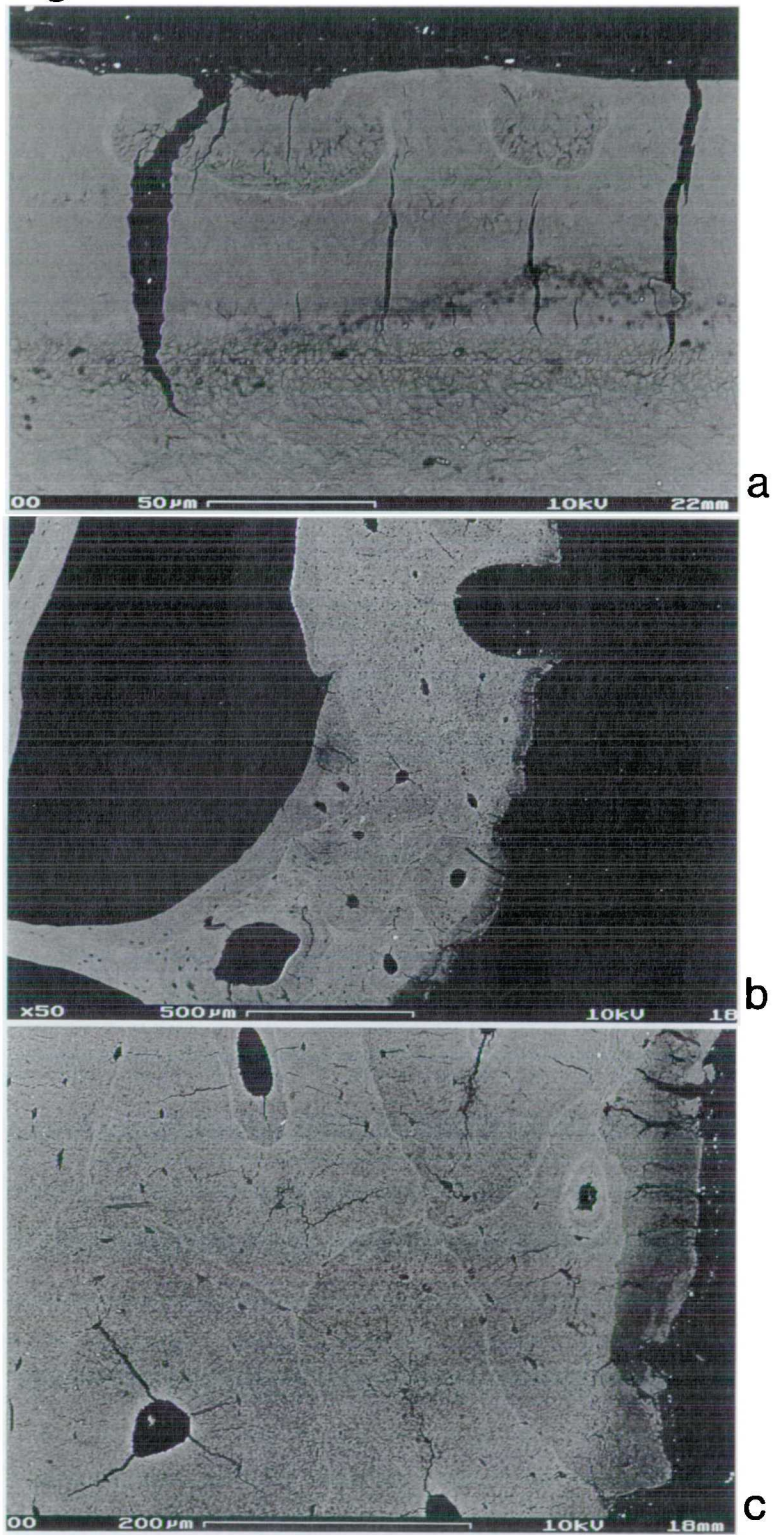
## **CAPTIONS**

**Figure 6.3**

6.3a SEM/BSE image of radicular cementum with two possible post mortem lesions situated halfway down root. The lesions are small and exhibit an area of slight demineralisation with a clear remineralised leading band of increased density. 7 years since death. Retrieved from partial lacustrine /burial context. Field width = magnification bar.

6.3b & c SEM/BSE image of diffuse band of demineralisation extending peripherally around the whole rib to a depth of 50-100 microns. 70 years since death by hanging. Buried 6 feet deep in a wooden coffin topped with unslaked lime. Field widths = magnification bars.

Figure 6.3



post mortem, concur with those of Yoshino et al.'s (1991) findings with regard to time.

The taphonomic relationship between environment and post mortem change in bones and teeth gains support from this new data. The localised change to the 3 month specimen is similar to the exposure change noted by Yoshino et al. (1991), and this is consistent with the possibility of partial skeletonization and disarticulation by an animal scavenger, although the effects of gut demineralisation cannot be ruled out (Andrews, 1990). The bacterial type of change to the waterlogged bog specimen, 15 months post mortem, is a new environmental location for this phenomenon. Possibly, the combined aspect of bog and air contributed favourably to a range of aerobic and anaerobic micro-organisms gaining access to the bones and teeth (the bog pH is unknown). The specimen retrieved 2 year since death, found in an intertidal zone of salt water, is exciting because it exactly replicates the post mortem marine morphology and distribution observed in the estuarine sea burial of the sailors of the Mary Rose (Chapter 2). This type of change is considered to begin at the point of skeletonization, potentially caused by a range of boring micro-organisms (Raghukumar et al., 1989; Golubic et al., 1975; Soudry, 1979) which use the skeleton as a fixed location for filter feeding silt free sea water. Interestingly, the post mortem change to the 7 year partial lacustrine/burial specimen, although very small and localised, was highly suggestive of bacterial type ingress (Chapter 2; Hackett, 1981), rather than tunnelling associated with the marine context (Chapter 2; Ascenzi & Silverstrini, 1984). In addition, the peripheral demineralisation of the 70 year specimen, observed as an exposure change in Yoshino et al.'s (1991) study, occurred in a burial



context, where no exposure had been documented (no such post mortem alteration was observed in the two individuals executed and buried under the same conditions [see Table 1]). Two explanations are possible: one is that the body was exposed and skeletonized prior to burial; or, and more likely, unknown co-factors predetermine whether such a change will occur or not. This variability is already known to exist within and between environmentally similar archaeological groupings e.g. the crew of the Mary Rose (Chapter 2) vis-a-vis the crew of the Vasa (During, 1990), the Spitalfields Crypt excavation (Molleson & Cox, 1993), and an English Civil War mass grave (Chapter 8).

The results from this study, although bringing forward the time-frame for post mortem change to the skeleton, do not refute the notion that this process begins at the point of, or after, skeletonization (it is acknowledged that the rate of skeletonization rate varies (Galloway et al., 1989)). It is a curious fact that although it is known that endogenous gut microflora promote early stages of body decomposition (Gordon et al., 1988) it is exogenous microflora (usually soil related) which are solely implicated in skeletal post mortem change (Yoshino et al., 1991; Berg, 1963). This idea has been adopted and utilised in archaeological and geochemical research which has tended to consider skeletal remains as depositional artefacts, subject to diagenetic alteration via the biologically porous network of empty vascular and cellular spaces (Piepenbrink, 1986; Piepenbrink & Schutkowski, 1987; Grupe et al., 1993; Tuross et al., 1989; Pate & Hutton, 1988; Kyle, 1986; Nelson & Sauer, 1984; Keeley et al., 1977). This notion has been accepted and utilised as defleshed bone in experimental protocols (see Introduction). However, the



idea has not been tested and the evidence for post mortem change potentially beginning earlier and being possibly of endogenous origin is strong.

In life the intestinal mucosa acts as a barrier preventing the invasion of endogenous microflora of the gut lumen transmigrating into the body (Marshall, 1991). Only under certain circumstances can gut microflora transmigrate, and when this occurs it is primarily into the portal vein and to a lesser extent via the mesenteric lymph system (Mainous et al., 1991). After death the intestinal mucosa no longer functions as an effective barrier and it has been experimentally demonstrated that bacteria can cross the intestinal mucosa within 15 hours post mortem (Kellerman et al., 1976). Bacteriological studies of post mortem blood have confirmed the rapid motility of this invasion, via the vascular network, reaching all the major organs of the body within 24 hours (Harper, 1989; Corry, 1978; Dolan et al., 1971). Indeed, invasion of the medullary cavity and Haversian canal has been reported as "bone taint" in the bones of cattle and pigs, by Clostridia, Proteus and faecal Streptococcus bacteria (Ingram, 1952; Haines & Scott, 1940). Is it not then conceivable that endogenous bacteria, given the right conditions, could rapidly transmigrate via the vascular network, to all the bones of the skeleton, passing into the marrow cavity via the nutrient arterial and venous vasculature, and so spreading intracortically into the Haversian supply. If this is the case, then initial post mortem change to skeletal microstructure could begin very soon after death, and well before skeletonization. Indeed, the very manner of death, with regard to disruption of the vasculature, could be highly significant.

## 6.6 Conclusion

The results from this study have brought forward the time-frame for post mortem change to skeletal microstructure. However, further studies are required to establish the earliest moment such change can occur prior to skeletonization. The unique contribution of the depositing environment has been shown to be taphonomically significant to the post mortem history of a skeleton, and warrants further study.

## CHAPTER 7: BUTCHERY AND DELIBERATE MUMMIFICATION

### 7.1 Introduction

The practices of domesticate butchery and deliberate mummification, although seemingly distinct from one another, represent systematic human interference with the body immediately after, or at the point of, death. This interference commonly imposes a disruption of the vasculature and of the soft tissues. As discussed in the previous chapter, post mortem alteration might occur soon after death if the vasculature has remained intact and the manner of death might influence this process. As butchery and deliberate mummification significantly disrupt vascular pathways, it is possible that post mortem alteration to the skeletal tissues will not occur.

### 7.2 Butchery in an archaeological context

Butchery has been defined as "the human reduction and modification of an animal carcass into consumable parts" (Lyman, 1994: 294). In the context of the archaeological record, butchery is determined via the detection of cut-marks on skeletal material and/or from the proportional representation of skeletal body parts per site. Little is known of the techniques employed for slaughter, but the methods of carcass division have been partially deduced from the location and orientation of cut-marks. In brief: skinning is represented by cut marks to the lower legs and phalanges and to the lower margins of the mandible and skull; disarticulation is evidenced from cut-marks situated at the edges or articulations of long bones and on the vertebrae and pelvic parts; whilst filleting is represented by cut-marks which are parallel to the long axis of bone

(Lyman, 1994). The modern method for carcass division of four common domesticates is shown below [Fig. 7.1], although it is doubtful whether this method was used in the past.

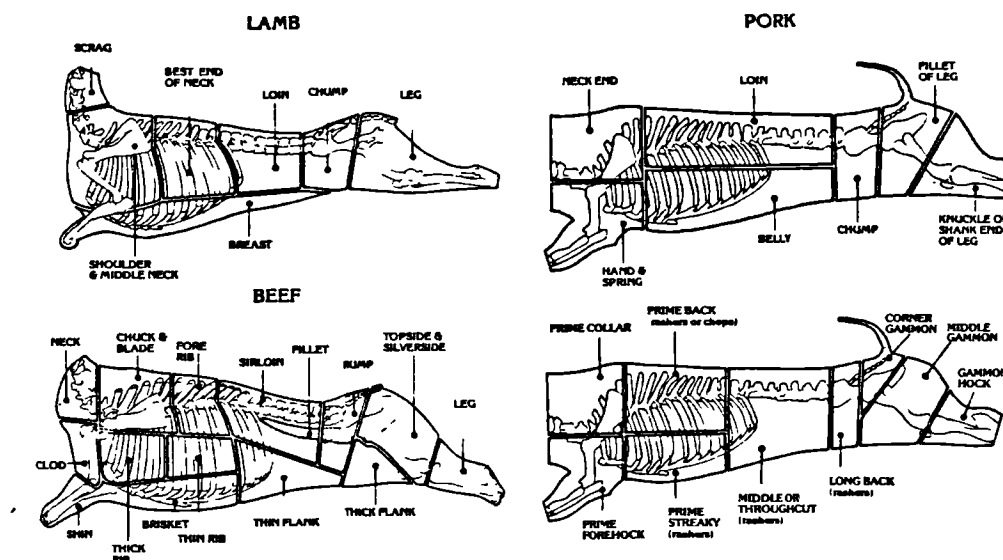


Figure 7.1 Modern schematic of carcass division in Britain (after Davis, 1987)

Previous studies of archaeological animal bone assemblages associated with settlement sites (Neolithic onwards), as opposed to ritual sites, have shown shifts of emphasis in husbandry terms from one species to another, and to the method of butchery and the tools employed for it (Maltby, 1989; Davis, 1987; Lyman, 1994). Hence, clear evidence exists for direct human intervention as a taphonomic factor influencing not only the deposit status of animal bone, but also its preservational status.

### 7.3 Mummification in an archaeological context

There are two kinds of mummification: one is accidental and the other is deliberate. Deliberate mummification is the subject of interest here and was practised mostly by the Egyptians between 2575 BC - 600 AD (Andrews, 1990). During this 3000 year period the success of the mummification or

embalming techniques varied. The methods were at their peak during 1085 - 945 BC, but declined towards the end of the period (Andrews, 1990; Spencer, 1982). What is common to all the methods described in ancient texts is that the Egyptians were knowledgeable about the decay process, and took considerable steps to allay it.

The general method of mummification is reviewed in detail in Andrews (1990) and Spencer (1982). It involved the removal, via an abdominal incision, of the stomach, intestines and occasionally the kidneys. The lungs and the liver were removed by puncturing the diaphragm. The heart was always left inside the body since it was considered to be the seat of intelligence. The brain was left untouched until approximately 1500 BC, whereupon the practice of removal began via penetration of the ethmoid bone or the superior orbital fissure. Once the internal organs had been removed the body was subjected to intensive dehydration by the combined actions of stuffing material inside the body and of covering the body with natron (a natural crystalline compound of sodium carbonate and bicarbonate with admixtures of sodium sulphate and chloride: it absorbs water and is mildly antiseptic). The material used for stuffing ranged from rags, straw and wood shavings to sand and dry grass. Aromatic resins and spices were also added, supposedly to offset the stench of the procedure. The body was then left in this state for a minimum period of 40 days. After this period the body became blackened in appearance and would be approximately 25% of its original weight, with much of the musculature dramatically reduced. The body was then emptied of stuffing, washed, dried and restuffed with the original stuffing, new stuffing soaked in resin and more natron. The organs, which had been removed earlier and treated with natron, were also

returned to the abdomen or chest. Any incisions that had been made were then stitched and the body was then massaged all over with juniper oil, beeswax, spices, milk and wine. At this point the body would be completely covered in resin to toughen it and render it waterproof. Some debate has taken place over the composition of the resinous material which was thought to turn black with time. However, Connan & Dessort (1991) have identified it as bitumen. It was at this stage that the body was wrapped with linen bandages over a period of 15 days.

It is acknowledged that the above description of the mummification process is a composite, and variations occurred throughout the period. Consider, for instance, Herodotus' description of his visit to an Egyptian embalmer's workshop in 450 BC, where he found an off-the-peg system of embalming existed (Herodotus: Burns (trans.), 1972). Of these, essentially three possible options existed: expensive, middling and cheap. The above description represented the most expensive option, whilst the cheapest involved simply washing out the abdomen with a purge for 70 days.

Indications of body decomposition prior to mummification have also been observed where the remains of maggots and beetles, associated with faunal succession during decay, have been found embedded within the bitumen (Spencer, 1982). Additionally, unwrapped mummies have been found to contain several incomplete individuals (Spencer, 1982). Another variation, less relevant to this discussion, was the practice of placing the internal organs in Canoptic jars or a box, instead of returning them to the body.

#### **7.4 Aim of this study**

The aim was to investigate whether post mortem alteration could be detected

in archaeological skeletal material which had been (potentially) butchered or deliberately mummified. Given previous results, it is hypothesised that no post mortem alteration would be evident, since the vascular pathway has been physically disrupted.

## **7.5 Material and methodology**

The animal bone used in this study came from a domestic Roman site (Old Grapes Lane, Carlisle) and was dated between 93 - 150 AD. The animal bone contexts examined belong to an enclosed rectilinear timber frame building, bordered by a contemporaneous drain, hedges and a road. The property was relatively large and included open cobbled yards. The excavated area indicated that an east-west ditch was constructed first, followed by the erection of the timber building, which itself showed multiple phases of internal reflooring and external resurfacing. The western side of the property was crossed by a plank-lined drain (Roman). On excavation the soil was wet, but not waterlogged. In addition, from the organic remains identified within deposits, conditions probably varied between dry to damp during the time of habitation. The animal bone sample is considered to constitute domestic debris, which is likely to have been either butchered and discarded, or butchered, cooked and discarded (Mr M. R. McCarthy and Dr S. Stallibrass, personal communication). Cutmarks were observed on specimen 181 and specimen 174 appeared charred.

The animal bone consisted of nine specimens taken from six separate contexts from the above site (for a full description of each context see Appendix 7.1). The species examined included cow, sheep/goat and pig. The specimens were taken from differing anatomical sites and include the

metacarpal, humerus, ulna, pelvis and femur (see Table 7.1). All cortical long bones, including the metacarpal, were sectioned transversely mid-shaft. The pelvic specimens were sectioned in the area of the pubis. The protocol for the embedding and examination of the specimens was the same as that outlined in Chapter 2, except that the SEM used for the analysis was a Zeiss DSM 962 operated at 1.19, 10 and 15 kV in BSE mode.

**Table 7.1**

**ANIMAL BONE SAMPLE**

LSB no.	context no.	species	bone
174	844	cattle	metacarpal
175	787	sheep	humerus
176	750	pig	humerus
177	787	sheep/goat	ulna
178	787	pig	ulna
179	749	sheep/goat	pelvis
180	776	pig	pelvis
181	749	sheep/goat	femur
182	745	pig	femur

The human material was Egyptian and had been deliberately mummified. The mummy was a 14 year old girl dating to 1000 BC. There was evidence of rewrapping, since some bones had been caught between bandages. In addition, little soft tissue remained. A mandibular tooth retained in its socket was removed and embedded, following the protocol for embedding



described in Chapter 2. The specimen was examined by reflection light microscopy using the Lasertec ILM11 microscope (see Chapter 4).

## 7.6 Results

Results of the examination of the animal bones from the civilian Roman site were mixed. Out of a total sample of 9 specimens, 4 were affected by post mortem alteration to microstructure, whilst the other 5 exhibited no changes. Of those specimens affected, two were classically bacterial in morphology, one was similar to an exposural change, whilst the other was altered in one localised area intracortically.

Specimen 179, from context 749, exhibited classical bacteria-related post mortem alteration to microstructure [Fig. 7.2a & b]. The changes were located primarily in trabecular bone and comprised an array of post mortem foci either showing evidence of remineralisation, or demineralised regions and voids [Fig. 7.2a]. Cortical bone contained some small post mortem foci located on osteocytic spaces, and the extent of change was less than that observed in the trabeculae [Fig. 7.2b]. Specimen 176, from context 750, similarly exhibited post mortem alterations to microstructure associated with bacterial activity [Fig. 7.2c]. The change was again concentrated in the bone trabeculae of the medullary area and occurred to a lesser extent in the cortex. Some of the post mortem foci appeared denser than the surrounding bone. Specimen 180, from context 776, exhibited peripheral periosteal demineralisation to an approximate depth of 10 microns [Fig. 7.2d]. The rest of the specimen's microstructure appeared normal. Specimen 178, from context 787, had one localised area of post mortem alteration located intracortically. The foci were small, measuring up to

50 microns across, and appeared to result from demineralisation [Fig. 7.2e]. Specimens 174, 175, 177, 181 and 182 exhibited no changes to microstructure.

The mummified specimen, examined using a confocal reflection microscope, had no observable changes to microstructure.

### 7.7 Discussion

The aim of this study was to ascertain if archaeological material which may have suffered vascular disruption soon after, or at the point of death, had undergone bacterially-related post mortem change. Apart from two specimens, admittedly in a very small sample group, no bacterially-related changes to skeletal microstructure were observed. No changes were evident in the deliberately mummified specimen. These equivocal results raise a number of questions which are worthy of discussion.

The microstructural changes exhibited by the animal bone of specimens 176 and 179, which are associated with bacterial action (Hackett, 1981), are interesting when viewed against the contexts from which the bones were derived. Specimen 176, a pig humerus, is particularly worthy of note since its context was a Roman drain. Even if butchered, it may have been exposed to intense bacterial activity within the drain, and this may explain the presence of a bacterially-related microstructural change. Specimen 179 is harder to explain in these terms since it derives from a soil context associated with a boundary hedge. There is no indication that secondary bacterial activity, other than that present in the soil, has contributed to the observed alteration to microstructure. Yoshino et al. (1991) have

## **CAPTIONS**

## Figure 7.2

7.2a Specimen 179. TS. Sheep/goat pelvis. Extensive post mortem or diagenetic alteration, of the bacterial-type, located primarily in the trabecular area. Note the presence of small holes within the partially remineralised diagenetic foci. Magnification bar = 50 microns.

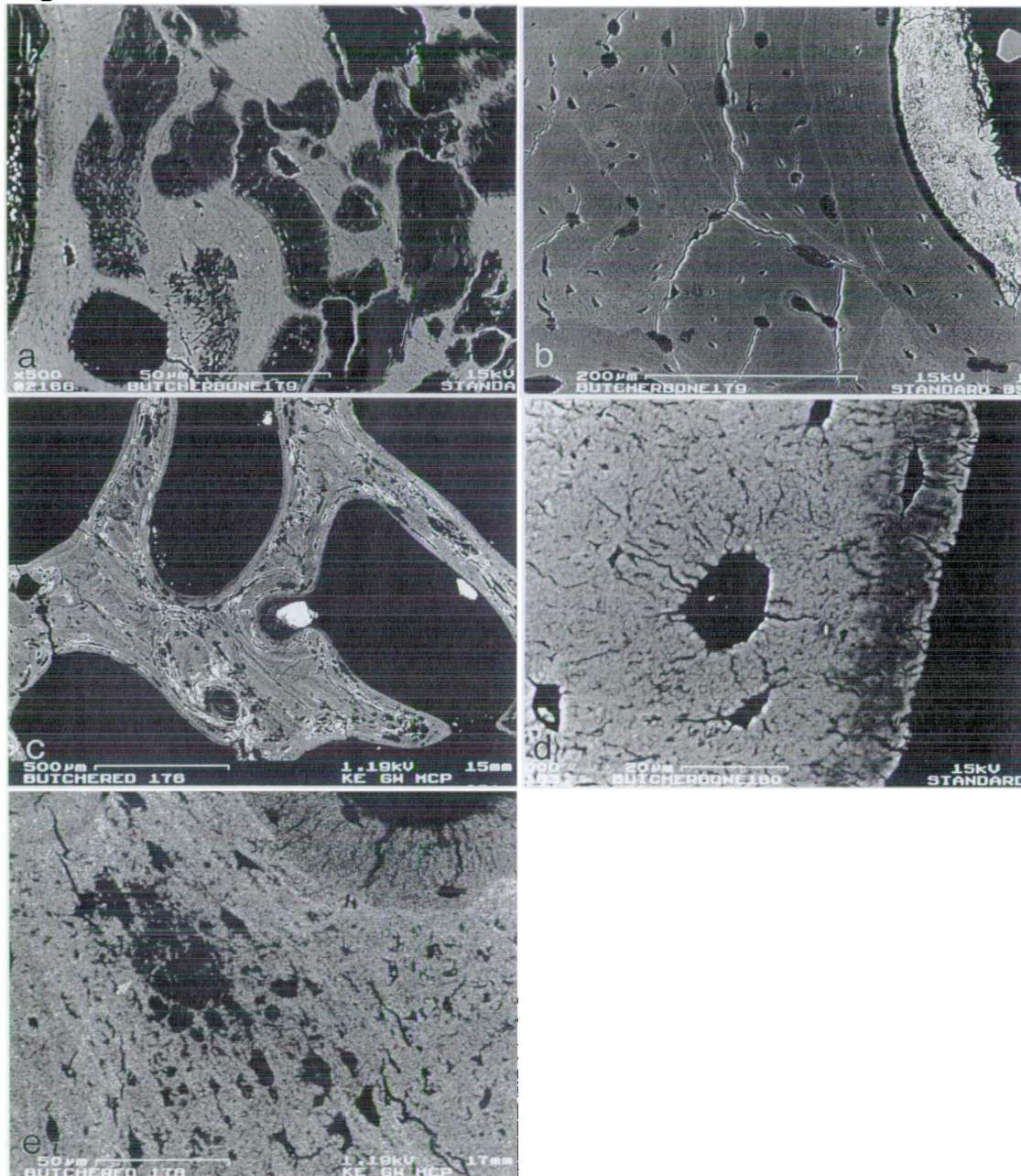
7.2b Specimen 179. TS. Sheep/goat pelvis. Small post mortem voids centred over osteocyte lacunae. This change was observable in cortical regions of the specimen. The bright edges to cracks and margins of lacunae are an artefact. Magnification bar = 200 microns.

7.2c Specimen 176. TS. Sheep/goat ulna. Extensive diagenetic foci of increased and decreased density were evident predominantly in the bone trabeculae of the medullary area. The morphology of this type of post mortem alteration has been associated with bacterial action. Soil matrix is present to right of centre (arrowed). Magnification bar = 500 microns.

7.2d Specimen 180. TS. Pig pelvis. This specimen exhibited peripheral demineralisation which encircled the subperiosteal aspect, to an approximate depth of 10 microns. No other post mortem changes were observed. This type of change has been associated with post mortem exposure. Magnification bar = 20 microns.

7.2e Specimen 178. TS. Pig ulna. This specimen had one localised area of demineralisation which was located intracortically (arrowed). No other changes in microstructure or density were observed. Magnification bar = 50 microns.

Figure 7.2



demonstrated that soil conditions can produce extensive bacterial changes within a 6 - 10 year period, and this factor cannot be ignored. However, given the speed of bacterially-related change documented in the previous chapter, some unknown factor of the post mortem history of the animal i.e. that the animal was not butchered for instance, may be possible, or, a secondary cascading process which was purely soil related may have occurred, as documented by Yoshino et al. (1991).

Another noteworthy microstructural change from the animal bone group was the peripheral periosteal demineralisation observed in specimen 180. This type of change has been previously associated with surface exposure (Yoshino et al., 1991), and the context from which the specimen derived was a surface. This may indicate that the butchered bone was discarded as rubbish, and remained exposed for some time prior to that surface becoming buried. This sort of information contributes towards an understanding of the human activity within the dwelling area. Specimen 178 is associated with ditch fill, and could also be associated with rubbish deposition. The demineralisation of the pig ulna is only superficial, but does not have the morphology associated with bacteria-related change. That the other specimens were unaffected is hard to interpret. For instance, the hedge context which produced a bacteria-related change to specimen 179 was shared by one other specimen, and yet that showed no changes to microstructure. This variation in preservation in bones which share the same or similar context has been noted in previous specimens examined throughout this thesis, and indicates that it is unlikely that soil burial alone is the primary factor driving post mortem alteration of skeletal microstructure. I contend that body status is probably the single most important factor for

terrestrially based post mortem alteration. As a caveat, the charred specimen (174) and the specimen which had cutmarks (181), had no changes to microstructure.

The mummified individual did not exhibit any post mortem microstructural alterations. This finding is encouraging, since so much is known about the Egyptian embalming process. However, it is acknowledged that many more specimens of this type need to be examined.

## 7.8 Conclusion

The notion that the vasculature acts as a pathway for intestinal bacteria to translocate to the skeleton was tested on archaeological material representing domesticated butchery and Egyptian mummification. The results, whilst equivocal, do suggest that the status of the body may be significant. However, the presence of bacterially-related change in two specimens underlines the complexity of the process of post mortem change to skeletal microstructure. Further studies in this area with modern well documented material are required, as is a wider study of mummy material.

## CHAPTER 8: SKELETAL DNA

### 8.1 PART I: Microstructural preservation and DNA recovery

#### 8.2 Introduction.

The retrieval of DNA from archaeological bone was first established as possible when Hagelberg et al. (1989), using the polymerase chain reaction (PCR) method, successfully amplified mitochondrial (mt) DNA from human material dating between 300-5500 years BP. Prior to this study it was considered impossible to obtain DNA from bone (Isen, 1988) and DNA had only been successfully retrieved from the skin of the extinct quagga (Higuchi et al., 1984), the skin and liver of an Egyptian mummy (Paabo, 1985), 7000 year old brain tissue (Paabo et al., 1988) and the skin of the extinct marsupial wolf (Thomas et al., 1989). In 1991 Hagelberg et al. reported successfully amplifying bone DNA taken from a 15 year old caucasian female murder victim (buried in a carpet for 8 years), which was subsequently co-matched to the DNA of the immediate family in order to confirm the victim's identity. The presentation of this new type of evidence was not only crucial to the final conviction of the murderer, but also firmly established the applicability of the PCR method to extract and amplify DNA from skeletal material, be it forensic or archaeological.

Following the work of Hagelberg et al. (ibid) further studies have successfully isolated mtDNA from skeletal material including the identification of the Romanov family from a mass grave site (Gill et al., 1994); the establishment of the potential geographic and racial origins of the Pacific islanders (Hagelberg & Clegg, 1993); and the retrieval of mtDNA from the dead of the American Civil and Vietnam wars



(Fisher et al., 1993; Holland et al., 1993). An intensive study of archaeological skeletal material from a 2000 year old double cemetery site revealed both different and shared maternal lineages within and between the two cemeteries (Shinoda & Kunisada, 1994). Other areas of success include the retrieval of DNA from a fossilized Miocene Magnolia leaf (Goldenberg, 1991); the extraction of the oldest ever DNA from a 120-135 Myr amber entombed weevil (Cano et al., 1993); and even the identification and regeneration of 25-40 Myr amber entombed bacterial spores (Cano & Borucki, 1995). It would appear that the ability of DNA to survive over great periods of time is now unquestionable, but the conditions under which this survival is possible are little understood.

Diagenetic alteration to skeletal tissues occurs after death and includes all processes which can affect degradation and remineralization, both in and out of the ground, but excludes the effects of high temperature and pressure (Lapedes, 1978; Rolfe & Brett, 1969). This geochemical term has become common in the archaeological literature to describe post mortem alteration to bones and teeth, and as such, has been shown histologically to be highly variable in its distribution and morphology (Chapter 2; Garland, 1989; Hackett, 1981; Poole & Tratman, 1978; Clement, 1963). Many of the detectable changes are thought to have been produced by the separate, or combined actions of bacteria and fungi (Hackett, 1981; Wedl, 1864); although other micro-organisms have been implicated, and may well be environment specific (Yoshino et al., 1991; Ascenzi & Silvestrini, 1984). Diagenetic alteration to the skeletal tissues is likely to have a profound effect on the survival of DNA.

### 8.3 Aim of this study

Given the evidence for variability in archaeological skeletal preservation, this study assessed relative microscopic preservation against mt DNA recovery and amplification.

### 8.4 Material and methodology.

The human skeletal material used in this microscopic study came both from a 17th century Civil War mass grave (numbered 3115, 3117, 3118 and 3123) [Fig. 1] and adjacent single grave (numbered 3071) situated in an Abingdon Civil War cemetery, and from a separate nearby medieval cemetery (Allen, 1989; 1990 ab). All the Civil War human material was male and was aged between 17-24 years of age, whilst the medieval specimen was male and aged between 20-25 years of age. Mid-shaft thick transverse sections were removed from five separate male femora and one male humerus using a wet diamond-edged circular saw and allowed to air dry. The sections were then placed in methacrylate, placed in a 32°C oven, and removed after the methacrylate had polymerised to polymethylmethacrylate (PMMA). The methacrylate monomer had been prepared by the flash distil method described by Boyde et al. (1986). The embedded specimens were then cut transversely using an Isomet-11-1180 circular saw, polished using graded abrasives, and finished with a 1µm diamond abrasive on a rotary lap. Each block face received a coating of carbon in vacuo and were mounted on an aluminium stub.

The specimens were examined using a Cambridge Stereoscan S4-10 SEM, operated in backscattered electron (BSE) mode working at 20 keV beam voltage. A four-segment solid-state BSE detector was used for

compositional imaging, collecting BSE electrons at all four segments. The resultant images were dominated by differences in the mean atomic number of the volume probed by the scanning beam, and thus provided sensitive information of mean density against micromorphology. Bone samples from the same specimens were simultaneously processed by Dr Hagelberg (Cambridge University) for mtDNA recovery. The relative recovery of mtDNA was then compared to the results from the microscopic study. For a full report of the methodology concerning the DNA work undertaken in this collaborative study, see the appended paper by Hagelberg et al. (1991) at back the of this thesis.

## 8.5 Results.

The results generally show that all the Abingdon 17th century mass grave bone and single grave bone underwent similar and sometimes extensive diagenetic alteration [Figs. 8.1a - 8.2d], whereas the spatially distinct 13th century specimen exhibited extremely good micromorphology [Figs. 8.2e & f].

### Abingdon mass grave and single grave bone.

The mass grave specimens exhibited similar diagenetic changes to those outlined in Chapter 2. The changes observed are those believed to be created by the invasive effects of bacteria. No fungal invasion was evident in any of the specimens examined. Specimen 3115 [Figs. 8.1a - c] had quite good microscopic preservation. The medullary third and central third of the cortex had relatively good microscopic preservation, with large areas of the cortex containing intact osteonal systems with osteocyte lacunae clearly recognisable. However, post mortem foci were present in amongst

these large fields of intact bone, and diagenetic alteration was extensive at the subperiosteal aspect. Specimens 3117 [Figs. 8.1d - f] and 3118 [Figs. 8.1g - i] exhibited a similar level of poor preservation, with diagenetic alteration concentrated in the medullary and subperiosteal thirds of the cortices and little recognisable bone could be identified. The inner third of the cortices had undergone diagenetic changes within every osteonal system in the plane of each section, but more bone was recognisable, as were intact osteocyte lacunae, in this region than anywhere else. Specimen 3123, also from the mass grave group [Figs. 8.2a - c], exhibited extremely poor preservation: almost its entire cortex from the medullary aspect through to the subperiosteal aspect had been remodelled post mortem. Closer inspection at locations between diagenetic focal lesions revealed occasional intact osteocyte lacunae, with very small areas of bone of unaltered morphology and density. Specimen 3071, which came from an adjacent single grave close to the mass grave group [Fig. 8.2d], exhibited similar changes to those affecting 3117 and 3118 and contained large regions of intact osteonal systems mid-cortex. For all those specimens above, it was always possible to identify some intact osteocyte lacunae within even heavily altered areas of bone, but the greater the diagenetic change the fewer the osteocyte lacunae could be observed. No mineralised osteocytes were observed in any of the specimens examined.

#### Abingdon Medieval specimen.

The 13th century specimen, which came from a separate cemetery in Abingdon, had by far the best state of preservation. This specimen had nearly perfect micromorphology, with its osteonal and osteocytic network intact

[Fig. 8.2e]. Only a very small area of the circumferential lamellae showed localised demineralisation [Fig. 8.2f], a negligible change considering the excellent state of the specimen overall.

#### 8.6 Brief summary of DNA results

All specimens examined in this study (except specimen 3123) produced DNA to a greater or lesser extent. Specimens 3115 and 3118 of the Civil War mass grave group produced similar amounts of DNA, whilst 3117 produced relatively more base pairs. The single grave, specimen 3071, produced similar amounts to that recovered from specimens 3115 and 3118 of the mass grave group. The best result was obtained from the older medieval specimen, which produced a similar amount to that of the modern control specimen.

The relative differences in the amplification results were considered to reflect the relatively damaged nature of the archaeological DNA. However, a second possibility which might have explained the observed differences would have been the presence of an unknown inhibitor, which could block the Taq polymerase reaction. Aliquots of DNA extracted from the archaeological specimens were added to modern DNA in an attempt to identify the presence of an inhibitor. Only a slight inhibitory presence was observed, and certainly not enough to explain the failure of 3123 to amplify.

For a full account of the DNA results refer to the appended paper (Hagelberg et al., 1991) attached at the back of this thesis.

**CAPTIONS**

**Figure 8.1**

8.1a Specimen 3115. Transverse section (TS). Extensive diagenetic changes to bone concentrated at subperiosteal aspect. A small amount of circumferential lamellae is still intact. Field width 320 microns.

8.1b Specimen 3115. TS. Mid cortical region exhibiting osteonal systems with localised areas of diagenetic alteration, usually centred on osteocyte lacunae. Field width 320 microns.

8.1c Specimen 3115. TS. A single trabeculum with recognisable areas of bone, combined with focal areas of diagenetic demineralisation. Field width 320 microns.

8.1d Specimen 3117. TS. Extensive diagenetic remodelling at subperiosteal aspect. Several circumferential lamellae remain intact. Field width 330 microns.

8.1e Specimen 3117. TS. Mid cortical region showing a moderate amount of diagenetic remodelling. Field width 330 microns.

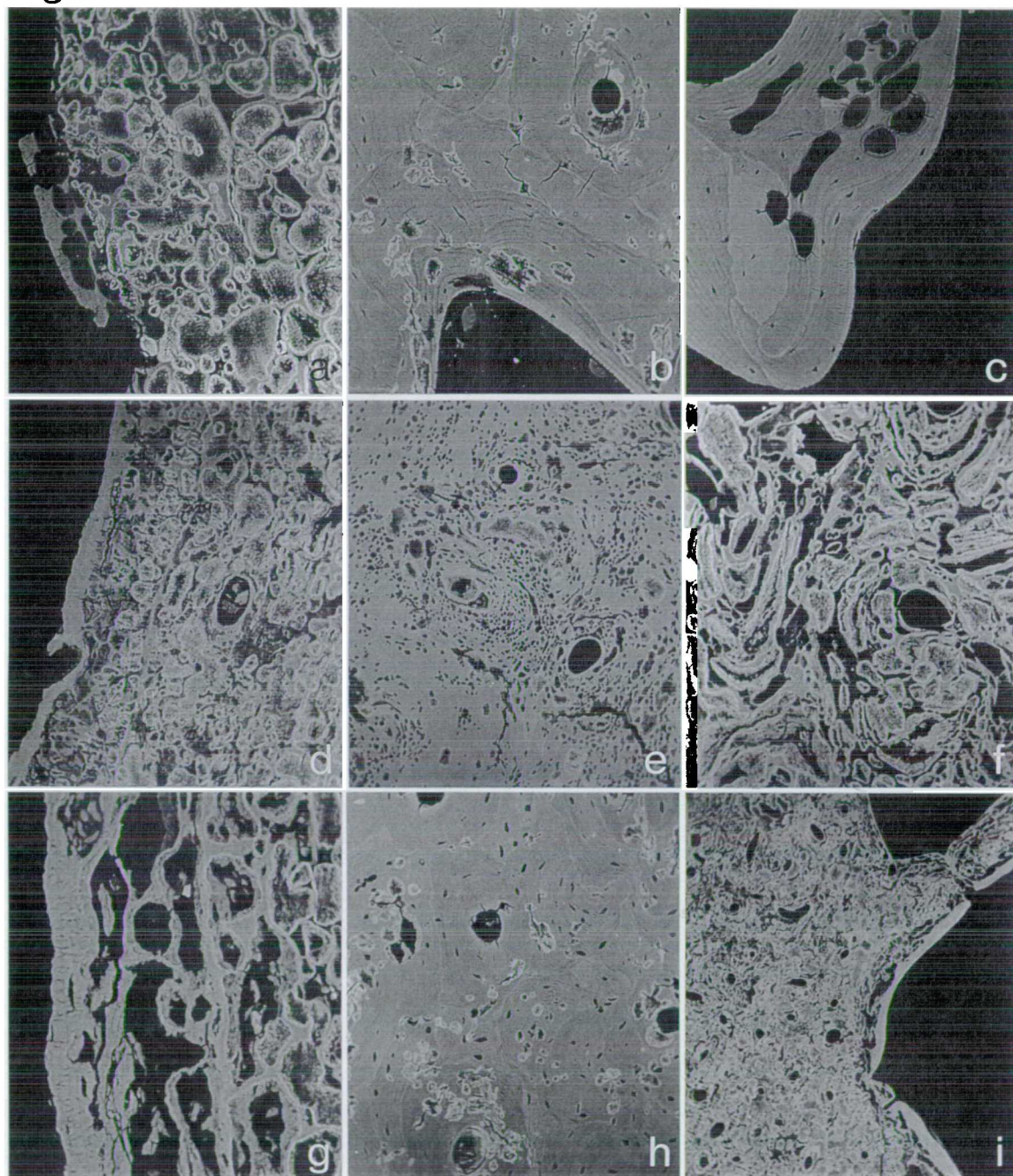
8.1f Specimen 3117. TS. Region close to medullary aspect affected by extensive diagenesis. Field width 330 microns.

8.1g Specimen 3123. TS. Subperiosteal region showing extensive diagenetic remodelling, although some bone is intact at the most external aspect. Field width 670 microns.

8.1h Specimen 3123. TS. Midcortical region extensively affected by diagenesis. Haversian canals are still evident. Field width 330 microns.

8.1i Specimen 3123. TS. Medullary aspect of bone showing extensive remodelling which is common throughout this specimen. Field width 1330 microns.

Figure 8.1





**CAPTIONS**

**Figure 8.2**

8.2a Specimen 3118. TS. Extensive diagenetic remodelling increasing and decreasing overall density. some circumferential lamellae are intact with two osteocyte lacunae visible. Field width 150 microns.

8.2b Specimen 3118. TS. Small area of midcortical bone with osteonal systems and interstitial lamellae altered by focal diagenetic lesions, many incorporating osteocyte lacunae. Field width 365 microns.

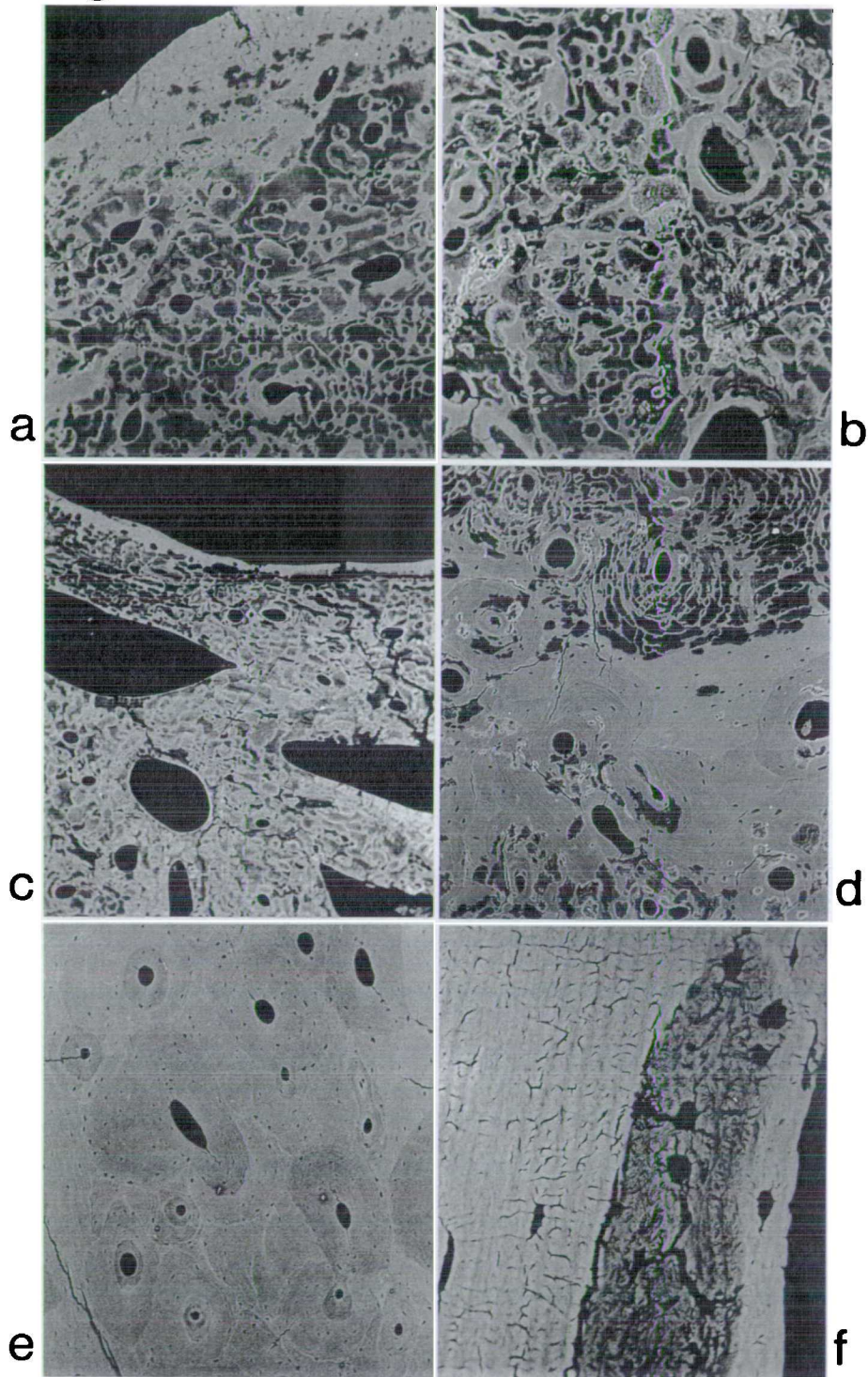
8.2c Specimen 3118. TS. Medullary aspect and adjoining trabecular bone affected extensively by diagenetic remodelling. The endosteal rim remains unaltered. Field width 3640 microns.

8.2d Specimen 3071. TS. Border between subperiosteal, altered bone (left) and relatively unaltered bone (right). Field width 670 microns.

8.2e 13th century specimen. TS. Typical field of excellent bone preservation. Osteonal systems with varying relative densities reflecting their maturation, with interstitial lamellae, and cement lines more highly mineralised, and a network of osteocyte lacunae. Field width 1260 microns.

8.2f 13th century specimen. TS. Small area of localised diagenetic demineralisation situated just deep to the subperiosteal surface of the bone. Note enlarged osteocyte lacunae within this demineralised zone, and the evident canalicular network throughout the adjacent bone. Field width 650 microns.

Figure 8.2



## 8.7 Discussion and conclusion.

The microscopical analysis and DNA study have both shown that a relationship does exist between the microscopic internal preservation of bone and the relative survival and recovery of mtDNA.

It is therefore not surprising that the microscopically well preserved medieval specimen produced much better DNA results than the bone from the relatively less well preserved mass grave group, or that the specimen which had extremely poor preservation produced no amplifiable DNA at all.

However, as observed in the DNA study, there are gradations of preservation within the mass grave specimens. These gradations appear to be related to the total volumetric area of diagenetic ingress, which in turn, causes a relative overall decrease in the number of identifiable osteocytic cell spaces. If one assumes that residues of DNA are most likely located within morphologically intact osteocyte lacunae and Haversian canals, then the invasion and destruction of these cell spaces and vascular canals by post mortem bacterial remodelling must contribute towards the fragmentation and destruction of any in-situ DNA and, as a consequence, lessen its subsequent recovery. It is, therefore, advisable to screen archaeological and forensic specimens for diagenetic alteration prior to attempting mtDNA extraction and amplification in order to maximise the chances of recovery.

No unequivocal information is available to suggest why the older material was so much better preserved, but the type of death, season of death, depth of burial, soil drainage and reworking will have contributed as co-factors in an unknown way to the observed variation in microscopic preservation and mtDNA recovery. In addition, the survival of mineralised osteocytes, a

process which occurs in vivo in aging adults (Boyde et al., 1986), may act to protect any mineral entombed DNA post mortem. If this proves to be the case, selecting bones with low bone turnover and/or a high incidence of mineralized osteocytes, such as ear ossicles, for DNA analysis might be advantageous. It should be noted, however, that no mineralised osteocytes were observed in any of the specimens examined in this study, although few would be expected in young individuals (Boyde et al., 1986).

## **8.9 PART II: Mineralized osteocytes: a possible location of bone DNA**

### **8.10 Introduction**

With the advent and success of the PCR method in reproducing mtDNA from extremely small amounts of fragmented ancient mtDNA (1 molecule is sufficient), a question remains as to its precise location within the bony tissues. This section includes a short discussion of one possible location and presents a collection of micrographs obtained from a range of skeletal material, both human and animal.

Bone, in life, is a highly vascularized tissue containing large numbers of encased osteocytes which form an interconnecting cellular network throughout cortical and trabeculated bone. After death the body skeletonizes, via decomposition processes, leaving an empty array of vascular canals and cell spaces intracortically. It therefore follows that if DNA is extracted from cortical bone, as has been the case in previous studies, then it must originate from either the Haversian canals which provided a vascular supply, or from the osteocyte lacunae which once

contained single cells. This is considered possible only if cells have survived in some way (Maat, 1993), or if a cell's DNA has adsorbed to bone mineral during autolysis, either ante or post mortem.

It is known that osteocyte lacunae can infill with mineral ante mortem, although the frequency of this occurrence is unknown. Pritchard (1972) referred to the presence of such infilled lacunae as "pyknotic remains" in bone from elderly individuals and also in necrotic bone. Boyde et al. (1986) reported observing large numbers of infilled lacunae present in human auditory ossicles and felt that there was "...strong suggestive evidence that the residue of the cell itself constitute(d) the matrix for mineralization" (Boyde et al., 1986: 1550). The authors ascribe this phenomenon to the required longevity of auditory ossicle osteocytes, due to their encasement in a bone which has matured at birth and hardly remodels throughout life. No one knows how long an osteocyte can survive within bone, but it has been estimated that the mean life of an adult osteon is 15 years (Pritchard, 1972), and it is also known that osteocytes can remain vital until their release by osteoclastic resorption, whereupon some are thought to return to the active osteoblast population (Boyde, 1980). No pathological condition affecting bone is known to cause mineral infilling of osteocyte lacunae, nor is it considered to be a post mortem phenomenon. For the purposes of this discussion such infilled osteocyte lacunae will be referred to not as "mineralized osteocytes", since this implies definite cell residue survival, but as "MIOL" (mineral infilled osteocyte lacunae).

That osteocyte death is synonymously linked with bone necrosis (Wong et al., 1982) is confusing, since it is both true and false. Using a vital stain Wong et al. (1982) demonstrated that post operatively removed femoral heads exhibited areas of empty/nonvital osteocytic bone. Cameron (1972) commented on work by Remagen et al. (1969), where rats had been overdosed with Vitamen D, that the osteocytes looked ultrastructurally "sick". Conversely, the work by Boyde et al. (1986) demonstrated that mineralized osteocytes (dead osteocytes) were present in amongst viable auditory ossicular bone, as well as in ossicles which had suffered inflammation due to infection. Hence, a commonality seems to be that if an osteocyte is to die ante mortem (but not necessarily mineralize) then it may initially be physiologically compromised by ischemia or toxic shock, or be resident in sites of low bone turnover, whereupon it dies of old age (Wong et al., 1982; Cameron, 1972; Boyde et al., 1986; Pritchard, 1972). This means that it is true that osteocyte death equals bone necrosis when accompanied by ischemia, but it is false to say osteocyte death equals necrosis when aged packets of bone contain mineralized osteocytes, since the Haversian or periosteal supply may still be viable.

In considering the biology of the osteocyte it is possible to postulate what mechanisms contribute towards it's ante mortem death and mineralization. The osteocyte is an osteoblast which has become encased within it's own extracellular matrix. When encased it no longer synthesizes osteoid (although it can produce a small amount of perilacunar bone (Boyde, 1980)) and consequently has a reduced rough endoplasmic reticulum and Golgi complex, with reduced nuclear chromatin (Junqueira et al., 1986). The cell itself becomes a flattened ovoid which interconnects

with neighbouring osteocytes via gap junctions situated on extending filopodial processes (Junqueira et al., 1986). Each osteocyte may have approximately 50 filapodia spread over a cell-centred radial diameter of 100 microns (Pritchard, 1972). This means that within each osteon nutrients (ions and small molecules) can be passed from the Haversian aspect to it's farthest lamellar region. During normal remodelling, small groups of osteocytes become cut off from a vascular supply in areas of bone called interstitial bone. Previously, it was established that MIOL occur in areas of low bone turnover and in pathologically affected bone. Hence, three possible scenarios are suggested for osteocytic mineralization and potential DNA survival:-

1. That a cell overproduces perilacunar bone, due to it's excessive longevity, gradually constricting and fatally closing the canaliculae containing the filapodial processes. This would cause not only a thickening of mineral within the lacuna, but also reduce nutrients being passed to itself and neighbouring osteocytes. Once closed, the cell lyses and fragmented nucleic material probably adheres to the encroaching mineral phase until an ionic balance is achieved and dessication is completed. This would produce an empty space surrounded by a thickened layer of mineral within the lacuna, and would also promote the infilling of mineral into the canaliculae [Morphological type 1].

2. That a cell becomes dysfunctional due either to a lack of nutrient or due to toxicity caused by disease or radiation. Either state could produce Cameron's (1972) "sick" cell, where perhaps an aberrant production of mineral nucleating proteins and increased calcium uptake causes not only cell lysis, but spontaneous sites of mineralization intracellularly. This



again may take up nucleic fragments as before. Since the canaliculae, to the now dead osteocyte, are still open, salts may still be pumped from surrounding vital osteocytes into the lacunar space causing a possible phasic build-up of mineral around the original sites of mineralization. This would present an inner zone of mineralization which concentrically enlarges layer-by-layer, to finally infill the entire osteocyte lacunar [Morphological type 2].

3. The cell dies of apoptosis (Whyte & Evan, 1995) due to the lack of signals from other cells. Any nucleic material may fortuitously stick to the lacuna wall. This would represent an empty osteocyte lacunae on SEM inspection [Morphological type 3].

Admittedly, this is all very speculative, but work by Boyde et al. (1986) has demonstrated MIOL with morphologies which match 1 and 2, whilst empty cell spaces have been reported in post operatively removed bone by Wong et al. (1982). The essential point remains however, that it is highly likely that in interstitial areas of cortical bone, bone from individuals of considerable age, the auditory ossicles and pathologically affected bone, all represent good detection sites for MIOL, and therefore DNA. This DNA, once incorporated, becomes protected by a mineral layer which acts in much the same way as amber has acted to preserve DNA over millions of years (Cano et al., 1993).

Other potential sites of mineral infilled cellular lacunae (MICL) within the skeletal tissues include chondrocytes, cementocytes, odontoblasts and pulp stone centres. The death of the chondrocyte within its calcified

lacuna presents a possibility of DNA survival only in the unlikely event that this lacuna remains intact after chondroclasia and subsequent bony remodelling. Such a survival is considered extremely unlikely, although the irregular formation of the temporomandibular condyle, where chondroblasts grow in a multidirectional manner (as opposed to columnar growth found at the epiphyseal plates of long bones), presents a slight chance, since a chondrocyte-bearing lacuna may fortuitously avoid chondroclastic resorption and subsequent bony remodelling (survival of calcified cartilage after bone formation is known to occur (Boyde et al., 1986)) (Whitson, 1985; Enlow & Dale, 1985). Other potential sites for chondrocyte survival include the thin layer of calcified cartilage situated beneath articular cartilage and just above the osseochondral junction, which exists even in a resting state in adult bone; calcification of the trachea, larynx and costal cartilage can also occur in elderly individuals; similarly, calcification of fibrous cartilage in the areas of the symphysis pubis, intervertebral discs, sternoclavicular and interchondral cartilage, and tendonous insertions also occur in the elderly, but can also occur as the result of trauma (Williams & Warwick, 1980). The partial survival of the cementocyte as a MICL is again considered unlikely. Although this cell is similar to the osteocyte, in that it becomes encased by its own extracellular matrix, it usually resides above an acellular layer of cementum (although a cellular layer of cementum can exist below the acellular layer) and gains nutrients only indirectly from a vascular supply, via diffusion from the periodontal ligament (PDL). This means that deeply sited cementocytes, gradually cease to gain nutrients and may die in vivo, leaving empty lacunae (Freeman, 1985). However, although not considered a possible MICL site due to its lack of nutrients and fewer

interconnecting cell processes, DNA may adhere to the lacuna walls at the point of the cementocyte's death. The odontoblast is known to frequently become encased by its' own extracellular matrix when responding to a carious stimulus. This usually occurs in the region of the pulp horn where odontoblasts are relatively crowded, and only when there has been rapid predentine formation (Torneck, 1985). On mineralization of the predentine the odontoblast becomes properly included within the dentine. Whether it is possible for such a cell to mineralize is unknown. Finally, the formation of pulp stones (denticles) within the dental pulp can occur around blood thrombi and dying or dead cells (Torneck, 1985); it is possible that cellular DNA may initially adhere to the forming pulp stone, and latterly become encased deep to its' centre. Hence, it is suggested that bone-related MIOL are more likely to occur and survive into the post mortem record, than the less likely occurrence of MICL at other skeletal sites.

#### **8.11 Material and methodology**

All material presented here has been examined for other research purposes involved in the production of this thesis. No predictive methodology was employed and essentially the results represent a retrospective overview. The specimens were prepared for SEM/BSE analysis as outlined in Chapter 2, but some were also examined using a Zeiss DSM 962 SEM in BSE mode operated at 10 and 15 kV.

#### **8.12 Results**

A forensic specimen belonging to a white male aged 91 years of age was found to have MIOL situated in a small interstitial area of bone belonging

to the 4th rib [Fig. 8.3a]. The MIOL themselves exhibit the morphologies referred to as scenarios 1 and 2 in the Introduction. These were the only MIOL evident in that plane of section. This specimen had undergone bacterially related post mortem remodelling.

The only human archaeological material which produced MIOL were all from auditory ossicles which came from two medieval cemeteries and one marine context. The marine specimen exhibited considerable numbers of MIOL which tended to be located towards the ossicle's external aspect [Figs. 8.3b]. The MIOL themselves exhibited the layered and partially infilled morphologies (types 1 and 2), as well as empty osteocyte lacunae [Fig. 8.3c]. The identification of MIOL in the affected medieval buried bone was made more difficult owing to some extensive post mortem bacterial remodelling. However, it was apparent that MIOL can survive in this type of affected bone, even when bordered by a large focus of demineralization [Figs. 8.3d & e].

Of the archaeological animal bone examined three specimens were found to contain MIOL. All the animals could be judged to be adult (Silver, 1969), although the precise ages, or even potential longevity of the animals, is unknown. However, the pig pelvis contained many MIOL of the characteristic type 2 morphology [Figs. 8.4a - c]. Of these MIOL, the profiles were suggestive of the size and shape of the cell nucleus [Figs. 8.4b & c]. Of the sheep/goat cortical bone from a femur and humerus, the detected MIOL were again numerous and of the type 2 morphology [Figs. 8.4d - f]. Given that these animals may well have been butchered Roman domesticates, it may be that the above animals reached considerable maturity before slaughter.

**CAPTIONS**

### Figure 8.3

8.3a Two 'mineral infilled osteocyte lacunae' (MIOL) situated in a small interstitial area of bone from the 4th rib of a white 91 year old male (see arrows). One MIOL appears uniformly dense, whilst the other illustrates the laminar-type MIOL with associated differing layered densities. Note that the visible canaliculae for both MIOL have also become infilled. Field width 50 microns.

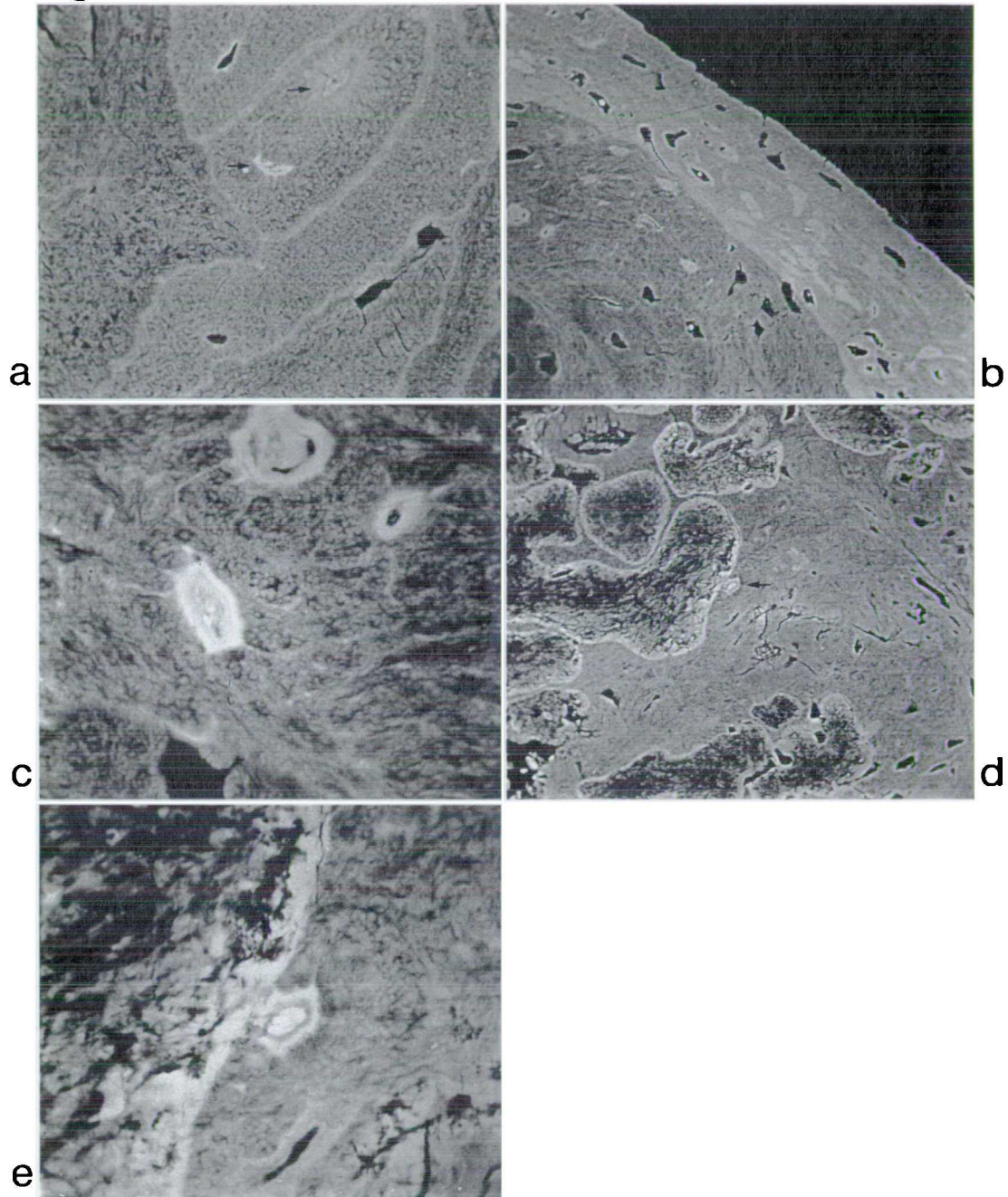
8.3b A large field of MIOL located on the external aspect of a human incus bone from the Mary Rose ship. Again the MIOL have an increased density over the surrounding bony matrix. Field width 340 microns.

8.3c Field of MIOL exhibiting the layered and partially infilled morphological types 1 & 2. Note empty osteocyte lacunae (top right) situated next to a cement line and in a separate packet of bone. Human incus from Mary Rose ship. Field width 34 microns.

8.3d A single MIOL (arrowed centre field) abutts an advancing diagenetic focus. The diagenetic foci themselves appear of decreased density to bone, and include empty osteocyte lacunae. Human incus from a Medieval cemetery site. Field width 140 microns.

8.3e Higher magnification of MIOL from previous Figure 20. The MIOL itself appears internally layered and is in direct contact with the advancing margin of the diagenetic focus. Field width 30 microns.

Figure 8.3



**CAPTIONS**



#### Figure 8.4

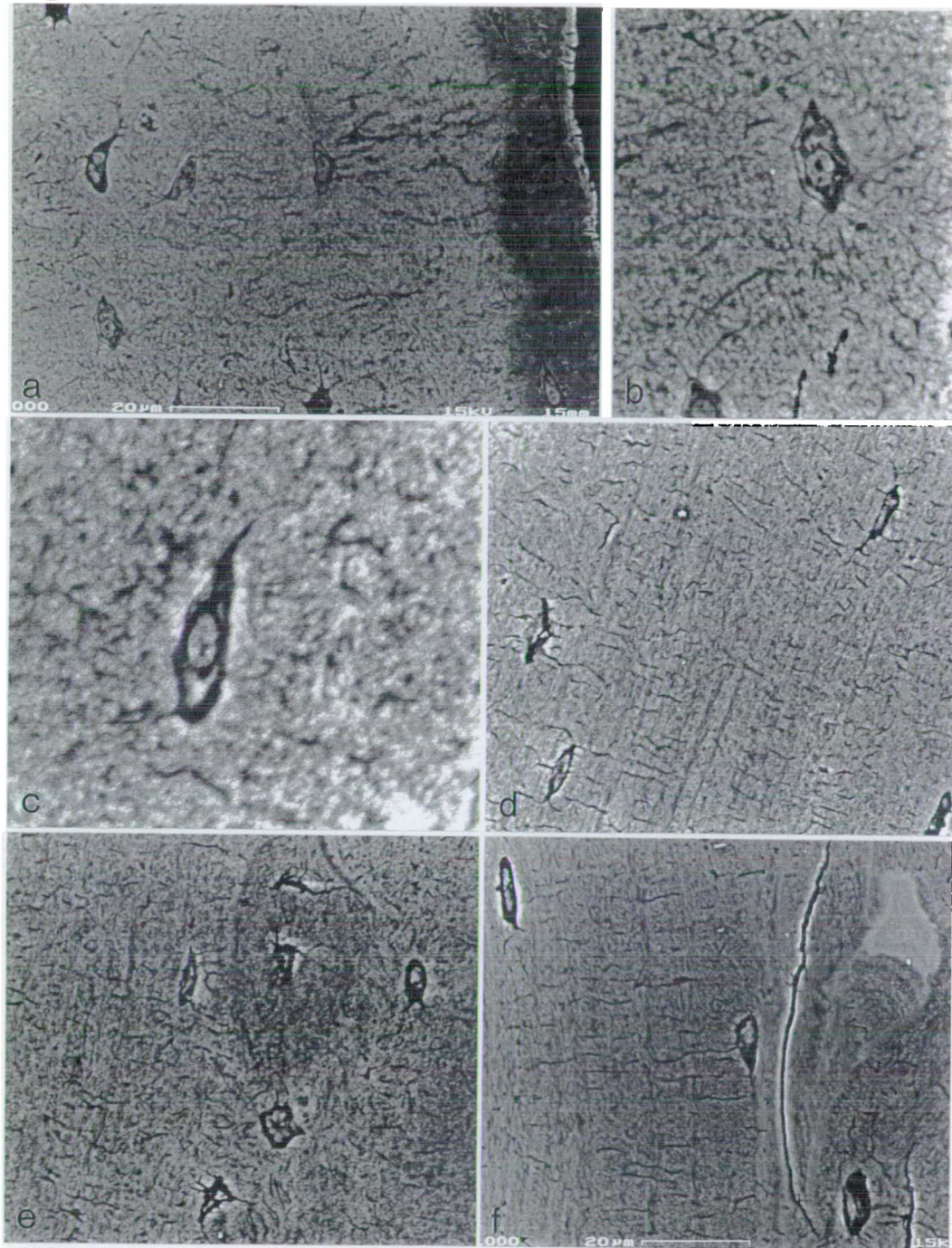
8.4a MIOL found in an adult pig pelvis (possibly butchered) from a domestic Roman site in Carlisle. The external aspect of the pelvis (orientation unknown) has a peripheral band of demineralization associated with environmental exposure, with the MIOL situated just beneath. No other post mortem alteration to bony tissue was evident. Magnification = scale bar.

8.4b & c Two MIOL with internal structures highly suggestive of fossilized cell nuclei both contained within a discrete membrane-like band of mineral. No mineral infilling of osteocyte canaliculae is evident. Both fields are taken from the previous pig specimen. Field widths respectively are 25 and 23 microns.

8.4d & e MIOL found in an adult sheep/goat humerus (possibly butchered) from a domestic Roman site in Carlisle. The MIOL appear as discrete mineral inclusions of similar density to the surrounding bony matrix, with no infilling of the osteocyte's canaliculae. Field widths are both 70 microns.

8.4 f Similar MIOL to the previous specimen but found within an adult sheep/goat femur (possibly butchered) from a domestic Roman site in Carlisle. Note (top right) localized region of higher density which is most likely physiologically calcified cartilage which has avoided bony remodelling (not characteristic of any known diagenetic morphology). Magnification = scale bar.

Figure 8.4



This type of observation, if the physiological processes involved are the same between humans and other mammals, would help to relatively age important death assemblages of disarticulated animal bone.

#### 8. 13 Discussion and conclusion

This retrospective study confirms previous observations made by Pritchard (1972) and Boyde et al. (1986) on human material. All human bone found to contain MIOL came either from bone belonging to an aged individual, auditory ossicles or interstitial areas of bone. However, it is now confirmed for the first time that MIOL do survive in archaeological bone from both terrestrial and marine contexts, even when the bone has undergone considerable diagenetic alteration. Further, MIOL have been detected in archaeological sheep/goat and pig cortical bone. The application of this finding is not only relevant to the survival of bone DNA, but also to relatively aging disarticulated adult bone belonging to important domestic death assemblages.

That these MIOL persist in archaeological bone may help to explain not only the survival of bone DNA post skeletonization, but also its apparent longevity over many thousands of years. Indeed, MIOL are comparable to the survival of bacterial spore DNA over millions of years (Cano et al., 1993; Cano & Borucki, 1995), due to the specialised nature and containment of essentially dessicated DNA. This survival of DNA has confounded Lindahl & Nyberg's (1972) experimental extrapolations on the short time DNA takes to degrade, and has since been criticised by Goldenberg (1991) who stated that such physiological models of decay are invalid set against unique environmental settings. Lindahl (1993) has since reappraised his earlier

work, but still believes there to be limits for skeletal material, and suggests many dramatic results are purely the result of modern contamination during execution of the PCR method. However, the recent work of Cano et al. (1993) and Cano & Borucki (1995) has been met with grudging acceptance (Fischman, 1995), and has pushed the boundaries for DNA recovery into millions of years, rather than thousands. Hence, although the frequency of MIOL is unknown, it is possible that this type of ante mortem physiological mineralization represents a potentially rich deposit of environmentally protected DNA. Therefore, the frequency and location of the MIOL need to be ascertained for the entire mammal group, in order to determine whether it is simply a hidden jewel or, more usefully, a semi-precious stone.

## CHAPTER 9: QUANTITATION

### 9.1 Introduction

The applicability of the SEM/BSE method to assess qualitative morphological and relative density changes to archaeological and forensic skeletal material has been extensively detailed within this thesis. This chapter addresses the need to quantify and validate some of the observations made using this method, and in particular, those of diagenetic foci which exhibit a perceived increase in their overall density, greater than that of the surrounding bone or dentine.

### 9.2 Bone.

The characteristic morphology of adult bone includes circumferential lamellae, secondary osteons and areas of interstitial lamellae. A radiating system of osteocyte lacunae and interconnecting canaliculae is present throughout the tissue. Within this general framework the process of remodelling results in areas of bone which have a relatively higher mean atomic number (Z) which appear lighter in BSE images, and areas which have a relatively lower mean Z appearing darker in BSE images, with holes or embedding medium appearing as black. This difference in bone matrix composition is a direct indication of the relative ages of packets of normal lamellar bone, the progress of mineralization being extended by a long maturation phase. Thus, due to the incremental structure of bone, where time and maturation are interrelated during growth and the normal bone turnover that occurs throughout life, BSE imaging should be an ideal method to observe such changes. Post mortem alteration or diagenetic foci have been shown generally to both alter the microstructural arrangement of

the host skeletal tissue and to summarily increase or decrease the observed bulk composition of the affected hard tissues. This type of diagenetic change is considered to be caused by the initial ingress of bacteria via the skeletal vascular and cellular network, creating areas of demineralised voids which terminally contain their mineralised residues combined with remineralised skeletal tissue. This type of bacterial mineralisation is considered comparable to the formation of oral calculus, where areas of dead bacteria and other microorganisms form mineralised regions of high and low densities, relative to bone and dentine, on the enamel and root surfaces of teeth (Jones, 1987).

### 9.3 Bone mineral density

All the skeletal tissues are composed of an organic and a mineral fraction. The mineral fraction varies between different tissues and during the stage of tissue maturation in a time-dependent manner. With maturation, the organic and water components decrease, unless affected by pathology or stress related growth disturbances (Fearne et al., 1994; Skinner & Hung, 1989; Boyde et al., 1986), and the mineral fraction increases. In brief, the adult dry weight mineral fraction is 96% of mature human enamel, 72% of dentine and 70% of compact bone (Williams & Elliott, 1979). The mineral phase itself is composed of a calcium-deficient carbonated apatite (Nelson, 1990) which may change in atomic number composition and crystal size during the maturation process (Fratzl et al., 1991; Bonar et al. 1983). Density gradient fractionation studies of human material have bracketed the various densities from bulk portions of the skeletal tissues and generally show mature enamel to lie between 2.6 - 3.0 gm/cm<sup>3</sup>, dentine 2.2 - 2.4 gm/cm<sup>3</sup>, cementum 2.2 - 2.4 gm/cm<sup>3</sup>, compact bone 1.65 - 2.3 gm/cm<sup>3</sup>

(Manly & Hodge, 1939; Manly et al., 1939; Richelle & Onkelinx, 1969; Williams & Elliott, 1979). Although these ranges do reflect the transitory state of mineral maturation, they are also crude approximations, due to bulk sampling of the hard tissue without regard to microstructure. This is particularly problematic with compact bone, where neighbouring packets of bone will be at differing stages of maturation. Pure crystalline hydroxyapatite (HA) has a density of  $3.2 \text{ gm/cm}^3$  and this represents the maximum value attainable. The only skeletal tissue which approaches this maximum value is mature enamel.

#### 9.4 SEM/BSE imaging and bone density

The first important point to make about SEM/BSE imaging is that it is not a measure of density (Nelson, 1990). The basic tenet of SEM/BSE imaging is that backscattering of electrons, within a homogenous substrate, increases with increasing atomic number (Neidrig, 1978; Watt, 1985). Hence, when the primary electron beam hits a substrate a proportion of the electrons will be deflected by topographical features present on the surface, whilst other electrons penetrate the substrate forming a spherical diffusion cloud of moving electrons, which are scattering either elastically or inelastically (Joy, 1988). A proportion of these electrons, with high energies, within the diffusion cloud are deflected back out of the specimen towards a detector which can discriminate between low and high energy electrons. Higher atomic numbered substrates increase the number of backscattered electrons detected and so conclusions may be drawn as to the atomic number composition of that substrate. Therefore, SEM/BSE images are atomic number maps derived from an unknown subsurface volume directly beneath the primary beam or spot.

The SEM/BSE method to skeletal tissues was first applied by Boyde & Jones (1983a; 1983b), and was shown to be highly sensitive to mineral density changes both between and within mineralised tissues. The images were reported to be of superior resolution to those obtained by microradiography. The fact that a density relationship appears to exist between the skeletal tissues and the BSE method seems curious and recently several workers have attempted to understand why atomic number contrast varies with bone mineral density. Nelson (1990), with the aid of Joy's (1988) Monte Carlo simulation of electron backscattering, established that if density were varied but the mean atomic number and weight kept the same, then there was no appreciable change to the BSE coefficient (number of backscattered electrons divided by the number of primary electrons incident on the sample) in a pure HAP/void model. However, when Nelson introduced a two-phase model simulating pure HAP combined with an organic phase, as is the case with the skeletal tissues, he then found that the BSE coefficient dropped progressively as the percentage of the organic phase increased and that of the HAP decreased. This also had the effect of decreasing net density. Nelson attributed this result to concurrent changes in atomic number, believing this to explain the atomic number contrast between dentine and enamel. Nelson then went on to investigate the effect of altering the composition of the mineral, since skeletal mineral is not composed of pure HAP and dental caries causes pathological changes to enamel mineral. He considered whitlockite ( $Z=14.05$ ), octacalcium phosphate ( $Z=13.51$ ) and brushite ( $Z=11.85$ ) in relation to pure HAP ( $Z=14.08$ ) and found a respective decrease in the BSE coefficient combined with a decrease in atomic number alongside a decrease in density. Hence, Nelson demonstrated that density alone does not effect the backscattering of



electrons, but a two-phase mineral/protein will, as will slight changes in mineral composition.

Howell and Boyde (1994) extended the work of Nelson (1990). They adapted Joy's (1988) programme to include a more representative atomic number bone composite which also included the embedding medium and assumed that "the more mineral is packed into a given microvolume of bone, the greater will be the mean atomic number" (Howell & Boyde, 1994: 286). They investigated the effect of varying the bone mineral volume, the size of the diffusion cloud depending on the energy of the primary beam and the effect of bone topography on BSE. They found that atomic number contrast did vary with differing bone densities; that the diffusion cloud increased in size with increasing beam voltage; and that the contribution of lamellar topography when polished is the main cause of a misleading BSE signal.

That BSE atomic number maps reflect bone mineral density is perhaps fortuitous. When considering a hypothetical substrate of fixed atomic number, the BSE signal should remain the same, no matter what its density within a fixed volume. Nelson's experimental HAP/voids simulation confirms this. That the BSE sample, derived from the diffusion cloud, represents a mean state of mineralization only appears to work because the net return of BSE reflects a proportional change between two fixed atomic number entities. It has been assumed not to reflect a compositional change to the mineral itself, although bone mineral composition can vary through pathology (Boyde et al. 1986) and age related increases in crystallinity (Bonar et al., 1983). Diagenetic or post mortem changes to the skeletal

tissues have been qualitatively assessed using the BSE method in this thesis, and represent a further complication to the above discussion.

#### **9.5 Aims of this study**

Apparent dramatic atomic number contrast is evident in those archaeological and forensic specimens affected by bacterial and fungal invasion. It is most likely, and has been interpreted by myself, to represent changes in mineral density, together with compositional changes to the mineral/organic fraction. However, diagenetic foci alter and probably increase the porosity of what is already a highly porous tissue. In addition, topographical relief is generated at the diagenetic focus/bone interface during polishing of the block face. Given the results of Howell and Boyde (1994) with regard to the artefactual contribution of topography to BSE signal, an attempt to verify the increase of atomic number contrast using X-ray microtomography (MCT) has been undertaken. Further, a selected group of specimens exhibiting a range of diagenetic ingress have been assessed using a quantitative BSE (QBSE) method of atomic number contrast.

#### **9.6 Material and methodology**

To assess whether the dramatic increase in density amongst diagenetic foci within bone and dentine is real, rather than solely topographical, a specimen was selected which had an unusually large amount of this type of change. The specimen was a soil-buried adult femur of medieval date, and exhibited slight periostitis on its anterior aspect (Ortner & Putschar, 1985). After a transverse mid-shaft anterior section had been removed from the periostitic area, embedded and examined following the protocol outlined in Chapter 2, it was found to contain a large band of high density foci

situated at the sub-periosteal border in a single tier of primary osteonal bone [Fig. 2.3d & 2.4a]. Polishing topography was evident both at the borders of the diagenetic foci themselves and also between the specimen and the PMMA [Fig. 2.4b].

For the purpose of undertaking MCT, a small radial section approximately 2mm in diameter was released from the embedded block and attached to a metal rod using a sticky wax. An aluminium wire was used as a standard. The analysis itself was done by Dr. Wong (London Hospital Medical College) following the protocol described in Fearne et al. (1994) and Elliott (1989). The benefit of undertaking MCT is that a radial, non-destructive cross section approximately 10 microns thick is obtained just below the blockface surface, via a precisely focused X-ray beam facing a detector. The specimen is rotated stepwise through 360° between the detector and the X-ray source over an 18 hour period [Fig. 9.1].

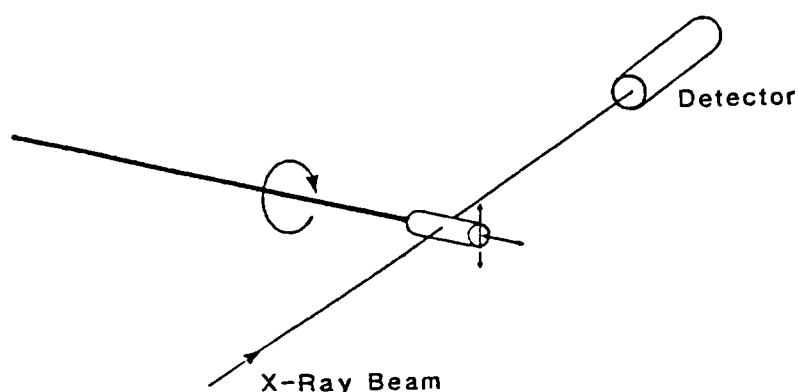


Figure 9.1 Diagram of specimen set-up and radial motion (after Elliott et al., 1989),

The benefits of such an approach are firstly that the artefactual contribution of blockface surface topography is not a factor and secondly, that X-ray linear absorption coefficients are directly affected by bone mineral density (Elliott et al., 1989b). Additionally, MCT is preferred over slab microradiography as its small plane section avoids superimposition of density information which is problematic in slab sections of 50-100 microns.

The second QBSE study involved a selection of archaeological specimens which exhibited a range of microstructural preservational states set against a modern standard. The method of quantitation used here was developed and described by Reid and Boyde (1987), and essentially brackets the BSE signal into 15 ranges or "bins". This allows for atomic number to be semi-quantitatively measured per sampling grid. The first 8 bins represent the range of values found in normal bone, whilst the other 7 represent increasing values over and above bone (Reid & Boyde, 1987). The specimens came from a range of sites both marine and terrestrial. The specimens were: two Mary Rose human incuses with excellent microstructural preservation, one human incus from a medieval soil-buried context from Barton-on-Humber with intermediate preservation, one human incus from a medieval soil-buried context from St. Oswalds Priory which exhibited poor microstructural preservation, and a small section of a human soil-buried femur described in the previous analysis from Barton-on-Humber, which exhibited almost total diagenetic reorganization to the specimen's microstructure. The modern standard was a laboratory human tibia without known pathology. All bones were embedded in PMMA and selected faces of the cut and ground blocks were finished by diamond ultramilling prior to carbon

coating. (Diamond ultramilling essentially cuts a flat surface which is almost topography free.) The specimens were mounted on a 25mm diameter stub with all block faces having the same working distance from the electron gun. The analysis was conducted using the system 80K interfaced to the S4-10 SEM operated at 19.7kV, 1mm diameter fields, with a sampling grid of 128x128. For the success of this analysis all experimental parameters, including the beam voltage, needed to remain stable and to this end high-speed driving between one specimen to another was critical. It is gratefully acknowledged that Prof. Boyde operated the SEM.

## 9.7 Results

The results from the MCT analysis confirm that the perceived high density of the diagenetic foci in SEM/BSE micrographs, is real and not artefactual [Figs. 9.2 & 3]. The colour bars at the top of the tomogram represent increasing mineral density from left to right, or decreasing linear absorption coefficients. It can be clearly seen that the region of primary osteonal bone at the subperiosteal surface, which contained a large area of diagenetically increased atomic number contrast in SEM/BSE imaging [Fig. 2.3d], is also the area which exhibited a high mean density well above that of surrounding bone in the tomogram [Fig. 9.2]. It is known that primary osteonal bone mineralises to a higher level than adult lamellar bone (Boyde, 1972). However, the included diagenetic foci are well above that expected for primary osteonal or woven bone. Additionally, those smaller diagenetic foci with increased densities which were contained within secondary osteonal systems of the cortex are either absent or not well defined in the tomogram. Areas of blue and light green are widely distributed throughout the cortex and represent a net decrease in density

relative to bone. This distribution of density values within the cortex can be more clearly discerned in Figure 9.3, where the colour bars have been recalibrated to include more density values, and it is clear that bone becomes both radically decreased in density in some regions although increased in others.

The results from the QBSE study are given in histogram form [see Fig. 9.4] and indicate a general shift towards a higher mean atomic number range of densities as diagenetic microstructural changes come to dominate the cortex. The modern tibial standard characterized the mean distribution of BSE signal levels for bone and occupied the first eight of the "bins" as predicted by Reid & Boyde (1987). One of the Mary Rose incuses examined exhibited a nearly identical distribution to that of the standard. The second Mary Rose incus, which also had good micromorphology, showed a slight increase in BSE signal associated with higher atomic number values. The Barton incus which exhibited intermediate preservation, with areas of diagenetic remodelling evident, showed a marked shift towards much higher BSE signal values. The St. Oswald's Priory incus, which represented extensive diagenetic remodelling, with little recognisable bone remaining, presented a marked shift towards much higher BSE signal values. The femur, which was previously examined using MCT, exhibited a slightly more pronounced shift towards BSE signal values than the previous specimen, and this correlates well with the presence of a large quantity of high density foci present at the subperiosteal surface. This dramatic shift or increase in mineral density is well illustrated in Figure 9.5, where the St. Oswalds incus and Barton femur have been plotted alongside the modern tibial standard for comparison. Overall, the atomic number composition of

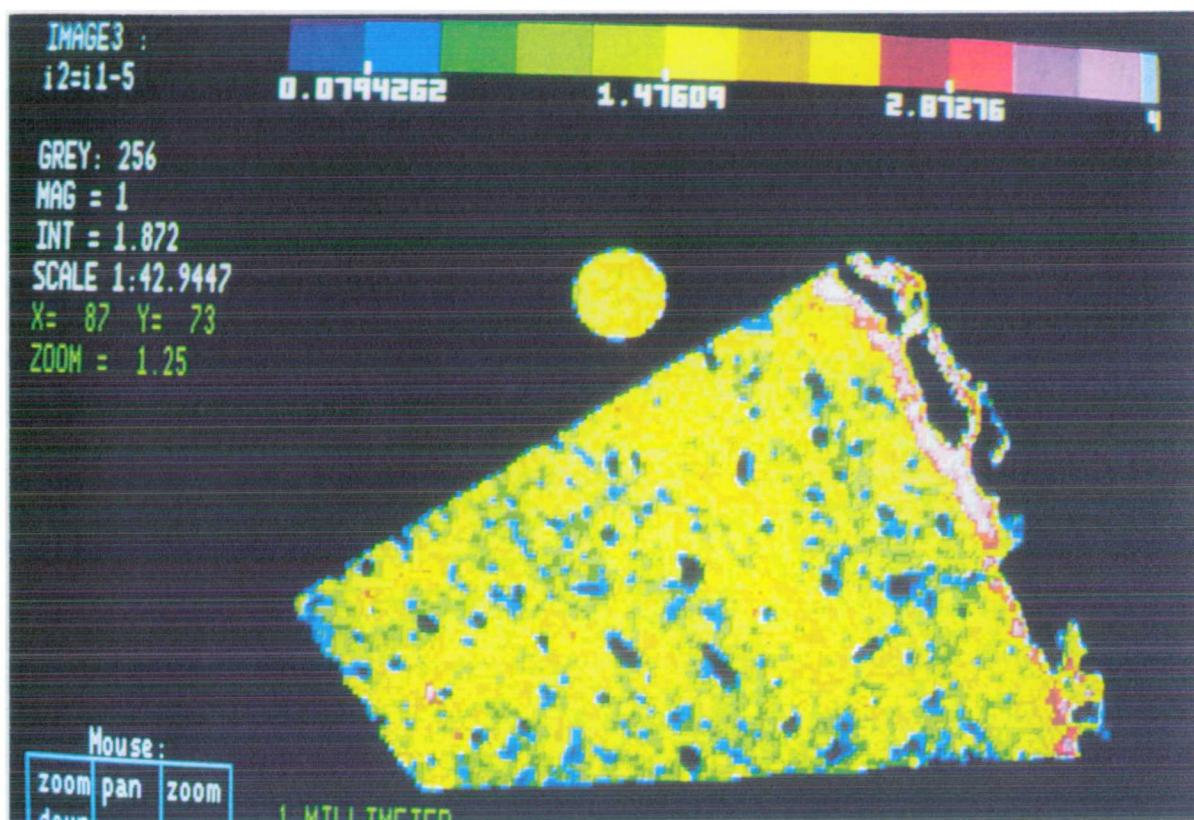


Figure 9.2

Tomogram of Barton femur with band of increased density evident within the primary osteonal bone present along the periosteal aspect. The increased area of density is shown as red to pink whilst normal bone appears green/yellow. Circular feature is aluminium standard.



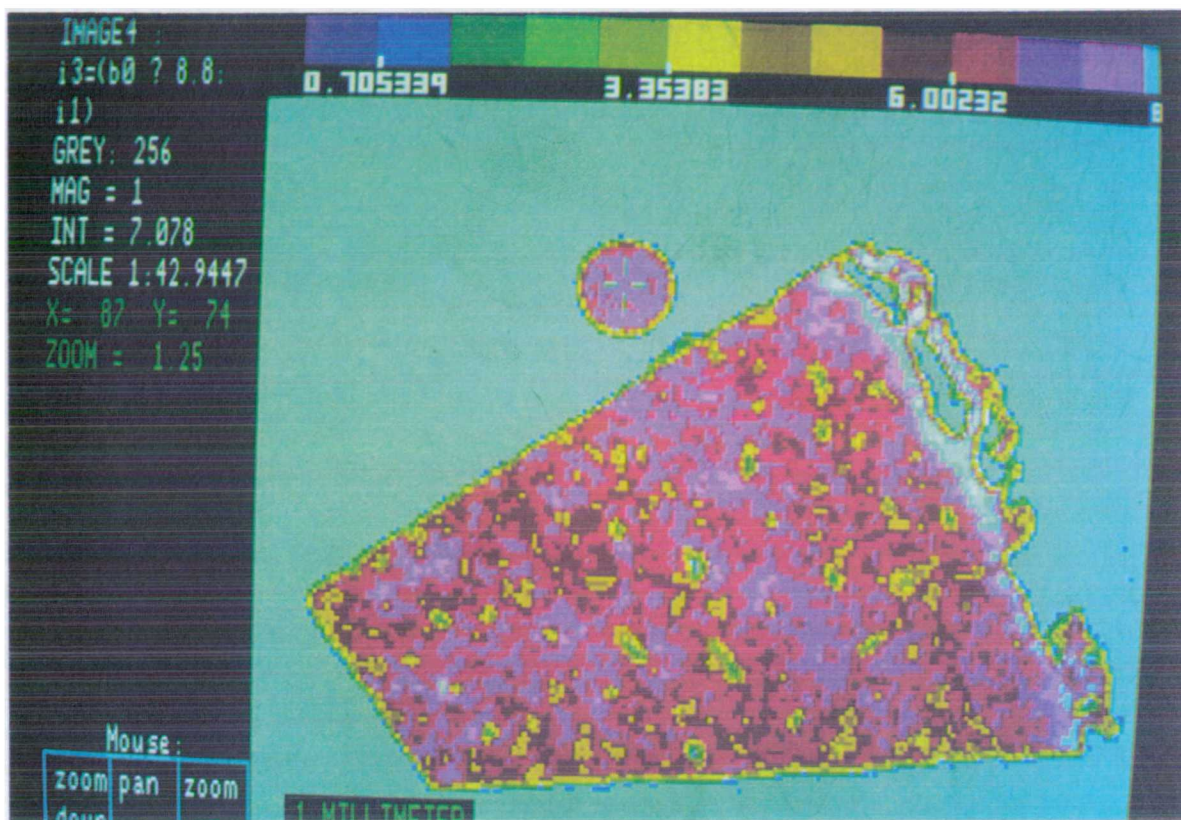


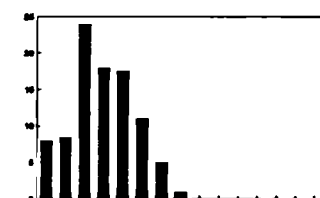
Figure 9.3

Tomogram of Barton femur with colour bar recalibrated to distinguish between density variation within the cortex. Blue represents lower density values relative to bone which increase to white. The cortex is seen to be decreased around Haversian canals, with only occasional diagenetic foci evident as pink to white pixels. Circular feature is aluminium standard.

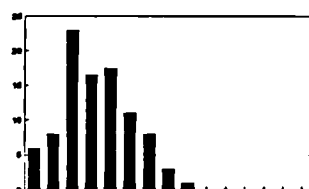


Figure 9.4 Diagenetic Shift in Sample Group

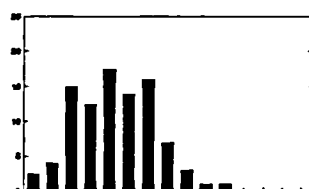
% of total in each mineral density bin



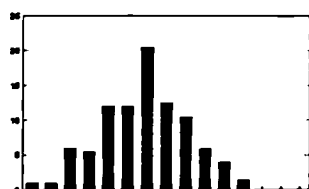
Standard



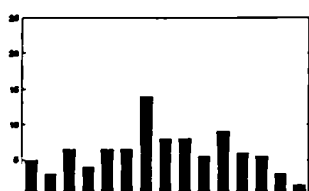
Mary Rose Inoue 1



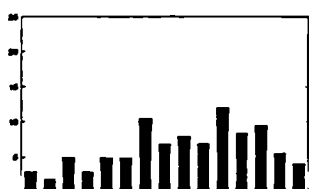
Mary Rose Inoue 2



Barton Inoue 1

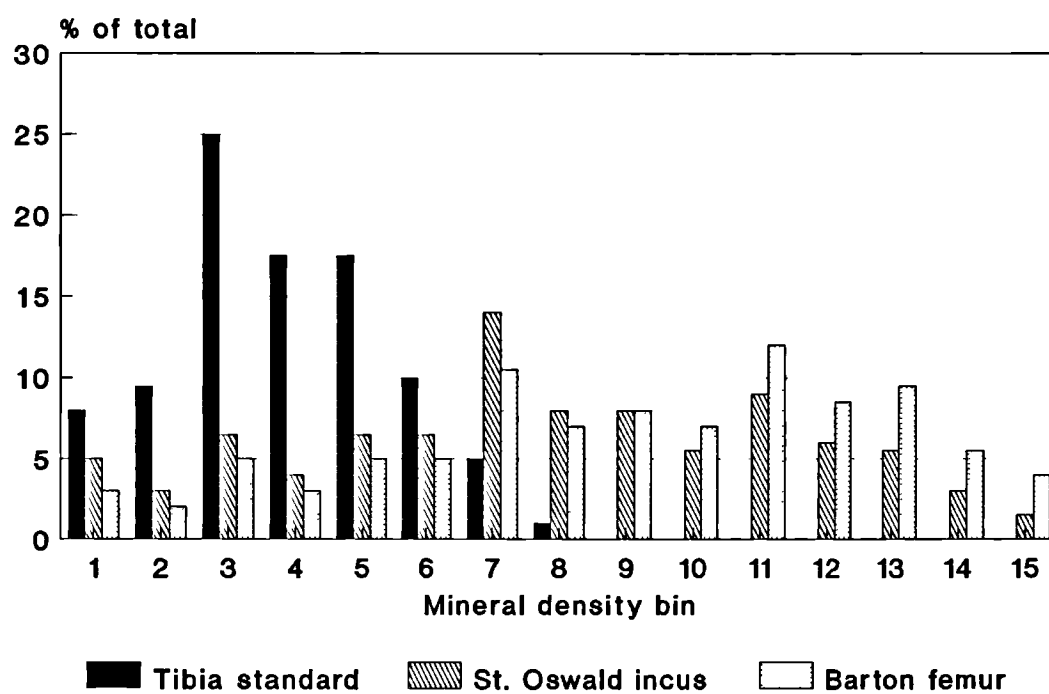


St Oswald Inoue



Barton Inoue 2

**Figure 9.5 Maximum Diagenetic Shift**  
QBSE of bone



archaeological human bone is seen to increase with increased diagenetic ingress and remodelling. This kind of change may be described as 'diagenetic shift'.

## 9.8 Discussion

The MCT analysis has confirmed that the high density foci identified throughout this thesis using SEM/BSE imaging in bacterially remodelled archaeological and forensic material, represent real localised increases in density, well above that of bone. The blockface surface topography generated by polishing, a contributory factor in the BSE signal, is not as significant as the change in composition. However, it is unclear whether the assumed increased porosity in regions of decreased density contributed an edge artefact to the BSE signal, since the resolution of the tomogram was not sufficient to resolve the small and complex sites where the mineralisation changes had occurred in this profoundly remodelled diagenetic bone. This relatively poor resolution in the tomogram may go some way to explain the lack of evidence for small high density diagenetic foci within the femoral cortex. Additionally, the diffusion cloud of electrons, which represents the sample volume per scanning point in SEM/BSE images, has been estimated to be 134 microns deep when using an accelerating voltage of 20kV (Howell & Boyde, 1994). This means that unless the diagenetic focus is large, and some can be, then a superimposition of differing density values may occur, providing misleading atomic number contrast. This last point is really a methodological problem for all material examined using the BSE method, since in order to reduce the size of the diffusion cloud (where energy is essentially dissipated)

one has to reduce the accelerating voltage, which in-turn causes massive irradiation damage to the specimen's surface (Howell & Boyde, 1994).

The QBSE study has usefully demonstrated the relationship between diagenetic microstructural change and the resultant shift towards a higher mean density. It is unclear whether this shift towards higher density is the result of bone mineral becoming more like HA, or changing its crystallinity or changing its composition towards other minerals such as octacalcium phosphate, whitlockite, brushite or calcite (as can occur in enamel caries). Given that the micromorphology of the bacteria-related change is similar to oral calculus, and therefore retains an elemental milieu of bacterial residue (LeGeros et al., 1988), then it is considered likely that unusual elemental substitutions will have occurred within areas affected by such post mortem ingress. Previous elemental studies on archaeological and fossil bone have demonstrated a large diversity in major and trace element composition relative to modern bone (Sealy et al., 1995; Sillen & LeGeros, 1991; Price, 1989; Buikstra et al., 1989; Tuross et al., 1989; Klepinger et al., 1986; Kyle, 1986). That bone mineral crystallinity appears to increase in archaeological and fossil specimens has also been documented (Bartsiokas & Middleton, 1992) with the suggestion that such changes occur only after at least 1000 years post mortem (Sillen, 1989). However, an increase in HA crystallinity has been reported elsewhere as an ante mortem function of age (Bonar et al., 1983).

## 9.9 Conclusion

The MCT study showed conclusively that the high density component of diagenetically altered bone, observed in this thesis by SEM/BSE imaging, is

real, and not an artefactual product. The application of QBSE to a range of archaeological specimens which represented a range of preservational states, from unaffected to profoundly diagenetically altered bone, demonstrated a gradual but highly significant shift in mineral density, well above that of normal bone. This diagenetic shift in mineral density or mineral composition has been additionally noted to affect terrestrial bone to a greater degree than marine deposited bone. Further studies are essential in this area if the processes of preservational or destructive fossilisation are to be more fully understood.

## CHAPTER 10: SUMMARY AND CONCLUSIONS

The research aim of this study was to assess the microstructural impact of diagenetic or post mortem alteration to predominately human skeletal tissues. The method of assessment selected was microscopical analysis, mainly using a scanning electron microscope in backscattered electron mode, and to a lesser extent using confocal reflection microscopy. With the use of these technologies the potential differing microstructural morphologies of post mortem alteration were investigated in archaeological material, both normal and pathological, from terrestrial and marine contexts. A baseline study provided new information on both the microstructural organization of post mortem alteration and on any alterations to tissue density. It also enabled the distinction of differing morphological types of post mortem alteration between terrestrial and marine contexts.

Further studies were then undertaken on a case-by-case basis on skeletal material which offered some unique pathology or environmental context. The speed of post mortem alteration was also assessed from well documented forensic material with reference to the depositing environment. On the basis of the results from the forensic study a small study was undertaken on archaeological material (both human and animal) which had suffered deliberate post mortem vascular disruption, in order to determine whether post mortem alteration to the skeletal tissues could still occur. In addition, an investigation into the relative survival of human DNA in archaeological bone versus its microstructural preservation status was undertaken. A retrospective study was made of all material examined for

this thesis for the presence of MIOL (mineral infilled osteocyte lacunae), as potential DNA survival sites within archaeological bone.

Finally, two quantitative studies were undertaken. The first utilized microtomographic (MCT) imaging to validate previous observations, made using the SEM/BSE method, of high density post mortem foci within bacterially remodelled bone. The second quantified the backscattering of electrons from a group of archaeological specimens which exhibited a range of microstructural preservational states, in order to measure changing mineral status or "diagenetic shift", evidenced by the SEM/BSE imaging method.

The results indicated generally that diagenetic change or post mortem alteration to the skeletal tissues can be extensive both in terms of altered microstructure and mineral density. The difference identified between the post mortem morphologies of terrestrial and marine contexts proved that the interaction between invading microfauna and environment are extremely important, governing not only the type of microstructural alteration, but also whether such a change will occur at all. It was discovered that environmental information can be ascertained from affected skeletal material, such that a clear stratigraphic relationship can be established. The speed of post mortem change, considered an irrelevance by previous authors, excepting Yoshino et al. (1991), has been established as occurring as soon as 3 months after death. In addition, the morphological changes associated with bacteria and marine deposition have also been brought forward to 15 months and 2 years post mortem respectively. These results set a new time-frame for the speed at which post mortem alteration

can occur, and it is hypothesized that such alterations can begin within 3 days after death, and certainly before skeletonization if translocated gut bacteria are responsible. Hence, post mortem alteration to skeletal microstructure - otherwise known as diagenesis - can occur very soon after death and does not represent a process that both begins and proceeds within a purely archaeological time-frame, nor is it a phenomenon which occurs solely post burial, as the use of the term diagenesis suggests. A cascading process of attack from gut to terrestrial microfauna may occur but the maximum duration of such an event, as yet, remains unknown.

Previous studies have established that mtDNA can be recovered from skeletonized human bone which is both forensic and archaeological. The work of this thesis has established that the presence and degree of post mortem alteration to microstructure can and does have a deleterious effect on relative mtDNA recovery. This result helps to explain the variation in results of other methods which attempt to recover bone related organic residues, since the presence of microbial acids and proteases would have wide-ranging effects which would go beyond the sole destruction of a relatively delicate nucleic acid. Once bacteria die and mineralise within post mortem voids, their cellular residues will be released by experimental demineralisation to mix freely with any skeletal ones, potentially combining with or contaminating them, to further complicate the constituent identity of the organic matrix. Hence, although this study was not concerned with the organic changes brought about by diagenesis, it is relevant that the degree of post mortem change to microstructure has a direct relationship to the preservational status of the organic component of the skeleton.



That mtDNA is recoverable from bone using the PCR method suggests that some preservational mechanism must exist for this to occur. It has been documented elsewhere that osteocytes appear to mineralise ante mortem in areas of the skeleton associated with low bone turnover. Such morphologically identifiable osteocytes or MIOL have, for the first time, been identified in archaeological material both human and animal. A MIOL was also identified in a profoundly diagenetically remodelled specimen, in a region which bordered morphologically intact bone. This finding helps to explain how it is that mtDNA is preserved and is therefore recoverable from bone which is of considerable antiquity and/or has undergone considerable microstructural post mortem alteration.

The SEM in BSE mode has proved to be a powerful method, well suited to investigating and identifying small changes to microstructure and density within forensic and archaeological skeletal material. The MCT study confirmed that the dramatic changes in tissue density, particularly in those foci exhibiting a higher density than bone, dentine and cementum, were real and not artefactual. The QBSE study, which quantitated electron backscattering, illustrated that increased post mortem alteration to microstructure of the bacterial-type resulted in a "diagenetic shift" toward increased density values, well above that of bone and dentine. Diagenetic shifts toward higher mean density values have serious contaminative implications for any technique which measures density or which assumes hydroxyapatite (bone salt) integrity, but also for understanding the progress or process of fossilisation itself.

To conclude, post mortem alteration or diagenetic change to skeletal material has been shown to be extensive, occurring within a relatively short time after death. It does not represent a post burial phenomenon as the term diagenesis suggests, but can begin above ground in a range of exposural contexts. The implication of gut bacteria in the promotion of early bacterially-related microstructural change is strong, as is the importance of body status at the point of, or soon after, death. Post mortem alteration to skeletal microstructure can also provide environmental information, since distinct post mortem morphologies have been identified between terrestrial and marine contexts. It can also provide localized environmental information within a stratigraphic matrix as evidenced by the Mary Rose results. Characterizing the post mortem microstructural and density changes to bone has helped to elucidate not only the preservational status of mtDNA in terms of its' relative retrieval in archaeological specimens, but also the potential location of the mtDNA itself. That diagenetic shift occurs in profoundly bacterially-remodelled specimens from terrestrial contexts, relative to the excellent preservation of marine specimens, may help to explain why marine vertebrates far outnumber terrestrial vertebrates in the fossil record. Bacterially driven microstructural change is considered a destructive form of fossilisation.

Clearly, post mortem alteration, or diagenetic change, to human and animal skeletal material represents an important taphonomic resource of relevance to archaeology, forensic science and vertebrate palaeontology. That it has been considered only as an irksome contaminative factor, although understandable, seems now quite shocking. A vast amount of work remains to be undertaken, especially in establishing the earliest moment that post

mortem alteration to microstructure can occur, the microfauna responsible for the such changes when set against body status and the deposit environment and the contribution of the aquatic environment as a special variable. Further studies are required also to establish the frequency of MIOL in detailed extant and archaeological populations and to extend the quantification of diagenetic shift in order to test the notion of destructive fossilisation.

A number of publications have arisen from this study and are contained in Appendix 10.

## REFERENCES

- Allen T. (1989) Abingdon Vineyard redevelopment. *South Middl. Archaeol.*, 19, 44-47
- Allen T. (1990a) Abingdon Vineyard redevelopment. *South Middl. Archaeol.*, 20, 73-74
- Allen T. (1990b) Abingdon. *Current Arch.*, 121, 24-27
- Andrews C. (1990) *Egyptian Mummies*. British Museum Publications, London
- Andrews M.L.A. (1978) *The Life That Lives on Man*. Arrow Books Ltd., London.
- Andrews P. (1990) *Owls, Caves and Fossils*. Natural History Museum, London
- Arnaud G., Arnaud S., Ascenzi A., Bonucci E. & Graziani G. (1978) On the problem of the preservation of human bone in sea-water. *J. Human Evo.*, 7, 409-420
- Ascenzi A. & Silvestrini G. (1984) Bone-boring marine micro-organisms: an experimental investigation. *J. Human Evo.*, 13, 531-536
- Behrensmeyer A.K. & Hill A.P. (1988) *Fossils in the Making*. Midway Reprint, University of Chicago, Chicago.
- Berg S. (1963) The determination of bone age. In: *Methods of Forensic Science*. Ed. F. Lundquist, Interscience Publishers, John Wiley & Sons, London & New York, II, pp. 231-252
- Blumberg J.M. & Kerley E.R. (1966) A critical consideration of roentgenology and microscopy in Palaeopathology. In: *Human Paleopathology*. Ed. S. Jarcho, Yale University Press, New Haven and London, pp. 150-170

Bonar L.C., Roufosse A.H., Sabine, Grynpas M.D. & Glimcher M.J. (1983) X-ray diffraction studies of the crystallinity of bone mineral in newly synthesized and density fractionated bone. *Calcif. Tiss. Int.* 35, 202-209

Boyde A. (1980) Evidence against osteocytic osteolysis. *Metab. Bone Dis. et Rel. Res.*, 2, 239-255

Boyde A., Howell P.G.T., Bromage T.G., Elliott J.C., Riggs C.M., Bell L.S., Kneissell, Reid S.A., Jayasinghe J.A.P. & Jones S.J. (1992) Application of mineral quantitation of bone by histogram analysis of backscattered electron imaging. In: *Chemistry and Biology of Mineralized Tissues*. Eds. H. Slavkin & P. Price. Excerpta Medica, Amsterdam, London, New York & Tokyo, pp. 47-61

Boyde A., Maconnachie E., Reid S.A., Delling G. & Mundy G.R. (1986) Scanning electron microscopy in bone pathology: review of methods, potential and applications. *Scan. Elec. Micros.*, 4, 1537-1554

Boyde A. & Jones S.J. (1983) Back-scattered electron imaging of skeletal tissues. *Metab. Bone Dis. Rel. Res.*, 5, 145-150

Boyde A. & Jones S.J. (1983) Backscattered electron imaging of dental tissues. *Anat. Embryol.*, 168, 211-226

Buikstra J.E., Frankenberg S., Lambert J.B. & Xue L. (1989) Multiple elements: multiple expectations. In: *The Chemistry of Human Bone*. Ed. T. D. Price, Cambridge University Press, Cambridge, pp 155-210

Burn A.R. (1972 trans.) *Herodotus: The Histories*. Penguin Books Ltd., pp. 160-161

Cameron D.A. (1972) The ultrastructure of bone. In: *The Biochemistry and Physiology of Bone*. Ed. G.H. Bourne, Academic Press, New York & London, I, pp. 191-231

Cano R. J. & Borucki M. K. (1995) Revival and identification of bacterial spores in 25-to-40-million-year-old Dominican amber. *Science*, 268, 1060-1064

Cano R. J., Poinar H. N., Pieniazek N. J., Acra A. & Poinar G. O. Jr. (1993) Amplification and sequencing of DNA from a 120-135-million-year-old weevil. *Nature*, 363, 536-538

Chamberlain A. H. L. & Moss S. T. (1988) The thraustochytrids: a protist group with mixed affinities. *Biosystems*, 21, 341-349

Chappard D., Alexandre C., Laborier J. C., Robert J. M. & Riffat G. (1984) Paget's disease of bone: a scanning electron microscopic study. *J. Submicrosc. Cytol.*, 16, 341-348

Clement A. J. (1958) The antiquity of caries. *Brit. Dent. J.*, 104, 115-123

Clement A. J. (1963) Variations in the microstructure and biochemistry of human teeth. In: *Dental Anthropology*. Ed. D. R. Brothwell, Pergamon Press, London, pp. 245-269

Connan J. & Dessort D. (1991) Du bitume des baumes de momies: determination de son origine et evaluation de sa quantite. *C.R. Hebd. Seanc. Acad. Sci.*, Paris, 312, 1445-1452

Cook M., Molto E. & Anderson C. (1989) Fluorochrome labelling in Roman period skeletons from Dakhleh Oasis, Egypt. *Am. J. Phys. Anth.*, 80, 137-143

Cook S. F., Brooks S. T. & Ezra-Cohn H. E. (1962) Histological studies on fossil bone. *J. Paleontol.*, Vol 36, 3, 483-494

Corry J. L. (1978) Possible sources of ethanol ante and post mortem: its relationship to the biochemistry and microbiology of decomposition. *J. App. Microbiol.*, 44, 1-56

Daniel G. (1975) A 150 Years of Archaeology. Duckworth, Trowbridge, pp. 29-56

Davis S.J.M. (1987) The Archaeology of Animals. B.T. Batsford Ltd., London

Denninger H.S. (1933) Palaeopathological evidence of Paget's disease. Ann. Med. Hist., 5, 73-81

Desmond A. (1982) Archetypes and Ancestors. Blond & Briggs, London

Doberenz A.R. (1967) Ultrastructure of fossil dentinal collagen. Calc. Tiss. Res., 1, 166-169

Doberenz A.R. & Wyckoff R.W.G. (1967) The microstructure of fossil teeth. J. Ultrastruct. Res., 18, 166-175

Dobney K. & Brothwell D. (1988) A scanning electron microscope study of archaeological dental calculus. In: Scanning Electron Microscopy in Archaeology. Ed. S.L. Olsen, BAR International Series 452, Oxford, pp. 372-385

Dolan C.T., Brown A.L. & Ritts R.E. (1971) Microbiological examination of post mortem tissues. Arch. Path., 92, 206-211

Duckworth W.H.L. (1901) Some dental rudiments in human crania. Trans. Odont. Soc. Brit., 33, 4, 89-121

Duerden B.I., Reid T.M.S. & Jewsbury J.M. (1993) Microbial and Parasitic Infection. Edward Arnold, London & New York.

During E. (1990) An osteological and anthropological analysis of the skeletal remains from the 362 years old Swedish warship Vasa. Report: Osteological Research Laboratory, University of Stockholm, Sweden

Efremov J.A. (1940) Taphonomy: a new branch of paleontology. Pan-Am. Geol., 74, 81-93

Elliot J.C., Bromage T.G., Anderson P., Davis G. & Dover S.D. (1989) Application of X-ray microtomography to the study of dental hard tissues. In: Tooth Enamel V. Ed. R.W. Fearnhead, Florence Press, Yokohama, pp. 429-433

Elliot J.C., Anderson P., Boakes R. & Dover S.D. (1989) Scanning X-ray microradiography and microtomography of calcified tissues. In: Calcified Tissue. Ed. D.W.L. Hukins, Macmillan Press, Basingstoke, pp. 41-63

Enlow D.H. & Brown S.O. (1956) A comparative histological study of fossil and recent bone tissues, Part I. Texas J. Sci., 8, 405-443

Enlow D.H. & Dale J.G. (1985) Childhood facial growth and development. In: Oral Histology: development, structure and function. Ed. A. R. Ten Cate, Mosby, St. Louis, pp. 398-445

Falin L.I. (1961) Histological and histochemical studies of human teeth of the Bronze and Stone Ages. Arch. Oral Biol., 5, 5-13

Fearne J.M., Elliot J.C., Wong F.S.L., Davis G.R., Boyde A. & Jones S.J. (1994) Deciduous enamel defects in low-birth-weight children; correlated X-ray microtomographic and backscattered electron imaging study of hypoplasia and hypomineralization. Anat. Embryol., 189, 375-381

Fischman J. (1995) Have 25-million-year-old bacteria returned to life? Science, 268, 977

Fisher D.L., Holland M.M., Mitchell L., Sledzik P.S., Wilcox A.W., Wadhams M. & Weedn V.W. (1993) Extraction, evaluation and amplification of DNA from decalcified and undecalcified United States Civil War bone. J. Foren. Sci., 38, 60-68

Fratzl P., Fratzl-Zelman N., Klaushofer K., Vogl G. & Koller K. (1991) Nucleation and growth of mineral crystals in bone studied by small angle X-ray scattering. Calcif. Tissue Int., 48, 407-413



Freeman E. (1985) Periodontium. In: Oral Histology. Ed. A.R. Ten Cate. C.V. Mosby Comp., St. Louis, pp. 234-263

Galloway A., Birkby W.H., Jones A.M., Henry T.E. & Parks B.O. (1989) Decay rates of human remains in an arid environment. J. Foren. Sci., 34, 607-616

Garland A.N. (1987) Palaeohistology. Science and Archaeology. 29, 25-29.

Garland A.N. (1989) Microscopical analysis of fossil bone. App. Geochem., 4, 215-229

Garland A.N. (1988) A Histological study of archaeological bone decomposition. In: Death, Decay and Reconstruction. Eds: Boddington et al., Manchester University Press, Manchester, pp.109-126

Gill P., Ivanov P.L., Sullivan K., Kimpton C., Piercy R., Benson N., Tully G. & Evett I. (1994) Identification of the remains of the Romanov family. Nature Genet., 6, 130-135

Goldenberg E.M. (1991) Amplification and analysis of Miocene plant fossil DNA. Phil. Trans. R. Lond. B, 333, 419-427

Golubic S., Perbuis R.D. & Lukas K.L. (1975) Boring microorganisms and microborings in carbonate substrates. In: The Study of Trace Fossils. Ed. R.W. Frey, Springer-verlag, Berlin, Heidelberg & New York, pp. 229-259

Gordon I., Shapiro H.A. & Berson S.D. (1988) Forensic Medicine. Churchill Livingstone, Edinburgh & London, pp. 1-62

Gould S.J. (1965) Is uniformitarianism necessary? Am. J. Sci., 263, 223-228

Graf W. (1949) Preserved histological structures in Egyptian and ancient Swedish skeletons. Acta Anat., 8, 236-250

Grupe G., Werrigloer U.D. & Parsche F. (1993) Initial stages of bone decomposition. In: Prehistoric Human Bone: Archaeology at the Molecular Level. Eds. J.B. Lambert & G. Grupe, Springer-Verlag, Berlin, pp. 257-274

Hackett C.J. (1981) Microscopical focal destruction (tunnels) in excavated human bones. Med., Sci. Law, 21, 243-265

Hackett C.J. (1976) Diagnostic criteria of Syphilis, Yaws and Treponarid (Treponematoses) and some other diseases in dry bone. Springer, Verlag, Berlin and New York.

Hagelberg E. & Clegg J.B. (1993) Genetic polymorphisms in prehistoric Pacific islanders determined by analysis of ancient bone DNA. Proc. R. Soc. B, 252, 163-170

Hagelberg E., Gray I.C. & Jeffreys A.J. (1991) Identification of the skeletal remains of a murder victim by DNA analysis. Nature, 352, 427-429

Hagelberg E. & Hedges R. (1989) Ancient bone DNA amplified. Nature, 342, 485

Haines R.B. & Scott W.J. (1940) An anaerobic organism associated with "bone-taint" in beef. J. Hygiene, 40, 154-161

Hamperl H. (1966) Problems in pathology and palaeopathology and bone. In: Human Palaeopathology. Ed. S. Jarcho, Yale University Press, New Haven and London, pp. 81-83

Harper D.R. (1989) A comparative study of the microbiological contamination of post mortem blood and vitreous humour samples for ethanol determination. Foren. Sci. Int., 43, 37-44

Hare P.E. (1980) Organic chemistry of bone and it's relation to the survival of bone in the natural environment. In: Fossils in the making. Eds. A.K. Behrensmayer & A.P. Hill, University of Chicago Press, Midway Reprint, USA, pp. 208-219

Hanson D.B. & Buikstra J.E. (1987) Histomorphological alteration in buried human bone from the lower Illinois Valley: implications for palaeodietary research. *J. Arch. Sci.*, 14, 549-563

Highsmith R.C. (1981) Lime-boring algae in hermatypic coral skeletons. *J. Exp. Biol. Ecol.*, 55, 267-281

Higuchi R., Bowman B., Freidberger M., Ryder M., Wilson O.A. & A.C. (1984) DNA sequences from the quagga, an extinct member of the horse family. *Nature*, 312, 282-284

Hodder I. (1991) *Archaeological Theory in Europe: the Last Three Decades*. Routledge, London, pp. 1-24

Holland M.M., Fisher D.L., Mitchell L.G., Rodriguez W.C., Canik J.J., Merrill C.R. & Weddn V.W. (1993) Mitochondrial DNA sequence analysis of human skeletal remains: identification of remains from the Vietnam War. *J. Foren. Sci.*, 38, 542-553

Hopewell Smith A. (1903) *The histology and patho-histology of the teeth*. The Dental Manufacturing Comp., London, pp. 345-351

Howell P.G.T. & Boyde A. (1994) Monte Carlo simulations of electron scattering in bone. *Bone*, 15, 285-291

Ingram M. (1952) Internal bacterial taints ('bone taint' or 'souring') of cured pork legs. *J. Hygiene*, 50, 165-181

Isaacs W.A. & Little K. (1963) Collagen and a cellulose substance in fossil dentine and bone. *Nature*, 197, 192

Iscan M.Y. (1988) Rise of forensic anthropology. *Yearb. Phys. Anthropol.*, 31, 203-230

Iscan M.Y. & Kennedy K.A.R. (1989) *Reconstruction of Life from the Skeleton*. Alan R. Liss Ltd., New York

Janaway R.C. (1985) Dust to dust: the preservation of textile materials in metal artefact corrosion products with reference to inhumation graves. *Science and Archaeology*, 27, 29-34

Jarcho S. (1966) *Human Palaeopathology*. Yale University Press, New Haven and London

Jones A.M. & Rule M.H. (1993) Preserving timber structures recovered from the marine environment: cold storage as a means of passive conservation. The Mary Rose a case study. *Biodet. Cult. Prop.*, 2, 117-140

Jones S.J. (1987) The root surface: an illustrated review of some scanning electron microscope studies. *Scan. Micros.*, 1, 2003-2018

Jones S.J. & Boyde A. (1987) Scanning microscopic observations on dental caries. *Scan. Micros.*, 1, 1991-2002

Jones S.J., Boyde A., Piper K. & Komiya S. (1992) Confocal microscopic mapping of osteoclastic resorption. *Micros. Anal.*, 18-20

Joy D.C. (1988) An introduction to Monte Carlo simulations. In: *Inst. Phys. Conf. Ser. No. 93, Vol I*, 23-32

Junqueira L.C., Carneiro J. & Long L.A. (1986) Bone. In: *Basic Histology*. Apple Century Crofts, pp. 140-165

Keeley H.C.M., Hudson G.E. & Evans J. (1977) Trace element contents of human bones in various states of preservation. *J. Arch. Sci.*, 4, 19-24

Keith M.S. & Armelagos G.J. (1988) An example of in vivo tetracycline labelling: reply to Piepenbrink. *J. Arch. Sci.*, 15, 595-601

Kellerman G.D., Waterman N.G. & Scharfenberger L.F. (1976) Demonstration in-vitro of post mortem bacterial migration. *Am. J. Clin. Path.*, 66, 911-915

Kelly P.J., Peterson L.F.A., Dahlin D.C. & Plum G.E. (1961) Osteitis deformans (Paget's disease of bone). *Radiology*, 77, 368-375

Kevorkian J. & Bylsma G.W. (1961) Transfusion of post mortem human blood. *Am. J. Clin. Path.*, 35, 413-419

Klepinger L.L. Kuhn J.K. & Williams W.S. (1986) An elemental analysis of archaeological bone from Sicily as a test of predictability of diagenetic change. *Am. J. Phys. Anth.*, 70, 325-331

Kyle J.H. (1986) Effect of post-burial contamination on the concentration of major and minor elements in human bones and teeth - the implications for palaeodietary research. *J. Arch. Sci.*, 13, 403-416

Lapedes D.N., Ed. (1978) *McGraw-Hill Encyclopedia of the Geological Sciences*. McGraw-Hill Inc., New York, pp. 153, 247-8.

Lawrence D.R. (1971) The nature and structure of paleoecology. *J. Palaeont.*, 45, 593-607

LeGeros R.Z., Orly I., LeGeros J.P., Gomez C., Kazamiroff J., Tarpley T. & Kerebel B. (1988) Scanning electron microscopy and electron probe microanalysis of the crystalline components of human and animal dental calculi. *Scan. Micros.*, 2, 345-356

Lindahl T. (1993) Instability and decay of the primary structure of DNA. *Nature*, 362, 709-715

Lindahl T. & Nyberg B. (1972) Rate of depurination of native deoxyribonucleic acid. *Biochem.*, 11, 3610-3618

Lyman R.L. (1994) *Vertebrate Taphonomy*. Cambridge University Press, Cambridge

Maat G.J.R. (1993) Bone preservation, decay and its related conditions in ancient human bones. *Int. J. Osteoarch.*, 3, 77-86

Mainous M.R., Tso P., Berg R.D. & Deitch E.A. (1991) Studies of the route, magnitude and time course of bacterial translocation in a model of systemic inflammation. Arch. Surg., 126, 33-37

Maltby M. (1989) Urban-rural variations in the butchering of cattle in Romano-British Hampshire. In: Diet and Craft: the Evidence of Animal Bone from Towns. Eds. D. Serjeantson & T. Waldron, BAR 199, pp. 75-95

Manly R.S. & Hodge H.C. (1939) Density and refractive index studies of dental hard tissues I. J. Dent. Res., 18, 133-141

Manly R.S., Hodge H.C. & Ange L.E. (1939) Density and refractive index studies of dental hard tissues II. J. Dent. Res., 18, 203-211

Marchiafara V., Bonucci L. & Ascenzi A. (1974) Fungal Osteoclasia: a model of dead bone resorption. Calc. Tiss. Res., 14, 195-210

Marshall J.C. (1991) The ecology and immunology of the gastrointestinal tract in health and critical illness. J. Hosp. Infect., 19, 7-17

Martin L.B., Boyde A. & Grine F.E. (1988) Enamel structure in primates: a review of scanning electron microscopic studies. Scan. Micros., 2, 1503-1526

McClanahan T.R. & Kurtis J.D. (1991) Population regulation of the rock-boring sea urchin *Echinometra mathaei* (de Blainville). J. Exp. Mar. Biol. Ecol., 147, 121-146

Meeks N. (1988) Backscattered electron imaging of archaeological material. In: Scanning Electron Microscopy in Archaeology. Ed. S.L. Olsen, BAR International Series 452, Oxford, pp. 23-44

Micozzi M.S. (1991) Post Mortem Change in Human and Animal Remains. Charles Thomas, Springfield Illinois

Molleson T., Cox M., Waldron A.H. & Whittaker D.K. (1993) The Anthropology: The Middling Sort. Spitalfields Project Vol. 2, Set no. 86, CBA, London

Morganthaler P.W. & Baud C.A. (1956) Sur une cause d'alteration des structures dans l'os humain fossile. Act. Soc. Helv. Sci. Natur., 136, 142-3

Neiburger E.J. (1988) Syphilis in a Pleistocene bear. Nature, 333, 603

Neidrig H. (1978) Physical background of electron backscattering. Scanning, 1, 17-34

Nelson D.A. & Sauer J. (1984) An evaluation of postdepositional changes in trace element content in human bone. Am. Antiq., 49, 141-147

Nelson D.G.A. (1990) Backscattered electron imaging of partially-demineralized enamel. Scan. Micros. 4, 31-42

Newman H.N. & Poole D.F.G. (1974) Structural and ecological aspects of dental plaque. In: The Normal Flora of Man. Eds. F.A. Skinner & J.G. Carr, Academic Press, London & New York, pp. 111-134

Nixon M. & Maconnachie E. (1988) Drilling by *Octopus vulgaris* (Mollusca: Cephalopoda) in the Mediterranean. J. Zool. Lond., 216, 687-716

Olsen S.L. (1988) Scanning Electron Microscopy in Archaeology. BAR International Series 452, Oxford

Ortner D.J. & Putscher W.G.J. (1985) Identification of Pathological Conditions in Human Skeletal Remains. Smithsonian Institution Press, Washington

Paabo S. (1985) Molecular cloning of ancient Egyptian mummy DNA. Nature, 314, 644-645

Paabo S., Gifford J.A. Wilson A.C. (1988) Mitochondrial DNA sequences from a 7000 year-old-brain. Nucl. Acids Res., 16, 9775-9787

Paget, J. (1877) On a form of chronic inflammation of bones (osteitis deformans). Trans. Med. Chirurgical Soc., 60, 37-64

Pate E.D. & Hutton J.T. (1988) The use of soil chemistry data to address post-mortem diagenesis in bone mineral. J. Arch. Sci., 15, 729-739

Piepenbrink H. (1986) Two examples of biogenous dead bone decomposition and their consequences for taphonomic interpretation. J. Arch. Sci., 13, 417-430

Piepenbrink H. & Schutowski H. (1987) Decomposition of skeletal remains in desert dry soils. Human Evolution, 2, 481-491

Poole, D.F.G. & Tratman E.K. (1978). Post-mortem changes on human teeth from late upper Palaeolithic/Mesolithic occupants of an English limestone cave. Arch. Oral Biol., 23, 1115-1120

Porter D. & Lingle W.L. (1984) Marine shell boring microorganisms include Thraustochytrids and other heterotrophic Protista. J. Protozool., 31, 20A-21A

Price T. D. (1989) The Chemistry of Prehistoric Human Bone. Cambridge University Press, Cambridge

Pritchard J.J. (1972) General histology of bone. In: The Biochemistry and Physiology of Bone. Ed. G.H. Bourne, Academic Press, New York & London, Vol. I, pp. 1-20

Purdy E.G. (1968) Carbonate diagenesis: an environmental survey. Geologica Romana, 7, 183-228



- Raghukumar C., Rao V.P.C. & Iyer S.D. (1989) Precipitation of iron in Windowpane oyster shells by marine shell-boring cyanobacteria. *Geomicrobiology*, 7, 235-244
- Reid S.A. & Boyde A. (1987) Changes in mineral density distribution with age: image analysis using backscattered electrons in the SEM. *J. Bone & Min. Res.* 2, 13-22
- Retallack G. (1990) *Soils of the Past: an Introduction to Palaeopedology*. Unwin Hyman, Boston
- Richelle L.J. & Onkelinx C. (1969) Recent advances in the physical biology of bone and other hard tissues. In: *Mineral Metabolism*, Vol III, Academic Press, New York, 123-190
- Rogers J. (1990) The human skeletal material. In: *Hazleton North: The Excavation of a Neolithic Long Cairn of the Cotswold Severn Group*. Ed. A. Saville, HBMC Report 13, London, pp. 182-198
- Rolfe W. D. I. & Brett D. W. (1969) Fossilization processes. In: *Organic Geochemistry: Methods and Results*. Eds. G. Eglinton & M. T. J. Murphy, Springer-Verlag, Berlin, pp. 213-244
- Roney J.G. Jnr. (1966) Palaeoepidemiology: an example from California. In: *Human Palaeopathology*. Ed: S. Jarcho, Yale University Press, New Haven and London, pp. 99-107
- Rothschild B.M. (1988) Existence of syphilis in a Pleistocene bear. *Nature*, 335, 595
- Rothschild B.M. & Turnbull W. (1987) Treponemal infection in a Pleistocene bear. *Nature*, 329, 61-62
- Roux W. (1887) Über eine Knochenlebende Gruppe von Faderpilzen (*Mycelites ossifragus*). *Z. wiss. Zool.*, 45, 227-254

Rule M.H. (1983) The Mary Rose: the Excavation and Raising of Henry VIII's Flagship. Conway Maritime Press, London

Sato-Okoshi W., Sugawara Y. & Nomura T. (1990) Reproduction of the boring polychaete *Polydora variegata* inhabiting scallops in Abashiri Bay, North Japan. Marine Biol., 104, 61-66

Saville A. (1990) Hazleton North: The Excavation of a Neolithic Long Cairn of the Cotswold Severn Group. HBMG Report 13, London

Schaffer J. (1889) Über den feineren Bau fossiler Knochen. S.B. Akad. Wiss. Wien. Math-nat. III, 98, 319-382

Schaffer J. (1890) Über Roux'sche Kanäle in menschlichen Zähnen. S.B. Akad. Wiss. Wien. Math-nat III, 99, 146-152

Schaffer J. (1894) Bemerkungen zur Geschichte der Bohrkanäle in Knochen und Zähnen. Anat. Anz., 10, 459-464

Sergis S., Ascenzi A. & Bonucci E. (1972) Torus palatinus in the Neandertal Circeo I skull: a histologic, microradiographic and electron microscopic investigation. Am. J. Phys. Anthropol., 36, 189-198

Shinoda K. & Kunisada T. (1994) Analysis of ancient Japanese society through mitochondrial DNA sequencing. Int. J. Osteoarch., 4, 291-297

Shipman P. (1988) Actualistic studies of animal resources and hominid activities. In: Scanning Electron Microscopy in Archaeology. Ed. S. L. Olsen, BAR 452, Oxford, pp. 261-286

Sillen A. (1989) Diagenesis of the inorganic phase of cortical bone. In: The Chemistry of Human Bone. Ed. T. D. Price, Cambridge University Press, Cambridge, pp. 211-229

Silver I.A. (1969) The aging of domestic animals. In: Science in Archaeology, Eds. D. Brothwell & E. Higgs, Thames & Hudson, London, pp. 283-302

Simpson K. & Knight B. (1985) Forensic Medicine. Edward Arnold Ltd., London, pp. 6-18 & 94-98

Skinner M.F. & Hung J.T.W. (1989) Social and biological correlates of localized enamel hypoplasia of the human deciduous canine tooth. Am. J. Phys. Anth., 79, 159-175

Smith K.G.V. (1986) A Manual of Forensic Entomology. British Museum (NHM), London

Smyth M.J. (1988) *Penetrantia clionoides*, sp. nov. (Bryozoa), a boring bryozoan in gastropod shells from Guam. Biol. Bull., 174, 276-286

Sognnaes, R.F. (1949) Studies on dental paleopathology. II. Differential diagnosis of the post-mortem histopathology of ancient teeth. J. Dent. Res., 28, 660

Sognnaes, R.F. (1955) Post mortem microscopic defects in the teeth of ancient man. A.M.A. Arch. Path., 59, 559-57

Sognnaes, R.F. (1956) Histologic evidence of developmental lesions in teeth originating from paleolithic, prehistoric, and ancient man. Am. J. Path., 32, 547-578

Sognnaes, R.F. (1959) Microradiographic observations on demineralisation gradients in the pathogenesis of hard-tissue destruction. Arch. oral Biol., 1, 106-121

Soudry D. (1979) Intervention de schizophytes dans la phosphomicrocritisation des debris osseux. C.R. Acad.Sc. Paris D. 288, 669-671

Spencer A.J. (1982) Death in Ancient Egypt. Pelican Books Ltd, London

Steinbock R.T. (1976) Palaeopathological Diagnosis and Interpretation. C.C. Thomas, Illinois.

Stirland A. (1985) The human remains of the Mary Rose wreck. Unpublished Post Excavation Report, Mary Rose Trust, Portsmouth.

Stirland A. (1991) Paget's disease (Osteitis Deformans): a classic case? Int. J. Osteoarch., 1, 173-177

Stout S.D. (1978) Histological structure and its preservation in ancient bone. Current Anth., Vol 19, 3, 601-603

Stout S.D. & Tietelbaum S.L. (1978) Histological analysis of undecalcified thin sections of archaeological bone. Am. J. Phys. Anth., 44, 236-270

Syssovena P.R. (1958) Post mortem changes to human teeth with time. Sudebnd-Medisthinskaya Ekspertiza I Kriminalistika na sluzhbe Sletsshviya. 2, 213-218 (Russian)

Teaford M.F. (1988) Scanning electron microscope diagnosis of wear patterns versus artifacts on fossil teeth. Scan. Micros., 2, 1167-1175

Thomas R.H., Schaffner W., Wilson A.C. & Paabo S. (1989) DNA phylogeny of the extinct marsupial wolf. Nature, 340, 465-467

Thomasset J.J. (1931) Sur un champignon fossile: mycelites ossifragus (Roux). Bull. Soc. geol. de France, 5, 1, 597-603

Tillman H.H. (1962) Paget's disease of bone. Oral Surg., Oral Med. & Oral Path., 15, 1225-1234

Tomes J. (1892) Casual Communication. Trans. Odont. Soc. Brit., 24, 89-92

Tompsett D.H. (1970) Anatomical Techniques. E. & S. Livingstone, Edinburgh and London.

Torneck C.D. (1985) Dentin-pulp complex. In: Oral Histology. Ed. A.R. Ten Cate., C.V. Mosby Comp., St. Louis pp. 146-182

Tuross N., Behrensmeyer A.K. & Eanes E.D. (1989) Strontium increases and crystallinity changes in taphonomic and archaeological bone. J. Arch. Sci., 16, 661-672

Ubelaker D.H. & Grant L.G. (1989) Human skeletal remains: preservation or reburial. Yearbook Phys. Anth., 32, 249-287

Watt I.M. (1985) The Principles and Practice of Electron Microscopy. Cambridge University Press, Cambridge

Watzman H. (1995) Israelis at odds over old bones. Nature, 1967, 10

Werelds R.J. (1961) Observations macroscopiques et microscopiques sur certaines alterations postmortem des dents. Bulletin du Groupement International pour la Recherche Scientifique en Stomatologic, 4, 7-60

Werelds R.J. (1962) Nouvelles observations sur les degradations post mortem de la dentine et du cement des dents inhumees. Bulletin du Groupement International pour la Recherche Scientifique en Stomatologie, 5, 554-591

Werelds R.J. (1967) Du moment ou apparaisseent dan les dents humaines les alterations post mortem en forme d'evidements canaliculaires. Presence de lesions dentaires identiques in vivo chez des poissons. Bulletin du Groupement International pour las Recherche Scientifique en Stomatologie, 10, 419-447

Wedl, C. (1864) Über einen im Zahnbein und Knochen keimenden Pilz. Akademie der Wissenschaften in Wien. Sitzungsberichte Naturwissenschaftliche Klasse ABI. Mineralogie, Biologi Erdkunde, 50 (1), 171-193

Weigelt J. (1927) Recent vertebrate carcasses and their paleobiological implications. Verlag Von Max Weg, Leipzig. [Trans. J. Schaefer (1989) University of Chicago, Chicago]

Wells C. & Woodhouse N. (1959) Paget's disease in an anglo-saxon. Med. Hist., 19, 369-400

Whitson S.W. (1985) Bone. In: Oral Histology. Ed. A.R. Ten Cate. C.V. Mosby Comp., St. Louis, pp. 109-128

Whyte M. & Evan G. (1995) The last cut is the deepest. Nature, 376, 17-18

Williams R.A.D. & Elliott J. (1979) Basic and Applied Dental Biochemistry. Churchill Livingstone, Edinburgh, London & New York

Wong S.Y.P., Dustan C.R., Evans R.A. & Hills E. (1982) The determination of bone viability: a histochemical method for identification of lactate dehydrogenase activity in osteocytes in fresh calcified and decalcified sections of human bone. Pathology, 14, 439-442

Yoshino M., Kimijima T., Miyasaka S., Sato H. & Seta S. (1991) Microscopical study on estimation of time since death in skeletal remains. Foren. Sci. Int., 49, 143-158

Young H.R. & Nelson C.S. (1985) Biodegradation of temperate-water skeletal carbonates by boring sponges on the Scott Shelf, British Columbia, Canada. Marine Geol., 65, 33-45

Yudin S.S. (1936) Transfusion of cadaver blood. J. Am. Med. Assoc., 106, 997-999

Zeff M.L. & Perkins R.D. (1979) Microbial alteration of Bahamian deep-sea carbonates. Sedimentology, 26, 175-201

Zimmerman M.R. & Angel J.L. (1986) Dating and Age Determination of Biological Materials. Croom Helm Ltd., London

## **APPENDICES**

# Appendix 4.1

## DATA SET OF TUBULE DIAMETERS (microns)

MR No.	LSB No.	SAMPLE SITES							
		1	2	3	4	5	6	7	8
1	53	6.5	5.6	5.5	6.0	7.0	5.0	5.0	6.8
2	52	0	0	0	0	10.7	7.4	13.3	10.6
3	57	0	0	0	0	7.1	0	0	0
4	64	4.8	5	5	5.2	6.2	5.1	5.0	4.8
5	68	6.6	4.7	5.5	5.5	4.8	6.0	6.5	4.6
6	58	0	0	0	0	0	13.4	15.6	18.6
7	62	13	17.6	12.7	13.9	12.8	12.4	8.1	0
8	54	6.7	7.5	7.2	8.4	0	0	0	5.2
9	55	8.3	5.0	6.0	5.0	0	0	9.0	10.0
10	59	0	0	0	0	0	0	0	0
11	61	OUT	-	-	-	-	-	-	-
12	60	0	0	0	0	0	0	0	0
13	63	0	0	0	0	0	0	0	0
14	70	6.7	6.0	5.3	5.8	5.7	5.7	6.2	5.9
15	67	7.9	7.3	8.2	0	0	7.3	5.9	0
16	65	0	0	0	0	0	0	0	0
17	66	0	0	0	0	0	0	0	0
18	69	0	0	0	0	0	0	0	0



## Appendix 4.2

### DATA SET OF MAXIMUM INGRESS

MR No.	LSB No.	SAMPLE SITES							
		1	2	3	4	5	6	7	8
1	53	155	132	235	140	140	74	45	85
2	52	0	0	0	0	11	16	38	22
3	57	0	0	0	0	123	0	0	0
4	64	921	882	1170	794	451	433	167	743
5	68	1411	1083	1050	679	904	753	701	853
6	58	0	0	0	0	0	40	65	48
7	62	67	99	77	110	70	70	83	0
8	54	633	570	376	534	0	0	0	853
9	55	385	390	250	256	0	0	95	92
10	59	0	0	0	0	0	0	0	0
11	61	OUT	-	-	-	-	-	-	-
12	60	0	0	0	0	0	0	0	0
13	63	0	0	0	0	0	0	0	0
14*	70	457	376	227	334	515	121	247	359
15	67	52	23	55	0	0	46	52	0
16	65	0	0	0	0	0	0	0	0
17	66	0	0	0	0	0	0	0	0
18	69	0	0	0	0	0	0	0	0

\* *invs. PDJ*

## APPENDIX 7.1

**Context description: Old Grapes Lane, Carlisle**

### **Context**

745 Status uncertain

749 A soil deposit in the vicinity of the bank on which the hedge grew. It probably dates to 140 - 160 AD. There was very little datable material, and what there was could have been residual, belonging to the late first century. The context was damp but not waterlogged. The pH was not measured.

750 A ditch-like drain defining the western side of the property. As the drain lies on the western side of the hedge it is arguable that its contents derived from a property other than the one excavated. Its status is ditch fill and dates from 93/94 - 150 AD. It contained a small amount of material that was probably residual from an earlier phase. The drain varied in width from 0.85 - 1.1 m across and was 0.45 m deep. It had vertical sides and a flat base, which suggests it had been lined with planks in the manner of other Roman drains in Carlisle. The context was damp but not waterlogged. The pH was not measured.

776 A deposit stratigraphically earlier than 749. This is the remnant of a surface and dates between 125 - 145 AD. This deposit contained residual material, as well as a couple of intrusive Medieval fragments. The status of the deposit is not as secure as the others. The context was damp but not waterlogged. The pH was not measured.

787 Is ditch fill of the east-west aligned ditch at the commencement of the period. It dates to the last decade of the first century. The ditch was 1.2 m wide. Its fill included many lenses of mixed clays, silts, sandy layers and organic deposits with straw and other cereal debris. Insects were abundant including mites, spiders, parasites, larvae and flies the majority of which would have been at home in the damp, but not a waterlogged, environment. These deposits were overlaid by surfaces which had slumped into the ditch fill. The status of the context is ditch fill. Its nature suggests that little residual material and certainly no intrusive material is likely to be present. It could represent the sweepings of a stable or byre. The deposits were damp but not waterlogged at the time of lifting. The pH was not measured.

844 This was a layer of silt overlying a cobbled surface inside the timber building. It was not a primary surface in the building but equally it is not one of the later ones. Its status is secure. It dates to approximately 100 AD. There were no associated finds. The layer was damp but not waterlogged. The pH was not measured.

The above information was kindly provided by Mr. M.R. McCarthy (Director of the Carlisle Archaeological Unit) prior to site publication.

## **Appendix 10**

**Publications arising from this study**



## **Palaeopathology and Diagenesis: An SEM Evaluation of Structural Changes Using Backscattered Electron Imaging**

Sydney S. Bell<sup>a</sup>

*Received 7 February 1989, revised manuscript accepted 10 September 1989*

This study addresses the problem of diagenetic change in normal and palaeopathological human skeletal material. Invasive sections were taken from adult human femora and tibiae for a structural and qualitative assessment of bone density changes using a scanning electron microscope (SEM) in backscattered electron (BSE) mode. The results obtained suggest that macroscopic and X-ray interpretations of archaeological bone, both normal and pathological, run the risk of misinterpretation due to its extensive diagenetic change. The progression of diagenesis was found to be ordered to some extent by the collagenous arrangement of bone and so potentially affected by any bone pathology present.

**Keywords:** BONE, HUMAN, PALAEOPATHOLOGY, DIAGENESIS, BACKSCATTERED ELECTRONS.

### **Introduction**

Palaeopathological studies have for many years relied heavily upon macroscopic appraisal of human bone to detect any abnormality or pathology. Such studies were based on the gross pathological studies undertaken in general medicine around the turn of the century (Greig, 1931), and were then expanded and utilized on archaeological material as a way to elucidate or interpret disease in ancient populations (Jarcho, 1966; Hackett, 1976; Weinbock, 1976; Ortner & Putschar, 1985). The results from such studies have not only provided archaeologists with putative information on the general health and diet of those populations, but have also assisted medicine in considering the epidemiology of certain specific pathological conditions (Roney, 1966). It has been suggested, however, that if the study of disease in past populations were to have any interpretable meaning with regard to present day medical conditions, then other techniques such as the use of X-rays and histology should also be applied to archaeological human bone (Ortner & Putschar, 1985; Rogers *et al.*, 1987; Garland, 1985, 1988). In standard recording work on archaeological populations, it is X-rays which tend to be used to assist interpretation of pathological conditions and not the more invasive and relatively time consuming histological techniques.

Diagenetic change to bone, or bone decomposition, is understood to mean dissolution, precipitation, mineral replacement and recrystallization (Pate & Brown, 1985). These

Hard Tissue Research Unit, Department of Anatomy and Developmental Biology, University College London, London WC1E 6BT, U K

changes have been morphologically noted in previous histological studies (Wedl, 1864; Hamperl, 1966; Blumberg & Kerley, 1966; Graf, 1949; Stout & Teitelbaum, 1978; Sefton *et al.*, 1972) and Hackett (1981) suggested a four-tiered classification of these diagenetically changed areas, foci or tunnels, namely Wedl, linear longitudinal, budded and lamellate. Wedl tunnels were considered by both Wedl (1864) and Hackett (1981) to have been produced by the lytic action of fungi, whilst the other three types were produced by the action of bacteria. Marchiafava *et al.* (1974) demonstrated that tunnels could be produced by the genus *Mucor* as quickly as 15 to 20 days after burial. Not all fungi, however, have this capability to dissolve away the organic and mineral fractions of bone to produce tunnels. Piepenbrink (1986) isolated fungal colonies which were present in the soil surrounding archaeological bone prior to lifting and obtained *Stachybotrys cylindrospora*, *Doratomyces stemonitis*, genus *Pythium* and genus *Rhizoctonia*. None of these fungi produced any tunnelling when reseeded on archaeological bone. Especially interesting though, was the finding that *Stachybotrys* produced a combination of several non-identified fluorescent antibiotics which tended to fluoresce around osteonal canals (Piepenbrink, 1986). Such an observation should stand as a salutary reminder that diagenesis incorporates many unknown components which could alter or mimic pathological conditions in life. Given the evidence for changes in bone after death (even after a very short period of time) including the secondary infiltrations of remineralization and extraneous fluorescence, microscopic study is essential to consider the validity of the assumption that one is actually testing bone and that the component being tested had resided in the bone during life (Rothschild & Turnbull, 1987; Nieburger, 1988; Rothschild, 1988).

Sea water burial effects have been considered by Arnaud *et al.* (1978) and Ascenzi & Silvestrini (1984). Both studies confirmed that human bone deposited in sea water would exhibit tunnelling features and a subsequent change to the perceived microscopic morphology of the bone. Ascenzi & Silvestrini (1984) found a variety of micro-organisms present in a network of boring channels similar to those produced by the action of fungi on soil-buried skeletons, but bacteria and algae did not appear to be directly involved in this case. Instead, protozoans of the amoebic type were found to contain aggregations of bone crystallites intracellularly. Ascenzi & Silvestrini (1984) suggest that these cells initially cause solubilization of the hydroxyapatite, but cannot explain the resultant take-up and aggregation of the crystallites intracellularly.

Remineralization within the foci or tunnels of soil-buried bone occurs in an unknown way at an unknown rate. Hackett (1981) noted that Wedl tunnels did not exhibit mineral redeposition, whereas the linear longitudinal, budded and lamellate foci did. Hackett described this redeposition and remineralization as "cuffing" around the edges of the foci with subsequent loss of birefringence and an increase in density. Such observations surrounding the complicated morphology observed by Hackett have also been confirmed by extensive histological work undertaken by Garland (1985, 1987, 1988). Garland (1988) also showed "infiltrations" of iron and brushite in the outer third of the cortex. Other authors too have attempted to identify the wide range of elemental compositional changes of archaeological and fossil bone (Hassan & Ortner, 1977; Hassan *et al.*, 1977; Henderson *et al.*, 1983; Lambert *et al.*, 1979, 1984, 1985; Kyle, 1986; Hanson *et al.*, 1987; Williams & Marlow, 1987; Williams & Potts, 1988; Klepinger *et al.*, 1986; Piepenbrink, 1986; Harcourt, 1986; Grupe, 1988). It has been shown generally by these authors that elemental distribution tends to vary in an unpredictable manner within individual sections and from one bone to another. These variations are recognized to be a product of diagenetic processes but are difficult to interpret in terms of the potential influencing factors to be found in soil. Janaway (1985) considered soil less important in the initial stages of decomposition, arguing that the body will create its own micro-environment which in turn modifies the

fects of the surrounding soil. Thus, the micro-floras involved in decomposing animals and other organic matter will have primacy in the initial stages and soil chemistry be involved more prominently later. This view is supported by the experimental work of Marchiafava *et al.* (1974), Arnaud *et al.* (1978) and Ascenzi & Silvestrini (1984). Soil chemistry must however to some degree control the floras present. Pate & Hutton (1988) consider it essential to evaluate as many aspects of soil chemistry as possible as they consider the ion exchange complex of different soils highly pertinent to the whole diagenetic process from dissolution through to recrystallization. Indeed, recent work by Allison (1988) has addressed directly, through an experimental anaerobic system, the time involved in decay and remineralization of soft bodied proteinaceous *Nereis*, *Nephrops* and *Alaemon*. He found that even in anaerobic marine, lacustrine and brackish environments decay could be almost total within 25 weeks, whilst remineralization could be observed within weeks of initiating an experiment. He concluded that if the decay rate is reduced, even slightly, then diagenetic remineralization can be very rapid and so enhance the specimen's chances of preservation for the fossil record. It is therefore evident that decay can commence very rapidly, as can remineralization, and more attention needs to be paid to the interactive system of diagenesis.

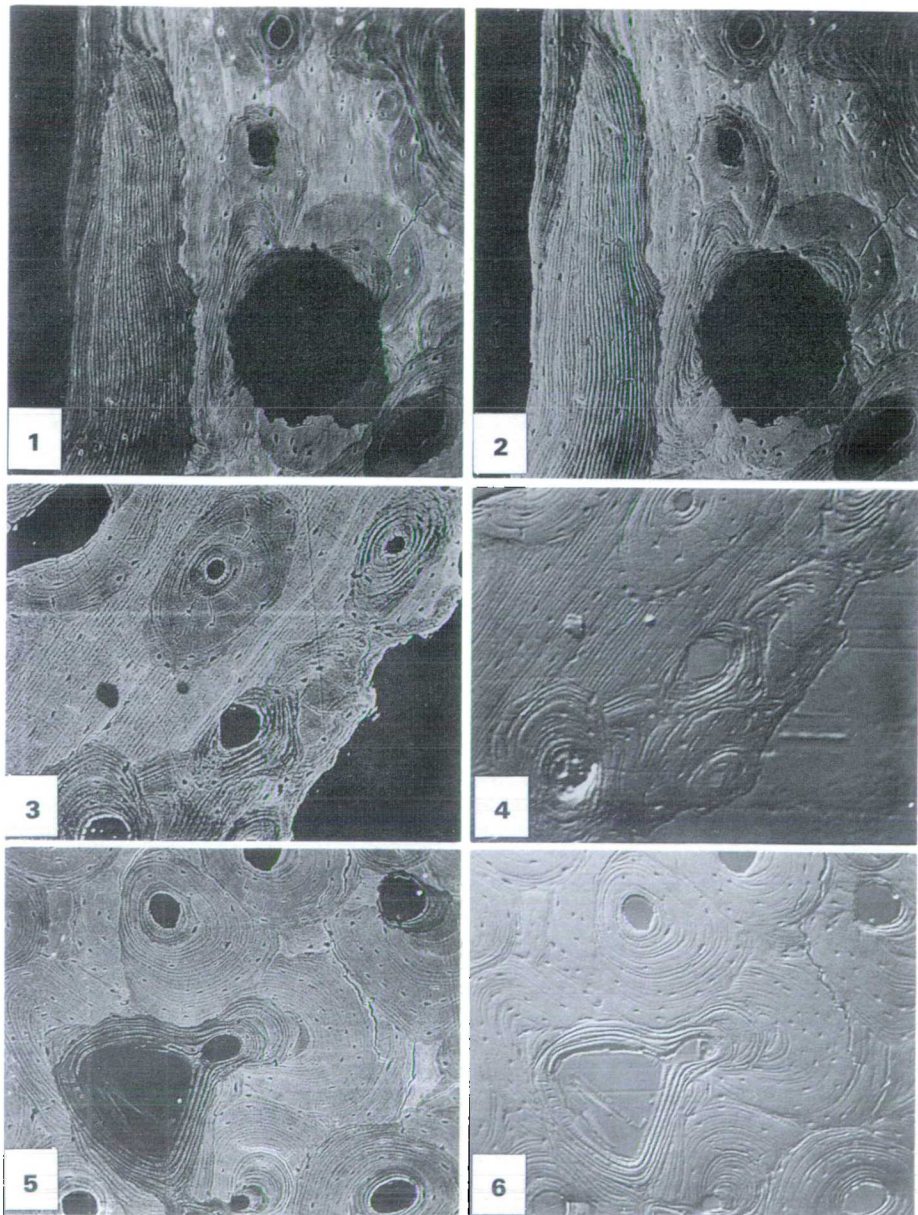
This study was undertaken to consider the morphological effects of diagenesis on normal and pathological archaeological bone with particular regard to any relative density variations found intracortically. BSE imaging is a method already utilized in basic medical research to illustrate density changes within bone and it has allowed the study of mineralization during growth and bone turnover and of impaired mineralization in certain pathological conditions such as Paget's disease, fluorosis, osteomalacia and osteogenesis imperfecta (Boyde *et al.*, 1986). BSE imaging was considered to be an entirely appropriate high resolution method to adopt for this archaeological bone study.

#### Material and Methodology

The skeletal material used in this study was adult human femora and tibiae taken from archaeological and modern sources. The archaeological material was taken from soil-buried mediaeval contexts and was adult but of unknown age and sex. One sample consisted of presumed normal bone in that it had no obvious gross pathology and was taken from a macroscopically well preserved skeleton. The remaining archaeological bone examined was considered pathological, it being affected by the non-specific condition of "periostitis", and was drawn from a miscellaneous group of bone. Two specimens were examined from this latter group: the first (specimen 1), an adult femur, macroscopically and on X-ray presented with slight striations of new bone distributed anteriorly and posteriorly along the femoral shaft; the second specimen (specimen 2), an adult tibia, showed extensive subperiosteal changes to the entire shaft and in complete longitudinal section showed that the entire medullary cavity had become infilled with bone so that no trabeculae were evident. The absence of the medullary cavity had not been clear from the X-ray, instead the medullary area appeared undefined and irregularly radiodense. The modern material was adult but of unknown age and sex, which had been prepared after Compsett (1970), and had been used as a laboratory specimen for several years. This specimen was considered normal in that it had no obvious gross pathology, and it was not routinely X-rayed as it had been provided as normal non-pathological bone.

Transverse and longitudinal sections (10 mm<sup>2</sup>) were taken from the mid-shaft anterior aspect of the femora and similarly from the mid-shaft medial and lateral aspects of the tibiae. The sections were cut using a wet diamond-edged circular saw and then allowed to air dry. They were then placed into reflux columns containing 50.50 chloroform and methanol to remove any residual water present through natural humidity within the bone. Ordinarily, reflux is used to remove any fatty material and water present in fresh

specimens (see Boyde *et al.*, 1986). Whilst this procedure is not necessarily required for deproteinized or inorganic specimens, vacuum embedding being a perfectly adequate alternative, it was done so that the results could, if necessary, be compared with fresh material. Reflux continued for 2 weeks. The sections were then removed and put through three changes of liquid polymethylmethacrylate (PMMA) every 24 h and subsequently placed in an oven set at 37 °C until the PMMA solidified. The methacrylate had been prepared by the "flash distil" method outlined by Boyde *et al.* (1986) which prevents bubbling in the methacrylate. The embedded specimens were polished using grade





abrasives and finished with a water-dispersed 1  $\mu\text{m}$  diamond abrasive on a rotary lap. Each block was mounted individually on an aluminium stub and the block face received a sputter coating of silver to render it electrically conductive and therefore suitable for SEM study in the backscattered electron imaging (BSE) mode.

The specimens were examined using a Cambridge Stereoscan S4-10 SEM, operated in SE mode, working at 20 kV beam voltage and about 10 amps probe current. The BSE flat section images were created using a solid state BSE detector in a four-segmented ring configuration and the topographical images were obtained by switching off the east and south quadrants simultaneously. Both topographical and flat section images were then taken. The topographical images were necessary for the identification of bubbles, holes, ridges or scratches which may have contributed to the overall signal artefactually, whilst the flat section images gave qualitative relative assessments of density changes within the specimen alongside any morphological changes. Such changes in density appear as a density map composed of dark areas which are less dense and light areas which are relatively more dense. This density dependence is the result of backscattered high energy electrons, which have an approximate escape depth of 1  $\mu\text{m}$ , being released from the specimen so that backscattering increases steeply with increasing atomic number (Z)

---

Figure 1. BSE image of a transverse section (TS) fresh human (80-year-old male) anterior midshaft femur. The most recent two sets of subperiosteal circumferential lamellae can be seen clearly as relatively less dense striations coursing across the left side of the field. At the base of this circumferential lamellae is a clear scalloped profile of osteoclastic resorptive lacunae, which pre-empted the successive laying down of the present circumferential lamellae. This line of resorption shows how natural cleavage planes play no part in limiting the removal of bone by osteoclasts, and this allows for the distinction made in Figure 3 between osteoclastic resorption and post-mortem loss. Variation in mineral density can be seen throughout the field of secondary osteonal remodelling. SEM BSE, PMMA-embedded bone. Field width (FW) 930  $\mu\text{m}$ .

Figure 2. Topographical image of the same field as Figure 1. This image shows clearly the lamellate nature of the subperiosteal circumferential lamellae as well as the presence of many osteocyte lacunae. This difference in mineral density and collagen orientation, seen as slightly raised or slightly depressed areas, is also well illustrated in the field of secondary remodelling. Small cracks can also be seen to follow and transect natural cleavage planes. FW 930  $\mu\text{m}$ .

Figure 3. TS lateral modern midshaft tibia showing clearly the loss of the subperiosteal circumferential lamellae. This removal is distinct from osteoclastic action as it follows the natural cleavage planes. SEM BSE, PMMA-embedded bone. FW 690  $\mu\text{m}$ .

Figure 4. Topographical image of same field as Figure 3 showing the removal of the subperiosteal lamellae follows clearly the natural cleavage planes provided by the bone. FW 690  $\mu\text{m}$ .

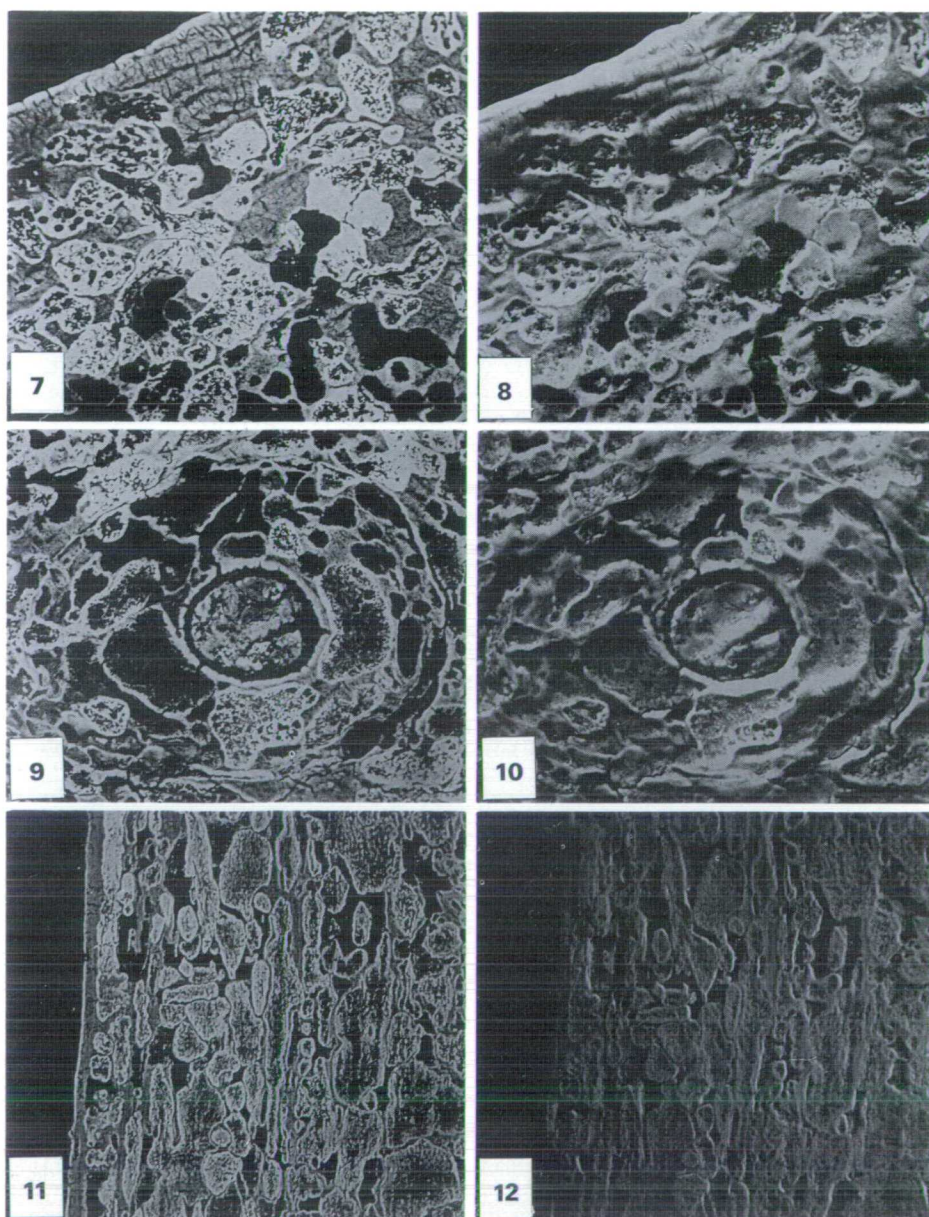
Figure 5. TS lateral midshaft modern tibia. Mineral density variation associated with secondary osteonal remodelling is comparable to that resulting from normal bone turnover. Note the cracking which follows the natural cleavage planes within the specimen. SEM BSE PMMA-embedded bone. FW 930  $\mu\text{m}$ .

Figure 6. Topographical image of same field as Figure 5 showing varying topography created by polishing PMMA-embedded section of bone with the secondary remodelling of normal bone turnover. Note the increased topography in the less well mineralized bone. This reflects the different collagen fibre orientations and contributes to the BSE image. FW 930  $\mu\text{m}$ .

values. Hence, any local variations in Z composition within the specimen will give variations in intensity and so image, due to modulations in the backscattered electrons signal (Boyde *et al.*, 1983, 1986; Watt, 1985).

### Results and Discussion

All the prepared archaeological specimens, both normal and pathological, show dramatic diagenetic change. The extensive changes had in all specimens removed, change



er obscured the characteristic morphology and density associated with adult human bone. Such changes therefore placed limitations on the interpretation of any pathological conditions present within the specimens but at the same time offered the chance to investigate the morphological and density variations present during the little understood process of diagenesis.

*Normal modern and archaeological bone(a) Circumferential lamellae: subperiosteal bone*  
The results from the specimens, both modern and archaeological, support the view expressed by Garland (1985) that macroscopic studies of the subperiosteal surface of bone to determine preservation and any pathological change is, on its own, a very uncertain practice. Macroscopic study relies upon the basic premise that the circumferential lamellae of the subperiosteal bone (Figures 1 and 2) survive the burial environment. However, even in the modern bone, the circumferential lamellae of the subperiosteal region were found to have been extensively removed (Figures 3 and 4), whereas the general osteonal architecture remained intact, although some cracks were present (Figures 5 and 6). This irregular removal of the superficial bone, which had cleaved along natural fracture planes, could be differentiated from a surface produced by osteoclastic resorptive activity as seen in Figures 1 and 2), since this type of surface would be characterized by a scalloped profile passing through and across secondary osteonal bone, quite irrespective of any natural cleavage planes. This post-mortem removal of the superficial bone was not detectable to the naked eye and must have occurred simply by students handling the

---

Figure 7. TS of lateral midshaft archaeological tibia. A small region of the subperiosteal lamellae was preserved intact with osteocyte lacunae morphologically identifiable. Extensive diagenetic change is present in the form of increased and decreased density. SEM BSE, PMMA-embedded bone. FW 145 µm.

Figure 8. Topographical image of same field as Figure 7. The relative topography associated with extensive diagenetic change results from foci of increased density standing proud of the apparently unaffected bone and areas of reduced or mixed density which appear as depressions in the overall matrix. The full interpretation of Figure 7 cannot be made without the topographic information. FW 145 µm.

Figure 9. TS of lateral midshaft archaeological tibia. A single osteon is enclosed and surrounded by extensive diagenetic change. An original cleavage plane has been preserved and can be seen partially encircling the osteon. The diagenetic foci are curved following the lamellae of the osteon. SEM BSE, PMMA-embedded bone. FW 185 µm.

Figure 10. Topographical image of the same field as Figure 9. Cracks partially encircle and cross a single osteon. The osteon had undergone extensive diagenetic change which is curvilinear or "lamellate" in shape. Note the raised rim surrounding diagenetic foci, indicating peripheral increased density. FW 185 µm.

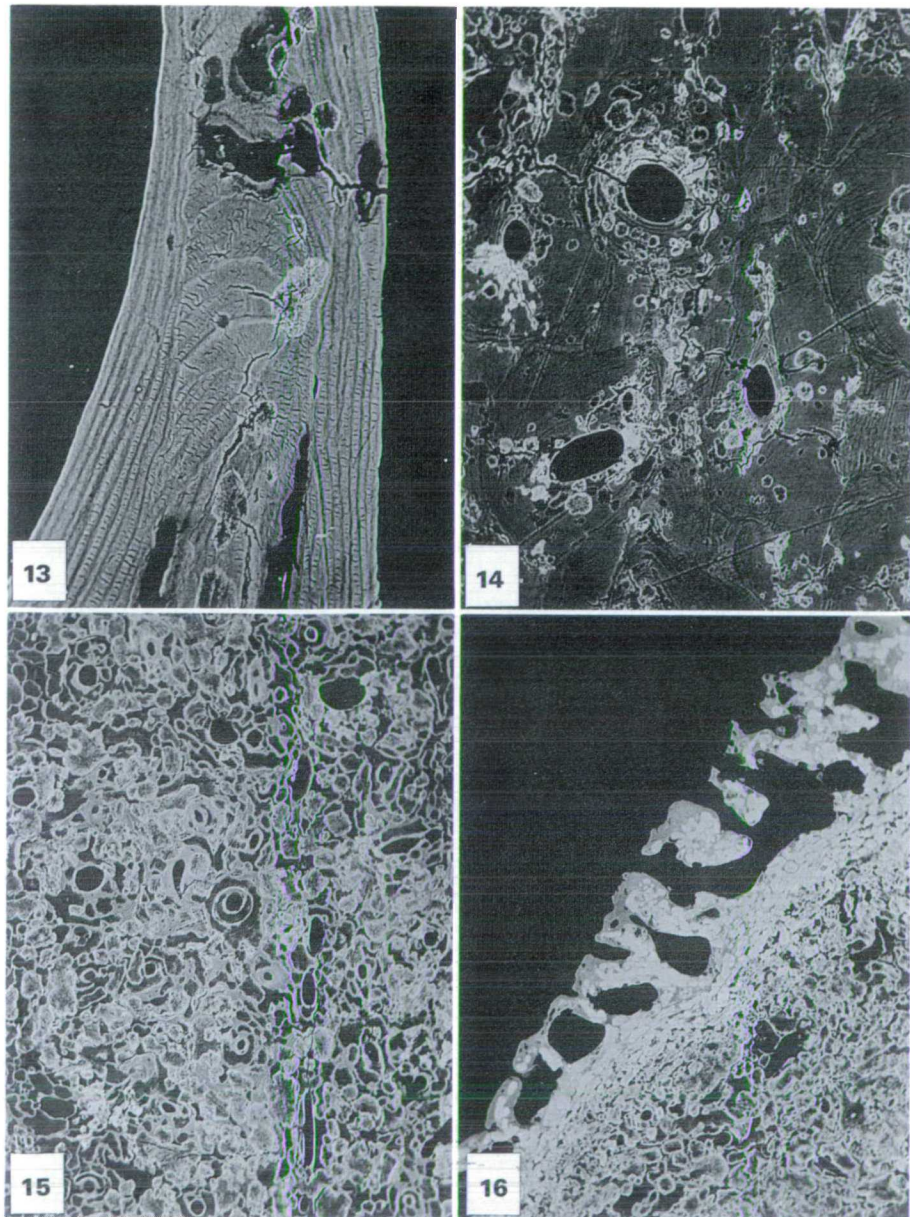
Figure 11. Longitudinal section (LS) of anterior midshaft archaeological femur. There is extensive diagenetic change with elongation of some areas of changed density, which had been curvilinear in transverse section. Such elongations are considered to follow the lamellae of osteonal systems. SEM BSE, PMMA-embedded bone. FW 325 µm.

Figure 12. Topographical image of the same field as Figure 11. The outermost circumferential lamellae appear intact but generally the field is one of extensive diagenesis. Elongations of some of the foci can be seen and most appear to follow the lamellae of the osteonal systems. FW 325 µm.



specimen over the years. Not surprisingly, the archaeological bone examined exhibits similar destructive removal of the circumferential lamellae and only fortuitously was that part of the bone preserved intact with an occasional osteocyte lacuna evident (Figures 7 and 8). Even when the lamellae could be seen, the bone had usually undergone extensive diagenetic change in the form of localized areas of decreased or increased density (Figures 7 and 8).

(b) *Cortical bone* The qualitative morphology of the normal archaeological transverse sections exhibited a similar pattern throughout the bone examined. The diagenetic



changes were extensive (Figures 7–14); only in the most central area of the cortex was there evidence of much bone being retained (Figure 14). Areas of changed density compared with the density of bone in the same field were present as discrete, irregularly shaped regions having dimensions of between 20 and 150  $\mu\text{m}$ . These presumably represented recrystallization where bone mineral would have been removed and then mineral redeposited in the same bone matrix. Alternatively (or additionally) crystals may have formed in altered organic material and or even extended into areas where no matrix remained at all. Areas of markedly decreased density, with similar dimensions, also occurred in all samples. Thus, two extremes of diagenetic change were noted in the BSE images: areas of bone which appeared uniformly very dense and areas from which the mineral seemed to have completely dissolved to create an appearance of holes in the matrix. However, the specimens exhibited areas of intermediate density between these two extremes. The borders of the altered regions were always clearly defined and of greater density than the surrounding, apparently unaffected, bone. The borders were continuous and enclosed regions which were often of lower density, giving the appearance of encapsulation. Within the altered region, the general density varied from close to that of the intervening bone, and was not uniform within any one region. Two main textural patterns were evident: holes of approximately 2–3  $\mu\text{m}$  in diameter, and a finer texture which represented the fibrous component of the bone. It was notable on the topographic images (Figures 8 and 10) that the most continuously dense altered regions were proud of the apparently unaffected bone, and this was proud of the zones of diagenesis which were not uniform in density, having been abraded more in polishing. Regions which were of negligible or very low density in the BSE images were most heavily abraded but mostly showed some texture. This whole arena of varying density was interpreted as diagenesis in progress, the overall appearance of the specimens suggesting that recrystallization is a continuous phenomenon, proceeding at rates defined by the numerous factors which contribute to diagenesis.

The artefact of cracking was noted in both modern (Figures 5 and 6) and archaeological specimens (Figures 9 and 10). This cracking could have occurred during diagenesis. Additionally, the cracking might have resulted in part from the preparation procedure of the specimens, presumably at the stage of reflux or solidification of the PMMA when shrinkage and expansion could have occurred. The cracks have presumably followed

---

Figure 13. LS of anterior midshaft archaeological femur. The trabecular bone is relatively well preserved with only small foci of changed density. Some cracking is evident within the central area of changed density which has been partially bisected. SEM BSE, PMMA-embedded bone. FW 315  $\mu\text{m}$ .

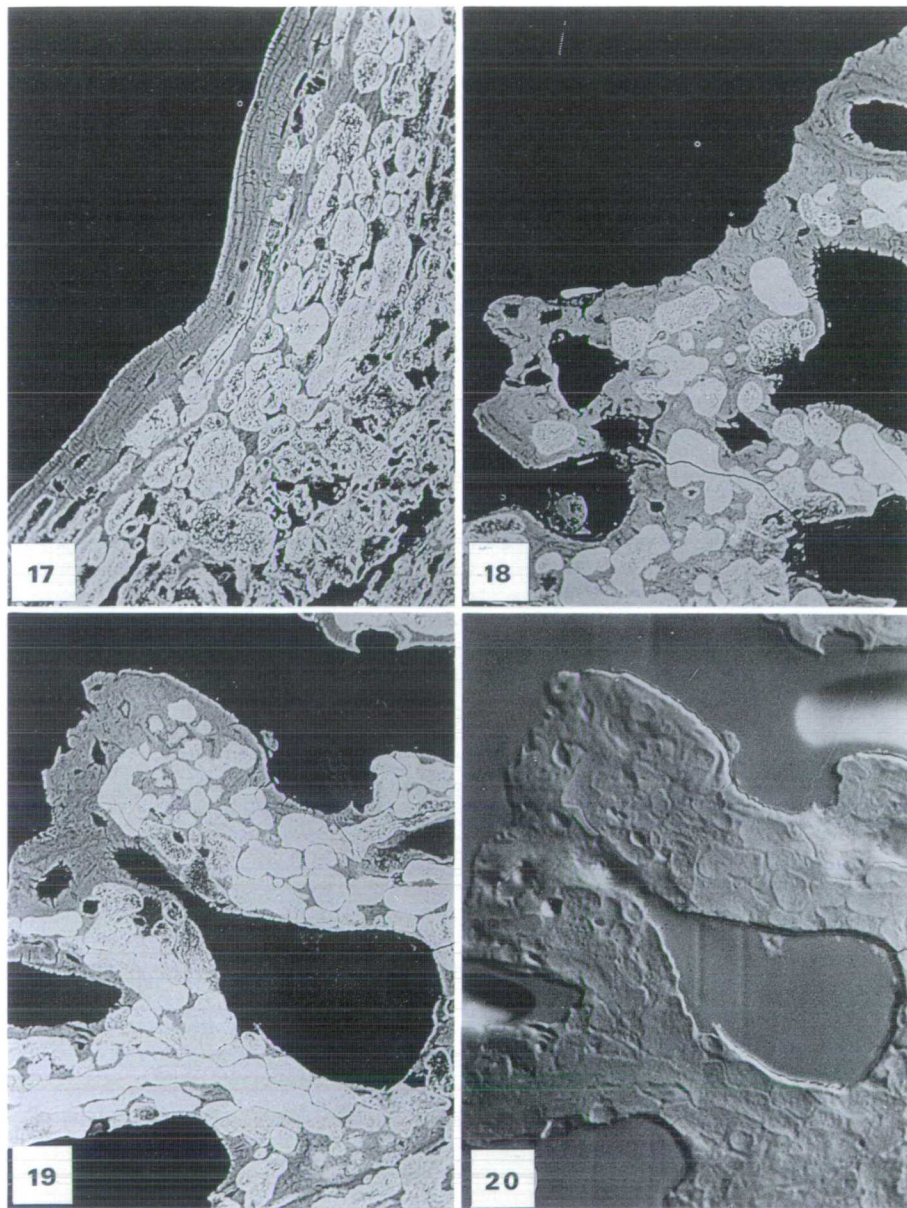
Figure 14. TS of medial midshaft archaeological tibia, showing a field from the most central area of the cortex with improved bone survival. The focal changes of diagenesis are located preferentially around osteonal canals. Cracks are present crossing natural cleavage planes to bisect foci of changed density for some distance. SEM BSE, PMMA-embedded bone. FW 620  $\mu\text{m}$ .

Figure 15. Pathological (specimen 1) archaeological bone. TS midshaft femur, shows extensive diagenesis toward the endosteal aspect of the cortex. Hardly any identifiable bone is evident. SEM BSE, PMMA-embedded bone. FW 1200  $\mu\text{m}$ .

Figure 16. Pathological (specimen 1) archaeological bone. TS anterior midshaft femur. Primary osteonal bone extending as a branching band, partly enclosing vascular spaces which ran longitudinally, has survived at the subperiosteal limit although diagenetic changes are extensive. SEM BSE, PMMA-embedded bone. FW 1200  $\mu\text{m}$ .



points of natural cleavage within the specimen. It was often noted that the cracks partly encircled single osteons, suggesting that although there had been extensive diagenetic change locally within and around the osteons, original fracture planes could be retained (Figures 9 and 10). The archaeological specimens also exhibited cracking which appeared to track from and through the foci of changed density (Figures 13 and 14). These cracks crossed morphologically identifiable areas of secondary osteonal systems, as well as cracking for some distance through islands or foci of recrystallization. Also much smaller cracks were noted within actual foci or recrystallization, often bisecting such features



either totally or in part, remaining entirely within the feature or extending beyond it for just a short distance. It would therefore appear that the artefact of cracking shows two important features: firstly, that natural fracture planes can be retained and may play a role in the orientation of the diagenetic process, i.e. Hackett's "lamellate" structure (Hackett, 1981); and secondly, the foci of changed density have not only orientated planes of weakness within themselves, but also aided cleavage across areas of morphologically identifiable bone which appear to ignore natural or ante-mortem fracture or cleavage planes.

Structurally recognizable but not necessarily unchanged bone could be seen amongst a complicated array of obvious diagenetic change in the archaeological bone. Osteonal systems within the cortex could be clearly observed, as could osteonal and interstitial lamellae, osteocyte lacunae and canaliculae. However, even where bone tissue was identifiable, areas of localized changes in morphology and density were invariably present, even within one osteonal system (Figure 14). The central regions of mid-cortical bone were best preserved, whilst the subperiosteal and endosteal aspects were found to be poorly preserved with extensive fields almost entirely affected by diagenesis. The importance of the osteonal canals in the initial spread of diagenetic change was clearly evident in those regions where most of the original bone structure remained (Figure 14). The bone trabeculae of the medullary region often retained good morphological details, displaying lamellar structure, areas of remodelling, osteocyte lacunae and canaliculae (Figure 13). This potential for preservation may be due to the protected location within the medulla; if so, it is perplexing that the endosteal aspect of the cortex undergoes such dramatic diagenetic change by comparison.

This report does not address directly the problem of the diagenetic changes that occur in the organic matrix of the bone. Where structurally recognizable bone was retained, it was the fibrous component that was evident, although mineralized cement lines round osteonal systems were also sometimes present (Figure 14). It is probable that, when demineralized, the collagenous component is more resistant to disruption than the non-collagenous proteins. Where these are less well preserved their loss might provide a track for the primary stages of diagenesis to extend along the collagen planes.

Longitudinal sections, taken from the transverse mid-shaft specimens, showed similar features of extensive diagenetic changes with small areas of bone preserved. Regions of changed density which were curvilinear in transverse sections now appeared elongated

---

Figure 17. Pathological (specimen 1) archaeological bone TS anterior midshaft femur, subperiosteal surface taken from the same specimen as Figure 16, in the region of macroscopic pathology. This does not have primary osteons at the surface, which is still intact. SEM BSE, PMMA-embedded bone FW 300 µm

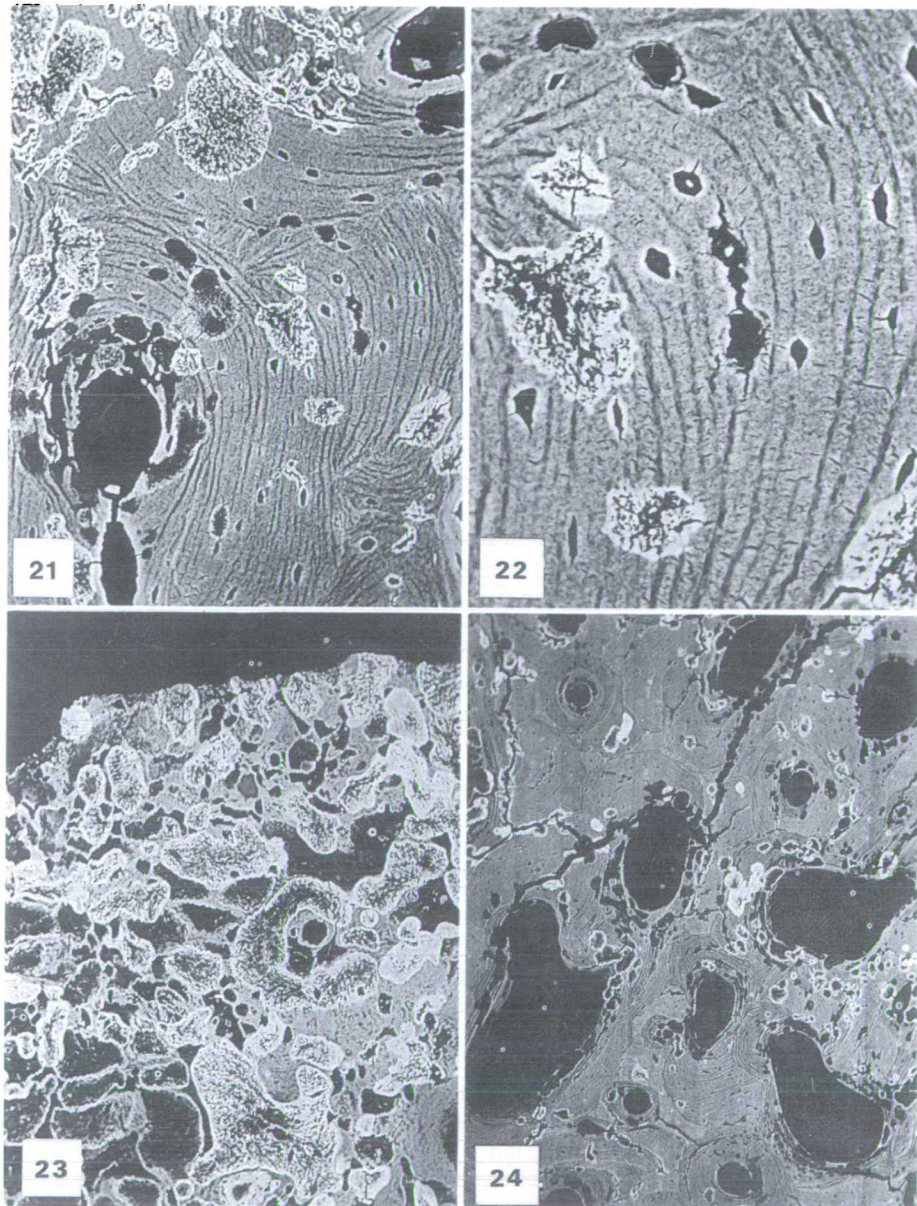
Figure 18. Pathological specimen 1 archaeological bone TS anterior midshaft femur. Osteoclastic activity is evident (centre field) as a scalloped resorptive border to the primary osteonal bone. Diagenetic foci have extended well into this new bone. SEM BSE, PMMA-embedded bone FW 300 µm.

Figure 19. Pathological (specimen 1) archaeological bone TS anterior midshaft femur, showing survival of bone at its subperiosteal limit. Note the irregularly shaped and larger osteocyte lacunae of rapidly formed bone. Diagenesis in this area is generally in increased density. SEM BSE, PMMA-embedded bone FW 300 µm

Figure 20. Topographical image of the same field as Figure 19, showing raised areas in the polished surface associated with the extensive increase in overall relative density to bone. (Two bubbles can be seen in the PMMA) FW 300 µm



as though following the lamellae of the osteonal systems (Figures 11 and 12). These elongations extended approximately 200  $\mu\text{m}$  in the plane of the polished longitudinal face and are highly suggestive of demineralization and recrystallization tracking in three dimensions along the fibrous structural organization of both the osteons and the circumferential lamellae at the subperiosteal surface. This extensive and eventual conjoining is presumably aided by the highly porous network of spaces within bone produced by osteonal canals, osteocyte lacunae and interconnecting canaliculae, and the natural boundary planes.





*Pathological archaeological bone*

The pathological sections (Figures 15–28) support in general the previous observations made in the non-pathological material. The subperiosteal circumferential lamellar bone is almost invariably absent (Figure 23), but where present, its lamellae were often preserved (Figure 17). Diagenesis was often extensive (Figure 15), particularly in peripheral regions of the cortex, the altered regions having similar size and distribution to those preserved in the non-pathological material. The artefact of cracking intracortically was also seen to track along natural and non-natural fracture planes.

The specimen which macroscopically presented with slight striations of periostitis (pathological specimen 1), was investigated to advantage by the BSE imaging technique (Figures 16–20). Primary osteonal bone was clearly seen extending as a branching band partly enclosing vascular spaces which ran longitudinally. The new bone had undergone extensive diagenesis with recrystallization (Figures 19 and 20). However, and perhaps surprisingly, the pathological intervascular ridge bone (Bromage, 1984), which is friable in archaeological specimens, had been preserved to its subperiosteal limit, together with small field of osteoclastic activity (Figures 16 and 18). This is in contrast with the non-pathological specimens which, although apparently robust, had lost subperiosteal circumferential lamellae almost entirely.

Information on the relationship of diagenesis to bone structure was obtained from intracortical locations in both pathological specimens (specimen 1: Figures 15–22; specimen 2: Figures 23–28). It was noted in transverse sections of the more pronounced periostitic osteitic specimen (specimen 2) that obvious diagenetic change seemed to be related preferentially in the lamellar bone close to the vascular canals (Figures 27 and 28). As with the non-pathological bone, it is difficult not to envisage the canals and osteocyte lacunae offering the primary route for diagenesis to begin and thereby extend deeper into the surrounding bone. Figures 24–28 show this process clearly: firstly the creation of mineralized zones; and secondly, infilling with an unidentified crystalline material. Figures 22 and 25 show an osteocyte lacuna situated within these foci of recrystallization in which the lamellar and/or fibrous organization is still evident. The foci of increased density do not always appear to be centred on osteocyte lacunae. However, this does not necessarily mean that osteocyte lacunae are only accidentally included in areas of recrystallization and thereby play no part in initiating diagenetic change. Many of the smaller foci do have osteocyte lacunae present and their frequency plus the distribution of early foci with increased density is very similar to that of the osteocyte lacunae.

---

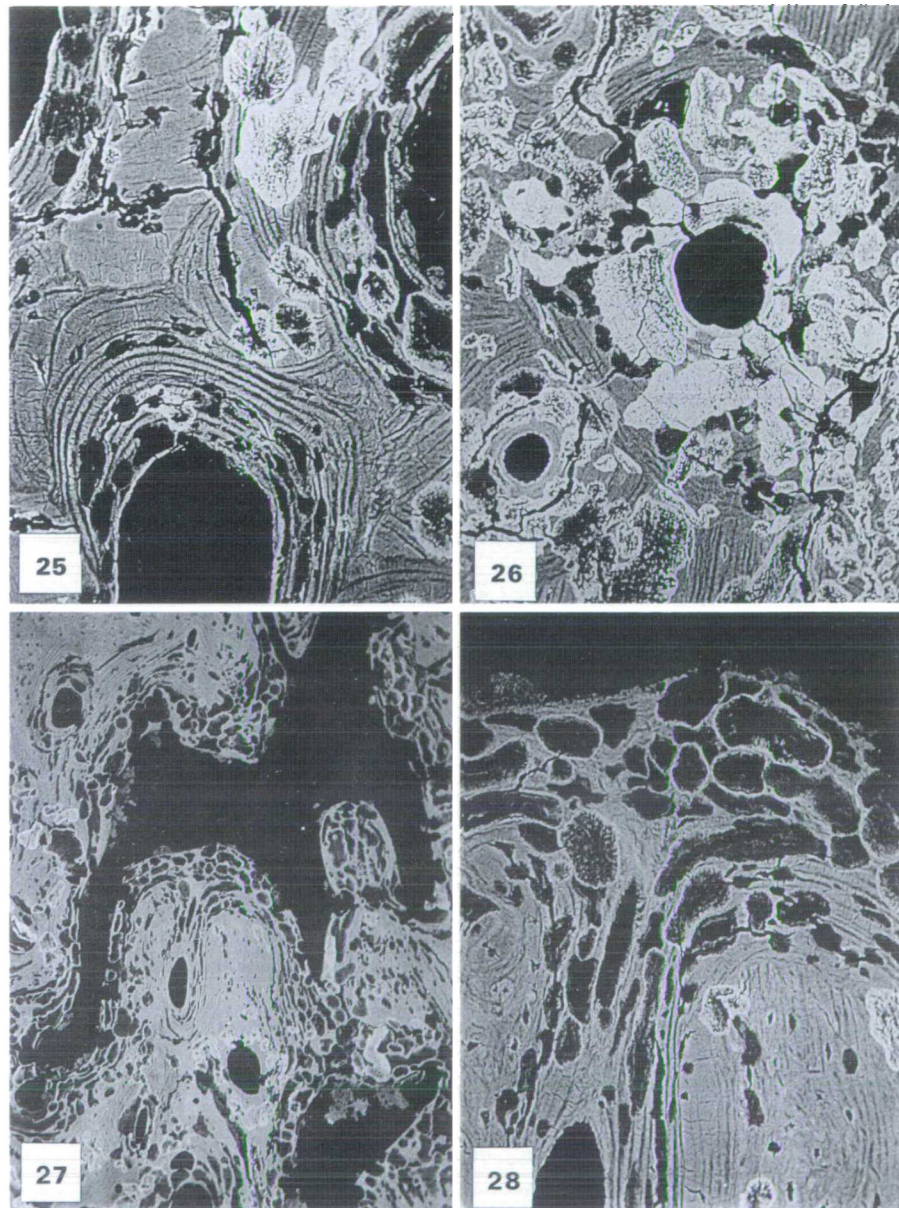
Figure 21 Pathological (specimen 2) archaeological bone. TS apical anterior mid-shaft tibia. There is considerable survival of bone endosteally with visible cement lines, osteocyte lacunae and osteonal lamellae. Foci of changed density are situated within and bridging osteonal systems and some are partially bisected by cracks. SEM BSE, PMMA-embedded bone. FW 300 µm.

Figure 22 Pathological (specimen 2) archaeological bone. TS apical anterior mid-shaft tibia. Higher magnification of field in Figure 21. The foci of changed density appear to be centred on osteocyte lacunae. SEM BSE, PMMA-embedded bone. FW 120 µm.

Figure 23 Pathological (specimen 2) archaeological bone. TS apical anterior mid-shaft tibia. There is extensive diagenetic change and the total absence of the subperiosteal circumferential lamellae. Loss of altered bone has also occurred. SEM BSE, PMMA-embedded bone. FW 3–5 µm.

Figure 24 Pathological (specimen 2) archaeological bone. TS apical anterior mid-shaft tibia. Cracks track for some distance across natural cleavage planes, partially bisecting focal areas of changed density. SEM BSE, PMMA-embedded bone. FW 1275 µm.

It was also noted in the more pronounced periostitic specimen (specimen 2), which had its medullary cavity infilled with bone, that an interesting comparison could be made with the observed diagenetic changes noted on those archaeological specimens with medullary cavity. In respect of the archaeological specimens which had an endosteal aspect, extensive diagenesis was noted both at this aspect and the subperiosteal aspect. These changes extended intracortically leaving more morphologically identifiable bone present at the most central area of the cortex. In contrast, the pathological specimen (specimen 2), which had no endosteal aspect due to the infilling of the medulla with bone



hibited no such changes at its most inner aspect i.e. the mid-point of the once present medulla. This was the region least affected by diagenesis. However, extensive diagenetic changes were well represented in its subperiosteal region, corresponding with previous observations on the archaeological specimens (both non-pathological and pathological). Therefore, where the endosteal aspect did not exist (specimen 2), the extensive effects of diagenesis had not occurred. This suggested that the highly porous nature of the medullary cavity in non-pathological and pathological archaeological bone contributed positively towards the extensive diagenetic changes noted.

A point counting technique was used to quantify this phenomenon. A systematic scheme was preferred as diagenesis has been considered from previous observations in this paper to be a non-random process of events. A small  $\times 60$  SEM BSE montage was created from an unembedded transverse section of the pronounced periostitic specimen (specimen 1) with a field width of 1880  $\mu\text{m}$  extending from its subperiosteal aspect to the bone-infilled proximate mid-point of the once present medulla. A grid containing  $11 \times 11$  intersections, each with an approximate interval of 115  $\mu\text{m}$ , was used to systematically sample the central area of the entire montage counting bone to non-bone (counts falling within vascular spaces were recorded but excluded from the non-bone totals). This provided a total of 8 counting grids. From the results of a correlation carried out on the number of intersections falling on bone to non-bone, it was found that a significant negative association existed between the two variables ( $\rho = -0.976$ ,  $N = 8$ ). Therefore, at the subperiosteal aspect one finds more non-bone, decreasing in sampled frequency with a strong negative gradient, as one approaches the bone infilled mid-point of the medulla. No gradient was present in the distribution of vascular spaces which represented 9.7% of the total number of grid intersections.

### Conclusion

Early, to understand the structural dynamics of diagenesis in human bone, be it pathological or otherwise, one needs to consider the role played by the extensive porous network provided by osteonal canals, osteocyte lacunae and canaliculae and also the influence of the subperiosteal and endosteal zones. The orientation and structure of those areas of changed morphology and density are also highly suggestive of the inherent ante mortem porous structure of bone influencing the pattern and progression of diagenesis to produce Hackett's (1981) "lamellate" structure, which he and others consider to be initiated by the complex actions of fungi and bacteria (Hackett, 1981; Wedl, 1864; Marchafava

---

Figure 25. Higher power of central region of Figure 24, showing details of the foci of changed density situated around osteonal canals. Cracks bisect foci, cross and exploit natural cleavage planes. SEM BSE, PMMA-embedded bone. FW 315  $\mu\text{m}$ .

Figure 26. Pathological (specimen 2) archaeological bone. TS apical anterior mid-shaft tibia. Two secondary osteons with extensive curvilinear diagenetic foci are shown. Note the centrifugal spread of diagenesis from the osteonal canals. SEM BSE, PMMA-embedded bone. FW 300  $\mu\text{m}$ .

Figure 27. Pathological (specimen 2) archaeological bone. TS apical anterior mid-shaft tibia. Diagenetic change occurred preferentially around vascular spaces. SEM BSE, PMMA-embedded bone. FW 1275  $\mu\text{m}$ .

Figure 28. Higher power of central field of Figure 27. The focal changes followed the orientation of osteonal lamellae as well as vascular spaces. The border of the focal regions is generally more sharply defined. SEM BSE, PMMA-embedded bone. FW 315  $\mu\text{m}$ .

*et al.*, 1974; Ascenzi & Silvestrini, 1984). The results from this study confirm the view of these authors that changes in bone are not randomly distributed but reflect the lamellar nature of bone and the distribution of external and internal surfaces. Furthermore the variation of density within diagenetically altered bone, dramatically illustrated by BSE imaging, may result both from the wide ranging elemental composition of the remineralized archaeological bone and from its stage of diagenesis.

An analysis of diagenetic changes in archaeological bone is therefore limited by the need to deduce the sequence of diagenesis. Further experimental investigation of the progression of diagenetic alterations in accelerated systems, particularly with regard to mineral density, should provide a valuable insight into this process in normal and pathological bone. It should be recognized that not only can unrecognized or discounted diagenesis invalidate one's interpretation of pathology in archaeological specimens but also pathology can play an important role in the progression of diagenesis itself.

#### Acknowledgements

I am very grateful to Sheila Jones, Alan Boyde and Tim Arnett for their help and guidance during this study. I would also like to thank Elaine Maconnachie, Maureen Arora and Roy Radcliffe for their expert assistance. The archaeological material was kindly provided by Dr Juliet Rogers, Bristol Royal Infirmary. This study was supported by grants from the MRC, SERC and Central Research Fund of the University of London.

#### References

- Allison, P. A. (1988). The role of anoxia in the decay and mineralisation of proteinaceous macrofossils. *Paleobiology* **14**(2), 139–154.
- Arnaud, G., Arnaud, S., Ascenzi, A., Bonucci, E. & Graziani, G. (1978). On the problem of the preservation of human bone in sea-water. *Journal of Human Evolution* **7**, 409–420.
- Ascenzi, A. & Silvestrini, G. (1984). Bone-boring marine micro-organisms: an experimental investigation. *Journal of Human Evolution* **13**, 531–536.
- Blumberg, J. M. & Kerley, E. R. (1966). Morphometry of bone in palaeopathology. In (S. Jarch Ed.) *Human paleopathology*. New Haven: Yale University Press.
- Boyde, A. & Jones, S. J. (1983). Back-scattered electron imaging and skeletal tissues. *Metabolic Bone Disease and Related Research* **5**, 145–150.
- Boyde, A., Maconnachie, E., Reid, S. A., Delling, G. & Mundy, G. R. (1986). Scanning electron microscopy in bone pathology: Review of methods, potential and applications. *Scanning Electron Microscopy* **IV**, 1537–1554.
- Bromage, T. G. (1984). Interpretation of scanning electron images of abraded forming bone surfaces. *American Journal of Physical Anthropology* **64**, 161–178.
- Garland, A. N. (1985). *A palaeohistological study of bone decomposition*. Unpublished M. A. dissertation. University of Sheffield.
- Garland, A. N. (1987). Palaeohistology. *Science and Archaeology* **29**, 25–29.
- Garland, A. N. (1988). A histological study of archaeological bone decomposition. In (A. Boddington, A. N. Garland & R. C. Janaway, Eds) *Death, Decay and Reconstruction*. Manchester: Manchester University Press, pp. 109–126.
- Graf, W. (1949). Preserved histological structures in Egyptian and ancient Swedish skeletons. *Acta Anatomica* **8**, 236–250.
- Greig, D. M. (1931). *Clinical observations on surgical pathology of bone*. Edinburgh and London: Oliver and Boyd.
- Grupe, G. (1988). Impact of the choice of bone samples on trace element data in excavated human skeletons. *Journal of Archaeological Science* **15**, 123–129.
- Hackett, C. J. (1976). *Diagnostic Criteria of Syphilis, Yaws and Treponematoses and Some other Diseases in Dry Bone*. Berlin: Springer Verlag.
- Hackett, C. J. (1981). Microscopical focal destruction (tunnels) in excavated human bones. *Medicine, Science and Law* **21**(4), 243–265.

- amperl, H. (1966). Problems in pathology and palaeopathology of bone. In (S. Jarcho, Ed.) *Human Palaeopathology*. New Haven: Yale University Press, pp. 81–83.
- anson, D. B. & Buikstra, J. E. (1987). Histomorphological alteration in buried human bone from the lower Illinois Valley: implications for palaeodietary research. *Journal of Archaeological Science* **14**, 549–563.
- are, P. E. (1980). Organic chemistry of bone and its relation to the survival of bone in the natural environment. In (A. K. Bahrensmayer & A. P. Hill, Eds) *Fossils in the Making*. Chicago: University of Chicago Press, Midway reprint. U.S.A., pp. 208–219.
- assan, A. A. & Ortner, D. J. (1977). Inclusions in bone mineral as a source of error in radiocarbon dating. *Archaeometry* **19**(2), 131–135.
- assan, A. A., Termine, J. D. & Haynes, C. V. (1977). Minerological studies on bone apatite and their implications for radiocarbon dating. *Radiocarbon* **19**(3), 364–374.
- enderson, P., Marlow, C. A., Molleson, T. I. & Williams, C. T. (1983). Patterns of chemical change during fossilization. *Nature* **306**, 358–360.
- naway, R. C. (1985). Dust to dust: the preservation of textile materials in metal artefact corrosion products with reference to inhumation graves. *Science and Archaeology* **27**, 29–34.
- rcho, S. (1966). *Human Palaeopathology*. New Haven: Yale University Press.
- leping, L. L., Kuhn, J. K. & Williams, W. S. (1986). An elemental analysis of archaeological bone from Sicily as a test of predictability of diagenetic change. *American Journal of Physical Anthropology* **70**, 325–331.
- yle, J. H. (1986). Effect of post-burial contamination on the concentration of major and minor elements in human bones and teeth – the implications for palaeodietary research. *Journal of Archaeological Science* **13**, 403–416.
- mbert, J. B., Simpson, S. V., Szpunar, C. B. & Buikstra, J. E. (1985). Bone diagenesis and dietary analysis. *Journal of Human Evolution* **14**, 477–482.
- mbert, J. B., Simpson, S. V., Buikstra, J. E. & Charles, D. K. (1984). Analysis of soil associated with woodland burials. *Archaeological Chemistry* **205**, 97–113.
- mbert, J. B., Szpunar, C. B., Buikstra, J. E. (1979). Chemical analysis of excavated human bone from middle and late woodland sites. *Archaeometry* **21**(2), 115–129.
- archiafava, V., Bonucci, L. & Ascenzi, A. (1974). Fungal osteoclasia: a model of dead bone resorption. *Calcified Tissue Research* **14**, 195–210.
- eiburger, E. J. (1988). Syphilis in a Pleistocene bear. *Nature* **333**, 603.
- rtner, D. J. & Putscher, W. G. J. (1985). *Identification of Pathological Conditions in Human Skeletal Remains*. Washington: Smithsonian Institution Press.
- ite, F. D. & Hutton, J. T. (1988). The use of soil chemistry data to address post-mortem diagenesis in bone mineral. *Journal of Archaeological Science* **15**, 729–739.
- ite, F. D. & Brown, K. A. (1985). The stability of bone strontium in the geochemical environment. *Journal of Human Evolution* **14**, 483–491.
- epenbrink, H. (1986). Two examples of biogenous dead bone decomposition and their consequences for taphonomic interpretation. *Journal of Archaeological Science* **13**, 417–430.
- ogers, J. (1987). Arthropathies in palaeopathology: the basis of classification according to the most probable cause. *Journal of Archaeological Science* **14**, 179–193.
- oney, J. G. Jr. (1966). Palaeoepidemiology. In (S. Jarcho, Ed.) *Human Palaeopathology*. New Haven: Yale University Press, pp. 99–107.
- othschild, B. M. (1988). Existence of syphilis in a Pleistocene bear. *Nature* **335**, 595.
- othschild, B. M. & Turnbull, W. (1987). Treponemal infection in a Pleistocene bear. *Nature* **329**, 61–62.
- rgi, S., Ascenzi, A. & Bonucci, E. (1972). Torus palatinus in the Neanderthal. Circeo I Skull. A histologic, microradiographic and electron microscopic investigation. *American Journal of Physical Anthropology* **36**, 189–198.
- einbock, R. T. (1976). *Palaeopathological Diagnosis and Interpretation*. Illinois: CC Thomas.
- out, S. D. & Teitelbaum, S. L. (1978). Histological analysis of undecalcified thin sections of archaeological bone. *American Journal of Physical Anthropology* **44**, 236–270.
- mpsett, D. H. (1970). *Anatomical Techniques*. Edinburgh: E. & S. Livingstone.
- att, I. M. (1985). *The Principles and Practice of Electron Microscopy*. Cambridge: Cambridge University Press.

- Wedl, C. (1864). Über einen im Zahnbein und Knochen keimenden Pilz. *Akademi der Wissenschaften in Wien Sitzungsberichte Naturwissenschaftliche Klasse ABl. Mineralogi biologi erdkunde* **50**(1), 171–193.
- Williams, C.T. & Potts, P.J. (1988). Element distribution maps in fossil bones. *Archaeometry* **30**(2), 237–247.
- Williams, C. T. & Marlow, C. A. (1987). Uranium and thorium distributions in fossil bone from the Olduvai gorge, Tanzania and Kanam, Kenya. *Journal of Archaeological Science* **14**, 297–309.

## Diagenetic Alteration to Teeth In Situ Illustrated by Backscattered Electron Imaging

L. S. BELL, A. BOYDE, S. J. JONES

The Hard Tissue Research Unit, Department of Anatomy and Developmental Biology, University College London, London, England

### Introduction

Diagenetic alteration to skeletal and dental tissues is a phenomenon which occurs after death. It includes all processes which can affect degradation and remineralization, both in and out of the ground, but excludes the effects of high temperature and pressure (Lapedes 1978, Pate and Brown 1985). The morphology and distribution of diagenesis within the hard tissues has been of interest to many authors and was initially observed as boring canals within dentine, thought to be created by fungi (Wedl 1864). Since this initial histological study, other similar light microscopic studies have demonstrated in both teeth and bone that diagenetic alteration can be extensive (Clement 1963, Falin 1961, Garland 1989, Graf 1949, Hackett 1981, Marchiafava *et al.* 1974, Piepenbrink 1986, Poole and Tratman 1978, Sognnaes 1955, Stout and Teitelbaum 1978, Wyckoff 1973). Diagenetic changes within the hard tissues spread from natural surfaces, including both the periosteal and endosteal surfaces of bone, and peripulpal, radicular and coronal surfaces of teeth. The invasive canals vary in diameter and course, and can exhibit remineralization at their peripheries (Bell 1990, Hackett 1981). Previous studies indicate that the time factor appears to be least important in the progress of these postmortem lesions. What is lacking in all these studies is a method which allows morphology, density, and total distribution of diagenesis to be assessed with all the hard tissues present and retained in their anatomi-

cal locations. We present a method whereby the investigation of diagenesis in archaeological material was extended to advantage using the backscattered electron (BSE) mode in a scanning electron microscope (SEM).

BSE imaging in a SEM is a technique already utilized in the study of bones and teeth in basic medical and dental research. Work from our laboratory has illustrated the density variations produced by initial mineralization and later maturation during growth and normal bone turnover, and also of impaired mineralization during pathological conditions such as Paget's disease, fluorosis, osteomalacia, and osteogenesis imperfecta (Boyde and Jones 1983a, Boyde *et al.* 1986, 1990). Dental and related tissues (and encrustations) such as enamel, dentine, cementum, Sharpey fibre alveolar bone, and calculus, have also been studied to advantage by this technique (Boyde and Jones 1983b, Jones 1987, Jones and Boyde 1987).

SEM/BSE imaging has been little applied to bones and teeth in the study of archaeological materials. To date most work in the archaeological field has been concerned with the Z composition of metals, ceramics, and glassware (Meeks 1988), even though scanning electron microscopy has been utilized extensively to study surfaces on many different types of archaeological material (see Olsen 1988). Recently, we have used BSE imaging to investigate diagenetic effects in adult human femora and tibiae with particular reference to archaeological normal and pathological bone (Bell 1990); while Dobney and Brothwell (1988) applied the same technique to the structure of calculus in archaeological samples. Other workers have employed the technique in wider studies and, in particular, to tooth enamel structure during primate evolution (Martin *et al.* 1988).

The study presented here examines the use of SEM/BSE imaging to assess the effects and distribution of diagenesis in teeth retained in situ in their supporting bone. The two important benefits of taking this approach are that all the hard tissues can be cross-compared in a single section; and that the contribution of a natural joint space can be assessed.

---

#### Address for reprints:

Lynne S. Bell  
The Hard Tissue Research Unit  
Department of Anatomy and Developmental Biology  
University College London  
Gower Street  
London WC1E 6BT, England



## Methodology

Macroscopically intact archaeological human mandibles and maxillae from five different soil-buried contexts (all cemeteries, Bronze Age to Medieval) and one marine context [the sudden sea burial of the crew of the *Mary Rose*, Portsmouth, 1545 A.D. (Rule 1982)] were used for this study. A single tooth and accompanying socket was removed from the mandible or maxilla by cutting the entire tooth and socket free using a wet, diamond-edged circular saw. Each section was then rinsed in tepid tap water and allowed to air dry. These sections were placed in methylmethacrylate, placed in a 37°C oven, and removed after the monomer had polymerised to polymethylmethacrylate (PMMA). The methacrylate monomer had been prepared by the flash distil method described by Boyde *et al.* (1986). The embedded specimens were then cut longitudinally buccolingually using an Isomet-11-1180 circular saw, polished using graded abrasives, and finished with 1 µm diamond abrasive on a rotary lap. Each block face received a coating of carbon in vacuum and was then mounted on an aluminium stub.

The specimens were examined using a Cambridge Stereoscan S4-10 SEM, operated in BSE mode working at 20 keV beam voltage. A four-segment solid-state backscattered electron detector was used. For compositional imaging, the signal used was the sum of that deriving from the four detector segments. For topographic imaging, the signal used was the sum of the components from the North and West segments minus the South and East segments. The compositional images are dominated by differences in the mean atomic number of the volume probed by the beam, but also show topographic contrast: high points and ridges allow increased chance of BSE escape, and conversely, it is more difficult for BSE to escape if the beam enters the sample below the general level of its surface; this explains the appearance of lamellae in Figure 1. The topographic images (e.g., Fig. 2), however, demonstrate no contrasts other than those originally in surface roughness (the lamellae and osteocyte lacunae in Fig. 2).

## Results and Discussion

All the hard tissues observed in this study, except enamel, had undergone quite radical diagenetic change. Further, the marine burial tissues proved to have highly distinctive and different morphologies when compared to soil-buried material.

### Bone

The characteristic morphology of adult bone includes circumferential lamellae, secondary osteons, and areas of interstitial lamellae. A radiating system of

osteocyte lacunae and interconnecting canaliculae is present throughout the tissue (Figs. 1 and 2). Within this general framework the process of remodelling results in areas of bone which have a relatively higher mean Z (lighter in BSE images) and areas which have a relatively lower mean Z (darker in BSE images), with holes or embedding medium appearing as black (Fig. 1). This difference in bone matrix density is a direct

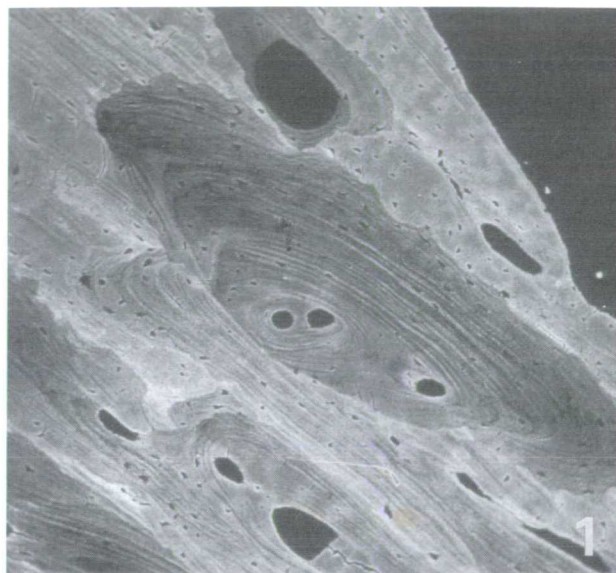


FIG. 1 Bone from cranial vault, 10-year-old girl: embedded in PMMA: BSE density image of polished blockface. Field width 855 µm.

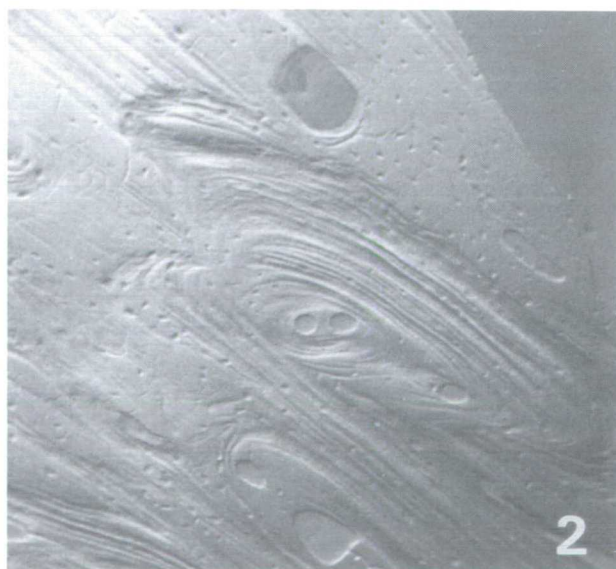


FIG. 2 Topographic image of same field as Fig. 1, using BSE detector with E and W quadrants subtracted. Polishing artefacts due to hardness and collagen orientation variation are evident and would contribute to the density image. Field width 855 µm.



indication of the relative ages of packets of lamellar bone, the progress of mineralization being extended by a relatively long maturation phase. Thus, due to the incremental structure of bone, where time and density are interrelated during growth and the normal bone turnover that occurs throughout life, BSE imaging should be an ideal method to observe such changes, even in archaeological material.

To interpret prepared samples, it was necessary to check topographic detail assiduously. BSE imaging detects high energy electrons released from the specimens surface to an approximate depth of 1–5  $\mu\text{m}$  (Boyde and Jones 1983a), with the BSE yield increasing with  $Z$ . Thus in a situation where the beam probe was incident to a homogeneous substrate, the total diffusion volume was greater than the BSE escape depth, and BSE were consequently released from a disc-like volume just beneath the surface of the substrate (Fig. 3a). However, in a situation where the lamellae of bone were scanned, then the topography created by the combined effects of collagen orientation between lamellae and their stage of maturation caused either an increase in the number of backscattered electrons released or a relative decrease as illustrated in Figure 3b. Thus, a ridge presented a convex-shaped escape volume, which had an in-

creased surface area and so allowed more BSE to escape, while a trough between ridges had a concave-shaped escape volume with a subsequent decrease in surface area which allowed far fewer BSE to escape.

Topographic detail due to polishing was observed in the normal nonarchaeological specimen (Fig. 2). This was due to three main factors. First, bone wears less than PMMA; second, bone containing collagen orientated parallel to the surface wears more than that vertical to the surface (Boyde 1984, Reid 1986); and third, for a given collagen orientation more highly mineralized bone wears less than less well mineralized bone (Boyde and Jones 1987). Thus the sites of osteonal canals and osteocyte lacunae were marked by slight depressions; younger less well mineralized osteons, or last formed regions of osteons, were less proud than older; and more mineralized zones, including interstitial lamellae, were generally proud of the mean surface level. Lamellar topography depended on collagen orientation and was enhanced in less well mineralized bone. Such topography created slight edge artefacts within the specimen. This resulted from an increased surface area at certain points in the scan where the size of the edge determined the amount of reflected high-energy backscattered electrons detected at that point. The net effect of this phenomenon was an observable apparent increase in density in the flat surface image (Fig. 1). Hence, in the flat section images it was generally seen that alternate lamellae and the free border of the Haversian canals were slightly brighter than the surrounding bone. However, although care had to be taken in interpreting the images so that effects of density and collagen orientation on the rate of abrasion during polishing were not ignored, the general features of varying density within the specimens were not contradicted by the topographic images.

The diagenetic effects in the soil-buried alveolar bone were similar to those found in long bones previously detailed by Bell (1990). The alveolar bone in all but one of the specimens (Fig. 4) was extensively affected by diagenetic alteration and appeared to have furnished no lasting protection to the enclosed root (Figs. 5 and 6). The primary or initial route of entry and spread of the micro-organisms appeared to follow the vascular and cellular network of bone and also had a strong orientation parallel to gross collagen direction in the soil-buried contexts (Fig. 7), supporting observations made in a previous paper (Bell 1990). In the *Mary Rose* marine specimen such a spread was not present. Instead, the route of entry of the micro-organisms almost completely ignored the vascular, cellular, and collagenous network of the bone, dentine, and cementum (Fig. 8). The peridental ligament "space," which once would have comprised the natural joint for the tooth, could not be implicated as a route for the spread of postmortem attack. Tissue destruction was located peripherally from the necks of the teeth crossing to the periosteal

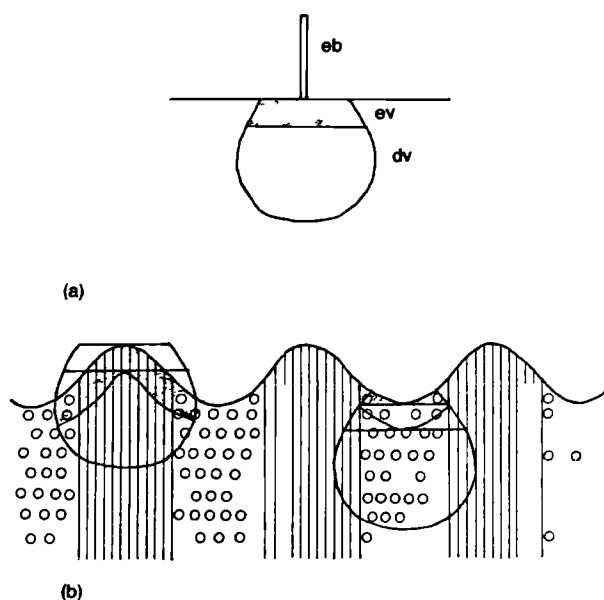


FIG 3 Represents the contribution of topography to the number of BSEs released from lamellar bone: (a) a homogeneous substrate struck by an electron beam (eb) will have a total diffusion volume of electrons (dv) with  $n$  the substrate as well as an BSE escape volume (ev) approximating to a disc with a fixed substrate surface area; (b) vertical collagen creates slight ridges during polishing causing the BSE ev to become convex in shape with a subsequent increased surface area, while collagen parallel to the surface plane abrades relatively faster, creating troughs which causes the BSE ev to become concave in shape with a smaller surface area.

aspect of the alveolar crest and continuing peripherally around the entire distance of the subperiosteal bone of the mandible (Fig. 9).

### Enamel

The enamel in the study, whether covered by calculus or not, appeared unaffected by diagenesis (Figs. 8 and

10). No general demineralization of the enamel surface was observed, although some apparently 'classic' carious lesions in the enamel were found (Figs. 11 and 12). In the limited regions where such an attack had taken place, cross striations of the enamel prisms could be more clearly seen than elsewhere, the approximately weekly incremental striae of Retzius were more prominent and the denser surface zone was evident. Microcavitation within the body of the lesion which resulted from partial localised removal of enamel, presumably by acid dissolution, was also present. The characteristic survival of this "white spot" type of carious lesion, and other more extensive enamel caries observed in this study,

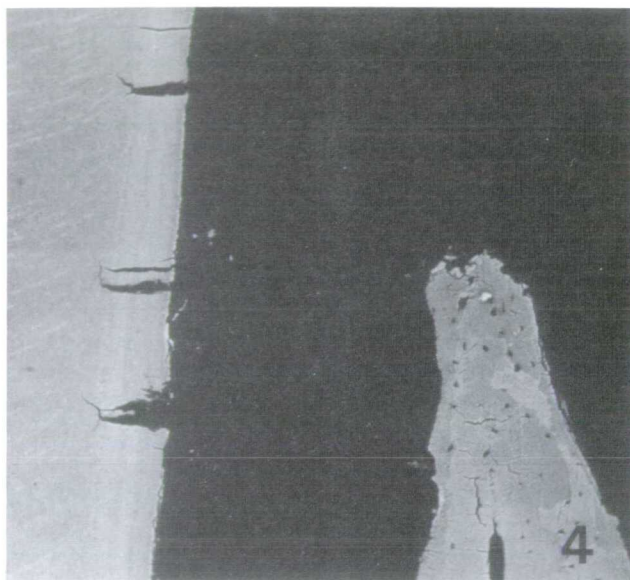


FIG 4 Soil-buried mandibular second premolar in situ showing dentine and cementum (left) and alveolar crest (right) unaffected by diagenesis. BSE image. Field width 885  $\mu\text{m}$ .



FIG 5 Soil-buried maxillary canine in situ: both apical cementum and alveolar bone are extensively altered by diagenesis. BSE image. Field width 1660  $\mu\text{m}$ .

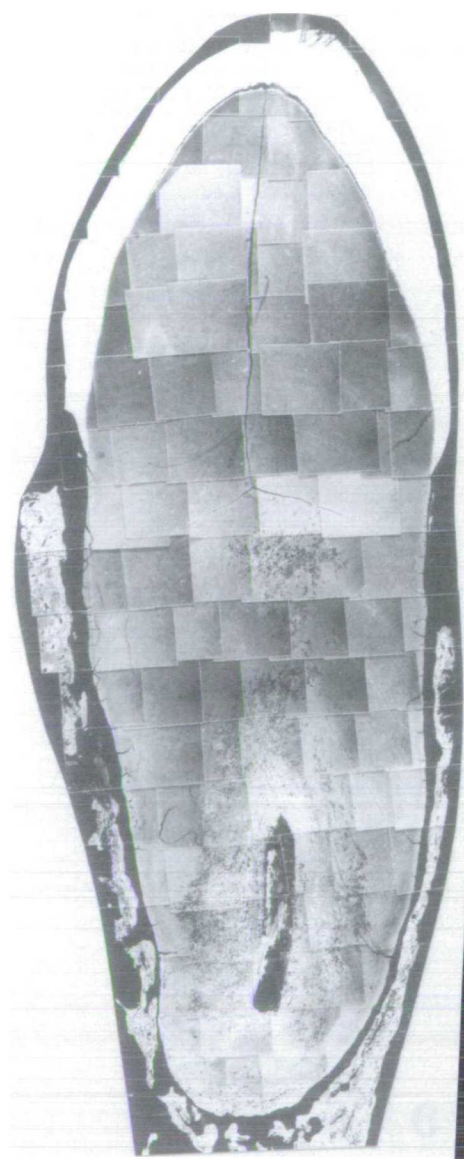


FIG 6 Montage of soil-buried maxillary canine and supporting bone. Diagenesis had affected all tissues except enamel. The tooth bears calculus and had presumed antemortem caries confined to enamel. BSE image. Max. field width 7 mm.



underlines the enamel's ability to be free of attack from body and soil flora, even when its own microstructure had apparently been compromised by antemortem attack. It is recognised, however, that enamel can suffer postmortem degradation to its surface as observed by Poole and Tratman (1978). The pattern of distribution of dental caries is characteristically localized, but the physicochemical changes that occur in acid dissolution of this tissue would be similar whatever the origin of the protons. In this study no such generalized changes were seen, and so it is concluded that the total depositional environment of both the soil and marine contexts studied were not conducive to such changes occurring. The acidity of the soils/sediments during the time of burial is unknown, unfortunately.

### Dentine

In striking contrast to the enamel, the soil-buried dentine was observed to have undergone extensive diagenetic change to its microstructure. These changes tended not to affect the mantle and adjacent circumpulpal dentine of the crown (Fig. 13), but were instead concentrated quite extensively both peripulpally in the root and crown (Fig. 14) and peripherally in the root (Fig. 15), while the enamel appeared to have protected the underlying dentine from external attack (Fig. 16). Interglobular spaces in the dentine below the enamel were also maintained without change (Fig. 17), but in the root the granular layer of Tomes was often not discernible because of extensive diagenesis (Fig. 15). Where diagenetic changes to the dentine had occurred, streaming foci tended initially to orientate along the

long axis of the collagen, following incremental planes, approximately at a 90° angle to the dentine tubules (Fig. 18). Peritubular dentine was often preserved in the diagenetic destruction foci (Fig. 19), in contradistinction to *in vivo* carious attack, which frequently initially follows and locates itself within the dentine tubules, demineralization then spreading to intertubular regions. With the formation of liquefaction foci, carious micro-organisms move outward into the intertubular dentine (Jones 1987, Jones and Boyde 1987). By contrast, diagenetic destruction foci were primarily placed in the intertubular dentine region, and the foci were discrete with clear boundaries between affected and unaffected tissue. Changes in the dentine became

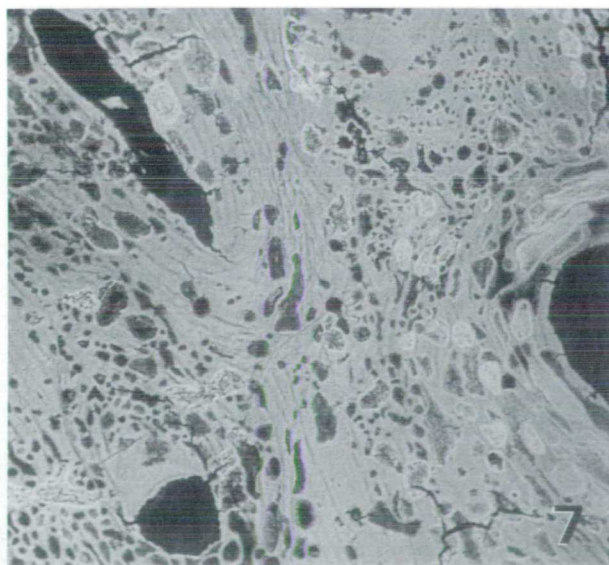


FIG. 7 Discrete diagenetic foci of varying mineral density in soil-buried maxillary lamellar bone. Spread of diagenesis was via the vascular and cellular network and incremental layers. BSE image. Field width 410  $\mu$ m.

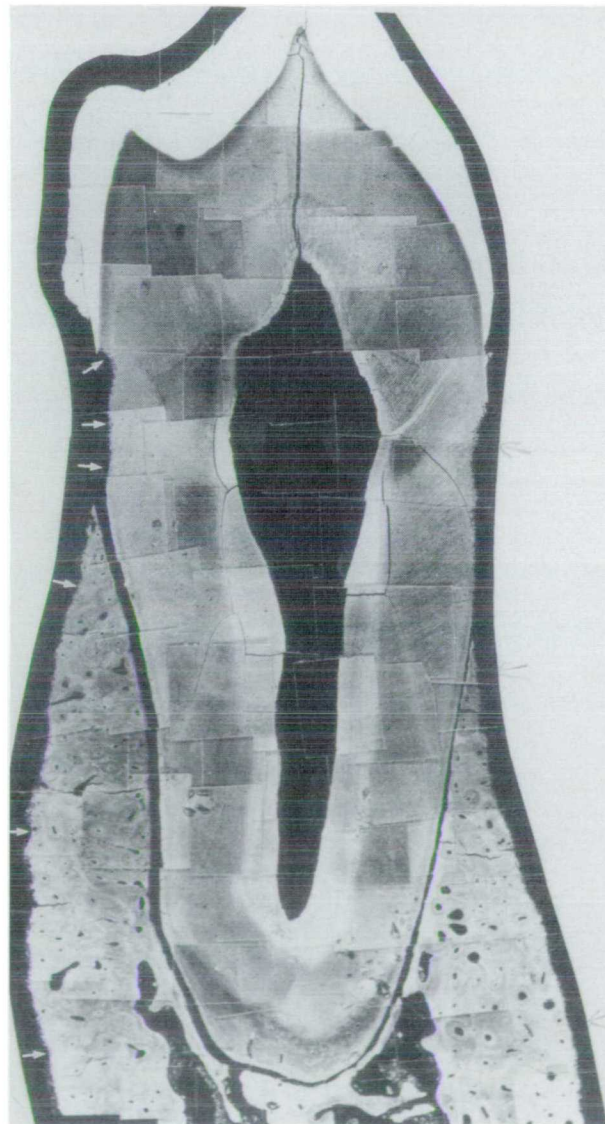


FIG. 8 Montage of marine-buried second premolar retained in mandibular bone. Diagenesis was confined to the surfaces arrowed. BSE image. Max. field width 9 mm.



extremely difficult to interpret or pick out when diagenetic alteration had been superimposed over an antemortem carious assault on the dentine (Figs. 20 and 21). The full distribution of diagenesis was obvious only where it deviated from antemortem microbial carious distribution. Consequently, if one were able to decide that the overall pattern and location of altered dental

tissues could not have been produced by carious attack alone, and the supporting alveolar bone shows evidence of diagenesis, then it would be reasonable to assume a degree of diagenetic intervention in the tooth.

The marine-buried dentine had an altogether different diagenetic morphology and distribution from that of the affected soil-buried material. The attack, as

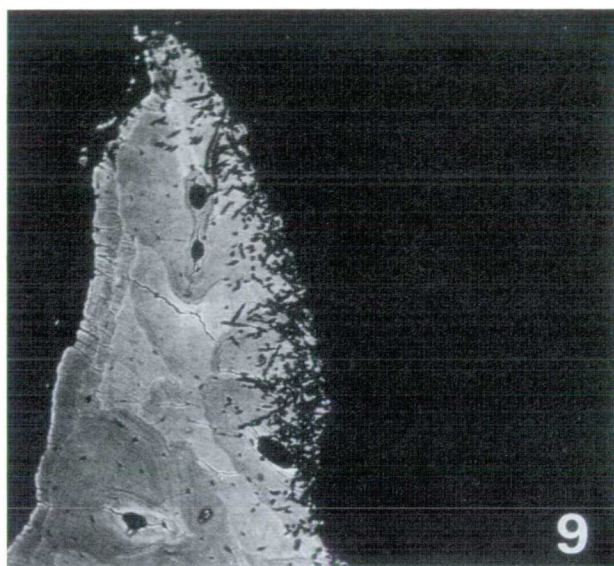


FIG. 9 Alveolar crest of marine-buried mandibular canine. Tunnels extend for a limited distance from the external surface (right). The Sharpey fibre bone of the socket wall is unaffected except at the margin of the socket. BSE image. Field width 855  $\mu\text{m}$ .

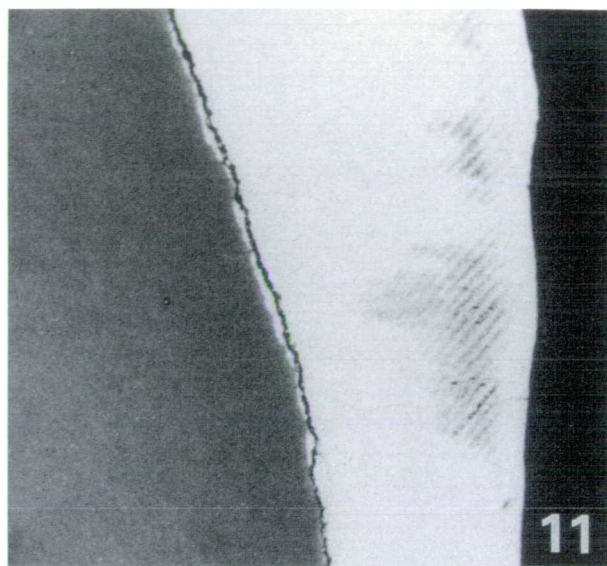


FIG. 11 White spot carious lesion in enamel showing characteristic peaks in spread of demineralization and intact surface layer: soil-buried maxillary canine; high power of Fig. 6. BSE image. Field width 1660  $\mu\text{m}$ .

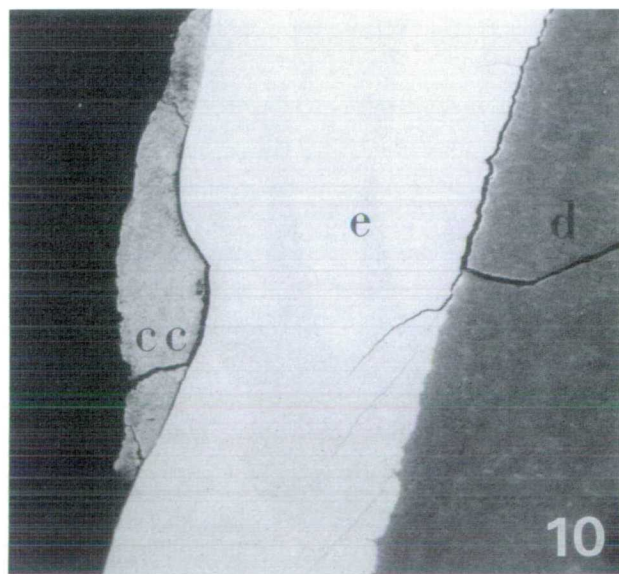


FIG. 10 Soil-buried mandibular canine: the dentine (d), enamel (e), and calculus (cc) were unaffected by diagenesis. BSE image. Field width 855  $\mu\text{m}$ .

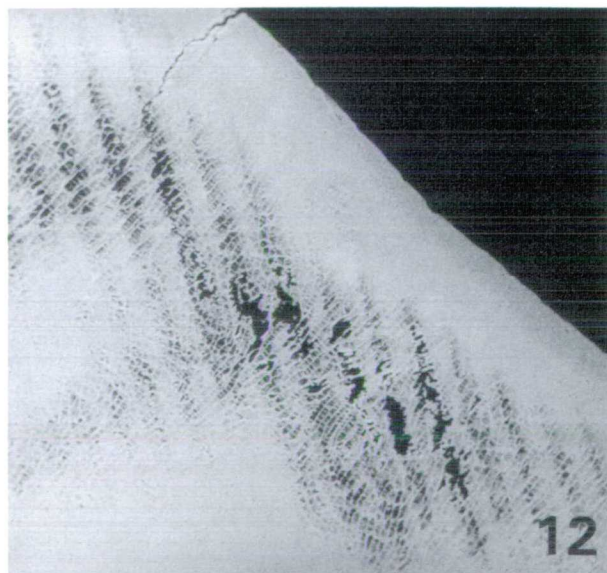


FIG. 12 Higher power of Fig. 11. Cross striations in the enamel prisms and incremental Brown Striae of Retzius are more prominent in the carious lesion, which has cavitated. BSE image. Field width 430  $\mu\text{m}$ .



mentioned above, was peripheral and therefore possibly shortlived (Fig. 8). The dentine was primarily attacked at the cervical margin where the enamel was partially undermined for a short distance (Fig. 22). The full spread of this postmortem attack appeared to have been self-limiting and only affected the root dentine to a level above the alveolar crest (Figs. 8 and 22). The invading micro-organisms appeared somewhat less affected by

the collagenous network of the dentine, but some tunnels followed incremental planes. Many tunnels either tracked along dentine tubules at the advancing edge of the attack, but some also crossed dentine tubule boundaries in almost any direction. There was no evidence of demineralization around any of these boring tunnel-like features, the smallest of which had diameters of approximately  $5\text{ }\mu\text{m}$ . Boring channels or tunnels from a

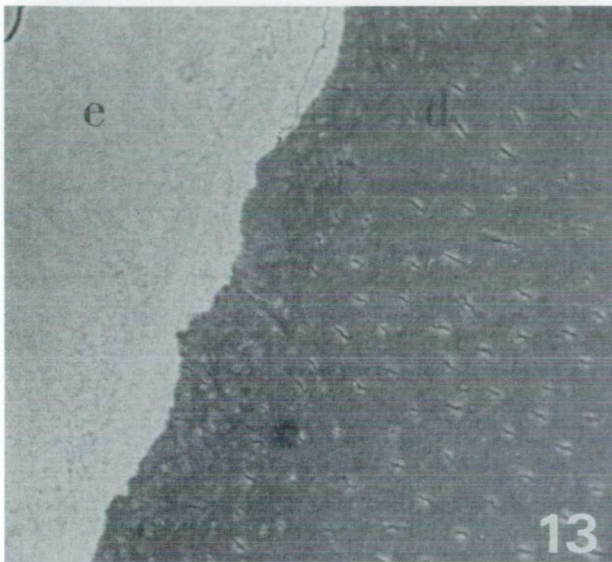


FIG. 13 Unaffected enamel (e) and adjacent, protected, dentine (d) in soil-buried mandibular canine. BSE image. Field width  $180\text{ }\mu\text{m}$ .

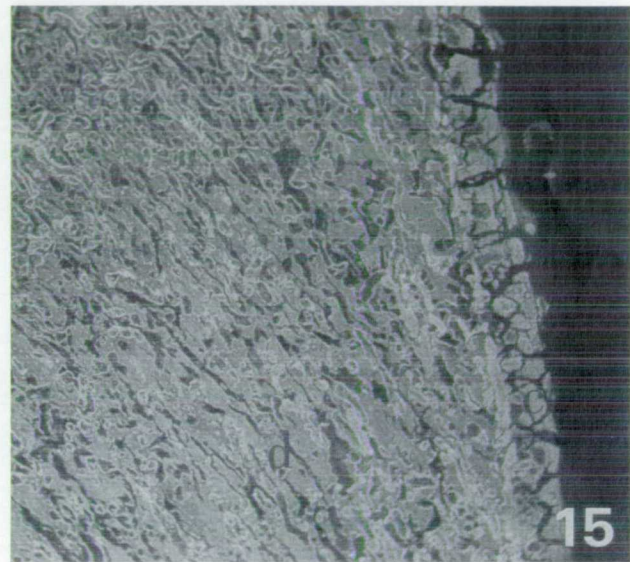


FIG. 15 Extensive postmortem alteration to dentine (d) and cementum (c) structure in soil-buried second premolar. BSE image. Field width  $895\text{ }\mu\text{m}$ .

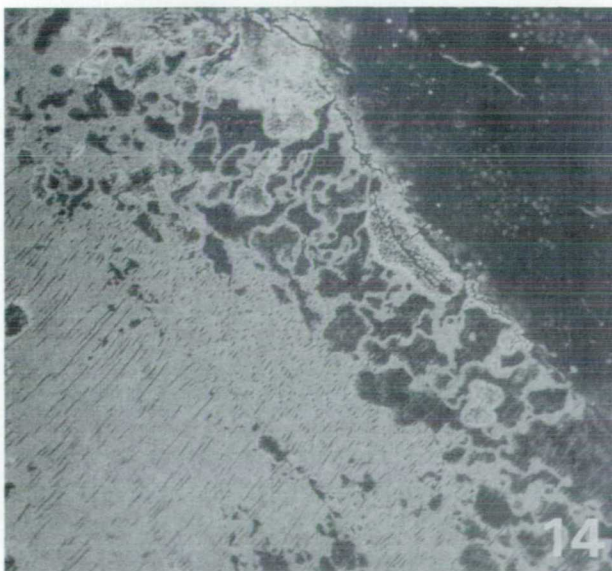


FIG. 14 Secondary dentine, bordering pulp chamber, riddled by diagenetic foci of varying density in a soil-buried maxillary canine. BSE image. Field width  $855\text{ }\mu\text{m}$ .

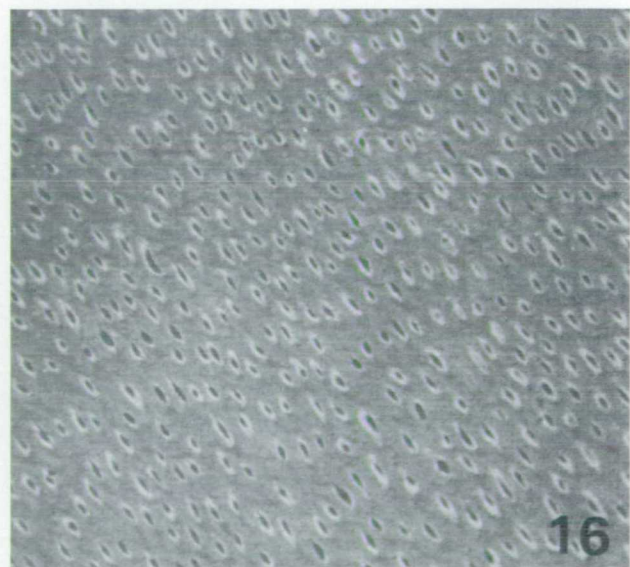


FIG. 16 Peritubular and intertubular dentine in the body of coronal dentine, unaffected by diagenesis: the varied diameter of the tubules is a feature of normal dentine. Soil-buried mandibular second premolar. BSE image. Field width  $170\text{ }\mu\text{m}$ .



marine context have been reported previously by Ascenzi and Silvestrini (1984), who found a variety of micro-organisms present inside the tunnels themselves. These authors implicated protozoans of the amoebic type as principal candidates for the tunnelling (ruling out bacteria and algae due to their absence). The actual in situ distribution of the boring tunnels was not demonstrated.

### Cementum

Soil-buried cementum, like bone and dentine, also underwent diagenetic change. Figure 15 shows considerable tissue alteration, and cracking which may have been due in total, or in part, to the methacrylate shrinking during polymerisation and possibly also expanding due to the exothermic heat of polymerisation. Diage-

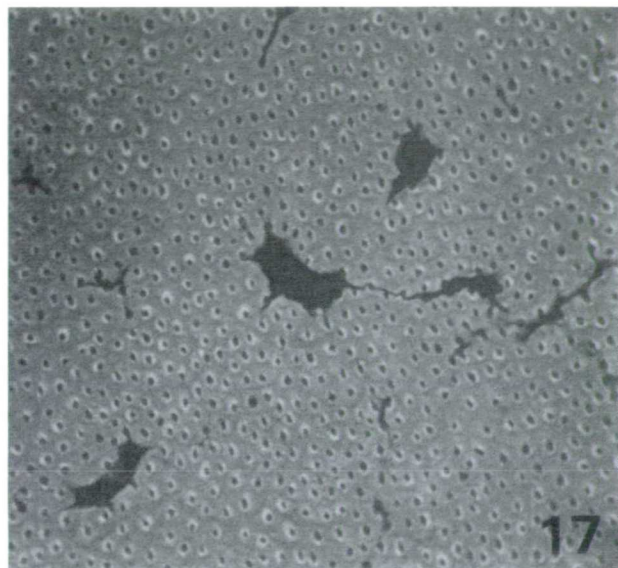


FIG. 17 Well-preserved interglobular dentine in a soil-buried maxillary canine crown. BSE image. Field width 170  $\mu\text{m}$ .



FIG. 19 Same tooth as Fig. 18. Note the variation in mineralization, the preservation of peritubular dentine and the peripheral hypermineralization of the diagenetic foci. BSE image. Field width 170  $\mu\text{m}$ .

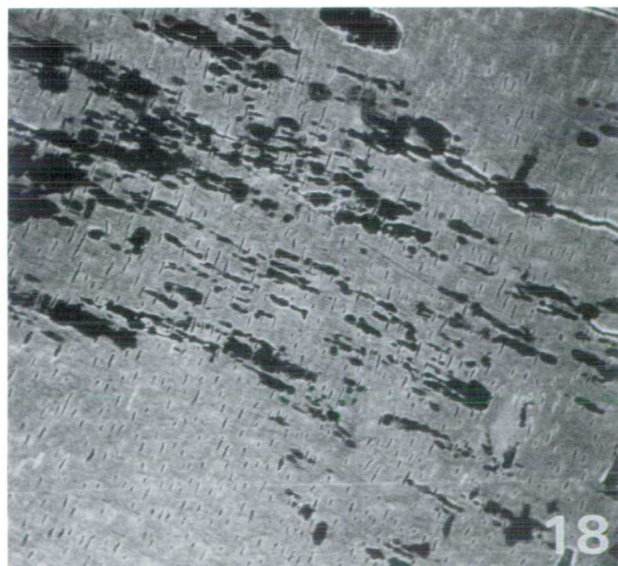


FIG. 18 Diagenetic foci extending along incremental planes in radicular dentine of a soil-buried upper canine. BSE image. Field width 430  $\mu\text{m}$ .

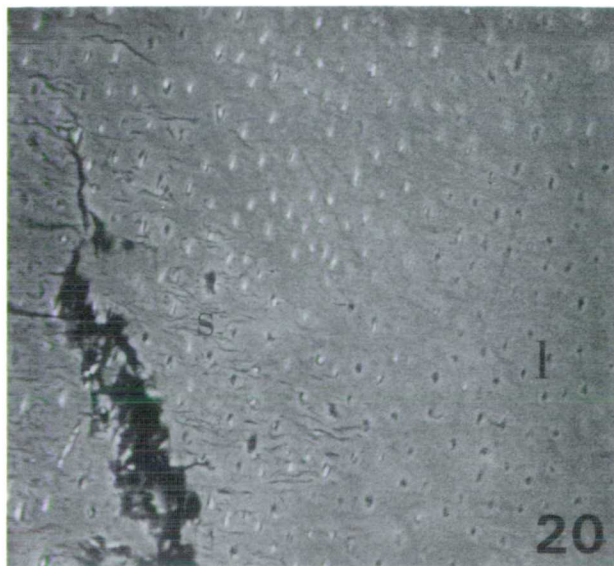


FIG. 20 Second maxillary premolar showing loss (l) of peritubular dentine and splitting (s) of decayed intertubular dentine. Soil-buried specimen. BSE image. Field width 170  $\mu\text{m}$ .



netic foci were clearly observable as partially demineralized and remineralized regions of varying densities (Fig. 23) similar to those observed in the alveolar bone (Fig. 24) and those detailed by Bell (1990) in long bones. The orientation of these foci appeared less clearly defined than those in dentine although they sometimes predominated at one incremental level, as seen in the longitudinal sections. Collagen order in cementum is similar to that of Sharpey fibre bone, the extrinsic fibres being approximately normal to, and the intrinsic fibres parallel to, the developing surface of the bone. On the whole, cementum was less affected by diagenesis than the related alveolar bone, presumably because it lacks the access routes provided by vascular canals.

The marine-buried cementum seemed hardly affected by diagenesis due to its location mostly within the preserved joint space (Fig. 25). However, the small amount that was affected, in a band parallel to the alveolar crest, showed similar tunnelling to that previously described in the marine bone and dentine (Fig. 26). Where cervical cementum was entirely absent, it was not possible to say whether this was due to antemortem or postmortem loss or whether root caries had complicated the picture.

## Conclusions

Backscattered electron imaging of the dental and supporting bony tissues proved a simple and effective method for investigating the changes in mineral density

and morphology that accompany diagenesis. All the hard tissues other than the enamel underwent diagenetic change to microstructure, and the microstructure of each calcified connective tissue influenced the pattern of diagenesis. A striking comparison was made possible between soil versus marine contexts examined in this study, illustrating the necessity of not only taking total account of the distribution and morphology of diagenesis throughout the hard tissues, but the contribution of the joint space to this whole process. It became clear from this study that had the teeth not been retained in situ of their alveolar and basal bone, the unique distribution of the soil to marine contexts would have been lost. Previous studies have not used this method of presentation, but it provides an important step toward understanding the microbial environment which promoted the consequent diagenetic morphologies.

It is clear from this study that the effects of diagenesis can be extensive even in apparently well-preserved

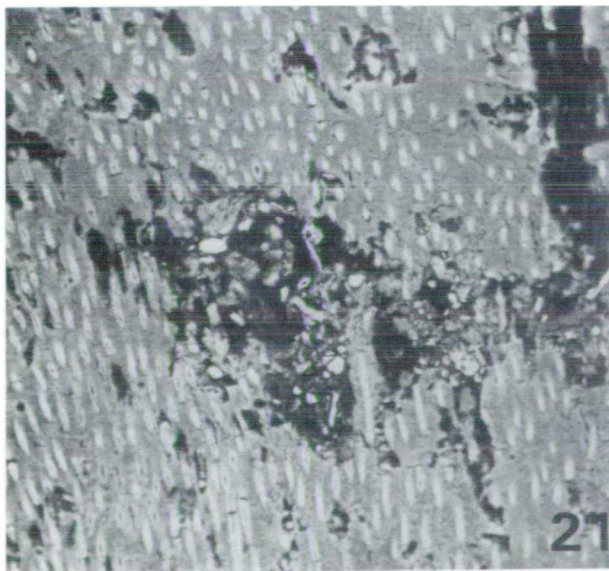


FIG 21 Same tooth as Fig. 20 showing a demineralized and cavitated area within the ante mortem carious dentine which could have been secondarily affected by diagenesis. BSE image. Field width 170  $\mu\text{m}$ .

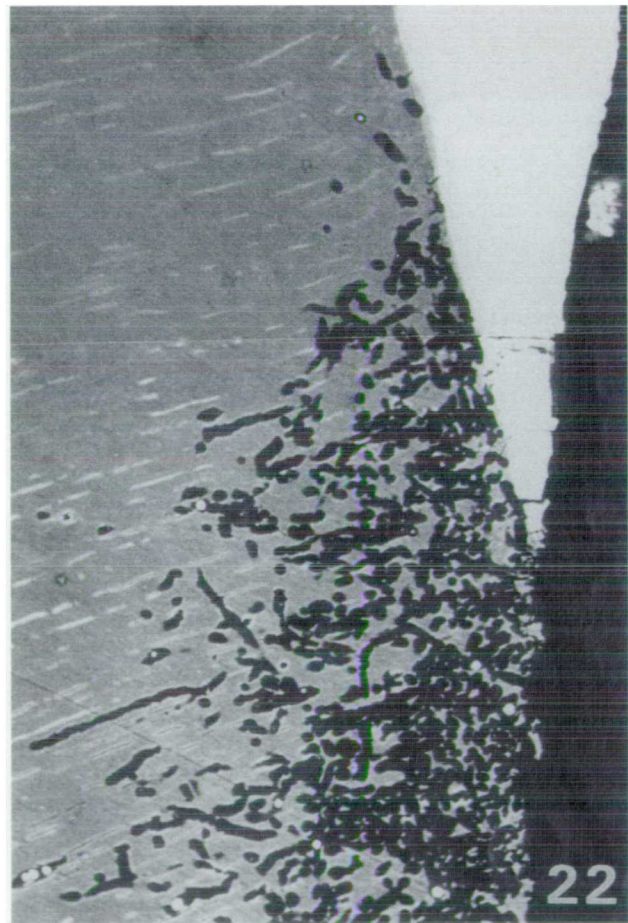


FIG 22 Marine-buried mandibular canine exhibiting diagenetic attack to dentine with tunnels undermining enamel for a short distance. The invading tunnels follow dentine tubule direction, the incremental planes and also directions apparently unrelated to dentine microstructure. BSE image. Field width 430  $\mu\text{m}$ .



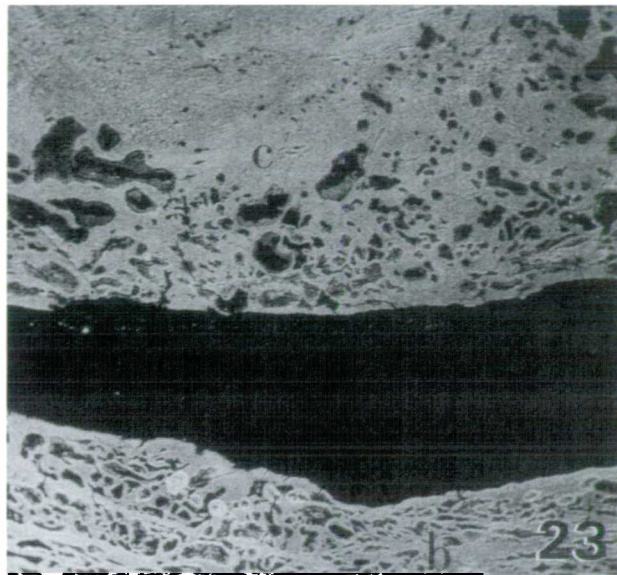


FIG. 23 Soil-buried maxillary canine showing diagenetic demineralized and remineralized foci within the apical cementum (c) and alveolar bone (b). BSE image. Field width 855  $\mu\text{m}$ .

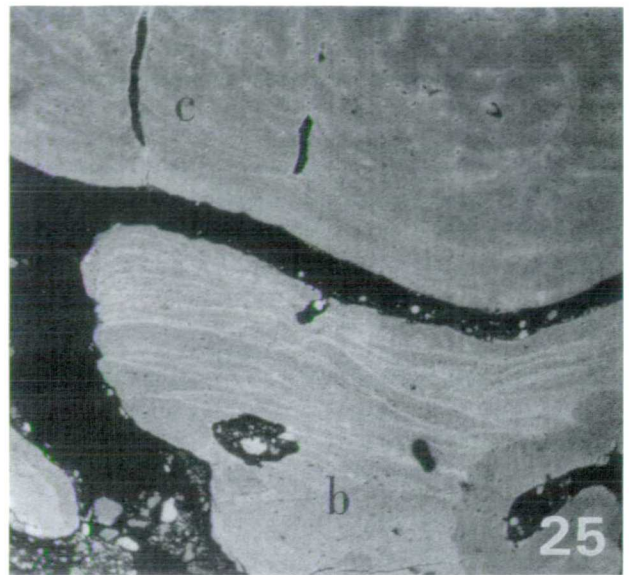


FIG. 25 Marine-buried mandibular second premolar and supporting alveolar bone (b) in region unaffected by diagenesis. The clefts in the cellular cementum (c) are not of diagenetic origin but anatomical features of the root apex. Sediment inclusions are present in ligament and vascular spaces. BSE image. Field width 1805  $\mu\text{m}$ .

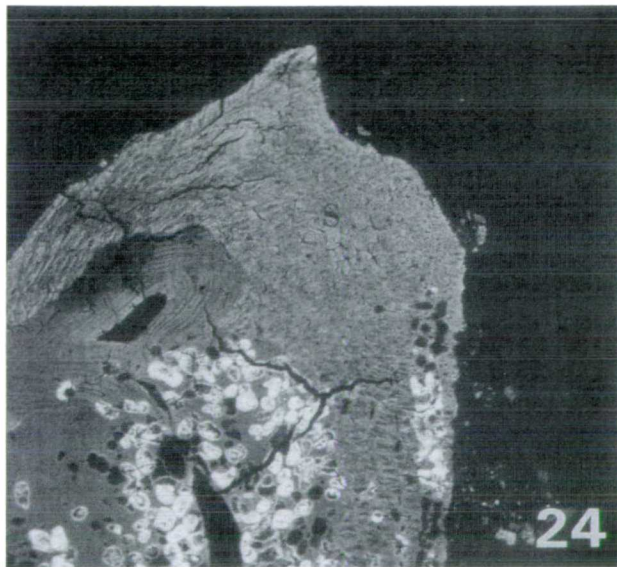


FIG. 24 Soil-buried alveolar crest exhibiting several discrete diagenetic foci of differing densities. The Sharpey fibre bone (s) contains postmortem lesions which followed intrinsic fibre incremental planes. In the osteon and adjacent bundle bone note the large area of demineralization (arrowed). BSE image. Field width 855  $\mu\text{m}$ .

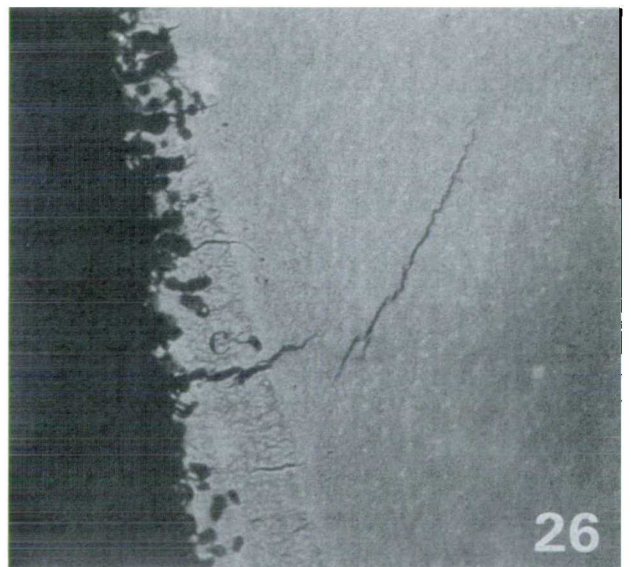


FIG. 26 Marine-buried mandibular canine: acellular cementum (c) at neck of tooth affected by boring tunnels only above the alveolar crest level. Same specimen as Fig. 6. BSE image. Field width 430  $\mu\text{m}$ .

dental and supporting skeletal tissues. Sampling protocols for biochemical and mDNA extraction studies could gain considerable benefit from identifying and locating microscopically the distribution of diagenesis before removal of bone or dentine. Moreover, rather

than considering diagenesis as an irksome contaminative factor only, it instead represents a little exploited taphonomic resource which could be of great use and interest to archaeological and forensic science.



## Acknowledgments

This manuscript relates to a paper presented at SCANNING '90, Crystal City, VA, April 20, 1990.

We thank Elaine Maconnachie and Roy Radcliffe for their technical assistance. The archaeological material was kindly provided by Ann Stirland, Juliet Rogers, Roger Flinn, and the Trust for Wessex Archaeology. Theya Molleson has provided continued interest and encouragement. This work was supported by grants from the MRC, SERC, and the Central Research Fund of the University of London.

## References

- Ascenzi A, Silvestrini G: Bone-boring marine micro-organisms: An experimental investigation. *J Human Evol* 7, 409–420 (1984)
- Bell LS: Palaeopathology and diagenesis: An SEM evaluation of structural changes using backscattered electron imaging. *J Archaeol Sci* 17, 85–102 (1990)
- Boyde A: Dependence of rate of physical erosion on orientation and density in mineralized tissues. *Anat Embryol* 170, 57–62 (1984)
- Boyde A, Jones SJ: Back-scattered electron imaging of skeletal tissues. *Metabol Bone Dis Rel Res* 5, 145–150 (1983a)
- Boyde A, Jones SJ: Backscattered electron imaging of dental tissues. *Anat Embryol* 168, 211–226 (1983b)
- Boyde A, Jones SJ: Early scanning electron microscopic studies of hard tissue resorption: Their relation to current concepts reviewed. *Scan Microsc* 1(1), 369–381 (1987)
- Boyde A, Hendel P, Hendel R, Maconnachie E, Jones SJ: Human cranial bone structure and the healing of cranial bone grafts: A study using backscattered electron imaging and confocal microscopy. *Anat Embryol* 181, 235–251 (1990)
- Boyde A, Maconnachie E, Reid SA, Delling G, Mundy GR: Scanning electron microscopy in bone pathology: Review of methods, potential and applications. *Scan Electr Microsc* IV, 1537–1554 (1986)
- Clement AJ: Variations in the microstructure and biochemistry of human teeth. In *Dental Anthropology* (Brothwell DR, Ed.). Pergamon Press, New York (1963) 245–269
- Dobney K, Brothwell DR: Dental calculus: Its relevance to ancient diet and oral ecology. In *Teeth and Anthropology* (Cruwys E, Foley RA, Eds.). BAR International Series 291, Oxford (1988) 55–81
- Falin LI: Histological and histochemical studies of human teeth of the Bronze and Stone Ages. *Arch Oral Biol* 5, 5–13 (1961)
- Garland AN: Microscopical analysis of fossil bone. *Appl Geochem* 4, 215–229 (1989)
- Graf W: Preserved histological structures in Egyptian and Ancient Swedish skeletons. *Acta Anatomica* 8, 236–250 (1949)
- Hackett CJ: Microscopical focal destruction (tunnels) in excavated human bones. *Med Sci Law* 21(4), 243–265 (1981)
- Jones SJ: The root surface: An illustrated review of some scanning electron microscope studies. *Scan Microsc* 1(4), 2003–2018 (1987)
- Jones SJ, Boyde A: Scanning microscopic observations on dental caries. *Scan Microsc* 1(4), 1991–2002 (1987)
- Lapedes DN, Ed: *McGraw-Hill Encyclopedia of the Geological Sciences*. McGraw-Hill Inc., New York (1978) 153–155
- Marchafava V, Bonucci L, Ascenzi A: Fungal osteoclasia: A model of dead bone resorption. *Calcified Tis Res* 14, 195–210 (1974)
- Martin LB, Boyde A, Grine FE: Enamel structure in primates: A review of scanning electron microscopic studies. *Scan Microsc* 2(3), 1503–1526 (1988)
- Meeks N: Backscattered electron imaging of archaeological material. In *Scanning Electron Microscopy in Archaeology* (Olsen SL, Ed.). BAR International Series 452, Oxford (1988) 23–44
- Olsen SL: *Scanning Electron Microscopy in Archaeology*. BAR International Series 452, Oxford (1988)
- Pate FD, Brown KA: The stability of bone strontium in the geochemical environment. *J Human Evol* 14, 483–491 (1985)
- Piepenbrink H: Two examples of biogenous dead bone decomposition and their consequences for taphonomic interpretation. *J Archaeol Sci* 13, 417–430 (1986)
- Poole DFG, Tratman EK: Post-mortem changes on human teeth from late upper Palaeolithic/Mesolithic occupants of an English limestone cave. *Arch Oral Biol* 23, 1115–1120 (1978)
- Reid SA: A study of lamellar organisation in juvenile and adult human bone. *Anatomy Embryol* 174, 329–338 (1986)
- Rule M: *The Mary Rose*. Conway Maritime Press, London (1982)
- Sognaes RF: Post mortem microscopic defects in the teeth of ancient man. *AMA Arch Pathol* 59, 559–570 (1955)
- Stout SD, Teitelbaum SL: Histological analysis of undecalcified thin sections of archaeological bone. *Am J Phys Anthropol* 44, 236–270 (1978)
- Wedl C: Über einen im Zahnbein und Knochen keimenden Pilz. *Akademie der Wissenschaften in Wien. Sitzungsberichte Naturwissenschaftliche Klasse ABI. Mineralogie, biologie Erdkunde* 50(1), 171–193 (1864)
- Wyck ff RWG: The microstructure and composition of fossils. In *Biological Mineralization* (Zipkin I, Ed.). J. Wiley & Sons Inc., New York (1973) 527–546



# Macroscopic and Microscopic Evaluation of Archaeological Pathological Bone: Backscattered Electron Imaging of Putative Pagetic Bone

LYNNE S. BELL AND SHEILA J. JONES

*Hard Tissue Research Unit, Dept. of Anatomy and Developmental Biology,  
University College London, Gower St., London, WC1E 6BT UK.*

**ABSTRACT** Reports on microscopic palaeopathological material are rare and have not addressed the potentially complicating effects of diagenesis on bone. This study examined the microstructural integrity of two putative cases of Paget's disease using a scanning electron microscope (SEM) in backscattered electron (BSE) imaging mode. The results obtained show that the SEM-BSE technique is a highly sensitive and informative microscopic method, which can be used to locate areas of morphologically intact bone within extensively altered diagenetic bone. Evidence for high bone turnover was present in both specimens and it was apparent that there was little relationship between macroscopic and microscopic preservation. The investigation also validated the use of gross X-rays as a diagnostic tool, since diagenetic reorganization of the bone coarsely replicated the general collagenous arrangement of the pathology sufficient for the resolving power of gross radiography.

**Keywords:** Paget's Disease, Human bone, Palaeopathology, Diagenesis, SEM, Backscattered electrons.

---

## Introduction

Paget's disease of bone derives its name from Sir James Paget's original description of "osteitis deformans" in 1877.<sup>1</sup> It is a disease of considerable antiquity and affects most bones of the skeleton.<sup>2</sup> Histologically it is characterized by excessive or rapid resorption and formation of bone. Consequently, it has a higher frequency of immature forms of bone, a greater number of reversal lines and larger osteocyte lacunae with less well mineralized walls, giving an overall mosaic-like appearance,<sup>3,4</sup> although in the early stages of the disease this mosaic appearance will be less obvious.<sup>5</sup> In archaeological material, Paget's disease is usually assessed from the gross and radiological appearance of the bones.<sup>2,6,7</sup>

Reports on the microscopy of such archaeological bone are rare and the potentially

complicating effects of diagenesis on bone structure have not been addressed. Diagenesis is known to alter and reorganize bones and teeth extensively after death.<sup>8–13</sup> This reorganization is believed to be mediated by the separate or combined actions of bacteria and fungi<sup>11,14–16</sup> although in marine contexts other microorganisms have been implicated.<sup>8,17</sup> In this study two cases thought to be Paget's disease from macroscopic and radiological findings have been examined for microstructural evidence supporting the tentative diagnoses.

## Methodology

The skeletal material used in this microscopy study came from two adult inhumations from separate medieval cemeteries: St Margaret *in cumbusto*, Norwich (SMI) and Sandwell Priory,

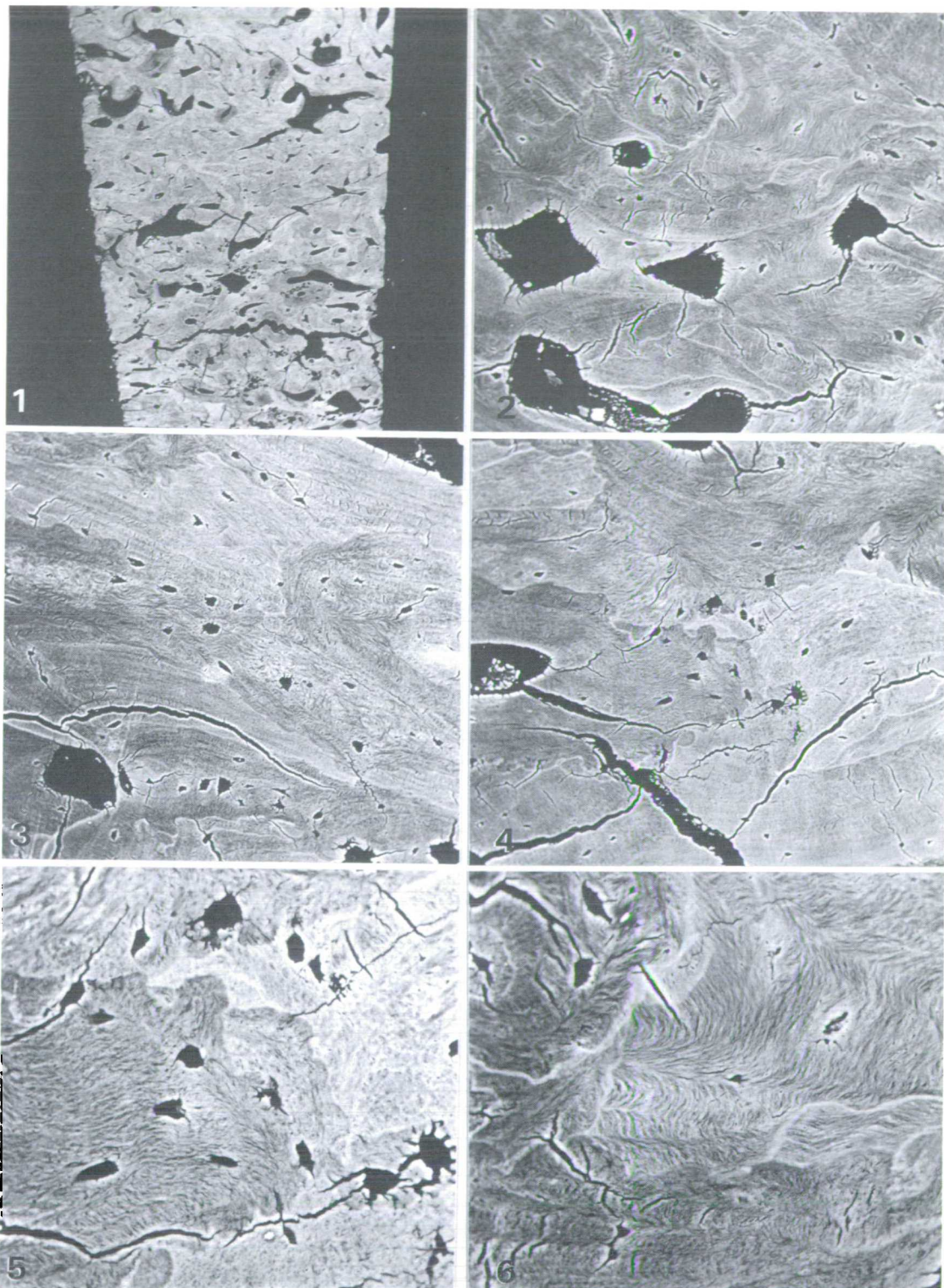


Figure 1. Sandwell Priory (SP) sagittal section of occipital bone. Increased vascularity with irregularly defined vascular canals evident amongst poorly organized and mineralized bone (less well mineralized bone is darker in tone than relatively more highly mineralized bone) (Field width (FW) 2625  $\mu\text{m}$ )

Figure 2. Sandwell Priory specimen showing irregularly defined vascular canals, among many reversal lines that are hypermineralized (whiter) compared with the surrounding bone (FW 445  $\mu\text{m}$ ).

Figure 3. Sandwell Priory specimen. Centre field shows irregular and enlarged osteocyte lacunae within poorly organized collagen (FW 440  $\mu\text{m}$ ).

Figure 4. Sandwell Priory specimen. Two osteonal systems are seen bordering each other and at an earlier maturation state than the interstitial areas of bone. Centre field, the osteonal lamellae are poorly organized with irregularly shaped and large osteocyte lacunae (FW 445  $\mu\text{m}$ ).

Figure 5. Sandwell Priory specimen. Higher power centre field of previous figure. A hypermineralized reversal line can be seen clearly with the characteristic scalloped outline of osteoclastic resorption lacunae. The irregular osteocytes are more clearly evident, as is the arrangement of collagen, particularly in the less matured bone at centre field (FW 185  $\mu\text{m}$ ).

Figure 6. Sandwell Priory specimen. An area of bone showing rapid remodelling as evidenced by several hypermineralized reversal lines close together and the generally lower state of mineralization of bone packets, (FW 185  $\mu\text{m}$ ).

Sandwell (SP). The gross and radiological distribution of SMI Paget's was postcranial (for a full description see Stirland in this issue), whilst the SP skeleton was affected only cranially and was not X-rayed. The macroscopic condition of the SMI was excellent, whereas that of the SP material was poor, being fragmentary and chalky.

A transverse midshaft section was removed from the left humerus and left radius (SMI), and a thick sagittal section was removed from the occipital bone (SP). The sections were then put in methylmethacrylate (with added styrene for stability<sup>3</sup>), placed in a 32°C oven, and removed after the methylmethacrylate had polymerized to polymethylmethacrylate (PMMA). The embedded specimens were then cut transversely using an Isomet-11-1180 circular diamond saw, polished using graded abrasives, and finished with a 1  $\mu\text{m}$  diamond abrasive on a rotary lap. Each block face received a coating of carbon *in vacuo*.

The specimens were examined using a Cambridge Stereoscan S4-10 SEM, operated in backscattered electron (BSE) mode working at 20 keV beam voltage. A four-segment solid-state BSE detector was used for compositional imaging, collecting BSE electrons at all four segments and summing the signal from all four segments. The images were dominated by differences in the mean atomic number of the volume probed by the scanning beam and so provided a sensitive indicator of mean density and micromorphology.

## Results

Examination by SEM/BSE imaging showed that the cranial SP bone, although considered poorly preserved macroscopically, had extensive regions unaffected by diagenesis. By contrast, the SMI material, which was considered in excellent macroscopic condition, was profoundly altered by diagenesis.

### *The Sandwell Priory bone*

The specimen had the appearance of a high bone turnover condition not dissimilar to the early stages of Paget's disease referred to by Tillman (1962).<sup>5</sup> There was evidence of increased vascularity (Figure 1), with irregularly defined vascular canals (Figure 2), and enlarged osteocytes within poorly organized collagen lamellae (Figure 5 and 6) which were seen easily in the BSE image because they were hypermineralized compared with the surrounding tissue. Small focal diagenetic lesions were evident on the endocranial aspect, located on sites where osteocyte lacunae would once have been (Figure 7). These focal alterations were distinguishable from osteoclastic activity.

### *The St Margaret in cumbusto bone*

The SMI bone had been altered extensively by diagenesis and little of the original bone tissue was recognizable. The left radial SMI specimen had the classic mosaic pattern of Pagetic bone,



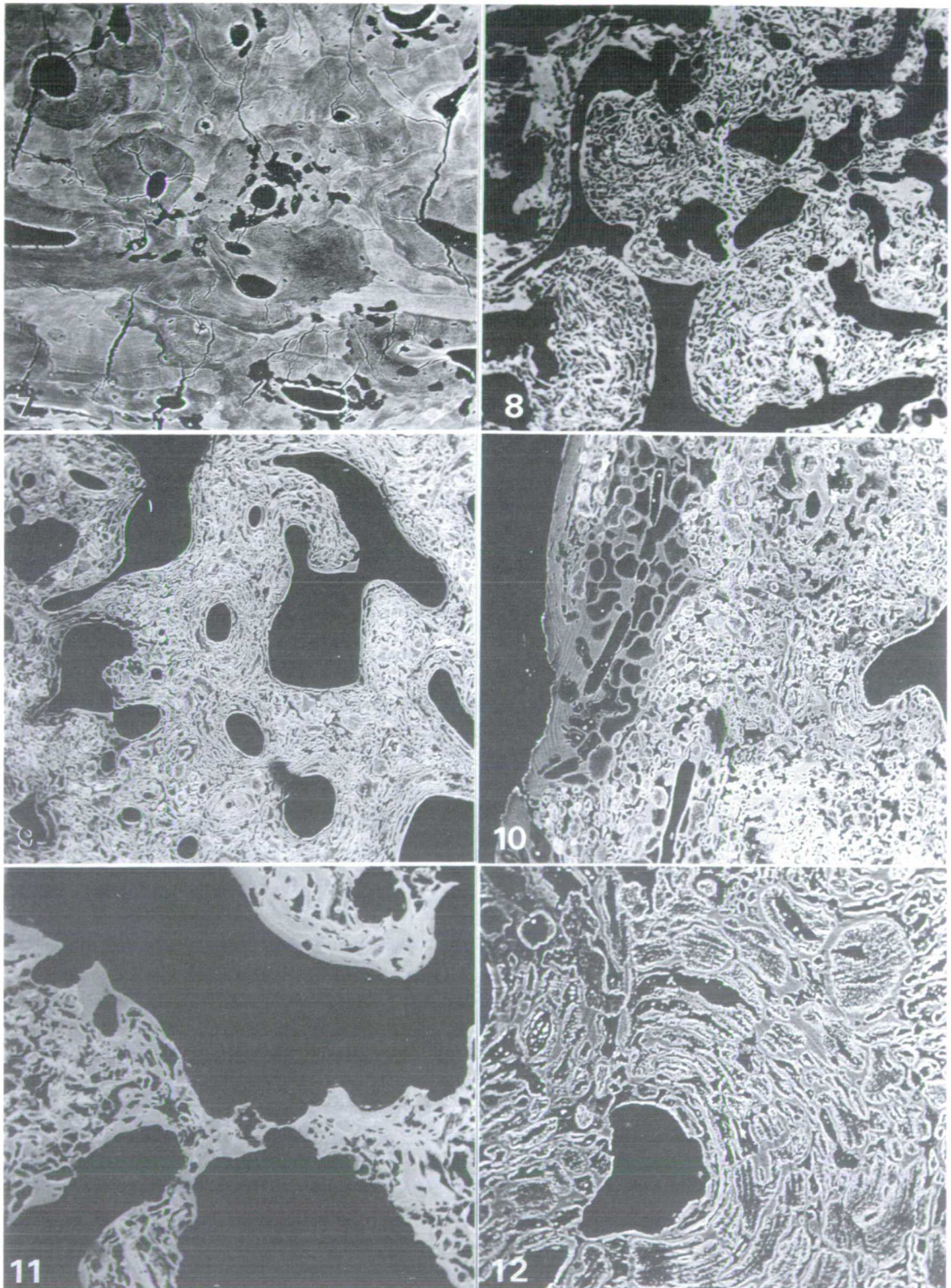


Figure 7. Sandwell Priory specimen. Small focal diagenetic lesions were evident on the endocranial aspect of the section. The diagenetic foci all had this type of morphology and were located mostly within osteonal systems (FW 875  $\mu\text{m}$ ).

Figure 8. St Margaret *in cumbusto* (SMI) left radius midshaft transverse section (TS). The classic 'mosaic' pattern of Paget's disease replicated by the diagenetic process. Very little of the original bone with its characteristic morphology and density is evident (FW 1910  $\mu\text{m}$ ).

Figure 9. St Margaret *in cumbusto* left humerus midshaft TS. Enlarged vascular canals characteristic of increased bone turnover found in a small area of the humeral cortex. Again diagenetic ingress is virtually total (FW 1665  $\mu\text{m}$ ).

Figure 10. St Margaret *in cumbusto* left humerus midshaft TS. The subperiosteal circumferential lamellae in both specimens often survived intact. However, regions just below the lamellae were entirely diagenetically reorganized in terms of morphology and density (FW 810  $\mu\text{m}$ ).

Figure 11. St Margaret *in cumbusto* left radius midshaft TS. Osteoclastic resorption lacunae clearly evident as scalloped edging at the periphery of enlarged vascular spaces. Although the diagenetic ingress is extensive, bone with its characteristic density is present at the periphery of the vascular spaces (FW 955  $\mu\text{m}$ ).

Figure 12. St Margaret *in cumbusto* left humerus midshaft TS. The process of diagenetic ingress is seen to orientate itself strongly with general collagen direction. Also a reversal line (top left centre) is highlighted by two different orientations of diagenetic ingress (FW 410  $\mu\text{m}$ ).

which had been retained, or rather replicated, by the diagenetic process (Figure 8). Similarly, the left humerus exhibited large irregular vascular canals within a field of diagenetically altered bone (Figure 9). At the subperiosteal aspect of both specimens there was survival of circumferential lamellae, external to regions of the bone with greatly diagenetically changed micromorphology and altered density (Figure 10). Internally, many regions of resorption lacunae profiles could be identified, edging the much enlarged vascular spaces (Figure 11). The diagenetic foci, described in detail elsewhere,<sup>8</sup> have a strong orientation along the long axis of gross collagen direction (Figures 10 and 12). Thus, although at a microscopic level very little bone with its correct structure and density was intact, the overall structure was coarsely replicated by the diagenetic process itself. It was therefore possible to read evidence for increased remodelling in the original bone even in regions where apparently none had survived.

## Discussion

The chalky fragmented appearance of the SP specimen presented a gloomy prospect in terms of ascertaining any useful information to add to the assessment of a potential pathology. It was therefore a pleasant surprise to find the microstructure of the bone in such good condition. Although the micromorphology indicated a high bone turnover pathology, this did not in itself

prove that Paget's disease was the cause of the condition. However, the microscopic study did add valuable information, and poor macroscopic survival of the bone should not pose a deterrent to microscopic investigation.

By contrast, the SMI specimens, although in excellent macroscopic condition and exhibiting both the gross and radiological appearance of Paget's disease, had been remodelled almost entirely by diagenesis. Although it might be supposed that the diagenetic alteration made it difficult to observe any signs of high resorption and apposition, the retention of the original vascular arrangement characteristic of Paget's disease and the mosaic pattern with many interrupted arcs mimicking the organization of the original lamellar groups, could be read as evidence for high bone turnover. This pattern was observed clearly in the grossly deformed SMI left radius, whilst the less altered SMI left humerus had a small area of enlarged vascularization within the cortex. Such characterization allowed validation of X-rays: the invasive lesions coarsely replicated the collagenous arrangement of the pathology with sufficient resolution for gross X-ray analysis. This observation, however, should not be considered the rule, since it has been shown by others that diagenesis can have other micromorphologies.<sup>8, 117</sup> It would therefore be prudent to ascertain the nature and type of diagenetic ingress microscopically before presenting important pathological case studies.

The investigation of the microstructure of the

bone was greatly simplified by the use of PMMA embedding: no further crumbling or fracturing of the archaeological bone occurred, whatever its original state of preservation. The bone was embedded intact without decalcification. All the histopathological information was revealed in a single polished facet of the block. Backscattered electron imaging was particularly useful because subtle changes in the degree of mineralization present were detected easily; these were of great value in the microscopical analysis of the bony tissues and in the appreciation of diagenetic changes. The sensitivity of the method<sup>8,18</sup> exceeds that of microradiography;<sup>19</sup> it is particularly apposite for palaeopathological specimens.

## Conclusions

Recent developments in the microscopy of bone and in particular the SEM/BSE imaging method, have provided highly useful investigative tools for palaeopathological study. The information yielded by this microscopical analysis has emphasized the need to be critical of macroscopic assessments of preservation, the requirement to validate the use of X-rays, and the opportunity to obtain further diagnostic information from the surviving microstructure in archaeological material.

## Acknowledgements

The St Margaret *in cumbusto* bone was kindly supplied by Ann Stirland, and the Sandwell Priory bone by Roger Flinn. This study was supported by grants from the MRC, SERC and the Central Fund of the University of London.

## References

1. Paget, J. On a form of chronic inflammation of bones (osteitis deformans). *Transactions of the Medical Chirurgical Society*, 1877; 60, 37-64.
2. Ortner, D. J. and Putschar, W. G. J. Identification of pathological conditions in human skeletal remains. Washington: Smithsonian Institution Press, 1985.
3. Boyde, A., Maconnachie, E., Reid, S. A., Delling, G. and Mundy, G. R. Scanning electron microscopy in bone pathology: review of methods, potential and applications. *Scanning Electron Microscopy*, 1986; IV, 1537-1554.
4. Chappard, D., Alexandre, C., Laborier, J. C., Robert, J. M. and Riffat, G. Paget's disease of bone: a scanning electron microscopic study. *Journal of Submicroscopic Cytology*, 1984; 16, 341-348.
5. Tillman, H. H. Paget's disease of bone. *Oral Surgery, Oral Medicine and Oral Pathology*, 1962; 15, 1225-1234.
6. Wells, C. and Woodhouse, N. Paget's disease in an Anglo-Saxon. *Medical History*, 1959; 19, 369-400.
7. Denninger, H. S. Palaeopathological evidence of Paget's disease. *Annals of Medical History*, 1933; 5, 73-81.
8. Bell, L. S., Boyde, A. and Jones, S. J. Diagenetic alteration to teeth *in situ* illustrated by backscattered electron imaging. *Scanning*, 1991; 13, 173-183.
9. Bell, L. S. Palaeopathology and diagenesis: an SEM evaluation of structural changes using backscattered electron imaging. *Journal of Archaeological Science*, 1990; 17, 85-102.
10. Garland, A. N. Microscopical analysis of fossil bone. *Applied Geochemistry*, 1989; 4, 215-229.
11. Hackett, C. J. Microscopical focal destruction (tunnels) in excavated human bones. *Medicine, Science and Law*, 1981; 21, 243-265.
12. Poole, D. F. G. and Tratman, E. K. Post-mortem changes on human teeth from late upper Palaeolithic/Mesolithic occupants of an English limestone cave. *Archives of Oral Biology*, 1978; 23, 1115-1120.
13. Clement, A. J. Variations in the microstructure and biochemistry of human teeth. In: *Dental Anthropology*, (edited by D. R. Brothwell), Oxford: Pergamon, 1963: 245-269.
14. Piepenbrink, H. Two examples of biogenous dead bone decomposition and their consequences for taphonomic interpretation. *Journal of Archaeological Science*, 1986; 13, 417-430.
15. Marchiafava, V., Bonucci, L. and Ascenzi, A. Fungal osteoclasia: a model of dead bone resorption. *Calcified Tissue Research*, 1974; 14, 195-210.
16. Wedl, C. Über einem im Zahnbein und Knochen keimenden Pilz. *Akademi der Wissenschaften in Wien. Sitzungsberichte Naturwissenschaftliche Klasse ABL. Mineralogie, biologie erdkunde*, 1864; 50, 171-193.
17. Ascenzi, A. & Silvestrini, G. Bone boring marine micro-organisms: an experimental investigation. *Journal of Human Evolution*, 1984; 7, 409-420.
18. Reid, S. A. and Boyde, A. Changes in the mineral density distribution in human bone with age: image analysis using backscattered electrons in the SEM. *Journal of Bone and Mineral Research*, 1987; 2, 13-22.
19. Kelly, P. J., Peterson, L. F. A., Dahlin, D. C. and Plum, G. E. Osteitis deformans (Paget's disease of bone). *Radiology*, 1961; 77, 368-375.



# Analysis of ancient bone DNA: techniques and applications

ERIKA HAGELBERG<sup>1</sup>, LYNNE S. BELL<sup>2</sup>, TIM ALLEN<sup>3</sup>, ALAN BOYDE<sup>2</sup>, SHEILA J. JONES<sup>2</sup> AND J. B. CLEGG<sup>1</sup>

<sup>1</sup> MRC Molecular Haematology Unit, Institute of Molecular Medicine, University of Oxford, John Radcliffe Hospital, Oxford OX3 9DU, U.K.

<sup>2</sup> Hard Tissue Research Unit, Department of Anatomy and Developmental Anatomy, University College London, London WC1E 6BT, U.K.

<sup>3</sup> Oxford Archaeological Unit, 46 Hythe Bridge Street, Oxford OX1 2EP, U.K.

## SUMMARY

The analysis of DNA from ancient bone has numerous applications in archaeology and molecular evolution. Significant amounts of genetic information can be recovered from ancient bone: mitochondrial DNA sequences of 800 base pairs have been amplified from a 750-year-old human femur by using the polymerase chain reaction. DNA recovery varies considerably between bone samples and is not dependent on the age of the specimen. We present the results of a study on a small number of bones from a mediaeval and a 17th-century cemetery in Abingdon showing the relation between gross preservation, microscopic preservation and DNA recovery.

## 1. INTRODUCTION

### (a) *The polymerase chain reaction and bone DNA*

Developments in molecular biology have provided new tools for analysing ancient DNA from archaeological remains and museum specimens Higuchi *et al.* 1984; Pääbo 1985; Pääbo *et al.* 1988; Thomas *et al.* 1989; Hagelberg *et al.* 1989; Golenberg *et al.* 1990. In particular, with the polymerase chain reaction PCR

Saiki *et al.* 1985, significant phylogenetic information has now been recovered from a number of ancient tissues preserved frozen, in dry environments, or in water-logged deposits. PCR is a technique for the enzymic synthesis of a DNA segment, whereby the exact sequence to be amplified is specified by two primers, short molecules of single-stranded DNA designed to match opposite ends of the two complementary strands of the target DNA, bounding the fragment to be replicated. Repeated cycles of denaturation, annealing of the primers to the target DNA and extension of the segment between the primers by a DNA polymerase, result in the exponential accumulation of the target DNA fragment that can then be sequenced by conventional techniques. In recent studies, PCR has been shown to be an essential tool for the analysis of ancient DNA, as it can be used for degraded and chemically modified DNA samples Paabo *et al.* 1989. The oldest tissue from which phylogenetically useful sequences have been recovered is a compression fossil of a *Magnolia* leaf from a Clarkian lake bed dating from 17–20 Ma, as described by Golenberg *et al.* 1990, and this symposium.

Hagelberg *et al.* 1989 described the amplification of mitochondrial DNA mtDNA sequences from

human bones several hundred years old. This has important implications for archaeology, anthropology and palaeontology as bones are preserved under a wider range of environmental conditions than those which allow preservation of soft tissue remains. Other studies have now been published describing the amplification of mtDNA fragments from ancient human skeletal material Horai *et al.* 1989; Hanni *et al.* 1990).

Reports of the analysis of bone DNA have met with some scepticism, as the results could be artefacts caused by amplification of trace amounts of modern DNA from people handling the material. However, Hagelberg & Clegg 1991 confirmed that authentic DNA can indeed be extracted and amplified from ancient bone, as analysis of DNA from a 16th-century pig bone revealed an unambiguous pig sequence. Additional evidence for the applicability of these techniques was provided by work done in the course of a murder investigation, in which bone DNA typing was used to confirm the identity of the victim Hagelberg *et al.* 1991. In this context, note that in a comprehensive review of forensic anthropology, Iscan 1988 stated that bone DNA typing was impossible unless some soft tissue remained on the skeleton.

Despite these developments, DNA typing from ancient bones is far from being a routine technique because little is known about the factors affecting DNA preservation and recovery. The preservation of DNA in bone is highly variable E. Hagelberg, unpublished observations and the relation between DNA content and parameters such as protein content is poorly understood. No work has yet been done to show how environmental conditions, such as depth of burial or

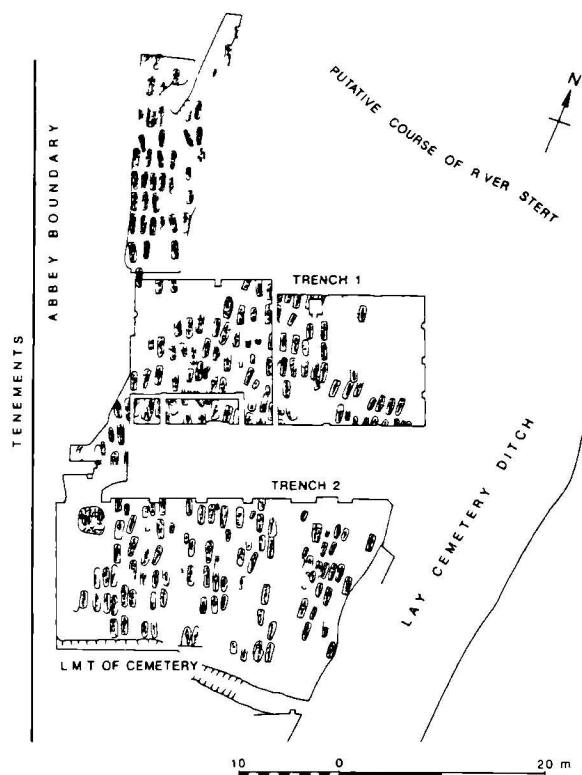


Figure 1. Plan of the Civil War cemetery in Abingdon. Four bone samples from the mass grave (3115, 3117, 3118 and 3123) and one from an adjacent single grave 3071 were used in this study. The unusual north-south orientation of the graves was part of the Puritan reaction against Anglican church ritual during the rule of Parliament.

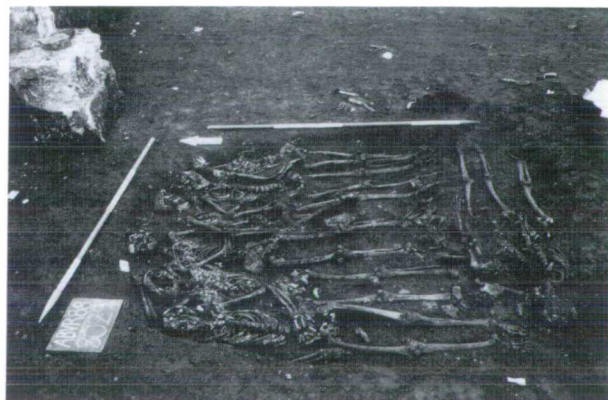


Figure 2. Mass burial of nine men, one with a musket ball between the ribs, from the Civil War cemetery in Abingdon.

soil pH, may affect DNA survival. The histological preservation of bone has also been shown to be variable, and skeletal material may be profoundly altered and reorganized by the effects of diagenesis (Hackett 1981; Bell 1990; Bell *et al.* 1991).

The purpose of this study was to investigate whether a relation exists between gross state of preservation of bone, as defined in archaeological terms, histological preservation, and the ability to extract DNA and amplify mtDNA sequences from the tissue. MtDNA is used frequently in ancient DNA studies because it is relatively small and well characterized: the human mtDNA genome consists of 16 569 base pairs and its sequence was published by Anderson *et al.* 1981,

evolves on average five to ten times faster than nuclear DNA and is inherited through the maternal line. Mammalian cells have approximately  $10^3$ – $10^4$  copies of mtDNA so it is fairly likely that some mtDNA could persist in degraded samples.

We describe here the preliminary results of DNA analysis of a small number of samples from skeletons recovered in the course of archaeological excavations in Abingdon, Oxfordshire, U.K.

### b) The Abingdon cemeteries

Excavations by the Oxford Archaeological Unit were done within the former precinct of Abingdon Abbey before redevelopment, and involved both the mediaeval town cemetery and a cemetery of the English Civil War period (Allen 1989, 1990a, b). In total, nearly 1000 skeletons have been recovered from the mediaeval cemetery and over 280 from the Civil War cemetery. The mediaeval cemetery was used from ca. A.D. 1100 to A.D. 1540 and has more than twenty successive layers of graves that overlay and cut into one another. In contrast, the Civil War cemetery was in use only between A.D. 1644 and 1663 and consisted of a single layer of burials that did not intercut.

Interestingly, the Civil War graves are all oriented north–south, in contrast to the mediaeval graves which all lie east–west. During the English Civil War and the rule of Oliver Cromwell much of the Anglican ritual was considered Papist, hence the unconventional orientation of the graves. The start of the cemetery can be dated from the capture of Abingdon by the Parliamentarians in May 1645, the end by the passing of the Test Act in 1663 when Anglican burial rites became compulsory again. The cemetery was not predominantly military, as the burials include old people, children and women. As shown in figure 1, most of the burials contained only one skeleton, with the exception of several group burials of a woman and child or two children, and one mass grave of nine individuals, one with a musket ball between his ribs (figure 2). The burial register for 1644–45 contains an entry for the burial of nine prisoners from the town gaol, which probably corresponds to the grave of the nine men, especially as the gaol at that time was in the Abbey gateway only 50 m away.

In addition, a small mediaeval graveyard approximately 1 km northwest of the Abbey was excavated between 1977 and 1978 by the Abingdon Archaeological and Historical Society (Harman & Wilson 1981). There were at least 19 adult and 3 child burials, all in individual graves, and no evidence of intercutting, although there were at least two successive layers of graves.

In this study we examined five human femur samples from skeletons excavated between 1988 and 1989 from the Civil War Cemetery and one femur from the small mediaeval graveyard.

## 2. MATERIALS AND METHODS

Mid-shaft sections of the femora were cut longitudinally and DNA extracted from one of the fragments, and the remaining portion was used for the

microscopic study. The bone fragments were processed for DNA analysis as described in Hagelberg & Clegg 1991. Care was taken at all stages to avoid contamination by modern DNA. Disposable sterile containers and pipette tips were used throughout, as well as sterile reagents and solutions dedicated solely for work on ancient DNA. Blank control extractions containing no bone were done in parallel with the bone extractions to monitor contamination from laboratory reagents and equipment.

DNA amplifications were done by the method recommended by Perkin-Elmer Cetus in 25 µl reactions containing 2 units *Thermus aquaticus* (Taq) DNA polymerase and 160 µg ml<sup>-1</sup> bovine serum albumin. The addition of bovine serum albumin in PCR reactions is useful to overcome the effect of a powerful PCR inhibitor of unknown origin present in many ancient DNA extracts Pääbo *et al.* 1988; Hagelberg *et al.* 1989. Two microlitres of bone DNA extract were used in each amplification reaction. A blank reaction containing no DNA was set up in each experiment to check for contamination of the PCR reagents. The amplifications consisted of 35 cycles of denaturation at 95 °C (1 min, annealing at 55 °C 1 min), and extension at 72 °C 1 min and were done in a Perkin-Elmer Cetus DNA Thermal Cycler. After amplification, 10 µl of the PCR reactions were subject to electrophoresis on agarose minigels and stained with ethidium bromide to visualize the DNA fragments under ultraviolet light.

The mtDNA primers used in this work are the previously described primers A and B which specify a 121 base pair b.p. fragment in a small non-coding region region V Wrischnik *et al.* 1987, primers D18, D6 and H408 of the hypervariable region (D-loop) of human mtDNA Higuchi *et al.* 1988; Vigilant *et al.* 1989, and the highly conserved mtDNA primers Kocher *et al.* 1989 specifying a 375 b.p. fragment of the cytochrome *b* gene primers L14841, H15149.

For the microscopic study, thick mid-shaft sections were taken from the femora using a water-cooled diamond saw and allowed to air dry. The sections were then placed in distilled methylmethacrylate monomer which was polymerized at 37 °C. After polymerization, the embedded specimens were cut transversely, polished using graded abrasives, and finally polished with fine diamond abrasive 1 µm on a rotary lap. Each block face was then coated with carbon *in vacuo*.

The specimens were examined by using a Cambridge Stereoscan S4-10 scanning electron microscope SEM operated in backscattered electron BSE mode working at 20 kV beam voltage. A four-segment solid-state BSE detector was used for compositional imaging, summing the signal from all four segments. The images were dominated by differences in the mean atomic number of the volume probed by the scanning beam and so provided a sensitive indicator of mean density and micromorphology.

### 3. RESULTS

We examined five human femur samples from the Civil War cemetery in Abingdon and one human femur from the small mediaeval cemetery. Of the five

bone samples from the Civil War cemetery, four were from the mass grave and one from a single grave adjacent to the mass grave figure 1, as follows: from mass burial, skeletons numbers 3115, 3117, 3118 and 3123 males aged *ca.* 17–24 years; single burial, skeleton number 3071 adult male. The femur sample from the mediaeval cemetery was from a male aged 20–25 radiocarbon date Har-3474 750 ± 80 before present 1950 = A.D. 1200.

#### (a) DNA amplification

DNA was extracted from 1.2 g of powdered bone, and little difference in the quantity of DNA was observed between all 17th-century bone samples after electrophoresis on an agarose gel and staining with ethidium bromide. Segments of mtDNA of 121 b.p. region V and 229 b.p. D-loop could be amplified from all DNA samples except bone DNA from skeleton 3123: DNA extracted from this sample could not be amplified, although the DNA extracted from the other three skeletons in the same grave could be amplified readily. To obtain an idea of the extent of damage of the bone DNAs, samples 3115, 3117, 3118 mass grave, 3071 single burial and the mediaeval bone DNA was subjected to PCR with four pairs of primers specifying DNA fragments of varying length, ranging

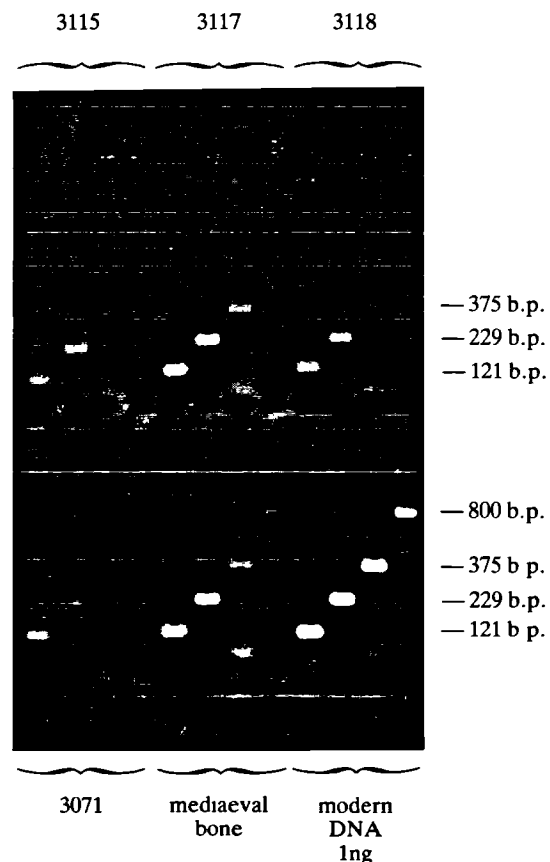


Figure 3. PCR amplifications of mtDNA from bone DNAs and control modern DNA, as follows: DNA samples from skeletons 3115, 3117, 3118, 3071 Civil War cemetery; bone DNA from mediaeval skeleton; control modern DNA 1 ng. The amplified products were 121 b.p. primers A and B; 229 b.p. primers D18 and D6; 375 b.p. primers L14841, H15149; 800 b.p. primers D18 and H408.

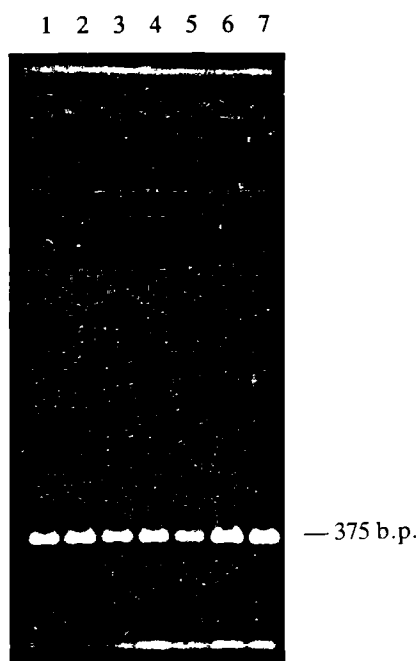


Figure 4. Effect of ancient bone DNA extracts on amplification of modern DNA. All the reactions contained 1 ng of modern DNA but reactions 1–6 contained 1 µl DNA from the following bone samples: 1 3115; 2 3117; 3 3118; 4 3123; 5 3071; 6 mediaeval bone. Reaction 7 contained modern DNA only. Note the slight inhibitory effect of several of the bone samples, particularly 3115, 3118, and 3071. The amplified product was the 375 b.p. fragment of the mtDNA cytochrome *b* gene.

from 121 to 800 b.p. The results (figure 3) suggested that DNA sample 3071 (single burial) was highly degraded, as only slight amplification of the 229 b.p. fragment could be obtained, whereas the three samples 3115, 3117 and 3118 from the mass burial were better preserved as the 375 b.p. fragment could be amplified (though not 800 b.p.). The most striking DNA preservation was observed with the mediaeval bone DNA, with clear amplification of the 800 b.p. fragment.

From the point of view of DNA preservation the mediaeval bone was better preserved than the 17th-century samples, assuming that failure to amplify reflects the extent of damage to the DNA. Samples may amplify poorly because of DNA damage, i.e. the DNA might be broken into small segments, but failure to amplify efficiently could also be a result of inhibition of the *Taq* polymerase by some unknown substance in the ancient DNA. We tested whether the ancient samples inhibited PCR by adding aliquots of the ancient DNA to reactions containing modern DNA (1 ng). The results (figure 4) show that the 17th-century samples inhibited slightly the amplification of modern DNA, with inhibition being stronger in 3115, 3118 and 3071 although there was little difference between them, and what inhibition there was could not account for the total failure to amplify sample 3123 described above.

#### (b) Microscopic examination

The microscopic examination revealed that the 17th-century bones had undergone similar, and some-

times quite extensive, diagenetic alteration, whereas the spatially distinct mediaeval specimen had extremely good micromorphology. The 17th-century specimens exhibited diagenetic changes similar to those described in Bell (1990), believed to be caused by invasive bacterial activity. No fungal invasion was evident in any of the specimens examined.

Sample 3115 (figures 5–7) had fairly good microscopic preservation. The medullary third and central third of the cortex showed large areas of bone with an intact system of osteocyte lacunae, although diagenetic foci were present among large fields of intact bone. Diagenetic alteration was only extensive at the subperiosteal aspect of this sample. In contrast, samples 3117 (figures 8–10), 3118 (figures 11–13) and 3071 (figure 17) showed a similar degree of poor preservation. The distribution of diagenetic alteration concentrated on the medullary and subperiosteal thirds of the cortex, where little recognizable bone could be identified. The middle third of the cortices had undergone diagenetic changes within every single osteonal system in the plane of each section, although more bone was recognizable and intact osteocyte lacunae could be seen (figures 9, 12 and 17). Sample 3123 (figures 14–16) had extremely poor preservation; its entire cortex from medullary aspect through to the periosteal aspect having been almost entirely remodelled *post mortem*. Closer inspection of locations between diagenetic focal lesions revealed occasional intact osteocyte lacunae and very small areas of bone with unaltered morphology and density.

The bone from the small mediaeval graveyard showed by far the best preservation. This sample (figure 18) had nearly perfect micromorphology, with its osteonal and osteocytic network intact. Only a very small area of the circumferential lamellae showed localized demineralization, but otherwise the state of preservation of this specimen was excellent.

#### 4. DISCUSSION

We have already shown in several studies (Hagelberg *et al.* 1989; Hagelberg & Clegg 1991; Hagelberg *et al.* 1991) that genetic information can be recovered from archaeological and forensic bones, but little is known about the factors affecting DNA preservation. To extract DNA from extremely ancient and valuable skeletal remains we will need to know the conditions under which DNA is preserved and which are the best samples to test. However, preservation may be defined in a variety of different ways; for an archaeologist, who is primarily concerned with gross morphology, the quality of preservation as assessed in the field depends on the weight, robustness and completeness of the bones. If the bones are dense, not brittle, and the surfaces are undamaged, the skeleton is said to be well preserved; if the bones are damp, the surfaces are pitted or rub off when touched and the bone is spongy, the preservation is poor.

The site of the Abingdon Abbey precinct, where the large mediaeval town cemetery and the Civil War cemetery were situated, sits upon gravel terrace deposits, overlaid by an orange sandy silt of post-



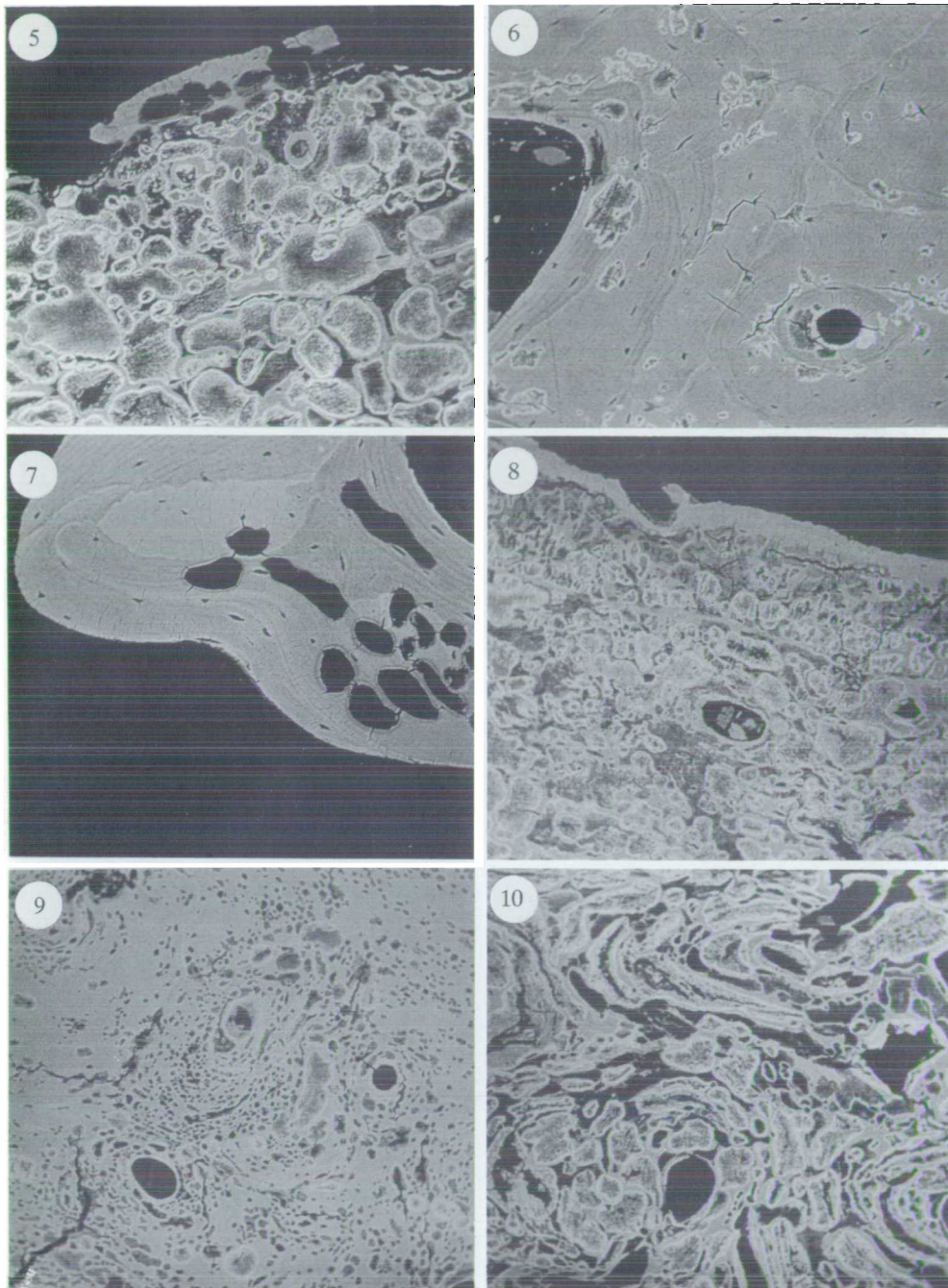


Figure 5. Specimen 3115. Transverse section *ts*. Extensive diagenetic changes to bone concentrated at subperiosteal aspect. A small amount of circumferential lamellae is still intact. Field width *fw* 320  $\mu$ m.

Figure 6. Specimen 3115. *ts*. Midcortical region exhibiting osteonal systems with localized areas of diagenetic alteration, usually centred on osteocyte lacunae. *fw* 320  $\mu$ m.

Figure 7. Specimen 3115. *ts*. A single trabeculum with recognizable areas of bone, combined with focal areas of diagenetic demineralization. *fw* 320  $\mu$ m.

Figure 8. Specimen 3117. *ts*. Extensive diagenetic remodelling at subperiosteal aspect. Several circumferential lamellae remain intact. *fw* 330  $\mu$ m.

Figure 9. Specimen 3117. *ts*. Midcortical region showing a moderate amount of diagenetic remodelling *fw* 330  $\mu$ m.

Figure 10. Specimen 3117. *ts*. Region close to medullary aspect affected by extensive diagenesis. *fw* 330  $\mu$ m.

glacial origin. Gravel deposits vary in their pH values depending on geographical location, but calcareous gravels are alkaline and are favourable to the gross preservation of bone (Brothwell 1981). The soils of Abingdon are alkaline-neutral, depending on the degree of mixing of the gravel into the overlying soils

by human agencies such as ploughing. The large mediaeval town cemetery was in use for more than 400 years and consisted of more than 20 layers of graves overlaying and intercutting each other. In consequence, the soil around the skeletons was very mixed and reworked, resulting in a friable loam with varying



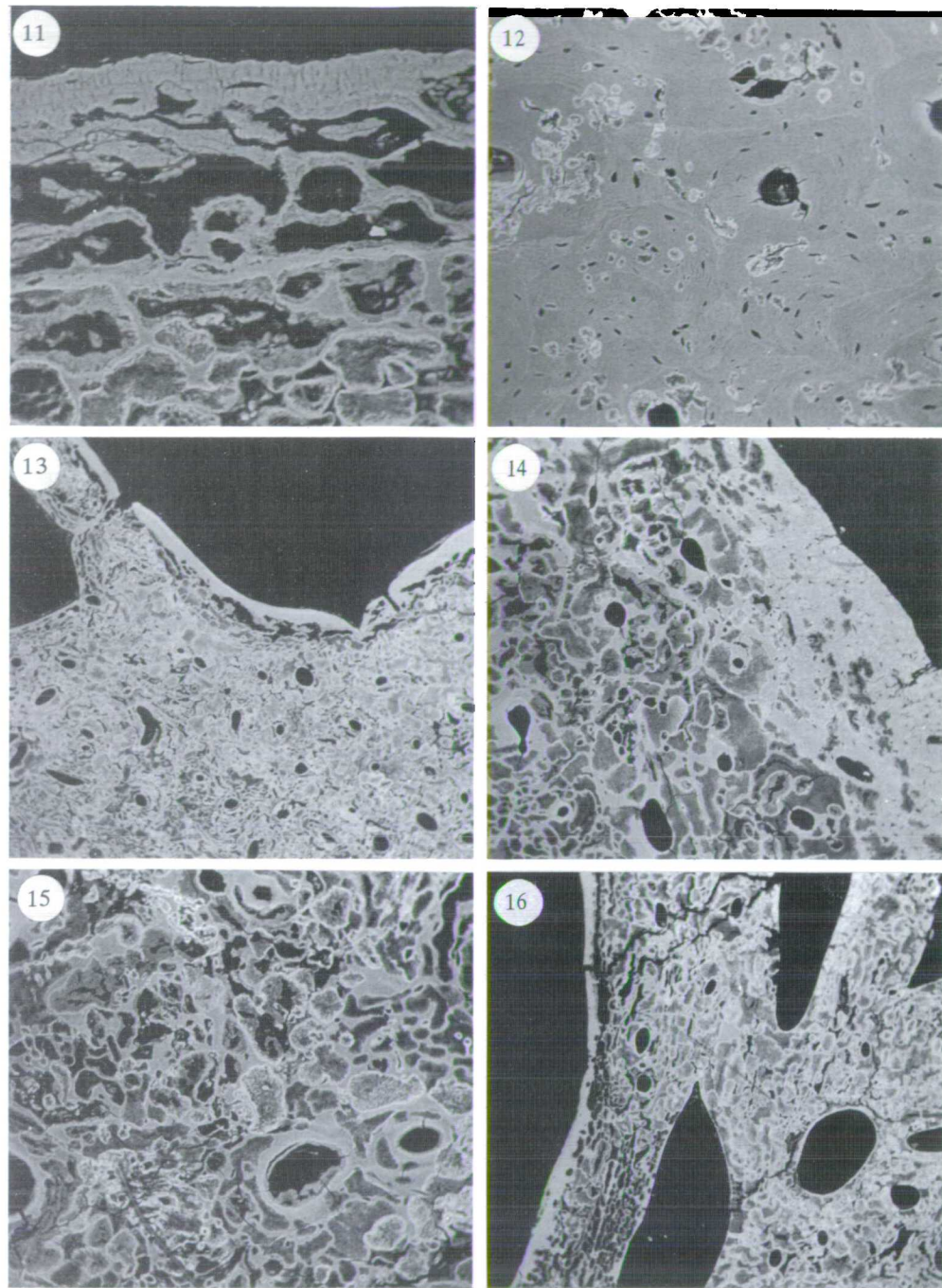


Figure 11. Specimen 3118. rs. Extensive diagenetic remodelling increasing and decreasing overall density. Some circumferential lamellae are intact with two osteocyte lacunae visible. fw 150  $\mu$ m.

Figure 12. Specimen 3118. rs. Small area of midcortical bone with osteonal systems and interstitial lamellae altered by focal diagenetic lesions, many incorporating osteocyte lacunae. fw 365  $\mu$ m.

Figure 13. Specimen 3118. rs. Medullary aspect and adjoining trabecular bone affected extensively by diagenetic remodelling. The endosteal rim remains unaltered. fw 3640  $\mu$ m.

Figure 14. Specimen 3123. rs. Subperiosteal region showing extensive diagenetic remodelling, although some bone is intact at the most external aspect. fw 670  $\mu$ m.

Figure 15. Specimen 3123. rs. Midcortical region extensively affected by diagenesis. Haversian canals are still evident. fw 330  $\mu$ m.

Figure 16. Specimen 3123. rs. Medullary aspect of bone showing the extensive remodelling common throughout this specimen. fw 1330  $\mu$ m.

percentages of gravel. No mediaeval skeletons from this cemetery have yet been examined for DNA survival the only mediaeval bone was from the small graveyard

1 km from the town cemetery) but the mediaeval bodies, although buried much longer than those of the Civil War, were very well preserved from an archaeo-



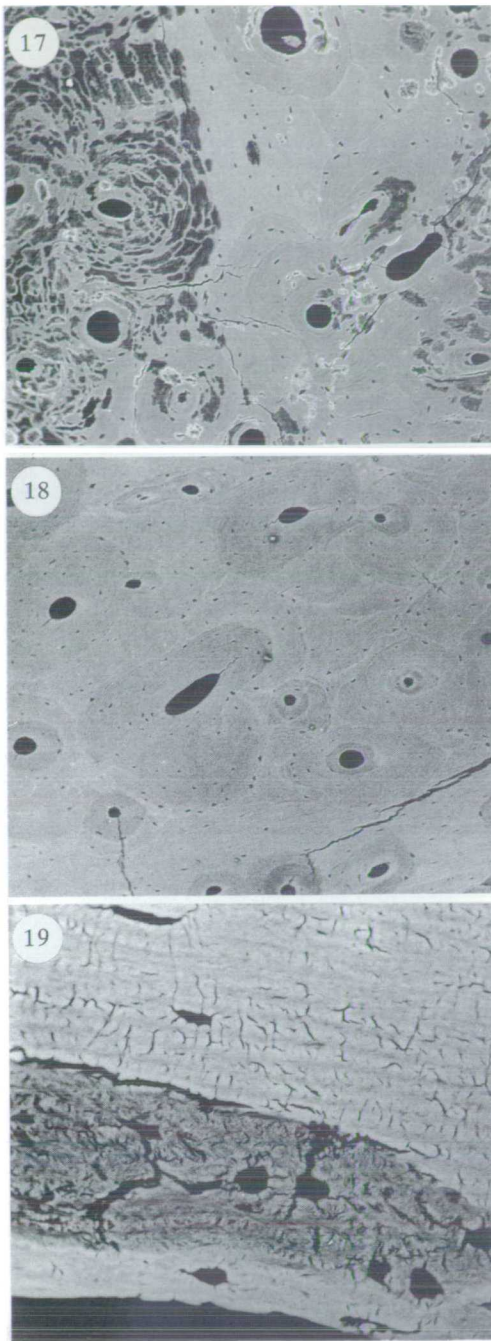


Figure 17. Specimen 3071. *ts.* Border between subperiosteal altered bone left and relatively unaltered bone right. *fw* 670  $\mu$ m.

Figure 18. Mediaeval specimen. *ts.* Typical field of excellent bone preservation. Osteonal systems with varying relative densities reflecting their maturation, with interstitial lamellae, cement lines more highly mineralized and a network of osteocyte lacunae. *fw* 1260  $\mu$ m.

Figure 19. Mediaeval specimen. *ts.* Small area of localized diagenetic demineralization situated just under the subperiosteal surface of the bone. Note enlarged osteocyte lacunae within this demineralized zone, and the evident canalicular network throughout the adjacent bone. *fw* 170  $\mu$ m.

logical point of view. The constant reworking of the soil may have influenced gross preservation by aiding drainage and circulation of calcareous material.

In contrast, the Civil War 17th-century cemetery was in use for less than 20 years and consisted of a single layer of discrete burials. The graves were cut into Saxon and mediaeval garden soils 0.8 m deep, below which was the orange sandy sealing gravel, although in places there were ditches and pits of Roman and earlier date filled with silty loam. Some of the graves were deep and cut into the gravel substrate, resulting in calcareous soil and good bone preservation; others were surrounded by the silt fills of earlier features or were shallow and did not reach gravel, and preservation was poor. The mass burial and the single burial 3071 were both shallow, being *ca.* 1 m and 0.9 m below the contemporary surface, and as such were in soft soil and did not cut into the gravel. The Civil War skeletons were quite orange or brown in colour on excavation, whereas the mediaeval ones were almost white, but colour was not a clear guide to gross preservation as some of the Civil War skeletons were orange but dense and well preserved.

From the point of view of tissue micromorphology, the changes to skeletal material are described in quite different terms. Here the geochemical term diagenesis is used to describe the alterations to skeletal and dental tissues after death. It includes all processes that can affect degradation and remineralization, both in and out of the ground, but excludes the effects of high temperature and pressure (Lapedes 1978; Pate & Brown 1985). This geochemical term is used commonly in archaeology to describe *post mortem* changes to bone and teeth, and has been shown histologically to be highly variable in its distribution and morphology (Clement 1963; Poole & Tratman 1978; Hackett 1981; Garland 1989; Bell 1990; Bell *et al.* 1991). Many of the changes are thought to be caused by the separate or joint action of bacteria and fungi Wedl 1864; Hackett 1981, although other microorganisms are implicated and may be environment specific Ascenzi & Silvestrini 1984; Bell *et al.* 1991.

In this study we show a clear relation between DNA recovery and the relative microscopic preservation of the bone. We had already assumed that DNA preservation was not directly related to the age of a specimen, as the mediaeval 13th-century bone had consistently given better results in DNA amplification than the 17th-century bones 21 skeletons from the Civil War cemetery have been examined for DNA recovery E. Hagelberg, unpublished observations. The mediaeval bone showed by far the best microscopic preservation, with nearly perfect micromorphology; it also showed very good gross preservation and was very dense and light in colour. The factors contributing to this excellent preservation are not understood; the depth of burial of the skeletons in the small mediaeval graveyard was difficult to measure owing to topsoil stripping caused by extensive building works, but was probably only 0.5 to 1 m in depth from the contemporary ground level Harman & Wilson 1981.

Relatively uniform preservation might have been expected within the mass grave from the Civil War, as all the skeletons were of young men of similar age, buried at the same time. However, skeleton 3123 was extremely badly preserved, with almost complete *post*

*mortem* remodelling; the sample taken from this skeleton has not yielded amplifiable DNA so far. The skeleton was buried slightly deeper than the other skeletons at the foot of the grave, partly covered by two other bodies, but this alone cannot explain its poor preservation compared with the three other samples from the mass grave, 3115, 3117 and 3118. These showed similar preservation to 3071 the sample from the single grave adjacent to the mass grave.

These results show that significant variability in preservation can occur within an archaeological site, whether described as gross preservation, microstructure, or DNA recovery. In population surveys of cemeteries it would be necessary to take several samples from the skeletons to be studied, particularly if a skeleton exhibited poor gross preservation, to maximize the chance of recovering some well-preserved tissue. Our study suggests that even in poorly preserved bones there might be regions of bone with unchanged morphology, particularly in the inner third of the cortex, between the diagenetically remodelled endosteal and periosteal layers. Histological screening of skeletal samples would optimize DNA recovery.

These results are encouraging for future research in bone DNA typing, although it remains to be seen to what extent DNA can be amplified from very ancient bone. Although many technical problems need to be solved, not least how to avoid or at least monitor contamination from modern DNA Hagelberg & Clegg 1991 and the occurrence of PCR artefacts such as 'jumping PCR' Pääbo *et al.* 1990, PCR and sequencing of bone DNA will become essential tools in anthropology and palaeontology.

This work was supported by a research grant to E.H. under the NERC Special Topic in Biomolecular Palaeontology. The Abingdon Vineyard project was funded by the Vale of the White Horse District Council. The microscopic examination of the bone samples was supported by grants from the MRC, SERC and the Central Research Fund of the University of London.

## REFERENCES

- Allen, I. 1989 Abingdon Vineyard redevelopment. *South Midl. Archaeol.* **19**, 44–47.
- Allen, T. 1990a Abingdon Vineyard redevelopment. *South Midl. Archaeol.* **20**, 73–74.
- Allen, T. 1990b Abingdon. *Curr. Archaeol.* **121**, 24–27.
- Anderson, S., Bankier, A. T., Barrell, B. G., de Bruijn, M. H. L., Coulson, A. R., Drouin, J., Eperon, I. C., Nierlich, D. P., Roe, B. A., Sanger, F., Schreier, P. H., Smith, A. J. H., Staden, R. & Young, I. G. 1981 Sequence organisation of the human mitochondrial genome. *Nature, Lond.* **290**, 457–465.
- Ascenzi, A. & Silvestrini, G. 1984 Bone-boring marine micro-organisms: an experimental investigation. *J. hum. Evol.* **7**, 409–420.
- Bell, L. S. 1990 Palaeopathology and diagenesis: an SEM evaluation of structural changes using backscattered electron imaging. *J. Archaeol. Sci.* **17**, 85–102.
- Bell, L. S., Boyde, A. & Jones, S. J. 1991 Diagenetic alteration to teeth *in situ* illustrated by backscattered electron imaging. *Scanning* **13** In the press.
- Brothwell, D. R. 1981 *Digging up bones: the excavation, treatment and study of human skeletal remains*, 3rd edn. Oxford University Press.
- Clement, A. J. 1963 Variations in the microstructure and biochemistry of human teeth. In *Dental anthropology*, ed. D. R. Brothwell. Pergamon Press.
- Garland, A. N. 1989 Microscopical analysis of fossil bone. *Appl. Geol.* **4**, 215–229.
- Golenberg, E. M., Giannasi, D. E., Clegg, M. T., Smiley, C. J., Durbin, M., Henderson, D. & Zurawski, G. 1990 Chloroplast DNA sequence from a Miocene *Magnolia* species. *Nature, Lond.* **344**, 656–658.
- Hackett, C. J. 1981 Microscopical focal destruction tunnels in excavated human bones. *Med. Sci. Law* **21**, 243–265.
- Hagelberg, E. & Clegg, J. B. 1991 Isolation and characterization of DNA from archaeological bone. *Proc. R. Soc. Lond. B* **244**, 45–50.
- Hagelberg, E., Gray, I. C. & Jeffreys, A. C. 1991 Identification of the skeletal remains of a murder victim by DNA analysis. *Nature, Lond.* **352**, 427–429.
- Hagelberg, E., Sykes, B. & Hedges, R. 1989 Ancient bone DNA amplified. *Nature, Lond.* **342**, 485.
- Hanni, C., Laudet, V., Sakka, M., Begue, A. & Stehelin, D. 1990 Amplification of mitochondrial DNA fragments from ancient human teeth and bones. *C.r. Acad. Sci., Paris.* **310**, Series III, 365–370.
- Harman, M. & Wilson, B. 1981 A mediaeval graveyard beside Faringdon Road, Abingdon. *Oxoniansia* **46**, 56–61.
- Higuchi, R., Bowman, B., Freiberger, M., Ryder, O. A. & Wilson, A. C. 1984 DNA sequences from the quagga, an extinct member of the horse family. *Nature, Lond.* **312**, 282–284.
- Higuchi, R., von Beroldingen, C. H., Sensabaugh, G. F. & Erlich, H. A. 1988 DNA typing from single hairs. *Nature, Lond.* **332**, 543–546.
- Horai, S., Hayasaka, K., Murayama, K., Wate, N., Koike, H. & Nakai, N. 1989 DNA amplification from ancient human skeletal remains and their sequence analysis. *Proc. Japan Acad.* **65**, 229–233.
- Iscan, M. Y. 1988 Rise of forensic anthropology. *Yearb. phys. Anthropol.* **31**, 203–230.
- Kocher, T. D., Thomas, W. K., Meyer, A., Edwards, S. V., Pääbo, S., Villablanca, F. X. & Wilson, A. C. 1989 Dynamics of mitochondrial DNA evolution in animals: amplification and sequencing with conserved primers. *Proc. natn. Acad. Sci. U.S.A.* **86**, 6196–6200.
- Lapedes, D. N. ed. 1978 *McGraw-Hill encyclopedia of the geological sciences* pp. 153–155. New York: McGraw-Hill.
- Maniatis, T., Fritsch, E. F. & Sambrook, J. 1982 *Molecular cloning: a laboratory manual*. Cold Spring Harbor University press.
- Paabo, S. 1985 Molecular cloning of ancient Egyptian mummy DNA. *Nature, Lond.* **314**, 644–645.
- Paabo, S. 1989 Ancient DNA: extraction, characterization, molecular cloning, and enzymatic amplification. *Proc. natn. Acad. Sci. U.S.A.* **83**, 1939–1943.
- Pääbo, S., Gifford, J. A. & Wilson, A. C. 1988 Mitochondrial DNA sequences from a 7,000-year-old-brain. *Nucl. Acids Res.* **16**, 9775–9787.
- Paabo, S., Higuchi, R. G. & Wilson, A. C. 1989 Ancient DNA and the polymerase chain reaction. *J. biol. chem.* **264**, 9709–9712.
- Paabo, S., Irwin, D. M. & Wilson, A. C. 1990 DNA damage promotes jumping between templates during enzymatic amplification. *J. biol. chem.* **265**, 4718–4721.
- Pate, F. D. & Brown, K. A. 1985 The stability of bone strontium in the geochemical environment. *J. hum. Evol.* **14**, 483–491.



- Poole, D. F. G. & Tratman, E. K. 1978 Post-mortem changes on human teeth from late upper Palaeolithic Mesolithic occupants of an English limestone cave. *Arch. Oral Biol.* **23**, 1115–1120.
- Saiki, R. K., Scharf, S., Faloona, F., Mullis, K. B., Horn, G. T., Erlich, H. A. & Arnheim, N. 1985 Enzymatic amplification of beta-globin genomic sequences and restriction site analysis for diagnosis of sickle cell anemia. *Science, Wash.* **230**, 1350–1354.
- Thomas, R. H., Schaffner, W., Wilson, A. C. & Paabo, S. 1989 DNA phylogeny of the extinct marsupial wolf. *Nature, Lond.* **340**, 465–467.
- Vigilant, L., Pennington, R., Harpending, H., Kocher, T. D. & Wilson, A. C. 1989 Mitochondrial DNA sequences in single hairs from a southern African population. *Proc. natn. Acad. Sci. U.S.A.* **86**, 9350–9354.
- Wedl, C. 1864 Ueber einen im Zahnbein und Knochen keimenden Pilz. *Mineral. Biol. Erdkunde* **50**, 171–193.
- Wrischnik, L. A., Higuchi, R. G., Stoneking, M., Erlich, H. A., Arnheim, N. & Wilson, A. C. 1987 Length mutations in human mitochondrial DNA: direct sequencing of enzymatically amplified DNA. *Nucl. Acids Res.* **15**, 529–542.

### Discussion

S. HUMMEL (*Institut für Anthropologie der Universität Göttingen, Göttingen, F.R.G.*). How does Dr Hagelberg distinguish between evolutionary changes in DNA sequences and those changes produced by diagenetic processes? Are there any safe tools for diagnosis?

E. HAGELBERG. Direct sequencing of PCR products should distinguish between these possibilities.

S. HUMMEL. In the case of highly repeated sequences, direct sequencing the PCR products will solve the problem. However, in the case of amplifying sequences that are less often repeated in the genome, or present only as single copies, the problem that a 'wrong' target might be the 'parent' of the overwhelming reaction should be kept in mind, I think, especially as ancient DNA might only reveal very few intact not nicked targets.

T. A. BROWN *Department of Biochemistry and Applied Molecular Biology, UMIST, Manchester, U.K.* Is the amount of human DNA present in human bones, and its length, dependent on the extent of microbial contamination present?

E. HAGELBERG. Yes, the heavily contaminated bones have less human DNA. The best bones with respect to human DNA amplification are undamaged ones.

R. P. AMBLER *Institute of Cell and Molecular Biology, Division of Biological Sciences, University of Edinburgh, U.K.* In the case of bone DNA that is destroyed by bacteria and fungi, does the decaying bone environment attract or support characteristic microorganisms (e.g. characterized by 16S rRNA)?

E. HAGELBERG. Yes, work of this kind is being done at present in several laboratories, although I myself have not worked in this area.



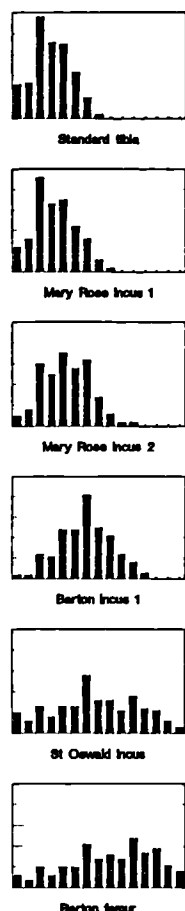


Figure 10. System 80K 15 bin Histograms of BSE signal level measured at 128x128 points in 1mm fields in carbon coated, micro-milled PMMA blocks: (a) Standard: 25y modern human tibia, TS; (b+c) fields from TSs of the long processes of incuses from sailors recovered from the wreck of the "Mary Rose" which sank off Portsmouth, England in 1545 AD; (d+e) similar fields from incuses from adults from medieval soil burials, (d) from Barton-on-Humber and (e) from St. Oswald's Priory, England; (f) adult femur from Barton-on-Humber. (a) through (f) show a general shift towards a higher mean atomic number (density) in diagenetically altered bone, with a corresponding increase in the range of densities compared with normal bone. This shift corresponds to morphological changes in microstructure.

Archaeological human bone from well documented and distinct environmental contexts was examined. Incuses were selected because on histological inspection they showed various stages of diagenetic change. The femurs selected showed gradients of diagenetic remodelling which had been established from morphological studies [15], ranging from slight, to intermediate, and extensive diagenesis. A recent, unburied human adult tibia was used as a control within this group. All bones were embedded in PMMA and the selected faces of the cut and ground blocks finished by UltraMilling before carbon coating. The analyses were conducted using System 80K interfaced to the S4-10 SEM, operated at 19.7kV, 1mm diameter fields, and with a 128<sup>2</sup> grid. The hits on bone were divided into 15 classes (the first 8 of which represented the range of values found in normal bone). The samples were mounted as one group on a 25mm diameter stub, the field co-ordinates previously recorded being refound by hand. This sufficed for rapid translation between such a low number of small samples (Figure 10).

The results indicated a general shift towards a higher mean atomic number in diagenetically altered bone, with a corresponding increase in the range of densities compared with normal bone. This diagenetic shift was seen to correspond to the degree of morphological change in microstructure. Bone fields which had little diagenetic alteration remained close to the control bone densities. Fields with intermediate diagenesis had higher mean signal levels. Fields with extreme or extensive diagenesis, where no "bone" was morphologically evident, covered a range with much higher BSE signal values.

This study is the first application of a method of quantification of diagenetic shift. The preliminary results show that it will help to map the fossilisation process at the morphological and mean atomic number level, particularly working at a slightly higher resolution and with a denser sampling grid.

Another group of archaeological samples which we studied were fourth lumbar vertebral bodies and femoral necks from bronze age sites (not

Boyde A., Howell P.G.T., Bromage T.G., Elliott J.C., Riggs C.M., Bell L.S., Kneissel M., Reid S.A., Jayasingh J.A.P. & Jones S.J. (1992) Applications of mineral quantitation of bone by histogram analysis of backscattered electron images. In: Chemsity and Biology of Mineralized Tissues. Eds. H. Slavkin & P. Price, Excerpta Medica, London, New York & Tokyo, pp. 47-60

**D. 23 Post-mortem changes in buried human bone.** By  
L. S. BELL, F. S. WONG\*, J. C. ELLIOTT,† A. BOYDE  
and S. J. JONES. *Department of Anatomy, University  
College London, and †Dept of Child Dental Health, The  
London Hospital Medical College, London*

Buried human bones are frequently used in the estimation of the age at death in archaeological populations, but have also been used as a source of material for studies of age changes in normal human material where the individual age at death is known. Internal changes are to be expected if there is an evident alteration in the density of the bone and may also have occurred even in the absence of such obvious change. Depending upon the circumstances at burial, the most common change is a substantial loss of mass with diagenesis. We have studied diagenetic structural changes using a variety of methods, but particularly those addressing questions of microscopic organisation and density, including backscattered electron-mode scanning electron microscopy (BSE-SEM) of carbon-coated, polished polymethyl-methacrylate-embedded blocks, X-ray diffraction and X-ray microtomography. Although the form of bones may be well preserved down to the level of finer structural features of trabeculae, BSE-SEM demonstrates internal substitution as the result of microbial and fungal activity. At completion, such processes result in the loss of all collagen and all lamellar structure, the resultant space being filled with structural domains reflecting the prior presence of the micro-organisms. The mean atomic number from the BSE-SEM image histogram is increased, and this increase in the density of microscopic voxels is confirmed by microtomography. These findings provide caveats for the use of such bone in other studies, but particularly regarding diffraction studies of mean crystal orientation and X-ray photon absorptiometry for the determination of bone mineral content. We show that bone mineral content may increase with post-mortem diagenetic change, even though the macroscopic density of the bone is starkly reduced.

J. Anat., 183, 196 (1993)

**THE SPEED OF POST MORTEM CHANGE TO THE HUMAN SKELETON  
AND ITS TAPHONOMIC SIGNIFICANCE**

**Lynne S. Bell, Mark F. Skinner and Sheila J. Jones**

**Forensic Science International  
(forthcoming)**